

A STUDY OF THE UPTAKE OF THORIUM  
ONTO ZEOLITES.

BY

LINDA CLAIRE JOZEFOWICZ

A thesis submitted for the degree of  
Doctor of Philosophy  
of  
The University of Salford

Department of Pure and Applied Chemistry,  
The University of Salford  
Salford, M5 4WT.

April 1989.

DECLARATION

I hereby declare that this thesis has not been accepted in any previous application for a degree, that it has been composed by myself and that the work described herein was performed by myself.

Linda Claire Jozefowicz.

Linda Claire Jozefowicz.

Date: 18th April 1989.

### ACKNOWLEDGEMENTS

I would like to express my special thanks to Dr. A. Dyer for his supervision and guidance in this work.

I am also grateful to British Nuclear Fuels plc (Springfields) for financial and technical support for this work, especially Dr. J.F. Ellis and Dr. H. Eccles, for their guidance and all the technical and chemical services staff at Springfields for helpful advice and support.

My thanks to Dr. H. Enamy for invaluable help and encouragement throughout this work and all members of the zeolite group, past and present, at Salford.

Thanks are due to Mr. D. Park (Shell) for obtaining EPMA and energy dispersive X-ray spectra, Mr. I. Vaughan for producing excellent X-ray powder diffractograms of thorium-zeolites at British Alcan plc and all technical staff and academic staff, at the University of Salford, who helped with this work.

I would like to thank Miss O. Wilson for providing many of the less well-known zeolites and her help with the reproduction of SEMs.

Finally, I would like to thank Mrs. Sylvia Thomson for the expert typing of this thesis.

*For Erika.*



## ABSTRACT

The presence of the  $\alpha$ - and  $\beta$ - emitters, uranium and thorium, in industrial waste streams poses a serious threat to the environment. This is due to both the potentially damaging nature of the radioactive emissions when incorporated into biological systems and to the general toxicity of these heavy metals.

A programme of work to remove these heavy metals especially thorium, from a particular raffinate was undertaken. It was desirable to use zeolites specifically to remove thorium and some uranium. A survey of the uptake of thorium onto a wide range of zeolites, both natural and synthetic is included. It was necessary to find a zeolite which could take up the radioactive cations, resist acid attack and which was suitable for use in a large scale, industrial removal plant.

Due to the nature of the radiochemical components in conjunction with zeolite behaviour, several radiochemical techniques had to be modified to provide analytical methods for this project. Effects of competing cations on the uptake of thorium onto zeolites were also studied.

The best all-round candidate was found to be an Eastgate zeolite, although clinoptilolite showed a reasonable uptake of thorium. The work carried out attempted to elucidate the mechanisms of thorium removal from solution.

## LIST OF CONTENTS

<u>CONTENTS</u>		<u>PAGE NUMBER</u>
CHAPTER 1	INTRODUCTION	1
1.1	Nuclear Waste	1
1.2	Production of the Plant Waste Stream	2
1.3	Uranium Fuel Rod/Pellet Production	5
1.4	Necessity for the Removal of Thorium and Uranium from the Plant Raffinate	7
1.5	Methods of Waste Management	9
1.6	Methodology of Medium-Low Level Waste Treatment	11
1.6.1	Fixation	11
1.6.2	Ultrafiltration	11
1.6.3	Electrochemical Methods	11
1.6.4	Biomass	12
1.6.5	Ion-Exchangers	12
1.6.6	Precipitation and Solvent Extraction	15
1.7	Liquid Wastes and Aims of the Project	17
CHAPTER 2	ZEOLITES	19
2.1	Occurrence	19
2.2	Natural and Synthetic Zeolites	20
2.3	Uses of Zeolites	21
2.4	Zeolites : Definition and Structure	22
2.5	Zeolite Structure and Ion-Exchange	24
2.6	Channel Types	29
2.7	Hydroxyl Groups	30
2.8	Characterization of Zeolites	31

<u>CONTENTS (continued)</u>		<u>PAGE NUMBER</u>
2.9	Zeolites and Zeolitic Materials used in this Work	32
2.10	Clinoptilolite	32
2.11	Erionite	37
2.12	Mordenite and ZEOLON 900 (Z900)	37
2.13	Chabazite	40
2.14	Zeolite Y	40
2.15	Zeolite A	43
2.16	Eastgate 2020	43
2.17	Other Zeolites	45
2.18	Ion-Exchange Capacity in Zeolites	45
2.19	Basic Ion-Exchange Theory	46
2.19.1	Kinetics	46
2.19.2	Ion-Exchange Mechanism	46
2.20	Langmuir Adsorption Isotherms	49
CHAPTER 3	THORIUM AND URANIUM	50
3.1	Thorium Occurrence and Uses	50
3.2	Uranium Occurrence and Uses	52
3.3	The Radioactive Decay of Thorium	53
3.3.1	Decay Equilibria	55
3.3.2	Other Isotopes of Thorium	59
3.4	The Radioactive Decay of Uranium	59
3.4.1	Equilibrium	62
3.4.2	Other Isotopes of Uranium	62

<u>CONTENTS (continued)</u>	<u>PAGE NUMBER</u>
3.5            Importance of Radioactivity Equilibria to this Work	62
3.6            The General Chemistry of Thorium	63
3.6.1        Aqueous Chemistry of Thorium	63
3.6.2        The Chemistry of Thorium in Nitric Acid	66
3.7            The General Chemistry of Uranium	67
3.7.1        General	67
3.7.1        The Aqueous Chemistry of Uranium	69
CHAPTER 4    EXPERIMENTAL METHODS	72
4.1            Quantitative Methods for the Determination of Thorium and Uranium	72
4.1.1        Colourimetry : Thorium	72
4.1.2        Colourimetry : Uranium	76
4.2            Titration : Thorium	77
4.3            Liquid Scintillation Counting	78
4.3.1        Theory	78
4.3.2        Čerenkov Counting	80
4.3.3        Quenching	81
4.4            Gravimetry	82
4.5            Qualitative Analysis Methods	83
4.5.1 $\gamma$ -Ray Spectroscopy	83
4.5.2 $\beta$ -Ray Spectroscopy	83
4.6.1        Electron Probe Micro-Analysis	85
4.6.2        The Electron Probe Microanalyser	86
4.6.3        Secondary Electrons	87

<u>CONTENTS (continued)</u>	<u>PAGE NUMBER</u>
CHAPTER 5      EXPERIMENTAL I	
5.1              Experimental	89
5.1.1           Preparation of Zeolites for Experiments	89
5.1.2           Wet Chemical Analysis of Specific Zeolites	89
5.1.3           Determination of Silica	91
5.1.4           Sample Preparation for Flame Photometry	93
5.1.5           Sample Preparation for Atomic Absorption Spectrometry	93
5.1.6           Water Content : TG Analysis	94
5.2              Specific Cation Exchange Capacity Measurements on Z900, Clinoptilolite, NaY, CaY	94
5.3              Preparation of Homoionic Forms of Zeolites for Isotherm Studies	95
5.4.1           Leaching Effect of Several Zeolites on Treatment with Water	97
5.4.2           Leaching Effect on Zeolites treated with Pure Thorium Solutions	97
5.4.3           Leaching Effect on Zeolites treated with Nitric Acid	98
5.4.4           Experiments to Determine the Release of Sodium and Potassium from Clinoptilolite and NaY with $10^2$ ppm Thorium Solutions	98
5.5.1           Colourimetry for the Analysis of Thorium	99
5.5.2           Preparation of a Standardized Stock Solution	99
5.5.3           Thorium Colourimetry Procedure : Morin	101
5.5.4           Thorium Colourimetry Procedure : Thoron	102
5.5.5           Colourimetric Determination of Uranium	103
5.6.1           Sample Preparation and Use of the Čerenkov Counting Technique	105

<u>CONTENTS (continued)</u>		<u>PAGE NUMBER</u>
5.6.2	Quenching	105
5.6.3	Liquid Scintillation Counting	108
5.6.4	Quenching	110
5.7.1	Preparation of a Th-234 Tracer Solution by Solvent Extraction of U-238	112
5.7.2	Radiochemical Extraction of Th-232 from its Daughter Isotopes	113
5.8.1	Screening of Zeolites for Th-232 and Ac-228/Ra-228 Uptakes	114
5.8.2	Variations of Experimental Conditions : Temperature	116
5.8.3	Variations of Experimental Conditions : Concentration	116
5.8.4	Th-234 Uptake on Clinoptilolite, Phillipsite, Chabazite 3	118
5.8.5	Ten-Hour Uptake Tests	118
5.9.1	Uptake Experiments : U-238 on Selected Zeolites	119
5.9.2	Uptake Experiments for Zeolites and Uranium $\beta$ -emitter Daughters	119
5.9.3	Experiments to show the Effect of Nitric Acid Concentration on the Uptake of U-238 $\beta$ -emitter Daughters on Zeolites	119
5.10	Competing Ion Effects	
5.10.1	Experiments to Determine the Effect of Competing Ions on the Uptake of Ra-228/ Ac-228 on Zeolites	121
5.10.2	Effect of the Uptake of Th-232 by Varying Concentrations of Competing Ions	123
5.10.3	Effects of $H^+$ , $Na^+$ , $K^+$ , $Ca^{2+}$ and $Al^{3+}$ on the Uptake of Th-232 on Clinoptilolite and Z900	123
5.11	Simulated Raffinate Solutions	125

<u>CONTENTS (continued)</u>		<u>PAGE NUMBER</u>
CHAPTER 6	EXPERIMENTAL II	127
6.1	Column Experiments	127
6.1.1	Procedure	127
6.1.2	Free Column Volume	129
6.1.3	Column Experiment	129
6.1.4	Variations of Column Experiments	130
6.2	Isotherm Experiments : Thorium	132
6.2.1	Repeated and Reversible Exchanges	134
6.2.2	Isotherm Experiments : Uranium	136
6.3	Wet Chemical Analysis of the Solids from Isotherm Experiments	136
6.4	Stripped Raffinate Solutions	139
6.4.1	Experimental	139
6.4.2	Fluoride Determination	142
6.5	X-ray Powder Diffraction (XRD)	143
6.6	Electron Probe Microanalysis (EPMA)	144
6.7	Differential Thermogravimetric Analysis (DTG)	145
6.8	$\gamma$ -Spectrometry	147
6.8	$\beta$ -Spectrometry	149
6.10	Scanning Electron Micrographs (SEM)	150
CHAPTER 7	RESULTS	(151 - 222)
	(See List of Figures and Tables for Contents)	

<u>CONTENTS (continued)</u>		<u>PAGE NUMBER</u>
CHAPTER 8	DISCUSSION OF RESULTS	224
8.1	Wet Chemical Analysis of Clinoptilolite and Eastgate	224
8.2	Cation Exchange Capacity	224
8.2.1	Leaching Effects of Solutions on Zeolites	225
8.2.2	Leaching Effect of Water	225
8.2.3	Leaching Effect of Nitric Acid	226
8.2.4	Leaching Effects of Pure Thorium Nitrate Solutions	226
8.2.5	Leaching Effect of a 1000ppm Th <sup>4+</sup> Solution	227
8.3	Quenching Effects of Na <sup>+</sup> , K <sup>+</sup> and Al <sup>3+</sup> on Cerenkov Counting	228
8.3.1	Quenching Effect of Na <sup>+</sup> , K <sup>+</sup> , Al <sup>3+</sup> on LSC (Th-232 and U-238)	229
8.4	Characterization of Solvent-Extracted Th-234 Solution	229
8.5	Characterization of Solvent-Extracted Th-232 Solution	229
8.6	Uptakes of Th-232 and Total Activity onto a Range of Natural and Synthetic Zeolites	230
8.6.1	Uptakes of Ac-228/Ra-228 onto Natural and Synthetic Zeolites (0.01N, Th-232)	232
8.6.2	Th-234 Uptakes onto Selected Zeolites	232
8.6.3	Ten Hour Uptakes of Th-234 onto Zeolites	233
8.7	Variations of Temperature and Concentration on the Th-232 Uptakes	233



<u>CONTENTS (continued)</u>	<u>PAGE NUMBER</u>
8.7.1 Variations of Temperature and Concentration	233
8.8 Uptakes of U-238 on Zeolites	233
8.9 Uptakes of U-238 ( $\beta$ -Emitter Daughters) onto Selected Zeolites	234
8.10 Competing Ion Effects of $K^+$ and $Na^+$ on Th-232 Daughter Uptakes	234
8.10.1 Competing Ion Effects of $K^+$ , $Na^+$ and $H^+$ on Th-232 Uptakes	234
8.10.2 Competing Ion Effects of $Na^+$ , $K^+$ , $Mg^{2+}$ , $Ca^{2+}$ , $Al^{3+}$ on the Uptake of Thorium in Nitric Acid Solution	235
8.11 Th-232 Uptakes from Simulated Raffinate Solutions	236
8.12 Column Experiments	237
8.12.1 Breakthrough Curves	237
8.13 Isotherms	242
8.13.1 Thorium	242
8.13.2 Langmuir Plots : Thorium	243
8.13.3 Langmuir Plots Involving the Thorium Daughter Isotopes	244
8.13.4 Ion-Exchange Isotherms : Uranyl Ions	246
8.13.5 Langmuir Isotherms : Uranium	247
8.13.6 Repeated Exchanges	248
8.13.7 Wet Chemical Analysis of Clinoptilolite treated with Thorium	248
8.13.8 Total Uptakes of Thorium in Isotherm Solutions	249
8.14 Stripped Raffinate Experiments	249
8.15 X-Ray Powder Diffractograms	250

<u>CONTENTS (continued)</u>		<u>PAGE NUMBER</u>
8.16	Energy-Dispersive X-ray Spectra	252
8.17	Differential Thermal Gravimetry	254
8.18	$\gamma$ -Spectra	255
8.19	$\beta$ -Spectra	257
8.20	Scanning Electron Micrographs	258
CHAPTER 9	GENERAL DISCUSSION, CONCLUSIONS AND FURTHER WORK.	
9	General Discussion and Conclusions	259
9.1	Thorium	259
9.2	Isotherms and Cation Positions	259
9.2.1	Clinoptilolite	259
9.2.2	NaY	261
9.2.3	Zeolite Z900	263
9.3	Isotherms : Uranium	264
9.3.1	Clinoptilolite	264
9.3.2	Z900	265
9.3.3	NaY	265
9.4	Langmuir Adsorption	266
9.5	Surface Precipitation of Thorium	268
9.6	Reproducibility of Results	269
9.7	Thermodynamic Parameters for Isotherms	269
9.8	Eastgate - A Special Case	270
9.9	Radiochemistry	272
9.9.1	Equilibrium Solutions	272
9.9.2	Čerenkov Counting	272

<u>CONTENTS (continued)</u>	<u>PAGE NUMBER</u>
9.9.3            Liquid Scintillation Counting	273
9.9.4            Counting Methods and Daughter Removal by Zeolites	274
9.9.5            Thorium-232 and Uranium-238	274
9.10 $\gamma$ - and $\beta$ - Spectroscopy	274
9.10.1 $\gamma$ -Spectroscopy	274
9.10.2 $\beta$ -Spectroscopy	274
9.11            Zeolites and Acid Solutions	275
9.12            Conclusions of This Work	276
9.13            Suggestions For Further Work	277
 <u>APPENDICES</u>	
APPENDIX I	279
APPENDIX II	280
APPENDIX III	283
APPENDIX IV	284 - 288
APPENDIX V	289
 <u>REFERENCES</u>	 290 - 300

PHOTOGRAPHIC PLATES (Situated at the end of Chapter 7)

PLATE 1

PLATE 2

PLATE 3

## LIST OF FIGURES

<u>FIGURE NUMBER</u>	<u>FIGURE TITLE</u>	<u>PAGE NUMBER</u>
1	Production of the Plant Raffinate	4
2	Raffinate Composition	6
3	Uranium Fuel Rod/Pellet Production	8
4	Silica and Alumina Tetrahedra in Zeolites	23
5	Secondary Building Units	25
6	Typical Zeolite Polyhedra	26
7	Cation Sitings for Zeolite Y	27
8	<i>Clinoptilolite</i>	36
9	Erionite	38
10	Mordenite	39
11	Chabazite	41
12	Zeolite Y	42
13	Zeolite A	44
14A	Isotherm Types	47
14B	Langmuir Adsorption Isotherms	49
15	Thorium-232 Decay Series	56
16	Uranium-238 Decay Series	57
17	Decay Equilibria for Th-232 and Th-228	58
18	Uranium-235 Decay Series	60
19	Hydrolysis Polymerization of Thorium	66
20	Thorium Species in Nitric Acid	68
21	Morin : Structure	72
22	Thoron : Structure	75
23	The $\beta$ -Spectrum of Th-234	85
24	Generation of Secondary Electrons	87

LIST OF FIGURES (continued)

<u>FIGURE NUMBER</u>	<u>FIGURE TITLE</u>	<u>PAGE NUMBER</u>
25	The Fox's Triangle Arrangement	108
26	Column Arrangement	128
27	Stripped Raffinate Composition	140
28	Quenching Effect of $\text{Na}^+$	157
29	Quenching Effect of $\text{K}^+$	157
30	Quenching Effect of $\text{Al}^{3+}$	158
31	Half-Life Curve for Solvent Extracted Th-234	158
32	Th-234 Uptake Curves (natural zeolites)	165
33	Ten-Hour Uptake Curves (Th-232)	165
34	Ten-Hour Uptake Curves (Ac-228/Ra-228)	166
35	Ten-Hour Uptake Curves (Ac-228/Ra-228)	166
36	Ten-Hour Uptake Curves (Ac-228/Ra-228)	167
37	Ten-Hour Uptake Curves (Ac-228/Ra-228)	167
	<u>BREAKTHROUGH CURVES:</u>	
38	Eastgate, Th-232	177
39	Clinoptilolite, Th-232	177
40	Clinoptilolite/Th-234/acid	178
41	Z900/Th-234/acid	178
42	CaY/Ac-228,Ra-228/acid	179
43	Z900/Ac-228,Ra-228/acid	179
44	Z900/Th-232/acid	180
45	Clinoptilolite/Th-232/acid	180
46	Clinoptilolite/Ac-228,Ra-228/acid	181
47	Eastgate/Th-232 Elution	181
48	Eastgate/Ac-228,Ra-228	182
49	Eastgate/Total Activity	182

LIST OF FIGURES (continued)

<u>FIGURE NUMBER</u>	<u>FIGURE TITLE</u>	<u>PAGE NUMBER</u>
	<u>ISOTHERM CURVES</u>	
50	Clinoptilolite. K/Th (0.01N)	183
51	Clinoptilolite. K/Th (0.001N)	183
52	Z900. K/Th (0.01N)	184
53	NaY. Na/Th (0.01N)	184
54	Clinoptilolite. Na/Th (0.1N)	185
	<u>LANGMUIR PLOTS</u>	
55	Clinoptilolite. K/Th (0.01N)	185
56	Z900. K/Th (0.01N)	186
57	NaY. Na/Th (0.01N)	186
58	Clinoptilolite. K/total activity (0.1N)	187
59	Z900. K/(Ac-228/Ra-228) (0.01N)	187
60	Clinoptilolite. K/(Ac-228/Ra-228) (0.1N)	188
61	Clinoptilolite. Na/(Ac-228/Ra-228) (0.1N)	188
	<u>ISOTHERM CURVES</u>	
62	Clinoptilolite ( $\text{UO}_2^{2+}$ )	189
63	Z900 ( $\text{UO}_2^{2+}$ )	189
64	Zeolite Y ( $\text{UO}_2^{2+}$ )	190
	<u>LANGMUIR PLOT</u>	
65	Clinoptilolite. Na/total activity	190
66	KY. K/total activity	191
67	NaY. Na/total activity	191
68	Clinoptilolite ( $\text{UO}_2^{2+}$ )	192
69	Z900 ( $\text{UO}_2^{2+}$ )	192
70	Z900 K/total activity	193

LIST OF FIGURES (continued)

<u>FIGURE NUMBER</u>	<u>FIGURE TITLE</u>	<u>PAGE NUMBER</u>
	<u>X-RAY POWDER DIFFRACTOGRAMS</u>	
71	Eastgate	197
72	Th Eastgate	197
73	Clinoptilolite	198
74	Th Clinoptilolite	198
75	Overlay Comparison	199
76	Na Z900	200
77	Th Z900	200
78	NaY	201
79	Erionite	201
80	Mordenite	202
81	Ferrierite	202
	<u>ENERGY DISPERSIVE X-RAY SPECTRA</u>	
82	Clinoptilolite treated with thorium	203
83	Clinoptilolite treated with thorium	204
84	Eastgate treated with thorium (acid washed)	205
85	Z900 treated with thorium (acid washed)	206
86	CaY treated with thorium	207
87	Clinoptilolite (batch)	208
88	Clinoptilolite (scales expanded)	209
	<u>DIFFERENTIAL THERMAL GRAVIMETRY</u>	
89	Clinoptilolite	210
90	Th on Clinoptilolite	210
91	Th-Clinoptilolite (caked phase)	211
92	Th-Clinoptilolite (powdery phase)	211
93	Na-Clinoptilolite	212

LIST OF FIGURES (continued)

<u>FIGURE NUMBER</u>	<u>FIGURE TITLE</u>	<u>PAGE NUMBER</u>
94	K-Clinoptilolite	212
95	Eastgate	213
96	Th(OH) <sub>4</sub>	213
97	NaY	214
98	NaY treated with thorium	214
	<u>γ-SPECTRA</u>	
99	Extracted Th-232 solution	215
100	Extracted Th-232 Daughters	215
101	Acid-washed Eastgate (Column) Th-232 Daughters	216
102	Acid-Washed Clinoptilolite (Column) Th-232 Daughters	216
103	Acid-Washed Clinoptilolite (Column) Th-234	217
104	Isotherm Solution at Equilibrium Th-232/Na	218
105	Isotherm Solid at Equilibrium	218
106	Isotherm Control Solution Th-232/Na	219
107	Solvent Extracted Th-234	219
108	Process Raffinate (R1)	220
109	Clinoptilolite Equilibrated with R1	220
	<u>β-SPECTRA</u>	
110	H-3	221
111	C-14	221
112	Tl-204	222
113	Th-234	222



## LIST OF TABLES

<u>TABLE No.</u>	<u>TITLE</u>	<u>PAGE NUMBER</u>
1	Channel System Types	30
2	Zeolites Used in this Work	33
3	Zeolites Used in this Work	34
4	Unit Cell Compositions of Zeolites	34
5	Summarized Data for Thorium Isotopes	54
6	Radiation Energies of Thorium Isotopes	54
7	Uranium Isotope Data	61
8	Physical Properties of Thorium	65
9	Physical Data of Uranium	69
10	Colourimetry Data : Thorium	74
11	Interfering Substances	74
12	Colourimetry Data : Uranium	74
13	$\gamma$ -Ray Energies of Thorium and its Daughters	84
14	Summary of Analyses	88
15	Variations in Colourimetry Procedures	100
16	Quencher Species ( $K^+$ , $Na^+$ , $Al^{3+}$ ) Used in Cerenkov Counting	106
17	Volumes of Acid Quencher	107
18	Quencher Proportions for L.S.C.	111
19	List of Zeolites	115
20	List of Zeolites and Zeolitic Materials	115
21	List of Zeolites and Competing Cations	122
22	Simulated Raffinate Solution Composition	126
23	Column Experimental Conditions	131
24	Experimental Conditions for Thorium Isotherm Experiments	135

LIST OF TABLES (continued)

<u>TABLE No.</u>	<u>TITLE</u>	<u>PAGE NUMBER</u>
25	Experimental Conditions for Uranium Isotherm Experiments	137
26	Various Raffinate Solutions	141
27	List of X-Ray Powder Diffractograms	143
28	Samples taken for X-Ray Microanalysis	144
29	List of Samples taken for DTG Analysis	146
30	Samples Analysed for $\gamma$ -Peaks	147
31	Samples Analysed for $\beta$ -Spectra	149
32	Zeolite Wet Chemical Analysis	151
33	Exchange Capacities of Tested Zeolites	152
34	Leaching Effect of Water on Selected Zeolites	153
35	Leaching Effect on Zeolites Treated with Acid Solution	153
36	Leaching Effect on Zeolites Treated with Thorium Solutions	154
37	Leaching Effect on Zeolites Treated with Thorium Solutions (Milliequivalent ratios)	155
38	Analysis for $\text{Na}^+$ , $\text{K}^+$ Release and $\text{Th}^{4+}$ Uptake Concerning Zeolites Contacted with Thorium Solutions	156
39	Results of Natural Zeolite Screening	159
40	0.1N Thorium Nitrate Uptakes	160
41	Synthetic Zeolite Screening ( $K_d$ Values)	161
42	Total Activity Removal - Thorium	162
43	Results of Zeolite Screening (Ac-228/Ra-228)	163
44	Results of Synthetic Zeolite Trials (Ac-228/Ra-228)	164
45	Effects of Temperature and Concentration Changes on the Uptake of Th-232	168
46	Effects of Temperature and Concentration Changes on the Uptake of Thorium $\beta$ -emitter Daughters	169

LIST OF TABLES (continued)

<u>TABLE No.</u>	<u>TITLE</u>	<u>PAGE NUMBER</u>
47	Results of Natural Zeolite Uptakes of $\text{UO}_2^{2+}$ (U-238)	170
48	Results of Synthetic Zeolite Uptakes of $\text{UO}_2^{2+}$ (U-238)	170
49	Percentage Uptake of U-238 $\beta$ -Emitter Daughters on Zeolites	171
50	Maximum Percentage and Uptake of U-238 $\beta$ -Emitter Daughters on zeolites in the Presence of Nitric Acid	171
51	Competing Cation Effects on Ac-228/Ra-228 Uptakes	172
52	Effect of $\text{Na}^+$ on the Uptake of Ac-228/Ra-228	173
53	Effect of $\text{K}^+$ on the Uptake of Ac-228/Ra-228	173
54	Effect on the Uptake of Th-232 by Varying the Concentration of Competing Cations	174
55	Effect on the Uptake of Th-232 of $\text{Na}^+$ , $\text{K}^+$ , $\text{Ca}^{2+}$ , $\text{Mg}^{2+}$ and $\text{Al}^{3+}$ in the Presence of $\text{H}^+$	175
56	Th-232 Uptakes for Zeolites Contacted with SOSIM Solutions	176
57	Free Column Volume Determinations of Zeolites	176
58	Repeated Exchange Results	194
59	Isotherm Solid Analysis	195
60	Isotherm Total Uptakes	195
61	Fluoride Determinations in Raffinate	196
62	$\beta$ -Spectrometry	223
63	The d-spacings ( $\text{\AA}$ ) of $\text{ThO}_2$ , $\text{K}_2\text{ThO}_3$ and Peaks A, B and C	251

## CHAPTER 1

### INTRODUCTION

## 1. INTRODUCTION

### 1.1 NUCLEAR WASTE

In 1946 British Nuclear Fuels established a plant at Springfields, near Preston, to produce uranium fuels for nuclear reactors. Since this time over 30,000 tonnes of nuclear fuel have been processed at the plant including all the uranium metal and uranium oxide fuel for the United Kingdom's Magnox and Advanced Gas Cooled Reactors (AGR's). As many as five million fuel elements and pins have been manufactured (this, in energy terms, is equivalent to 650 million tonnes of coal). At the plant it is possible to produce fuel for all major types of reactors and the plant has the facilities to manufacture speciality fuels for research and prototype reactors. The manufacture of uranium fuels involves a series of chemical reactions to convert uranium ore concentrate to the finished product. As with all chemical plants, large or small, waste streams or waste gases are generated. Some of these wastes are harmless to the environment, others are not and these generally are covered by legislation. Certain wastes must be specifically treated to remove harmful substances before being discharged to the biosphere. Other wastes may not be discharged at all and require long-term storage : e.g. safe containment and storage to allow a radio-active isotope, perhaps, to decay to a safe level before exposure to the biosphere.

The health and safety policy at Springfields is to make sure that possible hazards to its workforce and the general public are kept to a minimum and in compliance with internationally recommended safety guidelines. Any radioactive discharges are authorised by the Ministry of Agriculture, Fisheries and Food and the Department of the Environment. Regular monitoring of the environment around Springfields is conducted and there are stringent safety precautions that are observed by the workforce, e.g. the hydrogen fluoride plant.

British Nuclear Fuels plc. (Springfields) began a programme of funding projects to explore different methods of heavy-metal-removal from a particular radioactive waste stream produced on site. Presently most activity is removed from this waste-stream by solvent extraction and it is within industrial interests to use a cheaper method. It is planned to use inorganic ion-exchangers for the purpose of removing radioactive heavy metals from this waste stream.

## 1.2 PRODUCTION OF THE PLANT WASTE STREAM (RAFFINATE)

The waste stream is produced at a British Nuclear Fuels site at Springfields. The uranium ore concentrate [UOC or yellow cake] is imported from various countries around the world e.g. Australia, Africa and North America. In these countries, the uranium ore contains approximately 0.15% uranium and therefore, large amounts of rock must be mined to produce small quantities of uranium. The impure uranium, which is removed from the rock

by using acid or alkali, is further purified and enriched before it reaches Springfield. At this stage, these uranium ore concentrates may contain about 75% uranium and each batch that arrives at the plant is analysed for uranium content and impurities.

To be used in fuel rod or oxide pellet manufacture, uranium must be in a highly pure form. The yellowcake is dissolved in nitric acid and insoluble impurities are removed on a rotary filter. The bright yellow solution of "crude" uranyl nitrate is then passed through a solvent extraction plant to remove as many of the soluble impurities as possible. It is during this process that the plant raffinate is produced (FIG. 1).

The crude uranyl nitrate is contacted with tert-butyl phosphate in odourless kerosene (20% TBP/OK) in a mixer-settler system. In this process uranium-containing ions will pass into the organic solvent attracted by the phosphate components of the solvent, leaving most of the impurities in the aqueous phase. The odourless kerosene is purely used as a diluent as tert-butyl phosphate is a viscous liquid and this viscosity renders it unsuitable for use in solvent extraction processes. The uranium is then back-extracted from the organic phase by the use of dilute nitric acid. At this point in the process, some of the water is boiled off leaving a reasonably pure solution of concentrated uranyl nitrate.

The original aqueous solution from the solvent-extraction process contains a variety of impurities of both radioactive and non radioactive nature in rather concentrated nitric acid. This

## Production of the Plant Raffinate.

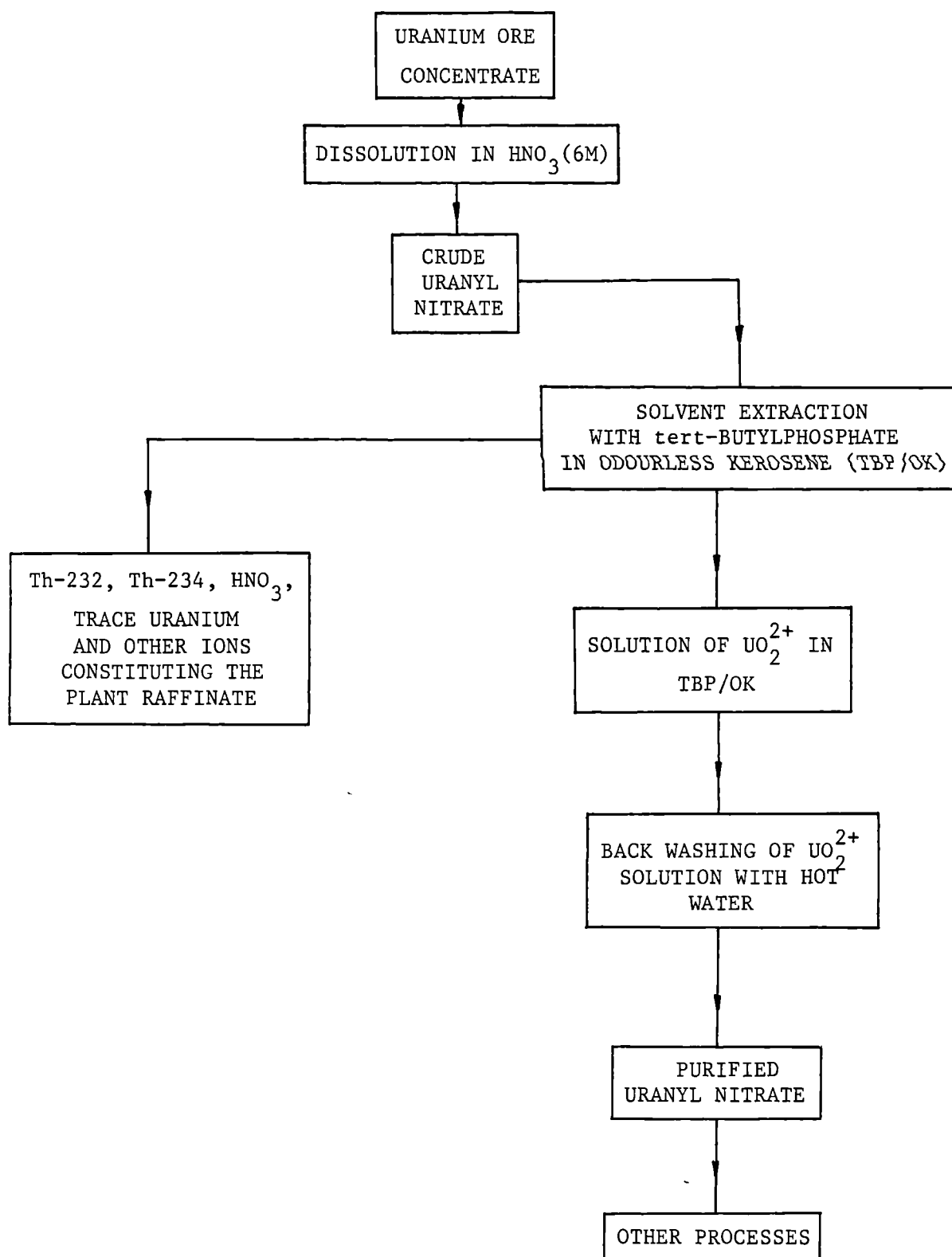


Fig. 1.



comprises the raffinate (FIG. 2) which is of variable composition depending on the original batch composition of the yellow cake.

### 1.3 URANIUM FUEL ROD/PELLET PRODUCTION

The concentrated uranyl nitrate must be converted to uranium tetrafluoride, by first reaction with air at elevated temperatures, then reduction processes by hydrogen and finally, reaction with hydrogen fluoride. The uranium tetrafluoride can be used in one of two ways :

a) it may be converted to uranium hexafluoride ( $UF_6$  or "HEX") by reaction with fluorine gas. The HEX gas produced is liquefied by cooling to about 90°C and passed into containers where it solidifies and is sent for enrichment by the "gas centrifuge method" to enrich the uranium -235 isotope of the HEX, which mostly contains uranium -238 (natural uranium). The enriched material returns to Springfields where it is treated with steam and hydrogen to directly convert it to uranium oxide powder. This powder is pressed into pellets and placed in stainless steel, or zirconium, cans which are then filled with helium and sealed. These are the uranium oxide "fuel pins" used in Advanced Gas-cooled Reactors and water moderated reactors.

b) it may be converted to the pure uranium metal to produce Magnox fuel rods by mixing with magnesium in an electric furnace. The uranium melt flows into a catchpot at the base of the reaction vessel followed by some magnesium fluoride slag. The slag floats and may be skimmed off during cooling, leaving a billet of uranium

## Raffinate Composition

COMPONENT	CONCENTRATION/mg l <sup>-1</sup>
Na <sup>+</sup>	2000 - 7000
K <sup>+</sup>	100 - 400
Mg <sup>2+</sup>	150 - 600
Ca <sup>2+</sup>	250 - 1000
Al <sup>3+</sup>	300 - 1200
Fe <sup>3+</sup>	250 - 1000
Cl <sup>-</sup>	50 - 100
PO <sub>4</sub> <sup>2-</sup>	5 - 50
COMPONENT	CONCENTRATION/g l <sup>-1</sup>
NO <sub>3</sub> <sup>-</sup>	20 - 80
SO <sub>4</sub> <sup>2-</sup>	2.5 - 7.5
F <sup>-</sup>	1 - 2
RADIOACTIVE COMPONENT	CONCENTRATION/mg l <sup>-1</sup>
Thorium	180 - 750
Uranium	5 - 50

Fig. 2 .

which is re-melted in a vacuum casting furnace and cast into rods. The cast rods are heat treated to produce a fine-grain crystal structure, straightened, machined and grooved to enable the Magnox cans to lock onto them. The cans are placed on the rods and helium gas inserted. The cans are capped producing Magnox fuel rods for use in Magnox reactors. (FIG.3)

#### 1.4 NECESSITY FOR THE REMOVAL OF THORIUM AND URANIUM FROM THE PLANT RAFFINATE

FIGURE 2 shows that the raffinate contains small quantities of thorium-232, thorium-234 and even smaller quantities of uranium-238, which have remained in the aqueous phase after solvent extraction. The daughter isotopes of these radioactive components must also be present in lesser concentrations, but nevertheless, contributing to the total activity of the waste stream.

Many heavy metals are toxic to biological systems.

Alpha-emitters may do serious damage if they are allowed to be incorporated into tissues. Luckily in many cases, heavy metals tend to pass straight through the natural processes of a biological system e.g. the human body, and may be excreted. However, the daughter isotopes of these emitters may cause damage. There is evidence to suggest that the daughters of thorium-232 and thorium-234 i.e. radium-228 and radium-226 respectively, cause osteosarcomas if ingested [REF.1]. This inevitably leads to leukaemia and other similar disorders. Ionizing radiation particles cause

## Uranium Fuel Rod/Pellet Production

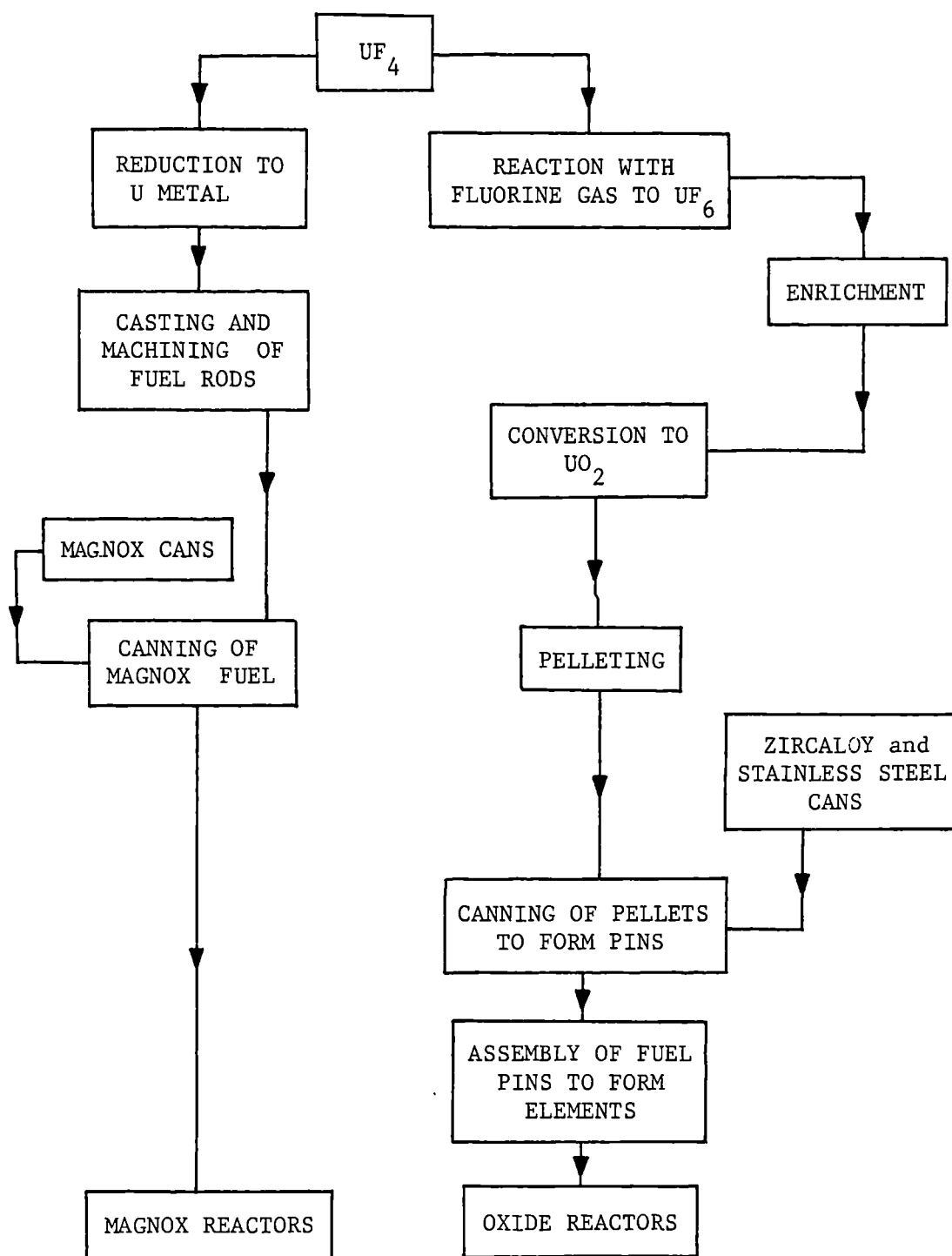


Fig. 3.

tissue damage if incorporated into the lung by inhalation. In addition to the radiation hazard it must be said that heavy metals such as uranium and thorium are toxic. Hence, removal of these heavy metals from industrial waste streams is necessary as they are toxic and naturally radioactive.

### 1.5 METHODS OF WASTE MANAGEMENT

The plant raffinate from the solvent extraction plant at Springfields is produced in volume and a method must be found to reduce this volume at the same time as removing the heavy metals. It would be advantageous to selectively remove these metals from the less harmful components of the waste-stream e.g. sodium, potassium and calcium. If any expensive removal system that was chosen was to allow the regeneration of the uranium and thorium then the method would become very cost-effective. If, however, the initial method chosen was cheap then it would be possible to store the thorium/uranium waste or encapsulate it in cement and dispose of it by deep burial. The choice of method is limited by several factors:

- a) The low pH of the raffinate.
- b) The requirement of selectivity for the removed species, hence the necessity of volume reduction.
- c) Cost.
- d) The nature of the radioactive species removed.

Radioactive waste may be classified into three groups:

- 1) High-level wastes consisting of materials from nuclear reactors. These activities are "man-made" and do not occur naturally, therefore they have high activities.

- 2) Intermediate-level wastes.
- 3) Low-level wastes. e.g. laboratory coats and gloves used in radiochemical laboratories.

High-level wastes may be stored in controlled surface sites whereby the waste is contained in cannisters, cooled by air or water to remove heat generated in the process of high-level radioactive decay, shielded by concrete and lead. A surveillance system must be able to detect rapidly any cannister failure and subsequent leak to enable prompt repair and thus, preventing harmful levels of activity reaching the biosphere. These wastes may be stored for a short period of time and reprocessed. They may need permanent storage. Deposition of the waste in stable, geological systems has been proposed as a possibility for permanent storage.

It is the intermediate to low-level waste category which concerns this project and many methods, old and modern, may be used to treat the waste.

- FIXATION of radio-ions by hydrothermal reactions with clays.  
FIXATION onto glass or cement matrices.
- ION-EXCHANGE.
- PRECIPITATION/ADSORPTION.
- SOLVENT EXTRACTION.
- ELECTROCHEMICAL METHODS.
- ULTRASOUND/ULTRAFILTRATION.
- BIOMASS.

## 1.6 METHODOLOGY OF MEDIUM-LOW LEVEL WASTE TREATMENT.

### 1.6.1 FIXATION

Radio-ions may be incorporated into glass or cement matrices after separation by other methods. The waste must be in a form compatible with cement or glass. In order to immobilise these radio-ions, work has been carried out on fixation of these ions into relatively insoluble alumino-silicate clay materials, which are allowed to react with aqueous caustic solutions of waste at temperatures 30-100°C. The reaction product from sodium and nitrate-containing wastes is a salt-filled, alumino-silicate in which radioactive ions are trapped [REF.2].

### 1.6.2 ULTRAFILTRATION

This is a technique where membranes with a capacity of less than 0.01  $\mu\text{m}$  are employed under cross-flow conditions. A waste stream containing solid, active particles may be decontaminated in this way and the cross-flow of effluent prevents fouling of the membrane. The process is dependent on feed composition and process conditions [REF.3].

### 1.6.3 ELECTROCHEMICAL METHODS

An electrode may be used in the form of an ion-exchanger to attract radioactive components depending on the applied electric potential. Elution of the attracted species is possible. The method can be used in conjunction with ultrafiltration membranes [REF.3].

#### 1.6.4 BIOMASS

Bacterial cultures have been found to absorb radioactive cations when fed a nutrient broth containing these cations. Problems are inevitable as the activity must be stored in suitable, non-biodegradable structures and mutation may result within the bacterial culture.

#### 1.6.5 ION-EXCHANGERS

A variety of ion-exchanger substances have been investigated including organic resins, zeolites, clays and other inorganic ion-exchangers.

Organic resins tend to break down from the radiation of the active ions accumulating within them. They are expensive and not as compatible with encapsulating media as inorganic ion-exchangers. Studies conducted for Springfields [REF. 5] using resins such as Dowex 50W, Duolite ES467 and Amberlite 200 showed that these resins will remove thorium-232 from 1.5M nitric acid solutions but difficulties were experienced in removing thorium from Duolite ES467 which had the best affinity for thorium. In most cases, regeneration of an organic resin will result in larger volumes of radioactive liquid waste being produced, thus causing more problems. At Springfields, it would be useful to regenerate the expensive resin and obtain reasonably pure uranium for commercial reasons.

Inorganic ion-exchangers in the radioactive waste treatment industry have been studied using substances such as



titanium phosphate, hydrous titanium oxide and zirconium phosphate to remove plutonium and other  $\alpha$ -emitters from wastes [REFS.6,17]. The ion-exchange properties of a wide variety of ion-hydrated oxides and substances such as mercarbide polymer have been studied in the removal of technecium and ruthenium anions from waste streams [REF.7]. Complex hexacyanoferrates have been studied as inorganic ion-exchangers [REF.8] but were found to have some sorption nature [REF.3]. Functionalised silicas are also being studied in the form of silica gels with covalently bonded groups. These have been used to remove ruthenium complexes from waste streams [REF.9]. This also, is strictly not an ion-exchange process but more akin to a co-ordination with the functionalised group so producing a monolayer of radioactive component on the surface of the silica. The radiation stability of these substances has been proved [REF.3] but the exchangers, especially silica gels, are expensive. Inorganic oxides have some drawbacks in that they are only useful over certain finite pH ranges.

Zeolites are three-dimensional alumino-silicates and differ structurally from two-dimensional clays. Zeolites have been used extensively as ion-exchangers in radioactive waste treatment [REFS.18,19,20,14]. Inorganic ion-exchangers and zeolites fulfil the criteria for use as waste treatment substances. These criteria are:

- Low leachability in water.
- Good chemical and physical stability towards heat and radiation.
- High mechanical strength/resistance to attrition.

- High thermal conductivity.
- Low volume and reasonably high capacity.
- Resistance to swelling or shrinkage on ion-exchange.
- Low cost.
- Regeneratability/compatibility with cement/glass.
- General chemical stability in acid or alkali conditions.

Much of the work done on zeolites has been conducted on the isotopes of caesium and strontium in alkaline pond waters. Original work on inorganic ion-exchangers was conducted in America and in Britain as early as the 1930's [REF.15]. By the 1960's zeolites such as clinoptilolite and zeolon 900 had been studied and were found to effectively remove caesium-137 and strontium-90 from spent fuel waste at the Idaho Chemical Processing Plant in the U.S.A. [REFS.2,10]. In 1963, a clinoptilolite ion-exchange column was commercially removing these isotopes from the waste stream just mentioned and reduced the radio-isotope components to drinking water levels. In more recent times, the Sixep plant at British Nuclear Fuels plc (Sellafield) utilizes clinoptilolite in the same way [REF.16].

Natural zeolite particle-size can be of any desired size but synthetically prepared zeolites may need to be treated to produce beads or may need to be modified with binders when used in fixed-bed column experiments. Inorganic ion-exchangers and clays tend to have very small particle sizes rendering them undesirable in fixed-bed columns due to the pressure drop created down the column. Most of the common types of zeolite are very

abundant and may be found in many parts of the world. They are cheap and similar versions may be produced synthetically and this leaves possibilities of preparing a zeolite that has been 'tailored' to specific requirements. A choice of zeolites with differing silica: alumina ratios is available. Hence, in acid pH solutions it would be preferable to use a zeolite with a high silica content to avoid significant structural breakdown [REF.21]. Many inorganic ion-exchangers, especially the oxide exchangers, may only be used over finite pH ranges. The disadvantage of using natural zeolites as opposed to the more expensive synthetic types is that natural zeolites contain impurities such as calcite, alumina, amorphous material and material from the rock depositions in which they are found [REF.21]. These impurities however may actually enhance any uptakes of radionuclides rather than deter them.

#### 1.6.6 PRECIPITATION and SOLVENT EXTRACTION

The methods of waste management so far discussed have been modern. The two oldest methods are precipitation and solvent extraction. Both methods are efficient but solvent extraction is very expensive on a large scale and also, can be dangerous, where flammable solvents are concerned. Radioactive ions such as  $\text{UO}_2^{2+}$  and  $\text{Th}^{4+}$  exist in acidic solutions and may be extracted out of strong acid solutions by solvents such as diethylether or tert-butyl phosphate in odourless kerosene. The two cations are strongly attracted to the oxygen-containing components of the solvents used. The process may be helped by addition of a 'salting-out' agent such as a high concentration

of sodium nitrate [REF.22]. Chemical precipitation and co-precipitation may be used to separate isotopes by the addition of a reagent which will cause certain ions to precipitate or by the use of subtle pH changes. The precipitate may then be filtered, washed and treated with another reagent to solubilize the isotope concerned. The precipitation of a selected species is governed by the solubility coefficient of the isotope-reagent system, the reagent used and/or the changes in pH necessary to precipitate the species. e.g. Thorium may be precipitated in the form of thorium hydroxide by adding sodium hydroxide. As soon as the pH rises above 3.8 the thorium hydroxide is formed as a gelatinous, white precipitate. In this way thorium may be separated from many impurities [REF.11]. Thorium precipitation techniques were initially used to separate thorium from impurities in its ore so to enable its analysis, after being freed from interfering substances [REF.12].

In a system as complex as the plant raffinate, precipitation becomes a difficult procedure, as iron and other metal hydroxides may co-precipitate with thorium and uranium. This would make subsequent separation necessary and is not particularly desirable.

Some inorganic ion-exchangers and zeolites with a high surface pH may be prone to surface precipitation of ions such as uranium and thorium [REF.13]. This effect will be discussed in more detail in subsequent chapters but it is sufficient to note here that it is important to know if ion-exchangers

are prone to surface precipitation or adsorption. If they do tend to precipitate radionuclides it must be considered that the ion-exchange process may not be total and may give rise to results that appear to be 'over-exchange', when considering the capacity of the exchanger.

#### 1.7 LIQUID WASTES AND AIMS OF THE PROJECT

All the waste management methods mentioned so far produce end products which are in the solid form. If a waste is in liquid form then it is voluminous, bulky and difficult to transport and handle. Liquid wastes pose problems where containment is necessary. Leakage from containers is always a possibility. The wastes themselves may be in the form of corrosive liquids. Heat generation from the decay of radioisotopes causes liquid expansion and pressure build-up in sealed containers. These factors cause structural-weakening of containers and give rise to concern about containment and storage of such wastes. Most of waste management is concerned with converting the radioactive components of a liquid waste into a volume-reduced, concentrated, isotope-filled solid for which containment and transport is relatively easy.

The aim of this project is to remove thorium and uranium from a liquid waste by using zeolites thus fulfilling the pre-requisites of Nuclear Waste Management to produce a smaller-volume, stable solid which is compatible with encapsulation substances and rendering the plant raffinate free from  $\alpha$ - and

$\beta$ -activity. The study was concentrated upon thorium-232 in its natural  $\alpha$ -activity form and several problems arose throughout the project and were overcome by techniques discussed in subsequent chapters.

## CHAPTER 2

### ZEOLITES

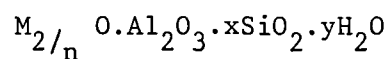
## 2. ZEOLITES

### 2.1 OCCURRENCE

Zeolites are one of the earths most common mineral types. There are several environments for zeolite geological deposition, these include:

Saline-alkaline lakes,  
 Open hydrological systems,  
 Saline-alkaline soils,  
 Sea-floor sediments,  
 Hydrothermal alteration of rocks in which zeolites may be found.

Zeolites may also occur by burial diagenesis of rock or may be found in volcanic tuffs. Substantial deposits of zeolites are to be found in the USA, Japan, Europe, Mexico, Cuba and on the beds of the oceans [REF. 4]. Zeolites may be defined as crystalline aluminosilicates with a tetrahedral framework surrounding interconnecting voids and channels, which contain mobile water molecules and cations. They have the empirical oxide formula:



where M represents one or more cations, n represents the cation valency, x and y represent the numbers of silica and water molecules respectively.

The total void volume of a zeolite may be as much as 50% of the total zeolite volume, e.g. chabazite. Zeolites are formed rapidly when considering relative geological timescales. They are formed over a period of a few thousands of years.



## 2.2 NATURAL AND SYNTHETIC ZEOLITES

The wide range of applications of zeolites led to studies of the preparation of synthetic zeolites. Natural zeolites are cheap but do contain impurities such as compounds, e.g. sodium chloride, calcite, and other occlusives such as quartz. These impurities may be expensive to remove and other impurities may exist as unaltered minerals, such as volcanic tuff, which did not undergo the slow chemical reaction when the zeolite itself was formed.

Natural zeolites are not pure in the chemical sense and two or more zeolites may be found together in deposits as intergrowths. Eastgate 2020, for example, is predominantly erionite found with mordenite. A zeolite like this may be difficult to classify as samples taken for analysis may vary from e.g. mordenite-rich to erionite-rich in the case of Eastgate, depending on the position of the deposit from which the sample was taken.

The advantage of preparing synthetic zeolites is that the presence of impurities may be regulated or omitted altogether, however, tonne for tonne, synthetic zeolites are more costly than their natural counterparts. Synthetic zeolites A, X and Y were prepared by workers at the Union Carbide Laboratories [REF. 31]. Zeolite Y has its natural counterpart in faujasite but A has no natural zeolite equivalent. Zeolites such as Y, with large cavities called "supercages" may be loaded with large rare earth cations [REF. 32] or platinum cations to aid catalysis [REF. 33].

The most common natural zeolites include analcime, clinoptilolite, heulandite and phillipsite. Other natural zeolites which are of potential commercial value include chabazite, erionite, mordenite and ferrierite.

### 2.3 USES OF ZEOLITES

Of the numerous uses of zeolites, the biggest use, per tonne, is as a detergent builder [REF. 23]. They are used as catalysts [REFS. 47,48] and as absorbents. Zeolites can be used as ion-exchangers, the mobile cations contained within the voids of the zeolite framework allow for exchange of these cations in external aqueous solutions to the zeolite [REF. 24]. Exchange may occur in aqueous or non-aqueous solutions.

Zeolites are used as drying agents and find such practical applications in organic solvent drying procedures. They are often used for their molecular sieving properties as many molecules can be separated, providing their sizes are suitably different. This property is dependent on the type and void size of the zeolite [REF. 25]. An application previously mentioned is in radioactive waste treatment, due to the ion-exchange properties of zeolites, but further applications in general waste-water treatment exist. Zeolites have been used in the farming industry to remove ammonia from confined spaces where animals are kept [REF. 26].

The composition of zeolites and their ion-exchange potential allows them to be loaded with fertilizing nutrients

enabling plants to utilize not only the loaded material but the nutrient minerals and elements provided by the zeolite itself, leaving only natural deposits [REF. 27]. Studies have been recently made on the uses of zeolites as slow drug-release systems [REFS. 28,29]. Here a drug such as dichlorovos (DDVP) which is an anthelmintic, may be loaded onto a zeolite and taken orally by a parasite-infested animal, such as a pig. The zeolite may then slowly release the anti-parasitic drug as it traverses through the digestive system of the animal, thus eradicating the parasite.

Other recent studies of the uses of zeolites include the utilization of zeolites as fillers in the paint industry [REF. 30]. These are just some of the uses of zeolites and it can be seen that their applications may lend themselves to many industries.

#### 2.4 ZEOLITES : DEFINITION AND STRUCTURE

Zeolites are aluminosilicates with a rigid, infinitely extending, open, three-dimensional structure. They may be classified into seven groups, in which their alumina/silica ratios are different. The sharing of the oxygen atoms at the corners of these alumina and silica tetrahedra enable the structure of a zeolite to extend in three-dimensions [FIG.4].

The net negative charge resulting from the  $(\text{SiO}_4)^{4-}$  and  $(\text{AlO}_4)^{5-}$  framework is balanced by positive charges from the mobile cations in the cavities and channels. These cations

## Silica and Alumina Tetrahedra in Zeolites.

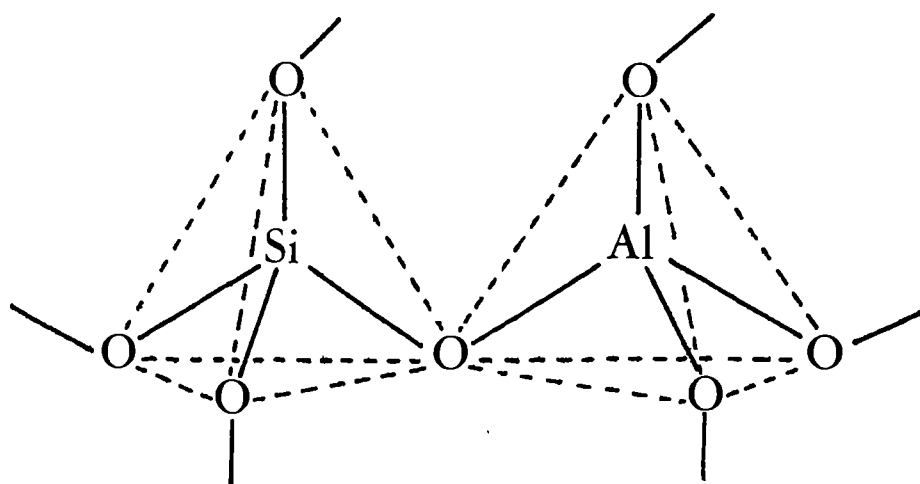


Fig.4.

are usually alkali or alkaline earths and are located at specific sites within a zeolite structure (FIG.7). The framework composition controls the framework charge and thus influences structural stability e.g. silica-rich zeolites such as mordenite are more stable than other zeolites in high temperatures and hostile environments. The internal void and channel volumes are determined by the framework topology and also by the presence of non-framework species such as water molecules, cations and other occlusives [REF. 34]. The internal voids consist of:

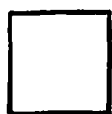
- 1) Channels (unidirectional or interconnected).
- 2) Cavity-like voids which are mutually interconnected through apertures which vary from 6-12 numbered rings of tetrahedra.

Zeolites are often discussed in terms of ideal structure and a zeolite structure may be broken down into 'secondary building units' (SBU's) which are repeatable throughout the zeolite framework. These units, proposed by W.M. Meier, are shown in FIGURE 5. The solid lines represent loci between tetrahedral centres i.e. aluminium or silicon. Oxygen atoms may be found near the centres of the lines but may not necessarily be positioned on them. Zeolite structures also contain polyhedral cages or voids described by R.M. Barrer [REF. 35]. Some more common polyhedra are shown in FIGURE 6. MEIER and BARRER have recently proposed and reviewed new approaches to zeolite framework classification [REFS. 36,37]. A zeolite structure is built up from these SBU's and gives rise to a characteristic system of interconnecting channels and voids. The entry of cations to these channels is restricted by the size of the channel aperture and is thus limited by the ring of comparatively large oxygen atoms from the silica and alumina tetrahedra. Water molecules may be contained within the cavities or channels of a zeolite or may be co-ordinated with the cations sited within these voids.

## 2.5 ZEOLITE STRUCTURE AND ION-EXCHANGE

Ion-exchange may occur in zeolites without significant changes to the zeolite structure. The rigidity of a zeolite structure plays a vital role here unlike clays, which do not possess a three-dimensional framework, and thus, may undergo shrinkage or swelling on cation-exchange. Cation exchange

## Secondary Building Units.



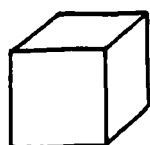
S4R



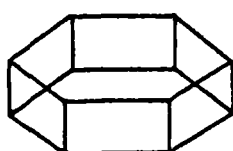
S6R



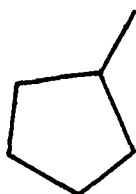
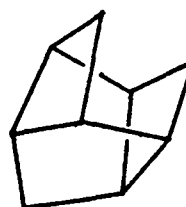
S8R



D4R



D6R

 $T_5O_{10}$  $T_8O_{16}$  $T_{10}O_{20}$ 

### Key

S: Single

D: Double

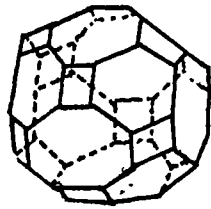
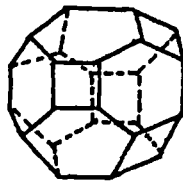
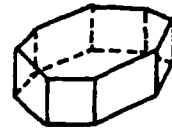
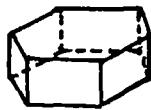
R: Ring

T: Tetrahedral centre

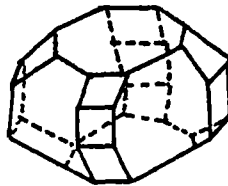
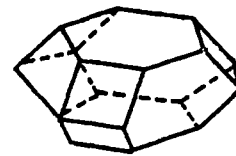
O: Oxygen

Fig. 5.

# Typical Zeolite Polyhedra.

 $\alpha$  $\beta$  $\delta$ 

D6R

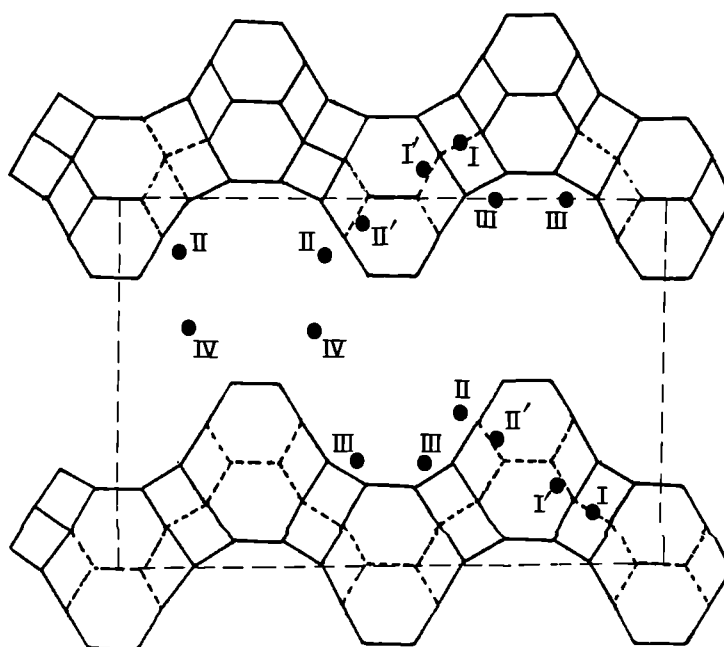
 $\gamma$  $\epsilon$ 

## Key

$\alpha$	26 - hedron
$\beta$	14 - hedron
$\gamma$	18 - hedron
$\epsilon$	11 - hedron
$\delta$	D8R, D6R

Fig. 6.

## Cation Sitings for Zeolite Y [Ref. 34]



- I      16-fold site in the centre of the D6R.
- I'     Site on the inside of the  $\beta$ -cage, next to the D6R.
- II'    Site on the inside of the sodalite cage near the S6R.
- II     Site which approaches the S6R outside of the  $\beta$ -cage  
lying within the large cavity opposite site II'.
- III    Positions in the wall of the large cavity (12-ring  
aperture).
- IV    12-ring sites.

Fig. 7.



selectivities in zeolites are not governed by the same principles as those for other inorganic ion-exchangers. The inherent zeolite structure is responsible for this and cation exchange may alter many physical and chemical properties of zeolites. For example, the stability of the zeolite may be affected along with its selectivity and adsorption qualities.

For ion-exchange to occur, a cation must diffuse into the zeolite structure and the outgoing cation must diffuse out via the zeolite apertures or "*n*-oxygen windows" (*n* is an integer). Thus the kinetic energy of the diffusing cation species with respect to the potential energy barrier of the aperture is important. The twisted-nature, size and shape of the channels can provide obstacles to ion-exchange and result in slower diffusion rates.

Cation-exchange is dependent on the size of the cation species (anhydrous and hydrated) and the cation charge. For exchange to occur the cation must be able to fit through an aperture and may need to shed its co-ordinated water molecules to do so. The cation may then co-ordinate with other water molecules once within a void or channel. The diameter of an aperture is based on the hard sphere model of atoms. Therefore, an oxygen atom from a silica tetrahedron would be considered as  $2.7\text{\AA}$  in diameter but in real terms the electron distribution falls off exponentially even beyond the  $1.35\text{\AA}$  ionic radius of the oxygen atom and so the hard-sphere model is idealized.

Other factors which govern ion-exchange are:

- 1) temperature, which causes thermal vibration changes in the atoms forming an aperture making the "effective" diameter of the aperture smaller.
- 2) the concentration of the cation species in solution.
- 3) the solvent.
- 4) the anion associated with the cation species in solution.

Cation exchange may fail to occur if the cation itself is too large in size to enter the smaller cavities and channels or if the charge distribution on the zeolite is unfavourable for the exchanging cation. The exchangeable cation of the zeolite also may be locked within a section of the structure due to anomalies or defects produced when the zeolite was made and are thus rendered non-exchangeable. Some cations within the zeolite structure may be held more strongly in certain parts of the framework structure.

The framework charge density of a zeolite decreases with increasing Si/Al ratio and is governed by the alumina content of a zeolite. Often, a zeolite containing larger amounts of aluminium will undergo ion-exchange more readily than a zeolite with a large amount of silica.

## 2.6 CHANNEL TYPES

The major types of channel systems are listed in Table 1 along with examples of zeolites displaying these systems [REF. 34].

TABLE 1                      MAJOR CHANNEL TYPES

SYSTEM	EXAMPLE
A 3-dimensional, non-intersecting system.	ANALCIME
A 2-dimensional, intersecting system.	CLINOPTILOLITE MORDENITE
A 3-dimensional, intersecting system containing equidimensional channels.	CHABAZITE ERIONITE A and X
A 3-dimensional, intersecting system with non-equidimensional channels.	OFFRETITE GMELINITE

2.7            HYDROXYL GROUPS

Surface hydroxyl groups exist at the edges of zeolite crystals where the framework structure has been broken. The quantities of these surface hydroxyl groups varies according to the crystal size and is directly proportional to the crystal size [REF. 38]. Solid potassium bromide/zeolite disc analysis, using Fourier transform infra red spectroscopy has shown that structural hydroxyl groups also exist [REF. 39,92]. During cation exchange in aqueous environments, cations may undergo hydrolysis which may give rise to <sup>apparent</sup> cation deficiency and replacement by hydroxyl groups or replacement by hydronium ions ( $H_3O^+$ ). Exchangeable cations in silica-rich zeolites

may be substituted by these hydroxyl groups when strong acid is used, which may also cause dealumination of the zeolite. There is less of a hydrolysis effect when most high-silica zeolites are used. The surface hydroxyl groups render the surface of a zeolite alkaline e.g. the surface pH of a zeolite such as clinoptilolite may be as high as 11.

## 2.8 CHARACTERIZATION OF ZEOLITES

The characterization of a zeolite involves the need to know information about the crystal structure, chemical composition and the physical and chemical properties exclusive to zeolites. X-Ray Powder Diffraction (XRD) techniques enable unit cell constants and crystallographic structure to be determined as well as elucidation of impurities.

Wet chemical analysis enables a complete elemental picture of the composition of a zeolite and enables the Si/Al ratio of the zeolite to be determined. Wet chemical analysis of zeolites will be discussed further in following experimental chapters. The classification of a zeolite may be confirmed by its ion-exchange and adsorption properties among other physical and chemical properties, such as stability and dehydration behaviour. Differential Thermal Gravimetry (DTG) is a useful tool as many zeolites give quite different DTG curves and is a quick and simple method to determine dehydration behaviour.

Crystal habit and crystal size may be obtained by the use of Scanning Electron Microscopy (SEM).

CD

## 2.9 ZEOLITES AND ZEOLITIC MATERIALS USED IN THIS WORK

In order to find zeolites which may be useful in the removal of thorium and uranium from aqueous solutions it was necessary to screen many zeolites and zeolitic materials. A wide variety of zeolites of different types were investigated, both synthetic and natural. The emphasis was placed on a zeolite which could remove thorium and its daughters from solution. A complete list of zeolites used in this work may be found in TABLES 2 and 3.

When considering the nature of the plant raffinate, containing the radioactivity, the zeolite structure must be able to withstand acid attack and to be reasonably selective for thorium. The  $\text{Th}^{4+}$  ion has an ionic radius of  $0.99\text{\AA}$  [REF. 51] and will exist as a hydrated ion in acid solution, so the zeolite aperture must be large enough to allow the ion to enter into the structure.

In the following, a few selected zeolites will be discussed in more detail and TABLE 4 shows the typical unit cell and Si/Al ratios for the zeolites discussed.

## 2.10 CLINOPTILOLITE

Clinoptilolite has a well defined framework structure with a high Si/Al ratio of between 4.25 and 5.25. Mudhills clinoptilolite has a Si/Al ratio of 5.36 and is thus compatible to that of mordenite. Clinoptilolite is well known as an ion-exchanger for  $\text{Cs}^+$  (and to a lesser extent for  $\text{Sr}^{2+}$ ) but the

A COMPLETE LIST OF ZEOLITES AND ZEOLITIC MATERIALS USED IN THIS WORK

TABLE 2

ZEOLITE (NATURAL)	AREA OF ORIGIN
ANALCIME	Wikieup, Arizona, USA.
BREWSTERITE	Whitesmith Mine, Strontian, Argyllshire, Scotland.
CHABAZITE 1	Christmas County, USA.
CHABAZITE 2	Beaver Divide, USA.
CHABAZITE 3	Bowie Divide, USA.
5050/F	Anaconda, USA.
CLINOPTILOLITE	Mudhills, California, USA.
1010/A	Anaconda, USA.
COWLESITE	Kingsburgh, Skye, Scotland.
EASTGATE 2020	Shoshone, USA.
ERIONITE 3030	Shoshone, USA.
FERRIERITE	Nevada, USA.
HEULANDITE	Iceland.
MORDENITE	Lovelock, Nevada, USA.
NATROLITE	County Antrim, N. Ireland.
PHILLIPSITE	Pine Valley, Nevada, USA.

Other zeolitic materials were tested for the removal of activity from radioactive solutions, these include ashy layers in lava flows, Brown tuff, Thannet Bed material (Pegwell Bay), zeolite in a palagonite tuff, Apatite and 5050 L etc..

TABLE 3

ZEOLITE (Synthetic)	MANUFACTURER
Na Y	Laporte Industries.
Zeolon 900	Norton, RD 569/85.
4A (powder)	Laporte.
K L	RD 737/86 Laporte.
5A (with binder)	RD 132 Laporte.
5A (powder)	Laporte.
13X	Laporte.

TABLE 4

TYPICAL UNIT CELL COMPOSITION AND Si/Al RATIOS FOR SELECTED ZEOLITES

ZEOLITE	UNIT CELL COMPOSITION	Si/Al RATIO
CLINOPTILOLITE	$\text{Na}_6[(\text{AlO}_2)_6(\text{SiO}_2)_{30}]\cdot 24\text{H}_2\text{O}$	4.25-5.25
ERIONITE	$(\text{Ca}, \text{Mg}, \text{K}_2, \text{Na}_2)_{4.5}[(\text{AlO}_2)_9(\text{SiO}_2)_{27}]\cdot 27\text{H}_2\text{O}$	3.0 -3.5
CHABAZITE	$\text{Ca}_2[(\text{AlO}_2)_4(\text{SiO}_2)_{16}]\cdot 24\text{H}_2\text{O}$	1.6 -3
MORDENITE	$\text{Na}_8[(\text{AlO}_2)_8(\text{SiO}_2)_{40}]\cdot 24\text{H}_2\text{O}$	4.17-5
Z900	$\text{Na}_{8.7}[(\text{AlO}_2)_{8.7}(\text{SiO}_2)_{39.3}]\cdot 24\text{H}_2\text{O}$	4.5 -5
Y	$\text{Na}_{56}[(\text{AlO}_2)_{56}(\text{SiO}_2)_{136}]\cdot 250\text{H}_2\text{O}$	4.8
A	$\text{Na}_{12}[(\text{AlO}_2)_{12}(\text{SiO}_2)_{12}]\cdot 27\text{H}_2\text{O}$	<1.5

exact sitings of these ions within the framework is not known, however A. DYER and A. ARAYA have proposed some ion sites [REF. 40]. There are five ion sites altogether, 3 in channels and at least one in a cavity.

The structure of clinoptilolite consists of sheet-like arrays of  $T_{10}O_{20}$  units of tetrahedra (where T represents a tetrahedral centre, silicon or aluminium, and O represents oxygen).

The plate-type structure is similar to the lamellar structure of heulandite [REF. 41,42]. The pore size of Mudhills clinoptilolite is  $4.0\text{\AA}$  and the pore volume accounts for 15% of the total volume. The solid density of the zeolite is  $1603\text{ Kg m}^{-3}$ . Due to its high Si/Al ratio the ability of clinoptilolite to stand up to acid attack is considerable compared with other zeolites such as A with a lower Si/Al ratio. E.G. Alkali stability is between pH 7 and 11, acid stability is in the pH range 1.5-7. In work done by D. Keir, clinoptilolite was found to resist acid attack when contacted with 8M nitric acid whereas chabazite was severely attacked by acid of greater concentration than 0.1N [REF. 21]. A typical clinoptilolite structure configuration may be seen in FIGURE 8. A study of the uptake of uranyl ions on clinoptilolite has been produced by N.R. ANDREEVA and N.B. CHERNYAVSKAYA [REF. 49].



## Clinoptilolite.

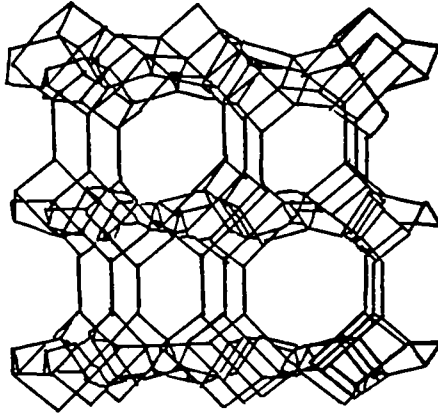


Fig. 8.

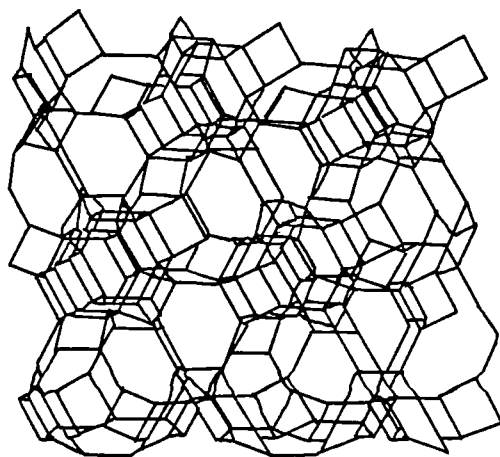
## 2.11 ERIONITE

Erionite [FIG.9] consists of double 6 rings (D6R) linked by single rings (S6R) and has 23-hedron and 11-hedron cages. Erionite has 3 channels and the main pore size (the free aperture of the main channel) is  $3.6 \times 5.2 \text{ \AA}$  and is thus elliptical in shape. The channels are tortuous and it is difficult for cation diffusion to occur because of this even though the large cages are present. Erionite is most commonly found with chabazite but surprisingly enough, is found with mordenite in the Eastgate sample used in this work. The crystals themselves are fibrous in nature and are considered to be carcinogenic to the lungs in the same way as fibrous asbestos [REF. 44]. Erionite is reasonably stable in acid being converted to the  $\text{H}^+$ -form of the zeolite, its metal cations being replaced by  $\text{H}^+$  or  $\text{H}_3\text{O}^+$ .

## 2.12 MORDENITE and ZEOLON 900 (Z900)

Mordenite consists of  $\text{T}_8\text{O}_{16}$  units and has two intersecting elliptical channels. These channels allow free movement of cations within them and have cavities available to cations next to them [FIGURE 10]. The channels have main free apertures of  $6.7 \times 7.0 \text{ \AA}$  and  $2.9 \times 5.7 \text{ \AA}$  and the cavities have a free diameter of  $3.9 \text{ \AA}$ .

The synthetic Z900 is a "wide port" version of mordenite [REF. 68] and has a more open structure allowing for the diffusion of larger molecules. Mordenite has the highest silica content of all natural zeolites [TABLE 4] and this allows

Erionite.Fig. 9.

Mordenite.

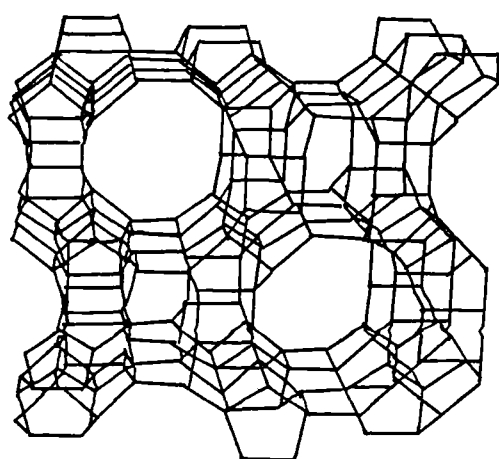


Fig. 10.

mordenite significant resistance to acid attack [REF. 21].

### 2.13 CHABAZITE

The structure of chabazite [FIGURE 11] consists of an array of double 6 ring units of tetrahedra. There are three channels which intersect at a large, ellipsoidal 20-hedron cage. The entry to the cage is governed by the  $3.7 \times 4.2 \text{ \AA}$  channel aperture. Ten cation sitings exist primarily in the 20-hedron cavity but there is a cation siting within the double 6 ring [Ref. 45].

The Si/Al ratio of chabazite is low and it is easily destroyed by acid attack. [REF. 21]. The adsorption and ion-exchange properties of chabazite vary greatly depending on the depositional origin of the zeolite as will be shown later.

### 2.14 ZEOLITE Y

Zeolite Y is a synthetic faujasite with 14-hedron cavities and 26-hedron "supercages". The structure consists of a double 6 ring array and there are three channels which have a large aperture of  $7.4 \text{ \AA}$  and a smaller aperture of  $2.2 \text{ \AA}$  [FIGURE 12]. The high silica version of Y used in this work (Si/Al = 4.8) was reasonably resistant to acid attack. The only detailed literature available pertaining to thorium uptake on zeolites has been by A.P. BOLTON and co-workers using zeolite Y [REF. 46]. Cation siting in zeolite Y may be seen in FIGURE 7.

# Chabazite.

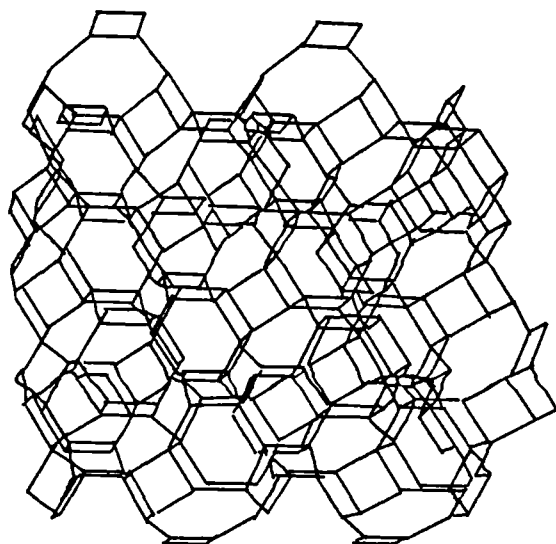
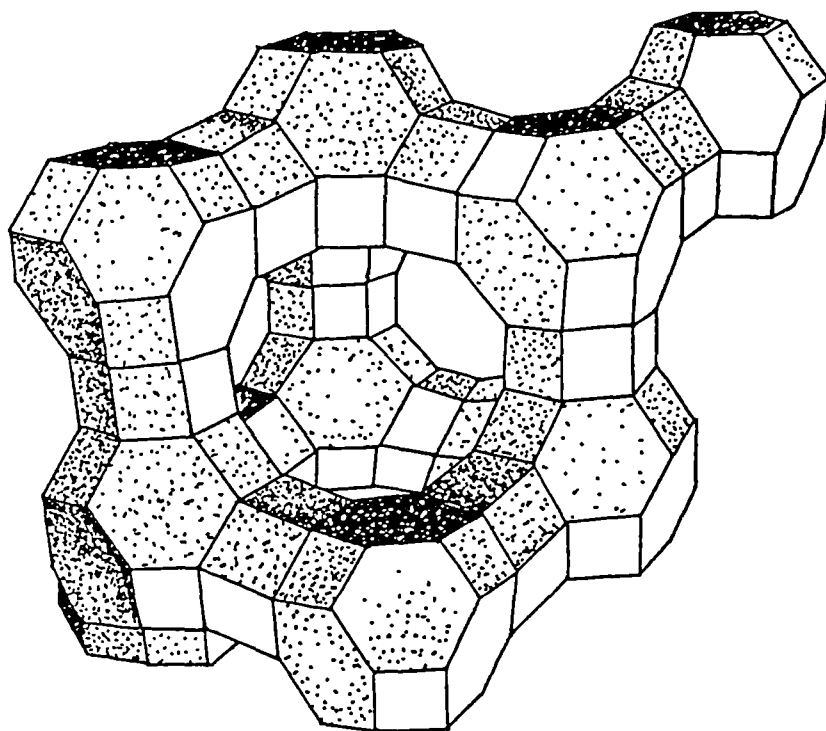


Fig. 11.

Zeolite Y.Fig. 12.

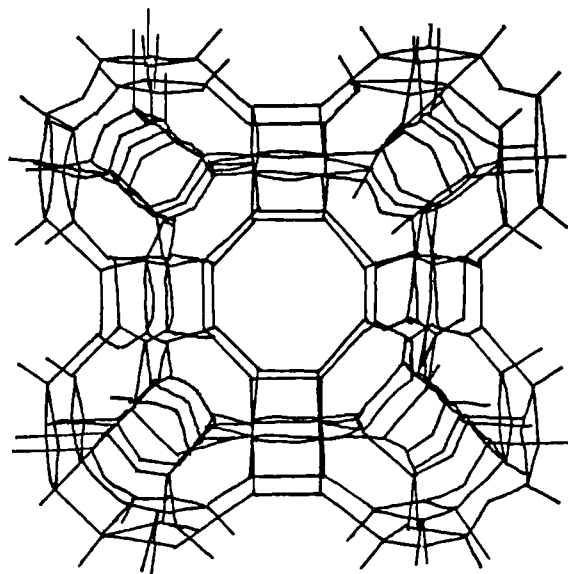
## 2.15 ZEOLITE A

In zeolite Y, the unit cell consists of truncated octahedra [FIG.6] joined by double six-membered rings, the unit cell of A is formed by truncated octahedra joined by double four-rings. The 3-dimensional channel system consists of large cavities with free-diameters of about  $11\text{\AA}$ , which are separated by eight-membered oxygen rings. The small apertures have free diameters of  $4.2\text{\AA}$ . The structure is shown in FIGURE 13. Cations are locked close to the apertures and changes in the cation type results in changes in the pore size. The low silica/alumina ratio (less than 1.5) of this zeolite renders it unstable in even weakly acidic solutions. It dissolves completely in 0.5M nitric acid and, depending on the volume of acid present, may form a gel.

## 2.16 EASTGATE 2020

Eastgate is not a single zeolite but is a mixture consisting of erionite, mordenite and some chabazite [REF. 43]. The zeolite used in this work appeared to be a mordenite-rich sample as shown by X-ray diffraction pattern analysis and wet chemical analysis. The sample itself will be discussed more fully in the discussion section of this work. The mineral is pale green in colour due to the presence of up to 5% iron(III)oxide. Eastgate may also contain reasonably large amounts of magnesium and calcium, unlike clinoptilolite which contains more potassium and sodium. Erionite is commonly found to contain large percentages of potassium but this is not the case with Eastgate 2020.



Zeolite A.Fig. 13.

## 2.17 OTHER ZEOLITES

The remaining zeolites and zeolitic materials mentioned in TABLES 2 and 3 will not be discussed here, but for convenience will be considered in the discussion chapters.

## 2.18 ION-EXCHANGE CAPACITY IN ZEOLITES

The base exchange capacity of a zeolite in solution depends on the hydrated zeolite composition i.e. the number of aluminium sites. The specific cation exchange capacity depends upon the exchange cation itself [REF. 34]. Capacity is usually expressed in units of milliequivalents per gram ( $\text{meq.g}^{-1}$ ) where milliequivalents of a cation = millimoles x valency of cation.

In this work, treatment of kinetics and equilibria has been conducted using the base exchange capacity of the zeolite, although some experiments were conducted to find the specific cation exchange capacity of selected zeolites. The measurement of ion-exchange capacity from aluminium content in natural zeolites may be found to be slightly larger than the real value, because often cations, in e.g. clinoptilolite, may not participate in easy exchange.

To measure the specific cation exchange capacity of a particular zeolite for a probe ion such as thorium would be difficult, as the mechanism of thorium uptake on different zeolites has not been quoted as ion-exchange in itself, [REF. 46], and may be due to adsorption or precipitation processes.

## 2.19 BASIC ION EXCHANGE THEORY

### 2.19.1 KINETICS

When considering molecules or ions (A) sorbing onto zeolites (Z)



at equilibrium, it can be said that the number of species entering the solid must be equal to those leaving the solid. This provides the basis for the measurement of distribution coefficients ( $K_d$ ) of ions in solid and solution (S)

$$K_d(A) = \frac{\text{No. of equivalents of A per gram of solid}}{\text{No. of equivalents of A remaining per cm}^3 \text{ solution}}$$

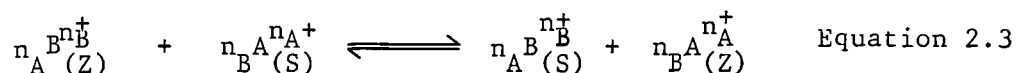
$$\text{i.e. } K_d(A) = \frac{[A]_Z \times \text{cm}^3 \text{ solution}}{[A]_S \times \text{g solid}} \quad \text{Equation 2.2}$$

The units of  $K_d$ 's are thus,  $\text{cm}^3 \text{g}^{-1}$ , but are usually omitted.

if a  $K_d$  value is high, then a good uptake of ion A is found.

### 2.19.2 ION EXCHANGE MECHANISM [REFS. 65,66,67,64]

When considering the following equation at equilibrium:



Where  $n_A$ ,  $n_B$  represent charges of the exchanging cations A and B and (Z), (S) represent the zeolite and solution phases respectively. If cation B, initially in the zeolite, is in contact with a solution containing cation A, providing conditions are favourable

and the zeolite has a preference for ion A, then exchange will occur, suggested by the previous equation.

An ion-exchange isotherm is a plot of  $A_S$  as a function of  $A_C$  where, with respect to the cation A,;

$$A_S = \frac{\text{milliequivalents of A in solution}}{\text{total of milliequivalents of A and B in solution}} \quad \text{Eqn. 2.4}$$

$$A_C = \frac{\text{milliequivalents of A in the crystal phase (zeolite)}}{\text{milliequivalents of Al}^{3+} \text{ in the zeolite}} \quad \text{Eqn. 2.5}$$

$$(A_C + B_C) = 1 \quad \text{Equation 2.6}$$

$$(A_S + B_S) = 1 \quad \text{Equation 2.7}$$

The isotherm must be constructed from data obtained at equilibrium and at constant temperature and pressure. The isotherm extends from a point of maximum A in solution to maximum B in solution. A series of variable proportions of A and B lie in between and isotherms fall into several groups as shown in FIGURE 14 A.

### Isotherm Types

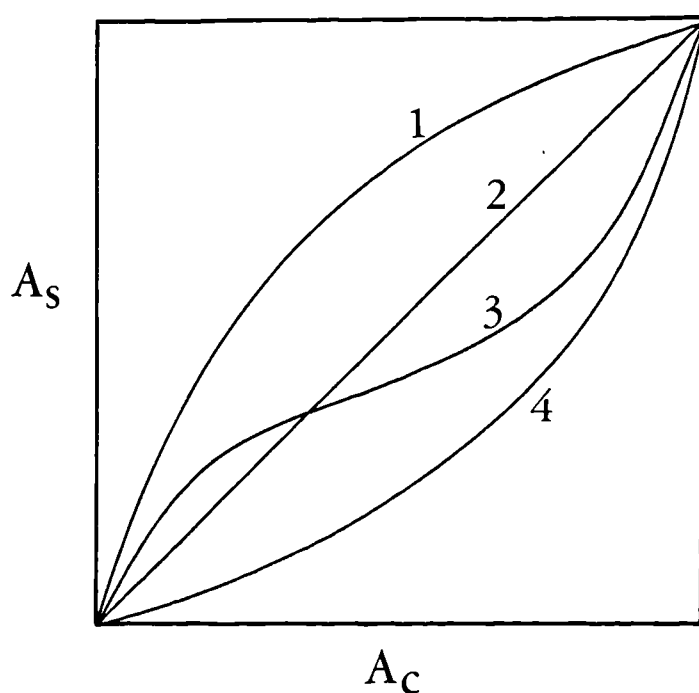


Fig. 14A.

Where the four curves shown represent:

- 1) The exchanger is not as selective for ions A over ions B.  
There must be a large concentration of A ions in solution.
- 2) The exchanger has no preference for either ion over the whole system.
- 3) There is a definite concentration dependence at which the exchanger will be selective for ion A.
- 4) The exchanger is selective for A ions.

The isotherm may be treated further to produce  $\Delta G$  values (Gibbs Free energy of the reaction) and diffusion constants. This treatment was not used for thorium for several reasons and only isotherm plots were obtained:

- 1) Activity coefficients of solution are not available for thorium.
- 2) In order to construct isotherms, there must be a closed system involving the ion A (e.g. thorium) and ion B (e.g. potassium) and the zeolite itself, in a homionic form e.g. (K-clinoptilolite)

As experimentation proceeded, it was found that what was taking place was not a simple ion-exchange. An ideal treatment of the equilibrium ion-exchange data was not possible and isotherm experiments were not considered further than the isotherm plot itself, which, in several cases had to be constructed in an additional way to that described earlier in this section. A fuller explanation of this is to be found in the discussion chapter involving isotherms.

## 2.20 LANGMUIR ADSORPTION ISOTHERMS

Zeolites may be considered to experience monolayer adsorption (corresponding to void-filling). Much work on the adsorption of gases onto zeolites has been carried out [REF. 94]. In this work, adsorption of species which are in solution are more relevant and adsorption is displayed by the following equation [REF. 93].

$$\frac{C_{eq}}{q_{eq}} = \frac{1}{Kq_{max}} + \frac{1}{q_{max}} C_{eq} \quad \text{Equation 2.8}$$

Where :  $C_{eq}$  represents equilibrium concentration of species in solution

$q_{eq}$  represents equilibrium concentration of species in solid

$K$  is a constant

$q_{max}$  is the maximum concentration in the solid.

If adsorption is occurring, a plot of  $C_{eq}/q_{eq}$  'vs'  $C_{eq}$  will be linear with slope  $1/q_{max}$  and intercept  $1/Kq_{max}$  as in FIGURE 14B.

### Langmuir Adsorption Isotherm.

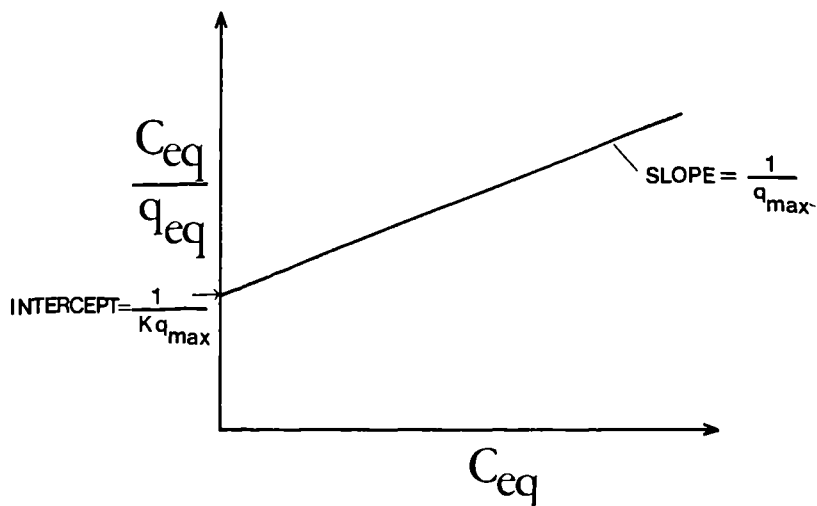


Fig. 14B.

CHAPTER 3

THORIUM AND URANIUM

### 3.1 THORIUM OCCURRENCE AND USES

The most stable isotope of thorium is  $^{232}\text{Th}$  which is an  $\alpha$ -emitter of very long half-life ( $t_{1/2} = 1.41 \times 10^{10}$  a). Thorium has no stable, non-radioactive counterpart. Even though thorium is a fairly abundant element, only a few hundred tonnes are extracted per annum. The earth's crust contains  $(1-2) \times 10^{-3}\%$  weight of thorium and thorium is about three times as abundant as uranium.

Thorium was first discovered in 1828 in a Norwegian mineral by Berzelius, but it was not used industrially until 1885 when Auer von Welsbach discovered that thoria became incandescent when heated. Von Welsbach developed the gas mantle and this was the largest single use of thorium upto 1973.

The principal source of most of the lanthanides and thorium and uranium is monazite, a mixed phosphate containing thorium, lanthanum, yttrium and uranium. The ore may be decomposed by concentrated sulphuric acid. Dilution, followed by careful adjustment of pH (by addition of a mixture of oxides) results in the selective precipitation of thoria ( $\text{ThO}_2$ ), this impure oxide is then dissolved in hydrochloric acid and the thorium extracted by tri-butylphosphate.

Thorium has recently been discovered in a new hydrous sodium thorium silicate named Thornasite, from Mont St. Hilaire, Quebec. Under ultraviolet radiation the mineral fluoresces a bright apple-green [REF. 52].



Thoranite contains up to 90%  $\text{ThO}_2$  and has been worked in Madagascar.

Thorite, a silicate material containing up to 62% thorium, is found in the Western USA and New Zealand. However, Monazite is more available and contains 1-10% thoria. On weathering of thorium-containing rocks, the heavy thorium-containing monazite sands are formed and are found in Australia, Brazil, India, South Africa, Sri-Lanka and the USA.

The world consumption of thorium in 1970 was estimated to be approximately 270 tonnes. From this, 50% was used as thorium nitrate in the preparation of gas mantles, 40% was used in the metallurgical industry, the remaining 10% was used for refractories, catalysts and in nuclear reactors [REF. 53].

More recently, the utilization of thorium in the nuclear industry is expected to increase. The estimated demands of thorium in the year 2000 by the U.S. Bureau of Mines are:

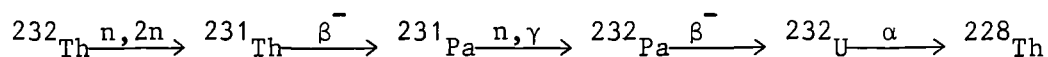
NON-NUCLEAR USES	50 - 520 tonnes.
NUCLEAR ENERGY	600 - 700 tonnes for thorium-burning nuclear reactor systems.

Due to the availability of the thorium, no supply problems are anticipated [REF. 53].

The potential for the utilization of thorium in nuclear reactors depends upon the fact that  $^{232}\text{Th}$  can absorb neutrons to produce fissile  $^{233}\text{U}$ , allowing it to be used as a fertile material in a nuclear breeder reactor. The method of using

thorium for nuclear power production is well documented [REF. 54].

Difficulties in the method arise from reprocessing the daughter products of the short-lived  $\alpha$ -emitter,  $^{228}\text{Th}$  formed from the chain:



### 3.2 URANIUM : OCCURRENCES AND USES

The oxide of the element uranium was discovered in 1789 in the pitchblende ores of Saxony by M.H. Klaproth. He named it after the planet Uranus which had been discovered a few years earlier in 1781. It was Berzelius who realised that the elemental uranium had yet to be isolated. E.M. Péligot, a French chemist, was the first to isolate the uranium metal in 1841. At this time, uranium was of little economic importance and was used only on a small scale, mainly for colouring glass and porcelain. Ores in which uranium was found were predominantly used for their thorium content until 1896, when Becquerel discovered radioactivity and the presence of radium was found to exist in uranium ores by the Curies (1898). When the demand for radium increased, the deposits of uranium ores in Saxony, the Belgian Congo and Canada were mined [REF. 55].

With the advent of the nuclear era, brought about by the discovery of nuclear fission (1938/39) and the outbreak of World War II, a fresh interest in uranium was aroused and has grown ever since. The 1940's Manhattan project in the USA produced much information on uranium chemistry, but it was only after the first "Conference on the Peaceful Uses of Atomic Energy" (1955)

that much of the information produced by the Manhattan Project became readily available. From 1942 onwards, uranium ores were mined specifically for their uranium content for use in nuclear reactors.

Uranium is widely distributed in the earth's crust and constitutes  $4 \times 10^{-4}\%$  of it, thus making the abundance of uranium more than that of gold, silver and mercury. Uranium generally occurs in high-silica, acidic rocks such as granites. Basalts (basic rocks) contain relatively little uranium. Sedimentary rocks rarely contain uranium but there are important exceptions such as in Monazite sands and carnotite-bearing sandstones of Colorado (50% uranium content). The oxidation of the silvery uranium metal often produces characteristically-coloured yellow ores. Uraninite is one of the most widely distributed uranium-containing minerals (45-85% Uranium) and is found as a dark rock. Pitchblende ( $\text{U}_3\text{O}_8$ ) usually contains traces of the rare earths and rarely contains any thorium.

Uranium ores may be found in France, Canada, South Africa, Colorado in the USA, Australia and the Belgian Congo. The extraction of uranium from its ore is a similar process to that used for thorium.

### 3.3 THE RADIOACTIVE DECAY OF THORIUM

Natural thorium, Th-232 is 100% abundant and exists along with Th-228. Relevant isotopes are found in TABLE 5 which shows their half-lives ( $t_{1/2}$ ), atomic number, atomic mass

TABLE 5SUMMARIZED DATA FOR THORIUM ISOTOPES

ISOTOPE	ATOMIC NUMBER	ATOMIC MASS	HALF- LIFE	DECAY MODES
Th-227	90	227	18.2 d	$\beta$
Th-228	90	228	1.91 a	$\alpha$ , $\gamma$
Th-229	90	229	7340 a	$\alpha$
Th-230	90	230	$8 \times 10^4$ a	$\alpha$
Th-231	90	231	25.52h	
Th-232	90	232	$1.4 \times 10^{10}$ a	$\alpha$
Th-234	90	234	24.1 d	$\beta^-$ , $\gamma$

TABLE 6RADIATION ENERGIES OF THORIUM ISOTOPES

ISOTOPE	ENERGY/keV	
	$\alpha$	$\beta$
Th-227	6040	-
Th-228	5430	-
Th-229	5050	-
Th-230	4680	-
Th-231	-	300
Th-232	4000	-
Th-234	-	190

and decay. The thorium decay series is found in FIGURE 15, and radiation energies found in this decay series can be seen in TABLE 6.

### 3.3.1 DECAY EQUILIBRIA

In the transmutation of the parent Th to the stable Pb, a total of ten other isotopes are produced [FIG. 15]. The thorium decay series differs considerably from the natural uranium decay series [FIG. 16] in that the half-lives of the thorium daughters are relatively short, the longest being  $^{228}\text{Ra}$  at 6.7 a.  $^{228}\text{Th}$  exists in equilibrium with  $^{232}\text{Th}$  in natural thorium nitrate, ( $t_{1/2}$  of  $^{228}\text{Th} = 1.9$  a). In the processing of thorium salts and ores, it must be noted that these decay products in the series fall into several columns of the periodic table and therefore behave in chemically different ways.

Due to the short half-lives concerned, the chemical problem is essentially one of handling two elements: thorium and radium. However, the short half-lives of some daughters also mean that after any separation into thorium and non-thorium fractions, the composition of the fractions changes rapidly.

The non-thorium fraction contains  $^{228}\text{Ra}$  which has, as one of its decay products, the strongly active  $^{228}\text{Th}$ . Even though this fraction may have less physical bulk than the thorium fraction, the percentage of  $^{228}\text{Th}$  in it may become relatively high. Additional thorium-228, produced by the decomposition of radium-228, must be accounted for in any counting procedures

## The Thorium Decay Series.

$A = 4n$  (Where  $n$  is an integer  
and  $A$  is mass number)

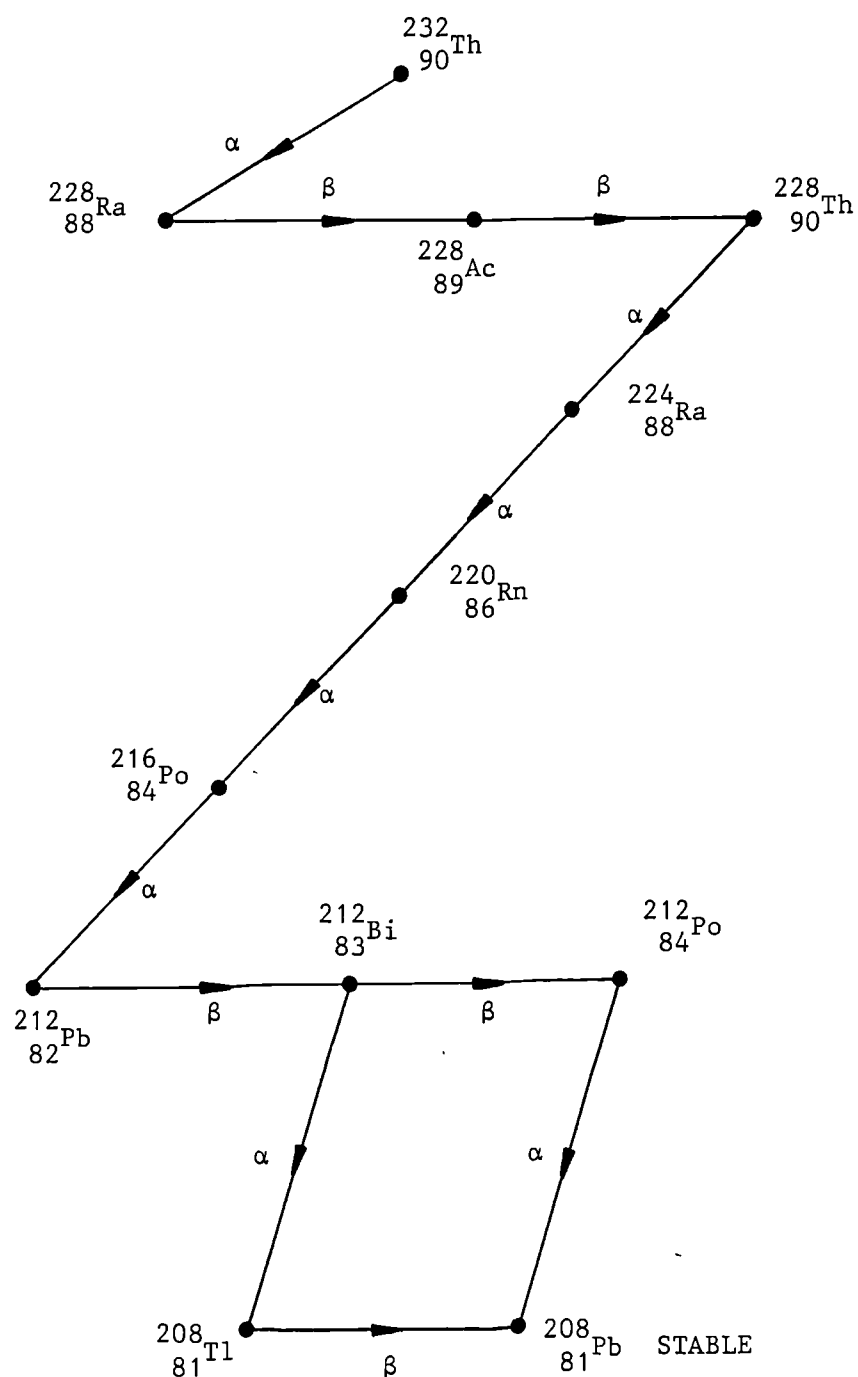


Fig. 15.

## Uranium - 238 Decay Series.

$A = 4n + 2$  (Where A is mass number  
and n is an integer)

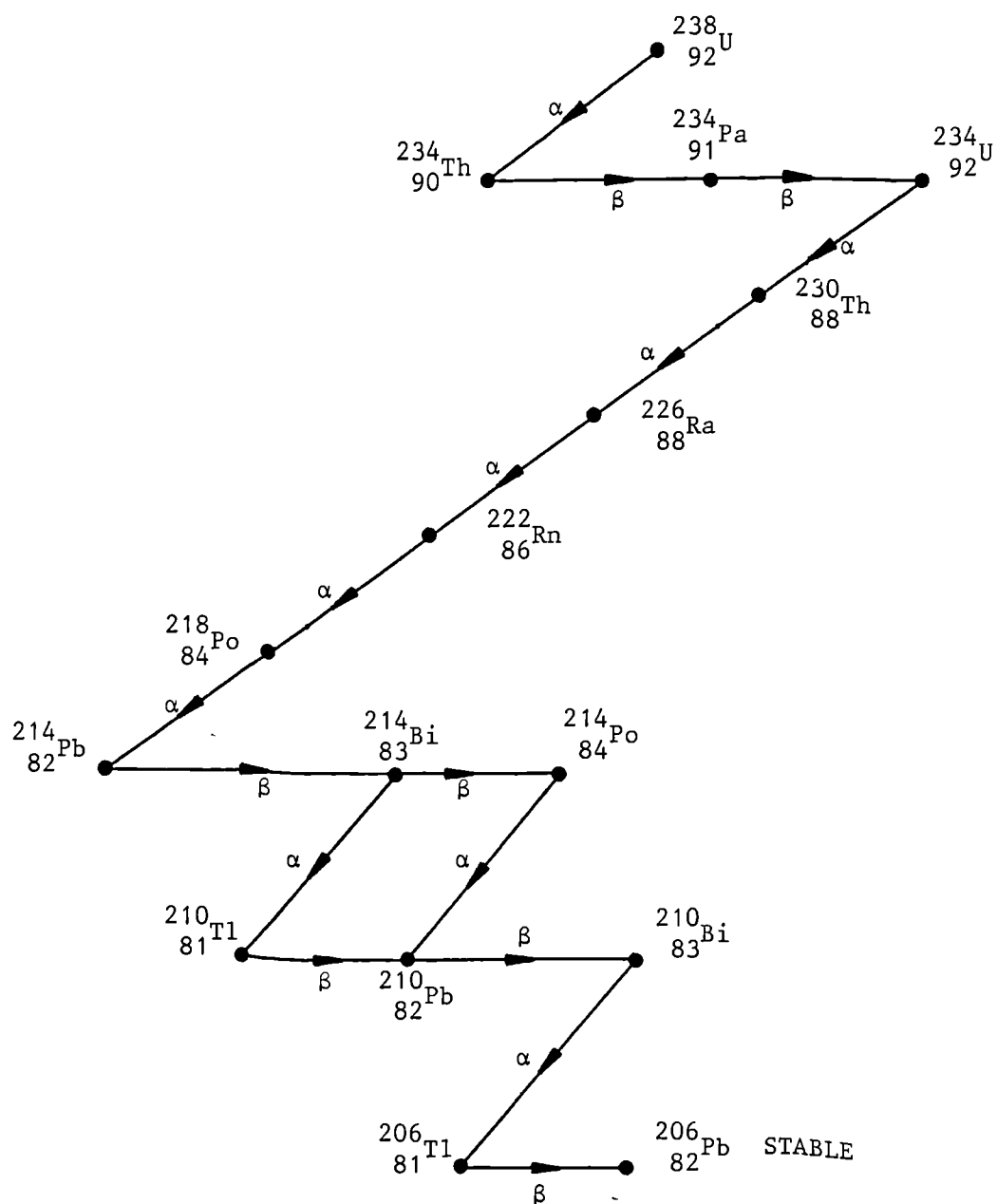


Fig. 16.

used even though the thorium-228 level gradually decreases as a result of its own decay into non-thorium products.

$^{224}\text{Ra}$  in the non-thorium fraction decays to  $^{220}\text{Rn}$ , a short-lived radioactive gas that may build up high levels of radioactivity in working areas.

When thorium is separated from other isotopes in the decay series [REF. 56] the thorium fraction has only a slight  $\alpha$ -activity, no  $\beta$ -radiation, and only a small amount of  $\gamma$ -radiation (from the 0.09 MeV  $\gamma$ -rays which emanate from  $^{228}\text{Th}$  decay). However, the activity from the  $^{228}\text{Th}$  side of the chain is quickly re-established and a first equilibrium state is achieved in about 36 days (10 half-lives of  $^{224}\text{Ra}$  which is the daughter product of  $^{228}\text{Ra}$ ). Activity then decreases as the  $^{228}\text{Th}$  decays faster than is replenished by the decaying  $^{228}\text{Ac}$ . About 3 years after separation the activity is lower than at any other time except at just after separation [FIG. 17].

## Decay Equilibria for Th-232 and Th-228

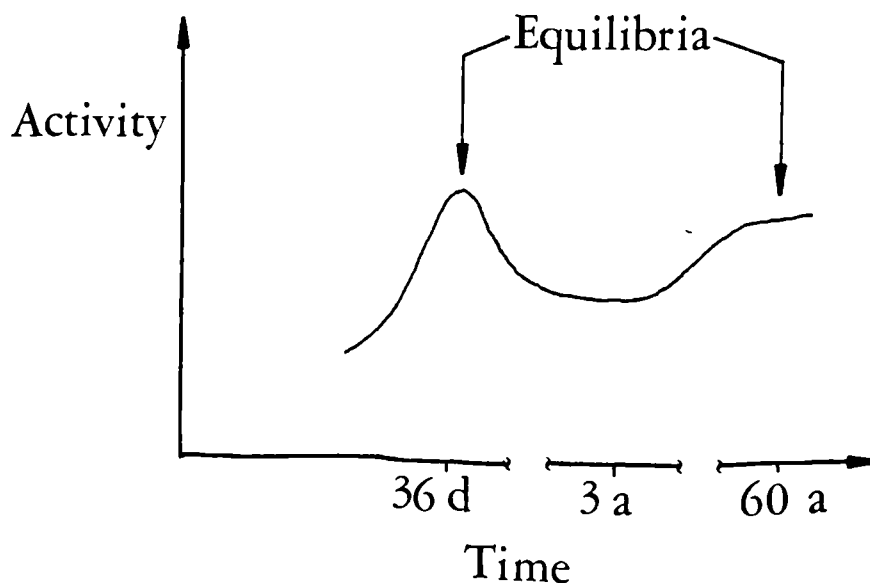


Fig. 17.



### 3.3.2 OTHER ISOTOPES OF THORIUM

Thorium-234 is produced as a daughter in the uranium-238 decay series [FIG. 16], it is a  $\beta$ -emitter of relatively short half-life (24.1 days). Thorium-230 also is produced in this decay series and is a long-lived  $\alpha$ -emitter ( $t_{1/2} = 8 \times 10^4$  a).  $^{234}\text{Th}$  may be separated from  $^{238}\text{U}$  by simple radio-chemical means. The uranium ore containing  $^{238}\text{U}$  is dissolved in medium concentrated nitric or hydrochloric acid. The  $\text{UO}_2(\text{NO}_3)_2$  or  $\text{UO}_2\text{Cl}_2$  produced is treated with tri-butylphosphate to remove the uranium by a solvent extraction process. A solution of  $^{234}\text{Th}$  and other isotopes and impurities from the ore is left and is discussed fully in Chapter 5.

A further two isotopes of thorium are produced by the decay of Uranium-235 which occurs at about 1% abundance of Uranium-238 [FIG. 18]. The two isotopes  $^{231}\text{Th}$  and  $^{227}\text{Th}$  both have relatively short half-lives ( $t_{1/2} = 25.52$  hours and 18.2 days respectively).

### 3.4 THE RADIOACTIVE DECAY OF URANIUM

The natural radioactive decay series of Uranium-238 is shown in FIGURE 16. The abundance of naturally occurring U-238 is 99.276%, U-235 is found at 0.72% abundance and a small contribution is made by U-234. Other physical data may be found in TABLE 7.

## Uranium-235 Decay Series.

$A = 4n + 3$  (Where A is atomic mass  
and n is an integer)

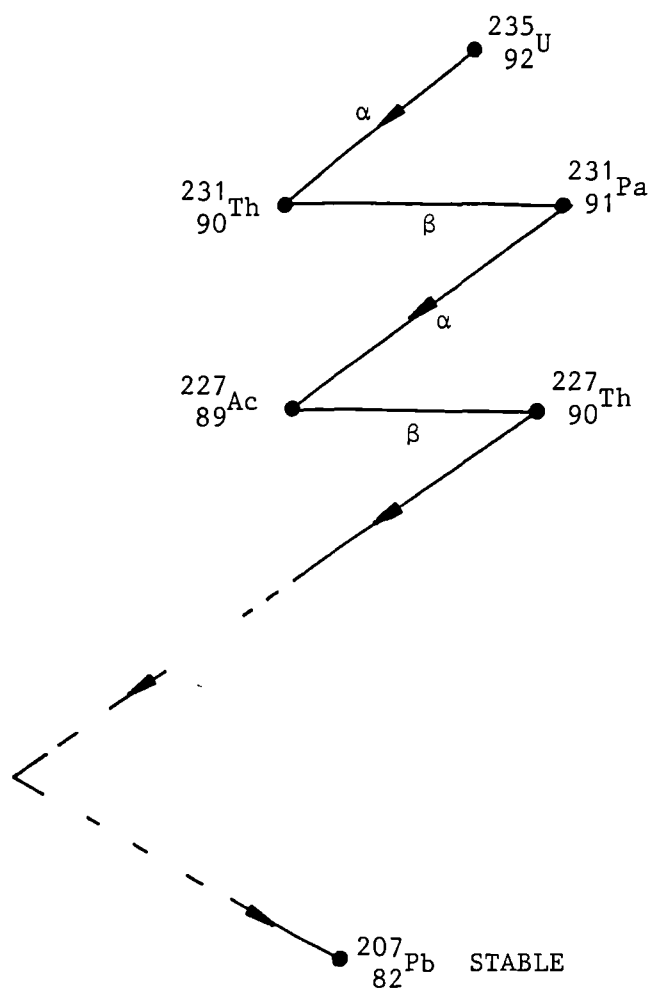


Fig. 18.

TABLE 7URANIUM ISOTOPE DATA

ISOTOPE	HALF-LIFE	DECAY
U-233	$1.6 \times 10^5 \text{ a}$	$\alpha$ , $\gamma$
U-234	$2.48 \times 10^5 \text{ a}$	$\alpha$ , $\gamma$
U-235	$7.13 \times 10^8 \text{ a}$	$\alpha$ , $\gamma$
U-236	$2.39 \times 10^7 \text{ a}$	$\alpha$ , $\gamma$
U-238	$4.51 \times 10^9 \text{ a}$	$\alpha$ , $\gamma$
U-239	23.5 minutes	$\beta$ , $\gamma$

### 3.4.1 EQUILIBRIUM

Considering U-238 that has been separated from its daughters (of which there are more than 10) the  $\alpha$ -activity from uranium is three times that of the thorium that has been isolated. After isolation of U-238 the equilibrium  $\beta$ -activity from  $^{234}\text{Th}$  and  $^{234}\text{Pa}$  is re-established in less than one year. At this stage of equilibrium there are 2  $\alpha$ - and 2  $\beta$ -particles emitted per U-238 disintegration. A stability which exists for thousands of years is set up and equilibrium with the remainder of the Uranium-series is not re-established until about 10 half-lives of  $^{230}\text{Th}$  have elapsed (approximately  $8 \times 10^5$  a).

### 3.4.2 OTHER ISOTOPES OF URANIUM

$^{233}\text{U}$  is produced by successive decays of  $^{241}\text{Pu}$  and is not dealt with in this work.

## 3.5 IMPORTANCE OF RADIOACTIVITY EQUILIBRIA TO THIS WORK

As seen in the previous sections, complex equilibria exist in salts of thorium nitrate ( $^{232}\text{Th}$ ) and uranyl nitrate ( $^{238}\text{U}$ ) which have been stored in laboratories. A problem arising in this work is what happens to the parents and daughters of these isotopes when contacted with a zeolite to remove a specific isotope from the decay chain. Counting results to quantify the species present must be interpreted carefully.

It is quite possible to separate  $^{232}\text{Th}$  and  $^{238}\text{U}$  from their daughters and the techniques used can be seen in the experimental section of this work. However, when using zeolites

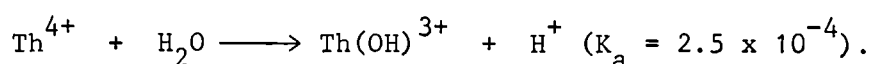
to remove radio-isotopes from an effluent stream, it is highly unlikely that the industry producing the effluent will be concerned as to whether daughter isotopes are present or not, as they inevitably will be. Detailed knowledge of exactly what a zeolite is taking up is useful and has been established in this work by not separating the parent isotopes, except in a few circumstances. There are few instances where zeolites would be required to remove a pure isotope from solution and this is certainly not the case in this project.

The use of a zeolite to remove activity from a solution will cause complex changes in the established equilibrium of the activity in the solution. This is an interesting problem and the complex equilibria of thorium and uranium have not been recorded in the literature pertaining to their removal from aqueous solution using zeolites.

### 3.6 THE GENERAL CHEMISTRY OF THORIUM

#### 3.6.1 AQUEOUS CHEMISTRY OF THORIUM

For the system  $\text{Th}^{4+}/\text{Th}$ ,  $E^0 = -1.9\text{V}$  and there is no evidence for any other oxidation state other than IV in aqueous media. Therefore, thorium forms only one series of salts in aqueous solution - those of the tetravalent thorium cation:  $\text{Th}^{4+}$ . This ion has very little tendency to hydrolyze at  $\text{pH} < 3$ .



The cation will combine with anions to form negative complexes with

an excess of such ions as  $\text{CO}_3^{2-}$ ,  $\text{C}_2\text{O}_4^{2-}$ ,  $\text{SO}_4^{2-}$  and  $\text{PO}_4^{3-}$  in acidic/neutral conditions. One or more positive complexes may be produced when added to  $\text{F}^-$  ions provided the mole ratio of  $\text{F}^-:\text{Th}^{4+}$  is less than 2.

Complexes also form with excess  $\text{SCN}^-$  and  $\text{NO}_3^-$  e.g. giving  $\text{Th}(\text{NO}_3)_4 \cdot x\text{H}_2\text{O}$  (where x is an integer).

Thorium has a strong tendency to form double salts like  $\text{K}_2\text{ThF}_6 \cdot 4\text{H}_2\text{O}$ ,  $\text{NaTh}_2(\text{PO}_4)_3$ . [REFS. 51,57,58].

Some of the more common compounds of thorium that are insoluble in acid solution and hence useful in separating thorium from other substances are the iodate, peroxide, oxalate, fluoride, phosphate, ferrocyanide and the double salt potassium thorium sulphate. The most characteristic trait of thorium is its extremely strong adsorption affinity. This is expected since it is adsorbed as the highly charged  $\text{Th}^{4+}$  ion with a radius of  $0.99\text{\AA}$  [TABLE 8] i.e. it has a high charge density and the ion is thus held by powerful electrostatic forces.

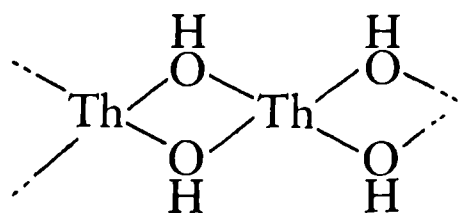
The structure of thorium complexes provides an illustration of the complexity of the crystal chemistry of the actinides e.g. the  $[\text{ThF}_8]^{4-}$  anion is dodecahedral in the  $(\text{NH}_4)_5\text{ThF}_9$  complex.

Above a pH of 3, aqueous solutions of thorium salts, as expected from the high formal charge on the cation, contain hydrolysis products e.g.  $\text{Th}(\text{OH})^{3+}$ ,  $\text{Th}(\text{OH})_2^{2+}$  etc. These polymeric-types may be seen in FIGURE 19.

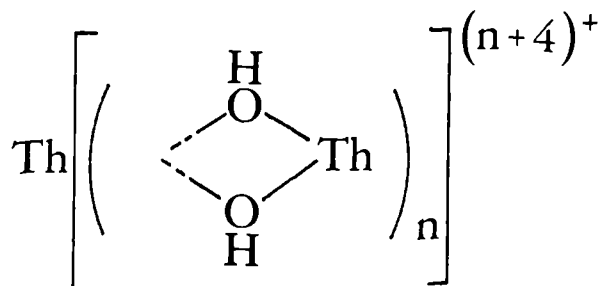
TABLE 8 PHYSICAL PROPERTIES OF THORIUM [REF. 51]

ATOMIC NUMBER	ELECTRONIC CONFIGURATION			IONIC RADIUS/Å		COVALENT RADIUS/Å
	Th <sup>0</sup>	Th <sup>3+</sup>	Th <sup>4+</sup>	Th <sup>3+</sup>	Th <sup>4+</sup>	
90	[Rn]6d <sup>1</sup> 7s <sup>2</sup>	[Rn]5f <sup>1</sup>	[Rn]5f <sup>0</sup>	1.00	0.99	1.65

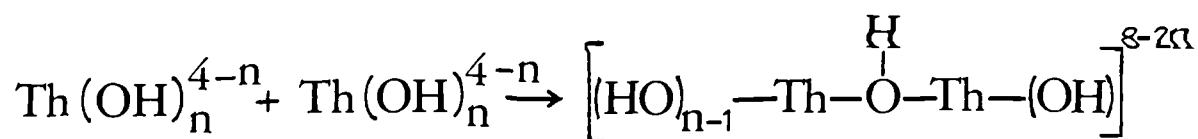
## Hydrolysis Polymerization of Thorium



Polymerization



Cross - Linkage



(where n is an integer)

Fig. 19.

### 3.6.2 THE CHEMISTRY OF THORIUM IN NITRIC ACID

It is generally accepted that in acid solutions, below a pH of 3.8, the thorium species is the  $\text{Th}^{4+}$  cation. KUMAR and TUCK have produced an extensive study of thorium nitrate and its complexes in aqueous and non-aqueous media and the paper includes details of infra red bands and Raman studies [REFS. 59,61]. The known thorium complexes are expected to exhibit high co-ordination numbers as do ruthenium nitrosyl complexes in nitric acid solutions [REF. 60].



Experiments have been conducted in the following acid systems:

- 1)  $\text{Th}^{4+} - \text{H}_2\text{SO}_4$  (0.05, 1.0, 3.0, 6.0M)
- 2)  $\text{Th}^{4+} - \text{HNO}_3$  (0.05, 1.0, 1.5, 2.0, 4.0 and 6.0M)
- 3)  $\text{Th}^{4+} - \text{HF}$  [REF. 62].

The complexes so formed are typical and the cationic species decrease with increasing acid concentration. In the case of system 2) it can be shown that there is greater than 50% conversion to the anionic species  $\text{Th}(\text{NO}_3)_5^-$  and  $\text{Th}(\text{NO}_3)_6^{2-}$  in 6M nitric acid. Total conversion to anionic species at this concentration of acid does not occur due to the weak nature of nitrate complexes. The free  $\text{Th}^{4+}$  ion concentration, which is high at lower acid concentrations decreases rapidly at 6M nitric acid. This can conveniently be seen in FIGURE 20. These facts also apply to system 1) but thorium chemistry in nitric acid differs from the other two systems in that there is little complexing between  $\text{H}^+$  and  $\text{Th}^{4+}$  and hence, little hydrolysis of thorium.

### 3.7 THE GENERAL CHEMISTRY OF URANIUM

#### 3.7.1 GENERAL

Uranium is the third member of the actinide series. Some physical data for uranium and its ions are found in TABLE 9. The metal must be used in the highly purified form when used in nuclear reactors. The metal itself is reactive and combines

# Thorium Species in Nitric Acid (0.5–6 M). [REF.62.]

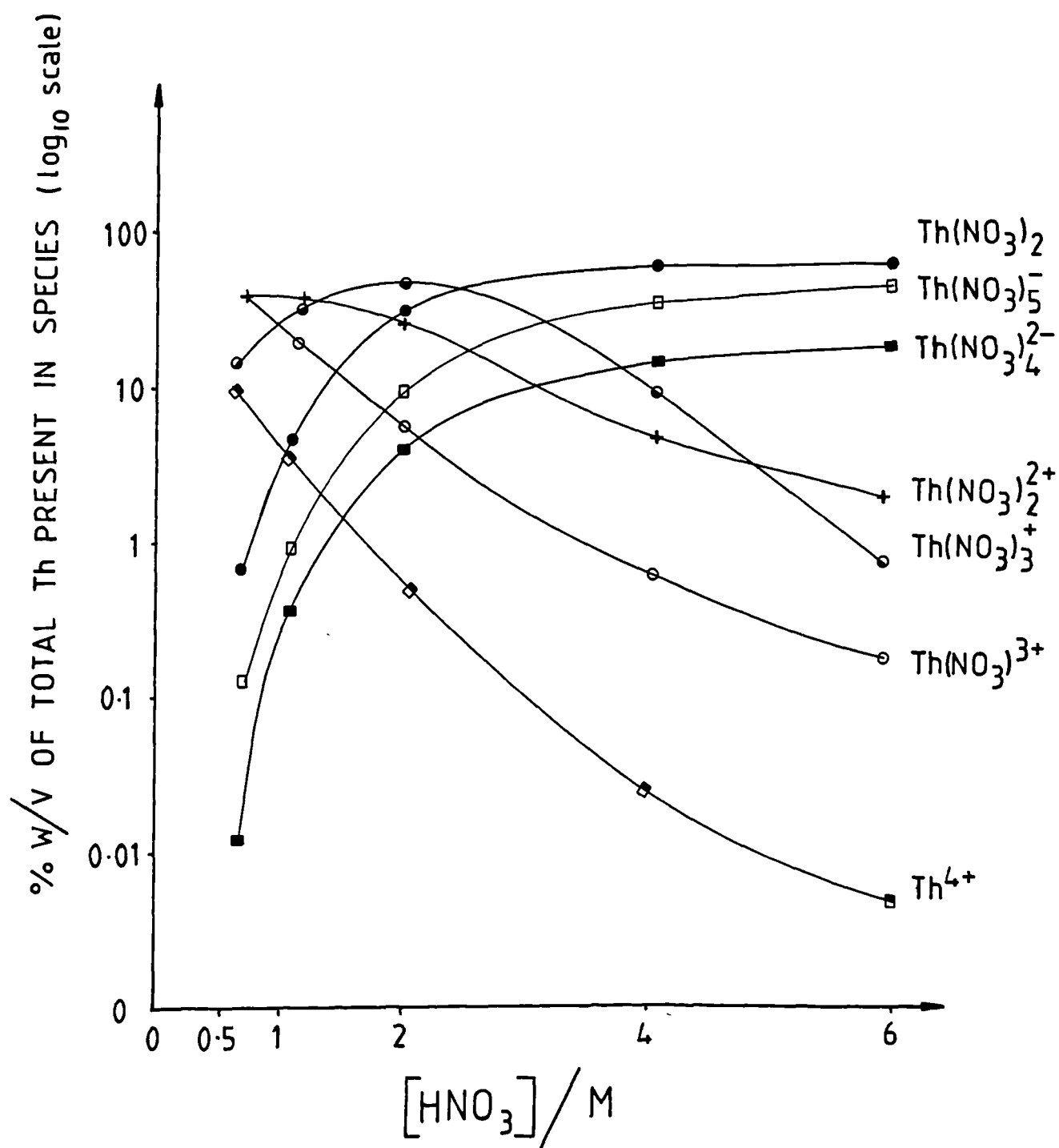


FIGURE 20.

directly with most elements. Reaction with boiling water produces  $\text{UO}_2$  and hydrogen which reduces the metal to the metal hydride. Many uranium compounds can be synthesized from uranium hydride.

TABLE 9

SOME PHYSICAL DATA USED FOR URANIUM.     $A = 92.$

	$\text{U}^{3+}$	$\text{U}^{4+}$	
Electronic Configuration	$[\text{Rn}]5f^3$	$[\text{Rn}]5f^2$	
Ionic Radius/ $\text{\AA}$	1.03	0.93	
Covalent Radius/ $\text{\AA}$	—	—	1.42

One of the most complex oxide systems known to chemistry exists for uranium due mainly to the fact that the uranium exhibits several oxidation states of similar stability. The main oxides are:

$\text{UO}_2$  (brownish-black)

$\text{U}_3\text{O}_8$  (greenish-black)

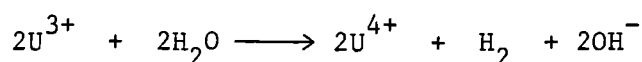
$\text{UO}_3$  (orange-yellow)

All the oxides of uranium dissolve in nitric acid to give  $\text{UO}_2^{2+}$  salts.

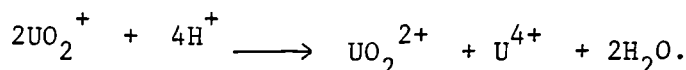
### 3.7.2 AQUEOUS CHEMISTRY OF URANIUM

The oxidation states of uranium give rise to  $\text{U}^{3+}$  (rose-purple),  $\text{U}^{4+}$  (deep-green) and  $\text{UO}_2^{2+}$  (bright yellow in solution) and  $\text{UO}_2^+$ . The properties of  $\text{U}^{3+}$  and  $\text{UO}_2^+$  are not fully known as the reducing property of  $\text{U}^{3+}$  is so strong that the

reaction in aqueous solution is:



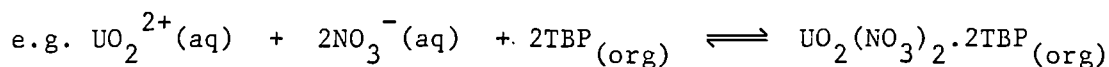
and studies are unable to be made. The pentavalent  $\text{UO}_2^+$  ion disproportionates into  $\text{U}^{4+}$  and  $\text{UO}_2^{2+}$  ions:



$\text{UO}_2^{2+}$  ions exist in solutions and solids e.g. uranyl nitrate.

The Uranyl ion ( $\text{UO}_2^{2+}$ ) is linear [REF. 63].

Uranyl nitrate in solution is bright yellow due to the presence of the  $\text{UO}_2^{2+}$  species. Uranium ore concentrate, or the trioxide, may be dissolved in nitric acid, the reaction is exothermic and produces uranyl nitrate and impurities brought into solution from the ore. The uranium content of the solution may then be solvent extracted by tert-butyl phosphate (TBP) in odourless kerosene. Co-ordination of the oxygen atom of the phosphate ligand of the solvent is favoured with uranium and the more polar the group that the oxygen atom belongs to, the more stable the co-ordination compound produced [REF. 55].



The neutral complex formed is anhydrous and is only soluble in the organic phase. The concentration of the TBP is usually between 25 and 40% in the diluent kerosene. The uranyl nitrate species is distributed in both the aqueous and organic phases in solvent extraction and the distribution coefficient,  $D$ , is influenced by the presence of nitric acid and  $\text{NO}_3^-$  ions:

$$D = \frac{[\text{UO}_2(\text{NO}_3)_2]_{\text{ORG}}}{[\text{UO}_2(\text{NO}_3)_2]_{\text{AQ}}}$$

It has been established that as the nitric acid (or nitrate) content of the aqueous phase is increased the distribution coefficient increases e.g. for a 30% volume TBP solvent extraction of uranyl nitrate, the distribution coefficient increases ten-fold for an increase in nitric acid normality from 1N to 3N at room temperature.

The uranium may be recovered from the organic solvent by back-extraction into very dilute acid or hot water (approximately 60°C) in order to depress the uranium distribution coefficient.

The original aqueous phase in the initial solvent extraction will contain impurities from the uranium ore and Th-234, a daughter product of the U-238, among other daughters in equilibrium with the uranium.

The hydrolysis of the uranyl ion has been extensively studied and polymeric ions have been suggested [REFS. 69,70].

These include  $\text{U}_2\text{O}_5^{2+}$ ,  $\text{U}_3\text{O}_8^{2+}$  in acid solution,

$\text{UO}_2(\text{OH})^+$  in dilute solution,

and later hydrolysis products such as  $(\text{UO}_2)_3(\text{OH})_4^{2+}$  but there is some argument as to the exact nature of these species.

It can be seen in section 3.6.2 that thorium also produces hydrous polymers in dilute acidic media. TOTH et al. have studied the behaviour of uranyl ion attachment to thorium(IV) hydrous polymers in dilute nitric acid solutions [REF. 71], and evidence is shown for dimers of hydrous uranyl ions by Raman spectroscopy.

CHAPTER 4

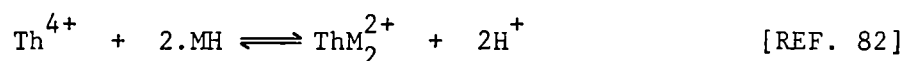
EXPERIMENTAL

METHODS

#### 4.1 QUANTITATIVE METHODS FOR THE DETERMINATION OF THORIUM AND URANIUM

##### 4.1.1 COLOURIMETRY : THORIUM

Spectrophotometric studies of thorium were initiated by chemists [REF. 83] and geologists to assay thorium ores. Two colourimetric reagents are widely used and these are Morin and Thoron [REFS. 72,73,51]. The specific details of these two reagents may be found in TABLE 10. Morin (5,7,2',4'-hydroxy-flavanone) has the structure shown in FIGURE 21(a) and forms the complex shown in FIGURE 21(b) [REF. 72]. The reaction may be conveniently shown by the equation:



Where M represents Morin.

#### Morin : Structure

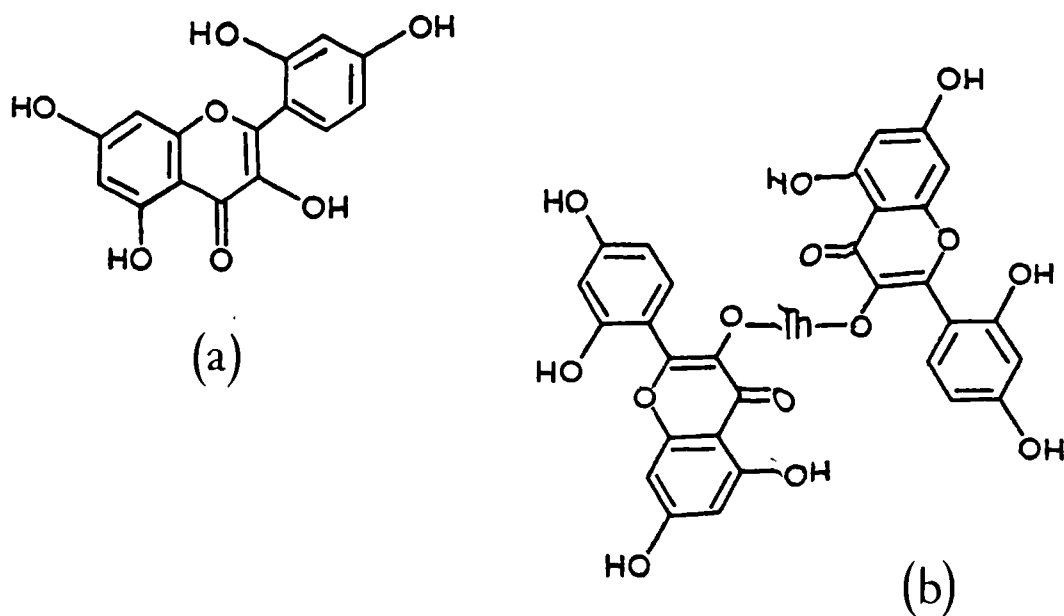


Fig. 21.

The method is simple and effective but care must be taken in choosing a reference material for the colourimetry of thorium by this reagent. Interfering substances [TABLE 11] can substantially change a result from the true value. The standard and reference solutions have to contain the same amount of interfering substances as the sample solution. In every colourimetric determination of thorium using the reagents Morin and Thoron, the possible interfering substances had to be accounted for. It was easier to do this rather than solvent extract the thorium for each sample, standard and reference, as many determinations of thorium would have to be made on varying solutions. The colourimetric method using Morin was found to be more accurate than titration as between 2 and 30 ppm of thorium could be determined at  $\text{pH} = 2$ . (The upper limit of determination varies as the presence of interfering substances increases and each experiment must have its own independent calibration curve to establish linearity). The alkali and alkaline earth metals do not interfere with Morin. Although aluminium is quoted as an interfering substance in Table 11, it must be present in about 20 times the unit weight of thorium to produce the same absorbance as unit weight of thorium.

Thoron is a bright orange-red colour and is less commonly termed 2-(2-Hydroxy-3,6-disulpho-1-naphthylazo) benzene arsonic acid and has the structure shown in FIGURE 22.



TABLE 10

REAGENT	THORIUM COMPLEX	pH	( $\lambda$ ) WAVE- LENGTH /nm	SENSITIVITY ( $\gamma/\text{ThO}_2$ FOR: $\log \frac{I_0}{I} = 0.001$ )
MORIN	YELLOW/GREEN	2.0	410	0.007
THORON	RED/ORANGE	0.4-1.2	545	0.013

TABLE 11

REAGENT	MAJOR INTERFERING SUBSTANCES
MORIN	Zr, FeIII, Al, U, Pb
THORON	CeIV, Zr, U(IV)

TABLE 12

REAGENT	U-COMPLEX COLOUR	pH	( $\gamma$ ) WAVE- LENGTH/nm	DETECTION SENSITIVITY	INTERFERING SUBSTANCES
H <sub>2</sub> O <sub>2</sub>	STRAW YELLOW	>12	392	0.01%	V, Mo, Cr, ORGANIC MATTER F <sup>-</sup> , PO <sub>4</sub> <sup>2-</sup>

## Thoron: Structure

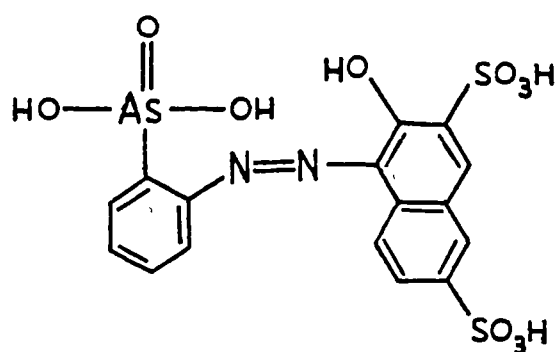


Fig. 22.

Two moles of thoron will combine with one mole of thorium (as with Morin) and linkage occurs via the arsono group of thoron [REF. 72]. Both of the arsono hydrogens are replaced forming the normal thorium arsonate, which is deep red in colour. Thoron as a reagent for colourimetry, is useful in the determination of thorium in acidic solutions and it is more sensitive for thorium than morin. The thorium arsonate colour intensity is constant over a pH range of 0.4-1.2 and thorium can be detected between 0.1 ppm and 30 ppm. Some interfering substances are listed in TABLE 11. Metals may be present in the following amounts (mg per 10 ml) without causing appreciable error: Mg(25), Mn(6), Zn(1), Al(1), Cu(1), CeIII(0.15), Ni(1), Pb(1), Ca(5).

#### 4.1.2 COLOURIMETRY : URANIUM

Many reagents are available for the colourimetric determination of uranium, these include potassium ferrocyanide, thiocyanate and hydrogen peroxide [REFS. 73,74,75]. The hydrogen peroxide method is used in this work as it is convenient to use. It is moderately selective for uranium as in basic solutions uranium(VI) forms pale yellow peruranates. Hence, the colour can be produced by adding hydrogen peroxide to a carbonate solution of uranium. The colour intensity is constant above pH = 12 and the specific characteristics of the determination, along with interfering substances, are shown in TABLE 12. This method only appears to have one drawback in the fact that extreme care must be taken in handling the solutions in colourimetry cuvettes. Due to the presence of solutions of carbonate and hydrogen peroxide, extensive bubble formation occurs on the inside surface of the silica cuvettes. This may be reduced by allowing as little reaction with the atmosphere as possible to occur to the colourimetry solutions and using air-tight lids on the cuvettes whilst in the photospectrometer. It is also essential to check for bubble formation during the noting of a reading on the instrument, as the bubbles change the 1.0 cm light path for absorption, thus affecting the results.

Other colourimetric reagents, such as Alizarin-S [REF. 84] have been studied and may be found in the literature.

A published method for the determination of uranium in thorium solutions is available [REF. 76] and involves careful

solvent extraction of uranium. A method which allows the direct absorbance determination of uranium in organic solutions of tri-butyl phosphate has been proposed by I. OBRENOVIĆ-PALIGORIĆ et al [REF. 78].

#### 4.2 TITRATION : THORIUM

The disodium salt of ethylene-diaminetetraacetic acid (EDTA) may be used to determine larger concentrations of thorium but the sensitivity of the method is prone to errors in solutions containing thorium concentrations of the order of < 150 ppm [REF. 79]. The reaction between thorium and EDTA-disodium salt is:



where the EDTA component is represented as Y. Xylenol orange indicator may be used and produces a blood-red complex with thorium at pH = 2.6. The addition of sufficient EDTA solution produces a very sharp, lemon-yellow, end point. The presence of aluminium interferes with the titration reaction and a background titration should be carried out especially if the thorium solution has been in contact with a potential source of aluminium.

A 'back-titration' may be used to analyse for thorium, whereby the EDTA (disodium salt) is added to the sample along with solid hexamine. The solution may then be titrated with standard lead nitrate solution with xylenol orange as indicator. For more accurate determinations of thorium, colourimetry is

preferred. No titration for the determination of uranium is used in this work, as a silver reductor is needed and the method of colourimetry using hydrogen peroxide was deemed to be adequate for quantitative determination of uranium.

#### 4.3 LIQUID SCINTILLATION COUNTING

##### 4.3.1 THEORY

Radionuclides may be quantitatively determined using a liquid scintillation counting technique [REF. 85]. Normally, emitted  $\alpha$ - or  $\beta$ -particles interact with primary solvent molecules. Dissolved within the primary solvent is a scintillator solute and the interaction with the radiation particle causes the solvent molecules to excite into levels higher than the ground state. The energy of the 'excited-state' solvent molecules is transferred, by collision, to the primary scintillator molecules. This transferred energy is re-emitted by the solute molecules as tiny flashes of light which are detected by a sensitive photomultiplier tube. A "wavelength shifter" or secondary solute may be used to shift the emitted light into a region of the spectrum where the photomultiplier is more sensitive to it.

A typical type of solvent-solute system may be used to count aqueous radioisotopes such as U-238, Th-232 is:

PRIMARY SOLVENT	Sulphur-free toluene.
PRIMARY SOLUTE	Diphenyl Oxazole (PPO).
SECONDARY SOLUTE	Bisphenyloxazolyl benzene (POPOP).

(These mixtures are often called cocktails and the composition for the cocktail, shown above, per litre of primary solvent would be 0.4 g POPOP and 4.0 g PPO).

If an aqueous solution of a radioisotope is to be counted by liquid scintillation techniques then it must be rendered entirely miscible with the organic solvents and solutes used. In order to achieve total miscibility, a detergent is often used to promote micelle-formation between aqueous and organic solutions. A typical detergent often used is TRITON X100.

In order to achieve a maximum count (thus reducing errors) and efficiency, the best ratios of aqueous sample solution, cocktail and detergent must be obtained. The optimum counting sample would be that giving a clear, homogeneous solution of maximum count. A Fox's Triangle experiment is the best way to determine an optimum counting system [REF. 80].

Hence, by preparing a set of standards of known activity a radioisotope may be quantitatively determined, provided that the total volume of each of the counting samples is exactly the same. The light emission is directly proportional to the amount of activity present.

Only total activity may be measured for U-238 and Th-232 as the isotopes used in this work, except in a few cases, contained their equilibrium daughter products and these also undergo light emissions in cocktail. The only real disadvantage of liquid scintillation counting is that some of the reagents, which need to be of scintillation grade materials, are expensive.

#### 4.3.2 ČERENKOV COUNTING

In 1934 P.A. ČERENKOV discovered that a beam of  $\gamma$ -rays passing through water was accompanied by the emission of a characteristic blue light [REF. 81]. This Čerenkov radiation may be detected by the photomultiplier in a liquid scintillation counter. There is no need to use a scintillator solvent or solute. Water may be used as the solvent, whose only requirements are a necessary high refractive index and transparency. A  $\beta$ -particle moving through a transparent medium can generate Čerenkov radiation provided that it travels through the medium with a velocity greater than that of light through the same medium. The minimum energy requirement for particles, in most cases, is about 0.29 MeV.

The  $\beta$ -emitters which are daughters of Th-232 and U-238 ( $^{228}\text{Ac}$ ,  $^{228}\text{Ra}$  and  $^{234}\text{Pa}$ ,  $^{234}\text{Th}$  respectively) can be detected by Čerenkov counting. As in liquid scintillation counting, the radiation produced by Čerenkov emission is directly proportional to the amount of isotope present. Therefore, activity from the weak  $\beta$ -emitters can be detected by Čerenkov counting independently from the total activity results obtained by liquid scintillation counting. It is possible to count more than one isotope in solution by liquid scintillation and Čerenkov counting. An assay for counting strontium isotopes in the presence of Cs-137 by the Čerenkov technique has been developed [REF. 86].

### 4.3.3 QUENCHING

Many substances, including samples, secondary solvents and solubilizers may affect the light output of the solute. Thus, the count of the sample may be "quenched". There are three types of quenching:

#### 1) Impurity quenching

This occurs where impurities, i.e non-fluorescent molecules, compete with the solute molecules for the excitation energy of the solvent molecules and release this energy as heat, by radiationless transfer. This type of quenching may be minimized by reducing the concentration of the quencher, and ensuring that the solvent excitation and solute fluorescence lifetimes are short. This provides less chance of a collision with a quencher molecule within the solution [REF. 87].

#### 2) Colour quenching

Coloured samples, e.g.  $\text{UO}_2^{2+}$  - containing solutions, which are yellow, decrease the mean free path of fluorescence photons and light-collection efficiency is reduced at the photomultipliers of the liquid scintillation counter.

#### 3) Photon quenching

Photon quenching is a type of self-adsorption effect. The maximum interaction between the  $\beta$ -energy and the solvent and solute in a cocktail may be reduced by the presence of impurities [REF. 85].



One or more types of quenching may affect a sample and quenching, in most cases, can be suitably corrected for. A "Quench Correction Curve" may be plotted from experiments where a concentration range of impurities or coloured solutions are prepared and "spiked" with the isotope to be counted. If a set of unquenched isotope standards are also counted, then the effect of quenching can easily be seen and a quench correction curve can be used for future reference. Other types of quench-correction methods may be seen in A. Dyer's comprehensive text on Liquid Scintillation Counting practice [REF. 85].

The Čerenkov counting technique is affected by colour quenching and to a lesser extent, impurity quenching, whereas liquid scintillation counting may be severely affected by both types of quenching.

#### 4.4 GRAVIMETRY

Thorium may be quantitatively determined by gravimetric analysis. It may be precipitated by the addition of sodium hydroxide producing a white gelatinous precipitate of thorium hydroxide  $\text{Th}(\text{OH})_4$ . This may then be filtered and ignited to thoria at  $1000^\circ\text{C}$ . Thoria is a stable, white powder which may draw water from the atmosphere and it has a relatively high molecular mass. These properties render thoria as an ideal gravimetric agent.

Gravimetry was used in this work to standardize pure thorium solutions. Less tedious methods, such as colourimetry and counting techniques were predominantly used for quantification purposes.

#### 4.5 QUALITATIVE ANALYSIS METHODS

##### 4.5.1 $\gamma$ -RAY SPECTROSCOPY

$\gamma$ -RAY spectroscopy in this work was used purely for the purpose of isotope identification. A germanium-lithium (GeLi) semi-conductor crystal type of detector linked to a multi-channel analyser provided adequate  $\gamma$ -spectra of both solid zeolite samples containing thorium and solution samples. The detectable  $\gamma$ -rays were those from the thorium daughters. [SEE TABLE 13].

##### 4.5.2 $\beta$ -RAY SPECTROSCOPY

By linking an SL-30 Intertechnique Liquid Scintillation Counter to a Canberra multichannel analyser, a suitable  $\beta$ -spectrum of Th-234 could be obtained showing an  $E_{\max}$  value of 191 KeV [SEE FIG.23].  $\beta$ -spectroscopy was used as an identification method and not a quantitative method.

Although the techniques of  $\beta$ - and  $\gamma$ - spectrometry were not used in this project to quantitatively determine thorium and uranium, it is possible to assay rock and soil by these methods. TALIBUDEEN and YAMADA have assayed rocks by these techniques using the  $^{208}\text{Tl}$   $\gamma$ -peak for thorium-232 which has been found to be directly proportional to the Th-232 content of the rock [REF. 88].

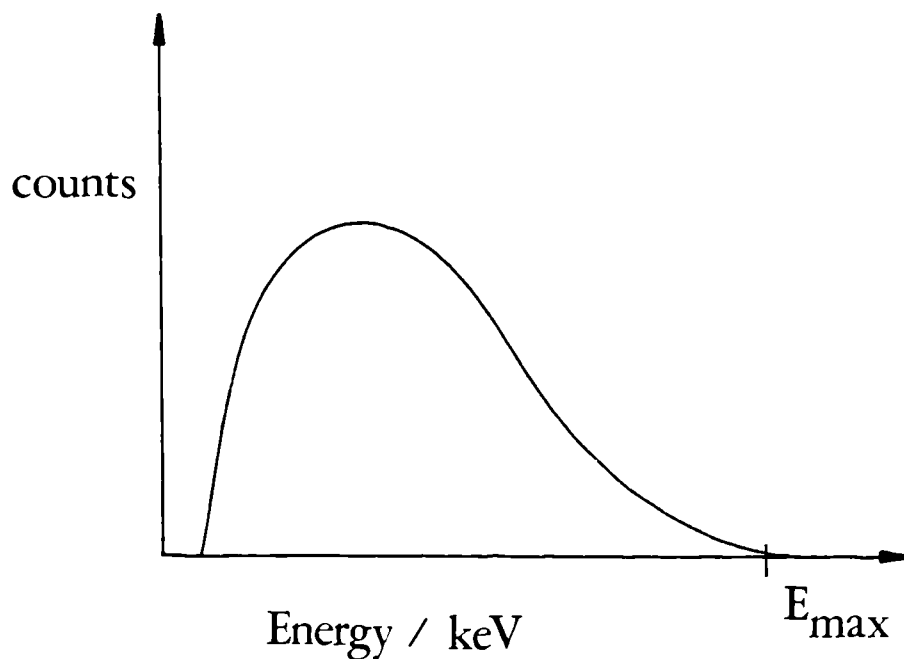
TABLE 13

SOME DETECTABLE  $\gamma$ -PEAK ENERGIES OF THORIUM AND ITS DAUGHTERS [REF. 90.]

ISOTOPE*	$\gamma$ -ENERGIES/keV
Th-232	59.0
Ac-228	56.8, 97.8, 127.5, 179.0, 184.0, 232.0, 336.0, 410.0, 458.0, 907.0, 911.9, 965.0, 1035.0, 1460.7, 1590.0, 1640.0.
Th-228	84.4, 137.0, 169.0, 205.0, 212.0.
Pb-212	115.1, 176.7, 236.0, 238.6, 300.1, 415.2.
Bi-212	144.0, 164.0, 228.0, 328.0, 432.0, 452.0, 472.0.
Tl-208	277.0, 510.6, 583.5, 859.0, 2620.0.
Th-234	29.0, 62.8, 91.4.
Pa-234	99.2, 125.0, 153.0, 225.0, 293.0, 333.0, 368.0, 556.0, 732.0, 767.0, 803.0, 877.0, 924.0, 1001.0, 1240.0, 1430.0, 1680.0.
Th-230	68.0, 110.0, 142.0, 184.0, 206.0, 235.0, 253.0.
Ra-226	186.0, 260.0, 420.0, 610.0.
Pb-214	53.2, 258.9, 295.2, 352.0.
Bi-214	609.4, 769.0, 935.0, 1120.0, 1155.0, 1238.0, 1416.0, 1509.0, 1728.0, 1764.0, 1849.0, 2017.0, 2117.0, 2204.0, 2432.0.
Tl-210	297.0, 780.0, $\sim$ 1100, $\sim$ 1300, $\sim$ 2360.

\*The half-lives of these isotopes are conveniently listed in Appendix III.

### The $\beta$ -Spectrum of Th-234.



$$E_{\max} = 191 \text{ keV for Th-234}$$

Fig. 23.

#### 4.6.1 ELECTRON PROBE MICROANALYSIS (EPMA)

The Scanning Electron Microscope (SEM) and the Electron Probe Microanalyser when used in conjunction with each other, enable the surface characterization of heterogeneous inorganic materials. Areas of the surface of a sample can be "pin-pointed" using the SEM and microanalyser.

In electron probe microanalysis, a finely-focussed electron beam is aimed at the surface region of interest and the signals

produced by characteristic X-rays, which are emitted as a result of the electron bombardment, are scanned. The interpretation of the data supplied by this technique can give qualitative and quantitative, elemental and compositional information from surfaces of only a few square microns [REF. 89]. A great advantage of this method is that the sample is not destroyed in the analysis and elemental losses are negligible when heavy metals are analysed.

X-ray scanning pictures can be obtained by using an electron probe microanalyser and detailed microcompositional data may be directly correlated to optical data in the form of scanning electron micrographs.

#### 4.6.2 THE ELECTRON PROBE MICROANALYSER

The machine is fitted with an electron gun focussed by reducing lenses creating an "electron beam" probe with a diameter of 0.1 - 1  $\mu\text{m}$  when applied to the sample. The interaction of the electron beam with the sample produces X-rays from a sample volume often exceeding 1  $\mu\text{m}$  in diameter and a few microns in depth.

An optical microscope is used to find a region of interest on the sample surface for electron bombardment, and in this respect, this feature of the electron probe microanalyser is basically a scanning electron microscope.

A set of energy dispersive spectrometers are used to analyse the intensity of the emitted X-rays. Comparison of the signals produced by the sample with those of a standard under the same operating conditions, enables quantitative elemental analysis.

### 4.6.3 SECONDARY ELECTRONS

The above description of electron beam-sample interactions is simplified and mentions nothing about secondary interactions other than X-ray production. The energy from the probe beam deposited in the sample is distributed among several other secondary processes including back-scattering of electrons and secondary electron emission from the sample. The fraction of beam energy which is associated with secondary electron emission is dependent on the nature of the sample and thus is useful in microanalysis. The generation of secondary electrons is shown in Fig. 24 below and it is interesting to note that the production of secondary electrons from interactions of back scattered electrons with the sample is more efficient than production of those produced by electron beam interactions, where heavy metals are concerned.

#### Generation of Secondary Electrons

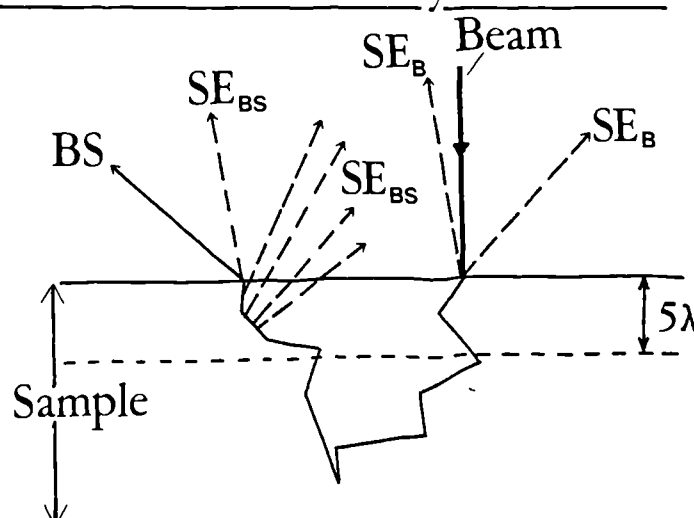


Fig. 24.

- $SE_B$  : Secondary electrons generated by beam-sample interactions.
- BS : Back Scattered electrons generate secondary electrons  $SE_{BS}$ , while exiting the sample.
- $\lambda$  : Mean free path of secondary electrons.

$\lambda$ , the mean free path of secondary electrons, is governed by the work function (the energy needed to overcome the surface potential barrier) to escape the sample and be detected. Many secondary electrons generated deeper within the sample are attenuated and eventually lose their energy and cannot escape.

A summary of the techniques used to analyse thorium and uranium may be found in TABLE 14.

TABLE 14

METHOD OF ANALYSIS QUALITATIVE	THORIUM	URANIUM
$\gamma$ -RAY SPECTROSCOPY	✓	✓
$\beta$ -RAY SPECTROSCOPY	✓	-
EPMA	✓	-
QUANTITATIVE	THORIUM	URANIUM
COLOURIMETRY	✓	✓
TITRATION	✓	-
LSC	✓	✓
ČERENKOV COUNTING	✓	✓
GRAVIMETRY	✓	-

CHAPTER 5

EXPERIMENTAL I



## 5.1 EXPERIMENTAL

### 5.1.1 PREPARATION OF ZEOLITES FOR EXPERIMENTS

All the zeolites used in these experiments were ground in a pestle and mortar and put through standard mesh sieves. The mesh fraction used was that between 150 $\mu$ m and 106 $\mu$ m unless otherwise stated. The zeolites were then sedimented down a 2m column filled with deionized water. *After 30 minutes the solid* that had collected at the base of the column was removed and dried in an oven at 110°C. In this way, the desired zeolite size-fraction was separated from any fines which remained in suspension in the column. All the zeolite mesh sizes were treated in this way unless otherwise stated. The zeolites were not purified. All the Clinoptilolite used in the experimental section was Mudhills Clinoptilolite (California) unless specified.

### 5.1.2 WET CHEMICAL ANALYSIS OF SPECIFIC ZEOLITES:

CLINOPTILOLITE 140/D Mudhills.

EASTGATE 2020.

In order to verify the chemical composition of clinoptilolite it was necessary to perform a full wet chemical analysis of the zeolite to compare to supplied data sheet values. The Eastgate sample had no data sheet and it was essential to know its composition in order to evaluate its silica to alumina ratio and hence its base exchange capacity. Other zeolites used had silica to alumina ratios which had been pre-determined.

## METHOD

### Determination of the oxides of sodium, potassium, calcium.

Approximately 0.3g zeolite (weighed accurately) was placed in a porcelain evaporating basin. Hydrochloric acid (AnalaR, 50%, 50ml) was added to the zeolite producing a pale yellow solution above the zeolite. The basin was placed on a steam bath in a fume cupboard and a watch glass was placed over the basin. The basin was heated for 6 hours after which time, the watch glass was removed and its convex surface was washed thoroughly into the basin with deionized water. The basin was then left on the steam bath overnight to allow the hydrochloric acid to evaporate slowly. A further aliquot of hydrochloric acid (AnalaR, 50%, 50ml) was added to the evaporate residues and the watch glass was replaced. The basin was heated again on the steam bath for 6 hours. The procedure of boiling the mixture and evaporation overnight was repeated a further four times in order to release the maximum number of cations from the zeolite structure. After the final evaporation, hydrochloric acid (AnalaR, 5%, 50ml) was added to the residue and was boiled for 3 hours after replacing the watch glass on the basin. A pale yellow solution resulted and a white solid mass remained at the base of the basin. The watch glass was thoroughly washed into the evaporating basin.

The pale yellow solution, and the white solids, after cooling in air, were then filtered through a Whatman 541, hardened, ashless filter paper into a 500 ml volumetric flask.

All traces of the solution and solid were transferred to the filter paper by thoroughly washing the basin out with deionized water and carefully rubbing the inside surface of the basin with a glass rod fitted with a rubber policeman. The solution in the volumetric flask was made up to the mark with deionized water. This solution was then transferred to a polypropylene bottle ready for analysis of potassium, sodium and calcium by flame photometry.

The experiment was conducted in duplicate and the average result calculated.

#### 5.1.3 DETERMINATION OF SILICA

Zeolite (40.3g, weighed accurately) was placed in a large, tall-form platinum crucible. Fusion mixture (41.5g, potassium carbonate : sodium carbonate = 69g : 53g, AnalaR) was added to the zeolite. A platinum lid was placed upon the crucible and the crucible was heated to red-heat, using a Meker burner (at 1000°C). The crucible was heated for 3 hours, cooled slightly, and was placed, with its lid, in a large ceramic evaporating basin filled with deionized water (30 ml). Concentrated hydrochloric acid (30 ml, AnalaR) was added. Effervescence occurred and the greenish, glassy solid began to dissolve. After the effervescence had ceased the crucible and lid were carefully removed and washed down into the pale yellow solution in the evaporating basin with dilute hydrochloric acid. The evaporating basin was placed on a steam bath and was allowed to evaporate to dryness overnight.

Hydrochloric acid (AnalaR, 50%, 50 ml) was added to the remaining solid and a large watch glass was placed over the basin. The procedure of boiling and evaporation was repeated four times as in section 5.1.2, and after the final evaporation hydrochloric acid (5%, 50 ml, AnalaR) was added to the solid. The solution produced was colourless and after boiling for 3 hours, a flaky white solid remained in the colourless solution. This solid was presumed to be silica. The solution and solid was filtered through Whatman 540 hardened, ashless filter paper under gravity. The filtrate was collected in a 500 ml volumetric flask and great care was taken that all silica residues were washed with dilute hydrochloric acid onto the filter paper. The filter paper itself was washed, along with the filter funnel, into the volumetric flask to ensure that all free ions were transferred properly. The filtrate was made up to the mark with deionized water and was transferred to a polypropylene bottle for analysis of aluminium, magnesium, iron, titanium and manganese by atomic absorption spectroscopy.

The filter paper and solid were dried in air and placed in a pre-weighed, platinum crucible. The crucible and lid were placed over a microburner. The crucible and its lid were gently heated in order to slowly char the paper to carbon with gradually increasing heat. When the charred filter paper turned white, after 5 hours, the microburner was replaced by a Meker burner. The lid was removed and the crucible was strongly heated at 1000°C for 1.5 hours. The crucible was then removed

from heat, cooled slightly and placed in a desiccator for 12 hours. The crucible and white solid were weighed, replaced in the desiccator and reweighed to constant weight. The white solid was deemed to be impure silica.

Hydrofluoric acid (48%, 5-8 ml, AnalaR) was added to the crucible and the crucible was placed on a sand bath on a hot plate in a fume cupboard overnight, allowing the hydrofluoric acid to evaporate. The remaining white solid was deemed to be pure silica. The crucible and solid were reweighed.

#### 5.1.4 SAMPLE PREPARATION FOR FLAME PHOTOMETRY

Very little sample preparation was necessary and only one step was taken. When using any analysis machine fitted with an aspirator tube it is necessary to ensure that the solution has been filtered properly from all particulate matter. In using hardened, ashless filter paper this requirement was met. Linear calibration curves for 0 - 25 ppm sodium and potassium were obtained as was a linear curve 5 - 100 ppm calcium on a Corning 400 Flame Photometer. No sample dilutions were necessary as the sample solution values fell directly on the calibration curves.

#### 5.1.5 SAMPLE PREPARATION FOR ATOMIC ABSORPTION SPECTROMETRY

Linear calibration curves were obtained for aluminium, iron, magnesium, titanium and manganese. Only the magnesium ppm values in both zeolites did not fall below the maximum ppm value for linearity on the calibration curve and needed to be diluted accordingly before a determination could be made.

The aluminium sample was diluted 1:1 with a 4000 ppm potassium solution as recommended by the atomic absorption operating manual in order to minimize interferences within the flame. A ThermoELECTRON S11 Atomic Absorption photospectrometer was used in these analyses.

#### 5.1.6 WATER CONTENT : TG ANALYSIS

To provide a full picture of the composition of a zeolite the water content must be known. The water content of a zeolite can be effectively determined by thermogravimetric analysis (TGA). In this method an accurately weighed amount of zeolite, which had been equilibrated over saturated sodium chloride solution was placed in a zero-weighted crucible on an accurate balance and was subjected to gradual heating in a furnace. The weight loss of the sample was analysed by a microprocessor linked to the balance. A METTLER TG50 Thermobalance was used in conjunction with a METTLER TC 10A TA processor. An accurate percentage weight loss of volatiles, i.e. water, was obtained.

#### 5.2 SPECIFIC CATION EXCHANGE CAPACITY MEASUREMENTS ON Z900, CLINOPTILOLITE, NaY, CaY

Generally, throughout this work, when a capacity measurement was required for a calculation, the base cation exchange capacity has been used based on the number of milli-equivalents of aluminium per gram of zeolite. The specific cation exchange capacity measurements for potassium were made on several zeolites to see how they compare with the base cation exchange capacity.

## METHOD

Zeolite ( $\sim 0.5\text{g}$ , weighed accurately) was placed in a  $100\text{cm}^3$  beaker. Ammonium acetate solution ( $20.0\text{cc}$ ,  $1\text{M}$ ) adjusted to pH 7 was added. This was stirred with a glass rod and allowed to stand overnight. The zeolite and ammonium acetate solution was put through a filter funnel fitted with a Whatman 540 filter paper into a  $100\text{ ml}$  beaker.

The sample, filter paper and the interior of the funnel were washed with ethanol (Absolute,  $5 \times 25\text{cc}$  portions) which were discarded. The "ethanol-leached" sample was further leached with successive  $10\text{cc}$  volumes of  $10\%$  w/v potassium chloride solution adjusted to pH 2.5 with hydrochloric acid ( $1\text{M}$ ). The extracts were collected in a  $100\text{cc}$  volumetric flask which was diluted to the mark with potassium chloride solution. The ammonium content of the analysis solution was measured using a Kjeldahl titration on a Kjeltach Auto 1030 analyser to find the cation exchange capacity (CEC).

### 5.3 PREPARATION OF HOMOIONIC FORMS OF ZEOLITES FOR ISOTHERM STUDIES

Zeolite ( $5\text{g}$ ) was placed in a three-necked, round bottom flask. The flask was then half-filled with respective metal nitrate solution ( $1\text{M}$ ,  $100\text{ ml}$ ).

ZEOLITE FORM TO BE PREPARED	METAL NITRATE SOLUTION (1M)
K-CLINOPTILOLITE	$\text{KNO}_3$
Na-CLINOPTILOLITE	$\text{NaNO}_3$
KY	$\text{KNO}_3$
NaY	$\text{NaNO}_3$
K-Z900	$\text{KNO}_3$
NaZ900	$\text{NaNO}_3$

A few anti-bumping granules were added and a condenser was fitted to the flask along with a thermometer. The apparatus was placed on a heating mantle equipped with a magnetic stirrer. A PTFE coated magnetic bar was added to the flask. The mixture was stirred and heated at 80°C for 20 hours. The solid was then filtered and returned to the flask and a fresh solution of metal salt added. The heating/stirring procedure was repeated, the solid being filtered after 20 hours. The whole method was carried out 4 times enabling four renewed exchange opportunities to provide exchange as fully as possible. After the final filtration the solid was washed with deionized water, dried in air and was placed on a watch-glass. The homoionic form of the zeolite was then allowed to stand in a desiccator containing saturated sodium chloride solution for two weeks. The zeolites were visually unchanged by the exchange process.



#### 5.4.1 LEACHING EFFECT ON SEVERAL ZEOLITES ON TREATMENT WITH WATER

Zeolites, especially natural ones, may leach cations on treatment with water. This may be due to cations being released from exchange with  $H^+$  or hydronium ions  $H_3O^+$ . This release of cations may also be due to the fact that impurities such as sodium chloride may be present, along with other non-zeolitic material, in the natural zeolites. This experiment was conducted on the natural zeolites clinoptilolite and Eastgate and the synthetic zeolites NaY and NaZ900.

##### METHOD

Zeolite (~0.1g, weighed accurately) was placed in a 22.5cm<sup>3</sup> capacity polyethylene vial. Deionized water (10.0 ml) was added and the vial was capped and secured with PTFE tape. The vial was placed in a drum on a mineralogical roller and the drum was rotated for 2 days. The vial was removed and centrifuged. An aliquot of the supernatant was taken for analysis of cations sodium, potassium by flame photometry and aluminium by atomic absorption spectrometry.

#### 5.4.2 LEACHING EFFECT ON ZEOLITES TREATED WITH PURE THORIUM SOLUTIONS

##### METHOD

Zeolite (~0.1g, weighed accurately) was placed in a 22.5cm<sup>3</sup> capacity polyethylene vial. Thorium solutions of varying concentrations (i.e. 5ppm or 100ppm solutions) were

added (10.0 ml) to the vials which were capped and secured with PTFE tape. The vials were placed in drums upon mineralogical rollers and the vials were rotated for 2 days at 20°C. After this time, the vials were removed, centrifuged and an aliquot of supernatant was taken for analysis of sodium and potassium ions by flame photometry.

#### 5.4.3 LEACHING EFFECT ON ZEOLITES TREATED WITH NITRIC ACID

##### METHOD

The above method was followed for Z900, Eastgate, NaY, Clinoptilolite with 0.1N and 0.5N nitric acid solutions. Aliquots of supernatant were analysed for sodium, potassium by flame photometry and aluminium by atomic absorption.

#### 5.4.4 EXPERIMENTS TO DETERMINE THE RELEASE OF SODIUM AND POTASSIUM FROM CLINOPTILOLITE AND NaY WITH 10<sup>2</sup> ppm THORIUM SOLUTIONS

##### METHOD

Zeolite (~1.0g weighed accurately) was placed in a 120cc capacity polypropylene bottle. The zeolites tested were NaY and clinoptilolite. Thorium nitrate solution (1000ppm, 100.0 ml) was added to the zeolite. The bottle was sealed with PTFE tape and capped. The bottle was placed in a drum on a mineralogical roller for an equilibration period of 3 days. The bottles were then removed and centrifuged for 20 minutes and 5.0 ml aliquots of the supernatant were diluted accurately to 100.00 ml. These diluted solutions were used to analyse for Na<sup>+</sup> and K<sup>+</sup> on a Corning 400 Flame Photometer.

Further aliquots of the supernatant were removed for thorium-232 analysis by colourimetry, using Morin as the reagent. [SEE SECTION 5.5.3].

#### 5.5.1 COLOURIMETRY FOR THE ANALYSIS OF THORIUM

Colourimetry using the reagents Morin and Thoron where appropriate (as explained in section 4.1.1), has been used extensively to quantify Th-232 in many experiments throughout this chapter and chapter 6. Since the nature of each colourimetry experiment conducted was slightly different, it would be impossible to list the exact procedure for each one, so the two general procedures for MORIN and THORON colourimetry to analyse pure thorium solutions will be listed here. TABLE 15 shows the varying conditions for each experiment.

#### 5.5.2 PREPARATION OF A STANDARDIZED STOCK SOLUTION

A stock solution of thorium nitrate (Relative molecular mass = 588.18, AnalaR, 1000.00 ml), was prepared by dissolving the thorium nitrate (23.7g) in deionized water, in a 1000 ml volumetric flask. This produced an approximately  $10^4$  ppm solution of thorium. This solution had to be standardized by gravimetric means. An aliquot of the stock solution (10.0 ml) was pipetted into a clean, pre-weighed, platinum crucible. (The experiment was conducted in triplicate). The solution was gently evaporated off using a microburner to heat the crucible. A white residue remained in the base of the crucible and this was assumed to be thoria. The platinum crucible was transferred

TABLE 15

## VARIATIONS IN COLOURIMETRY PROCEDURE

EXPERIMENT TYPE	REFERENCE PREPARATION	STANDARD PREPARATION
Pure $\text{Th}(\text{NO}_3)_4 \cdot 5\text{H}_2\text{O}$ solution.	Deionized Water	$\text{Th}(\text{NO}_3)_4 \cdot 5\text{H}_2\text{O}$ STANDARD in deionized water.
$\text{Na}^+$ or $\text{K}^+$ determinations	Relevant amount of $\text{Na}^+$ or $\text{K}^+$ added	$\text{Th}(\text{NO}_3)_4 \cdot 5\text{H}_2\text{O}$ STANDARD with relevant $\text{Na}^+$ or $\text{K}^+$
SOSIM experiments	Relevant amount of dummy SOSIM solution (without $\text{Th}_{4+}$ )	Thorium standards prepared in dummy SOSIM solution
Isotherm experiments	Control solution without thorium	* Control solutions containing thorium

\* Control solutions contained relevant binary cation mixtures of thorium and counter ion, but no zeolite.

by means of platinum-tipped tongues to a CARBOLITE ESF EURO THERM furnace. The furnace was closed and the temperature raised slowly (but not at a uniform rate) to 1000°C for several hours. After this period of time, the red-hot platinum crucible was removed from the furnace, cooled slightly and placed in a desiccator over silica gel.

After cooling completely, the platinum crucible (and the white powder it contained) were weighed to constant weight. From the mass of thoria produced from a 10.0 ml aliquot of the stock, the thorium content of the stock could be standardized at 9676ppm.

#### 5.5.3 THORIUM COLOURIMETRY PROCEDURE : MORIN

A set of thorium standards were prepared in 25 ml volumetric flasks by taking appropriate aliquots of standardized stock solution so that, when the aliquots in each flask were diluted to 25.00 ml, the thorium content would range from 30.0ppm thorium to 0.5ppm thorium.

Before dilution to 25.00 ml with deionized water, the pH of the aliquots were adjusted to pH = 2 (using short-range pH paper) with dilute nitric acid and nitric acid (0.5 ml, 0.63M, AnalaR) was added to each aliquot. Each flask was diluted to approximately 20 ml with deionized water.

A solution of MORIN (1.0 ml, 0.1% in absolute alcohol) was added to each flask and all solutions were made up to 25.00 ml with deionized water. On addition of the Morin and after

shaking, the thorium standard solutions attained a greenish-yellow colour ranging from straw yellow at 0.5ppm to intense greenish-yellow at 30ppm thorium.

#### SAMPLE PREPARATION

A known aliquot of sample solution was adjusted to pH = 2, as with the standard preparation, and then the procedure was the same as that above. A reference was prepared in the same way by omitting any thorium-containing component. The standards and samples were left for 30 minutes before taking any readings on the photospectrometer but the readings had to be taken within a few hours, as the absorbance was found to change after this time.

A pair of 1.0cm silica cuvettes were used in conjunction with a PYE UNICAM SP1800 UV Photospectrometer. The samples were read at 410nm (slit width 0.27nm).

#### 5.5.4 THORIUM COLOURIMETRY PROCEDURE : THORON

A set of standards were prepared in 25 ml volumetric flasks. The pH of the thorium solution had to be adjusted to between 0.4 and 1.2 with dilute nitric acid. 0.1% THORON (aqueous, 3.0 ml) was added and the standards were made up to the mark with deionized water.

The samples were treated in the same way. Each thorium-containing solution produced an orangy-red colour on addition of thoron. The absorbance of the thoron samples did not change appreciably in 24 hours.

As with the Morin procedure, the thoron samples were read in a PYE UNICAM SP1800 UV Photospectrometer using 1.0cm silica cuvettes. The wavelength used was 545nm (at a slit width of 0.27nm).

#### 5.5.5 COLOURIMETRIC DETERMINATION OF URANIUM

##### GENERAL PROCEDURE

An aliquot of standard uranium solution (1000ppm) was neutralized with dilute sodium hydroxide solution to pH 7. The solution was diluted to about 15 ml with deionized water and sodium carbonate solution (10%, 5.0 ml) was added. To this, hydrogen peroxide solution (30%, 0.2 ml) was added producing a straw-yellow coloured solution. The solution was made up to 25.0 ml in a volumetric flask. The solution was well shaken and transferred to an air-tight polyethylene bottle. In such a way, a set of standards were prepared in order to test the feasibility of this method.

The solutions were tested against a reference in 1.0cm silica glass absorbance cuvettes (with lids) on a PYE UNICAM SP1800 UV Photospectrometer. The main absorbances occurred at 380-400nm and 450nm at a slit width of 0.27nm.

The exact absorbance chosen was 392nm. When reading uranium samples that had been contacted with zeolites, it was necessary to use control uranium standard solutions containing a) the appropriate amounts of competing ion and b) aluminium (which leaches from the zeolite as when in contact with thorium solutions). The reference must contain exact quantities of aluminium and competing ion.

A plot of concentration of uranium 'vs' absorbance had to be made for each colourimetry experiment undertaken. The method was suitable for use with solutions in contact with zeolites as there were no interferences from aluminium. However when this method was used with isotherm solutions i.e.  $\text{UO}_2^{2+}/\text{K}^+$  or  $\text{UO}_2^{2+}/\text{Na}^+$ , then control solutions containing such binary mixtures of these ions were used to prepare standards.



#### 5.6.1 SAMPLE PREPARATION AND USE OF THE ČERENKOV COUNTING TECHNIQUE

Any aqueous sample that was counted by the Čerenkov counting technique for Ac-228 and Ra-228 was checked for the possibility of quenching substances (shown in the following section). All samples counted were of 5.0 ml proportions and the samples were placed in unused, low background polyethylene vials (22.5 ml capacity). The samples were then placed in a Beckman LS-233 Automatic Liquid Scintillation Counter, unless otherwise stated. The samples were all counted for 100 minutes (in duplicate) in the Tritium ( $^3\text{H}$ ) channel. A linear calibration curve of count rate 'vs' concentration percentage was plotted for all experiments.

Each counting result was corrected for background. The background count was considered to be that of 5.0 ml of the aqueous solution (without isotopes) in the same type of polyethylene vial.

#### 5.6.2 QUENCHING

A series of quench experiments were performed to observe the effects of cations, or acid, contained in sample solutions on the counting of isotope solutions.

#### METHOD

A 0.1N thorium nitrate solution was prepared containing equilibrium proportions of Ac-228 and Ra-228. The quenching properties of  $\text{K}^+$ ,  $\text{Na}^+$ ,  $\text{Al}^{3+}$  (0.01N stock solutions) and nitric

acid were tested by adding each of the following [SEE TABLES 16 and 17] volumes of thorium stock solution, cation stock solution and water to a counting vial and seeing the observed effect.

TABLE 16

VIAL NUMBER	0.1N Th <sup>4+</sup> /ml	H <sub>2</sub> O/ml	K <sup>+</sup> ,Na <sup>+</sup> OR Al <sup>3+</sup> : 0.01N/ml
1	1.0	3.5	0.5
2	1.0	3.0	1.0
3	1.0	2.0	2.0
4	1.0	1.0	3.0
5	2.0	2.5	0.5
6	2.0	2.0	1.0
7	2.0	1.0	2.0
8	2.0	-	3.0
9	3.0	1.5	0.5
10	3.0	1.0	1.0
11	3.0	-	2.0
12	4.0	0.5	0.5
13	4.0	-	1.0
14	5.0	-	-
15	4.0	1.0	-
16	2.0	3.0	-
17	1.0	4.0	-

TABLE 17

VIAL NUMBER	0.1N Th/ml	6M HNO <sub>3</sub> /ml	H <sub>2</sub> O/ml
18	1.0	-	4.00
19	1.0	0.25	3.75
20	1.0	0.50	3.50
21	1.0	0.75	3.25
22	1.0	1.00	3.00
23	1.0	1.25	2.75
24	1.0	1.50	2.50
25	1.0	1.75	2.25
26	1.0	2.00	2.00
27	1.0	2.25	1.75
28	1.0	3.00	1.00
29	1.0	3.00	1.00
30	1.0	3.50	0.50
31	1.0	4.00	-

A plot of counts 'vs' ml of added quencher was plotted for each cation and the acid. If there was no change in the count rate within counting errors the cation/acid was deemed to have no quenching effects.

### 5.6.3 LIQUID SCINTILLATION COUNTING

Sample preparation for liquid scintillation counting is more intricate than that for Čerenkov counting, but an enhanced count rate is produced thus minimizing counting errors. In order to find the optimum ratios of sample, detergent and cocktail a Fox's Triangle [REF. 80] experiment was conducted as follows.

#### SAMPLE OPTIMIZATION:

36 low-potassium content glass counting vials were placed and numbered as in the arrangement below [FIG. 25].

### The Fox's Triangle Arrangement

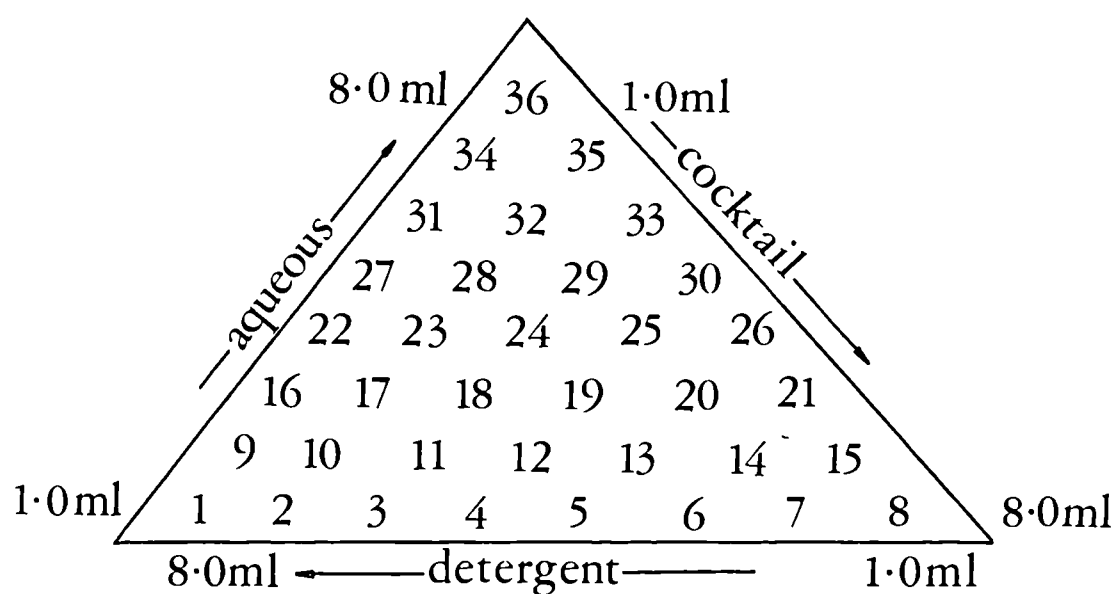


Fig. 25.

To each vial was added the appropriate volume of detergent, cocktail and aqueous sample as indicated by the volumes in the direction of the arrows in FIG. 25 thus keeping the total volume constant at 10.0 ml. e.g. vial number 13 would contain : detergent (3.0 ml), cocktail (5.0 ml) and aqueous sample (2.0 ml).

An aqueous Th-232 (0.01N) solution was used as the aqueous sample. TRITON X100 was the detergent used and a standard cocktail mixture was used (consisting of : POPOP ( $0.4 \text{ g l}^{-1}$ ) and PPO ( $4.0 \text{ g l}^{-1}$ ) in sulphur-free, scintillation grade toluene).

The vials were capped and vigorously shaken. Many of the mixtures gave a milky appearance or formed clear or opaque gels on shaking but vials 1, 2, 13 and 23 gave clear, ungelled, homogeneous solutions. These four vials were placed in a dark cupboard overnight to "dark adapt" the samples for counting. After 25 hours, the vials were examined and sample 23 was found to have gelled overnight. All gelled and/or opaque samples were discarded.

The three remaining samples were counted on the  $^{14}\text{C}/^3\text{H}$  channel of a BECKMAN LS-233 liquid scintillation counter. The sample with the highest, stable count rate, after deduction of the background count, was chosen as the optimum sample. This was found to be sample 2 for 0.01N thorium solutions. Thus the optimum ratios of aqueous sample, detergent and cocktail were found to be 1:7:2 ml respectively. This liquid scintillation system was found to be the ideal system for the counting of uranium-238 solutions (0.01N).

Therefore, in all liquid scintillation counting and quench correction experiments, only 1.0 ml of aqueous sample was needed. A linear calibration curve of concentration of total activity 'vs' count rate was plotted for all experiments.

#### 5.6.4 QUENCHING

A series of quench experiments were performed to observe the effects of cations contained in sample solutions on the counting of isotopic solutions.

#### METHOD

A 0.1N Thorium nitrate solution, deionized water and  $K^+$ ,  $Na^+$  or  $Al^{3+}$  (all 0.01N) were added to low potassium-content glass counting vials in the proportions shown in TABLE 18. All proportions total 1.0 ml of aqueous solution and cocktail (2.0 ml) and detergent (7.0 ml) was added to each vial. The vials were capped and shaken and 'dark-adapted' for 12 hours prior to counting. Any appreciable difference in observed count was taken to show a quenching effect. A plot of count rate 'vs' quencher concentration was plotted for each cation.

A Uranium-238 (0.01N) solution was tested in exactly the same way for the cations  $Na^+$ ,  $K^+$  and  $Al^{3+}$  (all 0.01N) in the proportions shown in TABLE 18.

TABLE 18

VIAL NUMBER	Th(0.1N)/ml	CATION (0.1N)/ml	WATER/ml
Q56	0.0	1.0 Na <sup>+</sup>	-
Q57	0.2	0.8 Na <sup>+</sup>	-
Q58	0.4	0.6 Na <sup>+</sup>	-
Q59	0.6	0.4 Na <sup>+</sup>	-
Q60	0.8	0.2 Na <sup>+</sup>	-
Q61	1.0	-	-
Q62	0.2	0.2 Na <sup>+</sup>	0.6
Q63	0.2	0.4 Na <sup>+</sup>	0.4
Q64	0.2	0.6 Na <sup>+</sup>	0.2
Q65	-	1.0 K <sup>+</sup>	-
Q66	0.2	0.8 K <sup>+</sup>	-
Q67	0.4	0.6 K <sup>+</sup>	-
Q68	0.6	0.4 K <sup>+</sup>	-
Q69	0.8	0.2 K <sup>+</sup>	-
Q70	0.2	0.2 K <sup>+</sup>	0.6
Q71	0.2	0.4 K <sup>+</sup>	0.4
Q72	0.2	0.6 K <sup>+</sup>	0.2
Q73	0.2	0.8 Al <sup>3+</sup>	-
Q74	0.4	0.6 Al <sup>3+</sup>	-
Q75	0.6	0.4 Al <sup>3+</sup>	-
Q76	0.8	0.2 Al <sup>3+</sup>	-
Q77	0.2	0.2 Al <sup>3+</sup>	0.6
Q78	0.2	0.4 Al <sup>3+</sup>	0.4
Q79	0.2	0.6 Al <sup>3+</sup>	0.2

5.7.1 PREPARATION OF A Th-234 TRACER SOLUTION BY SOLVENT  
EXTRACTION OF U-238 [REF. 91]

METHOD

Uranium Ore Concentrate, (UOC) (≈60g) was placed in a large beaker. Nitric acid (15.78M, 38 ml) was added and the  $\text{UO}_3$  dissolved, exothermically with stirring, to produce a clear, bright yellow solution. After dissolution, the solution was made up to 100 ml with distilled water. This solution was cooled and placed in a 500 ml separating funnel and was contacted with 5 x 200 ml portions of tri-butyl phosphate (TBP) (30% in Odourless Kerosene, OK). The organic solvent, which was the bottom layer, was run off (after shaking thoroughly with the aqueous solution and complete separation). After successive extractions, the aqueous layer began to lose its yellow colour completely.

The clear, colourless aqueous solution remaining was presumed to contain Th-234. In order to verify this, a  $\beta$ -spectrum was obtained by running a 5.0 ml sample in a polyethylene vial in a Kontron Roche Intertechnique SL30 Liquid Scintillation Counter which was linked to a Canberra Packard Series 35 Multi-channel Analyser.

A second test to verify the presence of Th-234 was conducted by counting 5.0 ml aliquots of sample, in polyethylene vials, by the Čerenkov method in a BECKMAN LS-233 Liquid Scintillation Counter over a period of several days, repeating the counting procedure each day. A plot of counts 'vs' time



could be plotted and extrapolated to find the half-life of the isotope within the sample.

The (Th-234)-containing sample was also analysed for  $\gamma$ -peaks.

#### 5.7.2 RADIOCHEMICAL EXTRACTION OF Th-232 FROM ITS DAUGHTER ISOTOPES [REF. 56]

##### METHOD

Chloroform (100 ml, 100%) was shaken with nitric acid (6M, 3 x 75 ml portions) in a 250 ml separating funnel. The upper aqueous phase was discarded after allowing the mixture to separate each time. This process saturated the chloroform with nitric acid.

Thorium nitrate hexahydrate (AnalaR, 3.0g) was dissolved in nitric acid (6M, 30 ml) and 10.0 ml of this solution was shaken in a separating funnel. After separation and removal of the organic phase the aqueous thorium phase was shaken with a further 3 x 10 ml portions of the acid-saturated chloroform solution. The remaining organic portion (approximately 8 ml) was re-extracted with dilute nitric acid (3 x 10 ml portions) and the solutions were analysed for thorium and thorium daughters by counting techniques.

The solutions containing Th-232 and Th-232 Daughters were also analysed qualitatively using  $\gamma$ -spectroscopy. [SEE SECTION 4.5.1] and TABLE 13.

### 5.8.1 SCREENING OF ZEOLITES FOR Th-232 AND Ac-228 / Ra-228 UPTAKES

A selection of zeolites, both natural and synthetic, SEE TABLES 19 and 20, were screened for uptakes at two different concentrations of Th-232 in the form of the nitrate salt. The percentage of uptake of daughter  $\beta$ -activity (Ac-228, Ra-228) was also measured.

#### METHOD

Zeolite (~0.1g, weighed accurately) was placed in a polyethylene vial (22.5cm<sup>3</sup> capacity). 10.0 ml of thorium nitrate solution (0.1N or 0.01N) was added. The vials were capped after sealing with PTFE tape to minimize leakage. The vials were placed in a drum which was put on a mineralogical roller. Five sample vials were prepared for each zeolite with each different normality of thorium solution used. The vials were agitated for a period of up to 1 week. At various time intervals (e.g. 1 hour, 6 hours, 24 hours, 48 hours and 168 hours) a sample vial was removed, centrifuged for ten minutes at 2500r.p.m. and an aliquot of the supernatant was removed for analysis of Th-232 by colourimetry with Morin (zeolites from TABLE 19 only). Aliquots (5.0 ml) were also removed for Čerenkov counting, (zeolites from both TABLE 19 and TABLE 20).

TABLE 19LIST OF ZEOLITES

Clinoptilolite	Phillipsite
Chabazite 1	Chabazite 3
Chabazite 2	Analcime
Mordenite	NaY
Eastgate	NaZ900
Ferrierite	

TABLE 20LIST OF ZEOLITES AND ZEOLITIC MATERIALS

Palagonite	13X
Palagonite containing zeolite	4A
Cowlesite	K - L
Natrolite	1010A
Brewsterite	5A (with binder)
Lava ash	5A (powder)
Heulandite	5050L
Brown Tuff	5050F
Thannet Bed Material	Apatite

### 5.8.2 VARIATIONS OF EXPERIMENTAL CONDITIONS : TEMPERATURE

- 1) Clinoptilolite was selected to observe the effect on  $\beta$ -activity and Th-232 uptakes with variations of temperature.

#### METHOD

Clinoptilolite ( $\sim 0.1$ g, weighed accurately) was placed in polyethylene vials. To each sample, thorium nitrate (10.0 ml 0.0418M) was added and the vials were sealed with PTFE tape, capped and rotated (60 revs. per minute) in an oven set at 36°C. After two weeks, equilibration was complete and the vials were removed from the oven and centrifuged for 10 minutes. 5.0 ml aliquots of supernatant were taken for Čerenkov counting and 1.0 ml aliquots were taken for Th-232 analysis by colourimetry, using Morin as the colourimetric reagent.

The experiment was repeated at 57°C and 75°C.

### 5.8.3 VARIATIONS OF EXPERIMENTAL CONDITIONS : CONCENTRATION

- 2) Clinoptilolite was also selected to observe the variation in effective uptakes of Th-232 and  $\beta$ -activity with different thorium tracer solutions, at constant temperature (18°C).

#### METHOD

Batch experiments were conducted as above on 0.1g samples of clinoptilolite (weighed accurately) but using various thorium nitrate concentrations (10.0 ml) as follows:  
0.0418M, 0.0209M, 0.0042M, and 0.0021M.

After two weeks equilibration, the vials were centrifuged and aliquots of supernatant were removed for analysis:

5.0 ml aliquots were removed for Čerenkov Analysis ( $\beta$ -emitters)

1.0 ml aliquots were taken for Th-232 analysis by colourimetry using Morin as the colourimetric reagent.

The different concentrations of thorium (mentioned above) were used to investigate the uptake of thorium on Ferrierite, Eastgate and Chabazite 3.

#### 5.8.4 Th-234 UPTAKE ON CLINOPTILOLITE, PHILLIPSITE, CHABAZITE 3

##### METHOD

Simple batch experiments as in section 5.8.1 were conducted on the three zeolites Phillipsite, Chabazite 3, and Clinoptilolite. The clinoptilolite was of two mesh sizes 1) between 106-150 $\mu$ m and 2) less than 106 $\mu$ m. A Th-234 tracer solution (10.0 ml) that had been solvent extracted from U-238, was placed in contact with approximately 0.1g zeolite (weighed accurately). The Th-234 tracer solution was present in 6M nitric acid i.e. pH  $\leq$  0. The zeolites were in contact with this solution for a maximum of 51 hours. At various time intervals a 5.0 ml aliquot was taken for Čerenkov counting after centrifugation of the solution from the zeolite.

#### 5.8.5 TEN-HOUR UPTAKE TESTS

Zeolite ( $\sim$ 0.1g, weighed accurately) was placed in polyethylene vials. The following zeolites were used: Clinoptilolite, Phillipsite, Chabazite 3, Erionite.

Thorium nitrate tracer solution (10.0 ml, 0.0418M) was added to each vial and twenty such vials for each different zeolite were prepared and capped. The vials were labelled, placed in a drum on a mineralogical roller for a maximum of ten hours. At half-hour intervals, a vial from each zeolite category was removed, centrifuged and aliquots of the supernatant removed in duplicate. The aliquots were either counted by Čerenkov counting techniques for Ra-228 and Ac-228 or analysed by colourimetry for Th-232 using Morin as the reagent.

### 5.9.1 UPTAKE EXPERIMENTS : U-238 ON SELECTED ZEOLITES

#### METHOD

Batch experiments were conducted on zeolites listed in TABLE 19 as in section 5.8.1. Approximately 0.1g zeolite (weighed accurately) was placed in a polyethylene vial and a 0.01N solution of  $\text{UO}_2^{2+}$  was added (10.0 ml). After equilibration (2 weeks), the vials were centrifuged and aliquots of supernatant were taken for colourimetric analysis of uranium, using hydrogen peroxide as the colourimetric reagent, as in section 5.5.5.

### 5.9.2 UPTAKE EXPERIMENTS FOR ZEOLITES AND URANIUM $\beta$ -EMITTER DAUGHTERS

#### METHOD

Batch experiments were conducted on zeolites NaY, Na-Z900 and Clinoptilolite as in section 5.8.1. Approximately 0.1g zeolite (weighed accurately) was placed in a polyethylene vial and a 500ppm uranium solution (10.0 ml) was added and the exact procedure as in section 5.8.1 followed. After equilibration, the vials were centrifuged and 5.0 ml aliquots of supernatant were removed for Čerenkov counting.

### 5.9.3 EXPERIMENTS TO SHOW THE EFFECT OF NITRIC ACID CONCENTRATION ON THE UPTAKE OF U-238 $\beta$ -EMITTER DAUGHTERS ON ZEOLITES

#### METHOD

Three uranium nitrate solutions were prepared in nitric acid solution as follows:

- 1) Uranyl nitrate (0.0954g) was dissolved in nitric acid (0.01N) in a 50 ml volumetric flask. The solution was then made up to the mark with 0.01N nitric acid giving a 452ppm U solution.
- 2) Uranyl nitrate (0.1036) was dissolved in nitric acid (0.1N) in a 50 ml volumetric flask. The solution was then made up to the mark with 0.1N nitric acid, giving a 491ppm U solution.
- 3) A 512ppm U solution was prepared in 0.5N nitric acid as in 1) and 2).

Using these 3 solutions in 10.0 ml portions respectively on ~0.1g (weighed accurately) Clinoptilolite, NaY and NaZ900, batch experiments were conducted as in section 5.8.1. After equilibration, the samples were centrifuged and 5.0 ml aliquots of supernatant from each sample were taken and counted by the Čerenkov method.



## 5.10 COMPETING ION EFFECTS

### 5.10.1 EXPERIMENTS TO DETERMINE THE EFFECT OF COMPETING IONS ON THE UPTAKE OF Ra-228/Ac-228 ON ZEOLITES

The plant raffinate contains ions other than thorium and its daughters, so a study was undertaken to see the effect of different concentrations of competing cations on the uptake of the Th-232  $\beta$ -emitter daughters.

#### EXPERIMENTAL

A selection of zeolites (SEE TABLE 21) (approximately 0.1g, weighed accurately) were placed in separate plastic vials. Thorium tracer solutions (0.169M) were prepared containing various amounts of competing cations (shown in TABLE 21) and were added (10.0 ml aliquots) to the zeolites. The batch equilibration procedure in section 5.8.1 was followed. After an equilibration period of about 2 weeks the vials were centrifuged and 5.0 ml aliquots of supernatant were removed for Čerenkov counting.

TABLE 21

ZEOLITE	COMPETING CATION	CATION CONCENTRATION/ppm
CLINOPTILOLITE	Na <sup>+</sup>	10 <sup>4</sup>
	K <sup>+</sup>	4 x 10 <sup>2</sup>
CHABAZITE 3	Na <sup>+</sup>	10 <sup>4</sup>
	K <sup>+</sup>	4 x 10 <sup>2</sup>
CHABAZITE	Na <sup>+</sup>	10 <sup>4</sup>
	K <sup>+</sup>	4 x 10 <sup>2</sup>
5050L	Na <sup>+</sup>	10 <sup>4</sup>
FERRIERITE	Na <sup>+</sup>	10 <sup>4</sup>
1010A	Na <sup>+</sup>	10 <sup>4</sup>
ERIONITE	Na <sup>+</sup>	10 <sup>4</sup>
PHILLIPSITE	Na <sup>+</sup>	10 <sup>4</sup>
EASTGATE	K <sup>+</sup>	4 x 10 <sup>2</sup>

### 5.10.2 EFFECT OF THE UPTAKE OF Th-232 BY VARYING CONCENTRATIONS OF COMPETING IONS

#### METHOD

The method used in section 5.8.1 was used for clinoptilolite, Z900, Eastgate, NaY. These zeolites were treated with the solutions (10.0 ml) shown below:

- 1)  $\text{Na}^+:\text{Th}^{4+} = 1:1$ , where 1 unit represents 500 ppm of respective ion.
- 2)  $\text{Na}^+:\text{Th}^{4+} = 2:1$
- 3)  $\text{K}^+:\text{Th}^{4+} = 1:1$
- 4)  $\text{K}^+:\text{Th}^{4+} = 2:1$
- 5)  $\text{H}^+:\text{Th}^{4+} = \text{A}$  1000 ppm thorium solution prepared with 0.1 N  $\text{HNO}_3$
- 6)  $\text{H}^+:\text{Th}^{4+} = \text{B}$  1000 ppm thorium solution prepared with 0.5 N  $\text{HNO}_3$ .

After an equilibration period of 2 weeks the samples were centrifuged and 1.0 ml aliquots of supernatant were removed for Th-232 analysis by colourimetry, using Morin.

### 5.10.3 EFFECTS OF $\text{H}^+$ , $\text{Na}^+$ , $\text{K}^+$ , $\text{Ca}^{2+}$ , $\text{Mg}^{2+}$ and $\text{Al}^{3+}$ ON THE UPTAKE OF Th-232 ON CLINOPTILOLITE AND Z900

Stock solutions of the cations  $\text{Na}^+$ ,  $\text{K}^+$ ,  $\text{Ca}^{2+}$ ,  $\text{Mg}^{2+}$  and  $\text{Al}^{3+}$  were prepared (0.1N) and a 0.1N stock solution of  $\text{Th}^{4+}$  was prepared in nitric acid (0.5M).

Zeolite (approximately 0.1g, weighed accurately) was placed in polyethylene vials. The stock cation solutions and acidic thorium solution was added to the zeolite in the following proportions:

CATION STOCK 0.1N/CC	Th-232 ACIDIC STOCK 0.1N/CC	VIAL NUMBER
0.00	20.00	1
2.00	18.00	2
4.00	16.00	3
6.00	14.00	4
8.00	12.00	5
10.00	10.00	6
12.00	8.00	7
14.00	6.00	8
16.00	4.00	9
18.00	2.00	10

thus keeping the total normality the same but varying the proportions of thorium, cation and acid in the solutions.

The vials were then sealed with PTFE tape and placed in a drum on a mineralogical roller for a period of 2 weeks. After this period of time, the vials were centrifuged and an aliquot of the supernatant was removed for analysis by EDTA (disodium salt) direct titration of pH = 2.6, using xylenol orange as the indicator.

## 5.11 SIMULATED RAFFINATE SOLUTIONS

A set of experiments were designed in order to test some of the screened zeolites for thorium uptake in the presence of all the competing cations contained within the plant raffinate [SEE FIG. 2]. Four solutions of the specific ion concentrations shown in TABLE 22 were prepared as the actual plant raffinate was of variable composition (within the limits shown in FIG. 2). These solutions were designated SOSIM 1, SOSIM 2, SOSIM 3 and SOSIM 4.

### METHOD

Zeolite (~0.1g, weighed accurately) was placed in polyethylene vials. The zeolites used were clinoptilolite, Z900, NaY, Eastgate and 4A. The SOSIM solution (10.0 ml) was added to each zeolite. (Hence each of the four SOSIM solutions was tested on each zeolite). The vials were sealed, placed in a drum on a mineralogical roller and agitated for 1 week. After this period of time, the vials were removed, checked for leakage and centrifuged for 20 minutes. Duplicate aliquots were taken from each vial, and analysed for Th-232 uptake by colourimetry. A set of standards and a reference solution were prepared by using a 'dummy' stock solution (i.e. a SOSIM solution containing exactly the same constituents as the original solution but not containing thorium).

TABLE 22

SIMULATED RAFFINATE SOLUTION COMPOSITIONS

ION	CONCENTRATIONS/g l <sup>-1</sup>			
	SOSIM 1	SOSIM 2	SOSIM 3	SOSIM 4
Na <sup>+</sup>	2.00	7.00	4.50	-
K <sup>+</sup>	0.10	0.40	0.25	-
Mg <sup>2+</sup>	0.15	0.60	0.37	0.15
Ca <sup>2+</sup>	0.25	1.00	0.62	0.25
Al <sup>3+</sup>	0.30	1.20	0.75	0.30
Fe <sup>3+</sup>	0.25	1.00	0.62	0.25
Th <sup>4+</sup>	0.15	0.80	0.48	0.16
NO <sub>3</sub> <sup>-</sup>	20.00	80.00	49.40	20.00

CHAPTER 6

EXPERIMENTAL II

## 6.1 COLUMN EXPERIMENTS

Column tests were run on zeolites (clinoptilolite, Z900, CaY, Eastgate) in order to observe uptake of thorium, where a potentially infinite source of thorium was available to simulate an industrial process.

### 6.1.1 PROCEDURE

A Pyrex glass column was made from a 10.0cm length of 1.0cm (inside diameter) precision glass tubing. A glass condenser jacket was fitted around the tube and a medium-course glass sinter fixed at one end of the tube. The column arrangement was as in FIGURE 26. The volume of the column and all tubing was observed by pumping through enough deionized water to fill all void space and this volume was obtained using a measuring cylinder at the outlet of the column set up in place of the fraction collector. Thorium solution (1000 ppm  $\text{Th}^{4+}$ ) was prepared and placed in the column reservoir as in the diagram. A GILSON MINIPULS 2 4-channel, high precision peristaltic pump was used to pump the solution into the column at a flow rate of 20 ml per hour. The column outlet tube was attached to an LKB REDIRAC 2112 fraction collector which was fitted with 40 polyethylene vials per rack.

The reservoir, pump, column and fraction collector were linked by silicone tubing.



## Column Arrangement

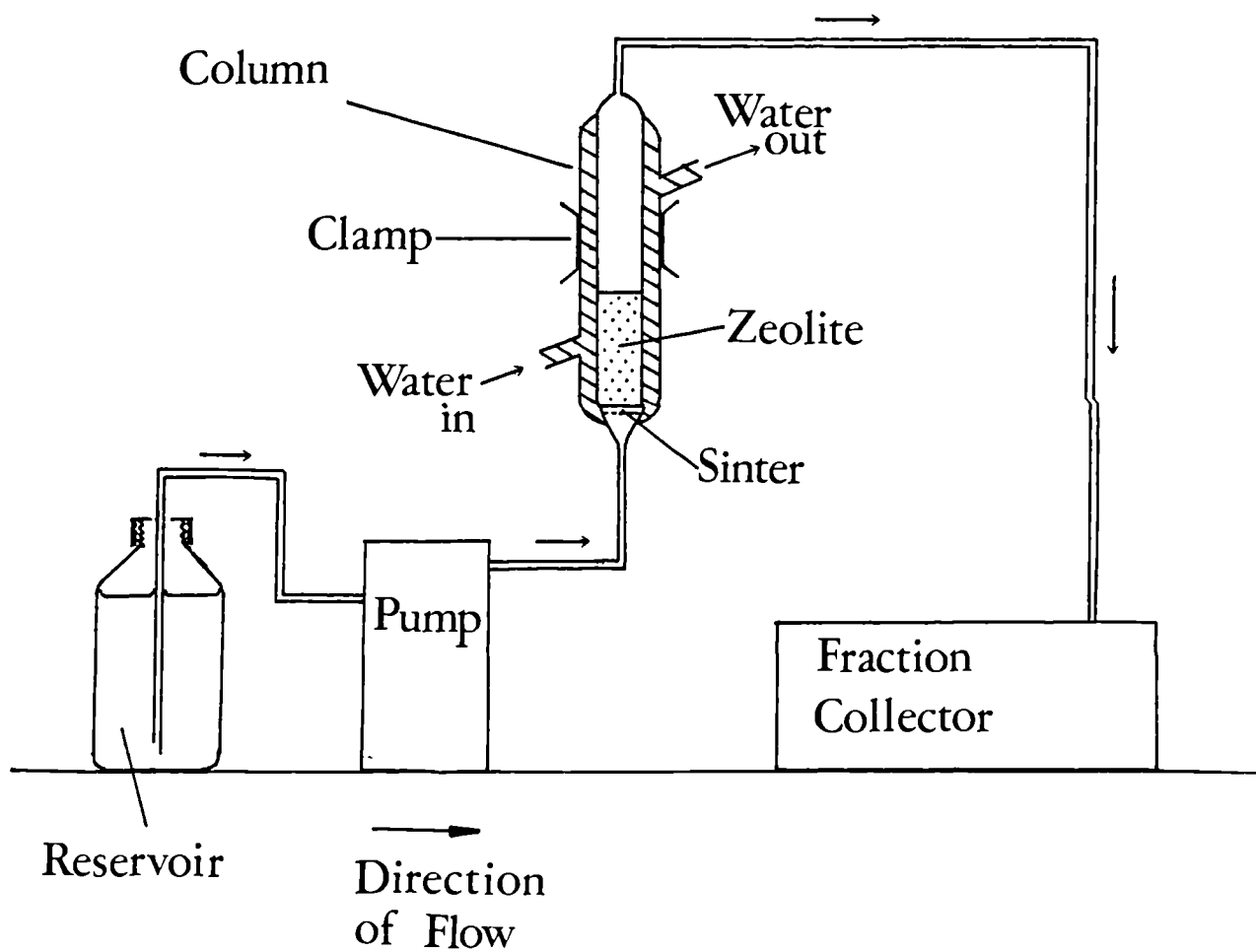


Fig. 26.

~3.0g (weighed accurately) zeolite was slurried into the column with deionized water. Deionized water was pumped into the column from a measuring cylinder and the total volume of water to fill the column and tubing was noted. Deionized water (500 ml) was pumped through the column overnight to ensure that very little air remained between the particles of zeolite. This was known as pre-conditioning the zeolite.

#### 6.1.2 FREE COLUMN VOLUME

~3.0g (weighed accurately) zeolite (particle size 150-250 $\mu$ m) was placed in a 10cm<sup>3</sup> measuring cylinder of approximate inside diameter 1cm. In to this was pipetted 5.0cm<sup>3</sup> of deionized water ( $V_3$ ). The cylinder was capped and shaken to elute as much air as possible from between the zeolite particles. The cylinder was left to stand for 12 hours and, after ensuring as much air as possible had been eluted from the solid by gentle tapping of the cylinder, the volume of wetted solid ( $V_1$ ) and solid plus supernatant ( $V_2$ ) were noted.

The BED VOLUME was approximated to  $V_1$  in cm<sup>3</sup>.

The FREE COLUMN VOLUME =  $V_3 - (V_2 - V_1)$  / all in cm<sup>3</sup>.

#### 6.1.3 COLUMN EXPERIMENT

The inlet tube from the pump was now attached to the thorium reservoir (the fraction collector had previously been calibrated using a 5.0 ml volumetric flask and an infra-red drop counter to collect 5.0 ml of eluted solution in each vial). The first 35 cm<sup>3</sup> of solution collected on the fraction collector was

assumed to be deionized water. After this volume had been eluted all 5.0cm<sup>3</sup> fractions of eluted solution were counted by the Čerenkov counting technique and aliquots were taken for EDTA titration.

In this way, the percentage removal of thorium daughters and the thorium-232 removal from solution could be assessed.

The results were expressed as break-through curves by plotting concentration, or percentage of detected species in the effluent 'vs' eluted volume.

#### 6.1.4 VARIATIONS OF COLUMN EXPERIMENTS

Certain experiments involved the uptake of thorium with nitric acid present. In cases such as this, the zeolite in the column was preconditioned with the appropriate nitric acid concentration (500 ml) of the experiment prior to the addition of any thorium solution in nitric acid.

Some column experiments were designed to remove the thorium which may have been deposited on the zeolite by ion-exchange with solutions of sodium nitrate or acid. The conditions for each experiment may be found in TABLE 23.

A column experiment could not be conducted for NaY as this zeolite was in a powdered form and the medium-to-course sinter was not able to contain the zeolite. A fine sinter and fine-to-medium sinter was prone to clogging. A form of binderless beads of CaY (Laporte Inorganic, Widnes) was available for use and this was used as a substitute for NaY.

The solids remaining at the end of the column experiments were filtered, washed with deionized water and dried. Portions of some of the zeolites were taken for  $\gamma$ -spectrometry, EPMA and/or XRD analysis.

TABLE 23

COLUMN EXPERIMENT CONDITIONS

ZEOLITE MASS AND MESH SIZE	PRE-CONDITION SOLUTION (500 ml)	INFLUENT SOLUTION AND ISOTOPE	FURTHER CONDITIONS OF EXPERIMENT AFTER LOADING THORIUM ON COLUMN
CLINOPTILOLITE 3.01g (150-250 $\mu$ m)	HNO <sub>3</sub> (1M)	Th <sup>4+</sup> (750ppm) in HNO <sub>3</sub> (1M) Th-232.	50ml DEIONIZED WATER 500ml NaNO <sub>3</sub> (1M)
CLINOPTILOLITE 2.99g (150-250 $\mu$ m)	HNO <sub>3</sub> (0.5M)	Th <sup>4+</sup> (750ppm) in HNO <sub>3</sub> (0.5M) Th-232	
CLINOPTILOLITE 300g (150-250 $\mu$ m)	HNO <sub>3</sub> (0.6M)	Th <sup>4+</sup> (1000ppm) in HNO <sub>3</sub> (0.6M) Th-234	
NaZ900 3.00g (150-250 $\mu$ m)	HNO <sub>3</sub> (0.5M)	Th <sup>4+</sup> (1000ppm) in HNO <sub>3</sub> (0.5M) Th-234	
NaZ900 3.01g (150-250 $\mu$ m)	HNO <sub>3</sub> (0.1M)	Th <sup>4+</sup> (1000ppm) in HNO <sub>3</sub> (0.1M) Th-232	
CaY 3.00g (binderless)	HNO <sub>3</sub> (0.1M)	Th <sup>4+</sup> (1000ppm) in HNO <sub>3</sub> (0.1M) Th-232	150ml DEIONIZED WATER 300ml 0.01N K <sup>+</sup> HCl (1%).
CLINOPTILOLITE 3.01g (150-250 $\mu$ m)	HNO <sub>3</sub> (0.5M)	Th <sup>4+</sup> (999ppm) AQUEOUS Th-232	
CLINOPTILOLITE 3.02g (>150 $\mu$ m)	DEIONIZED WATER	Th <sup>4+</sup> (999ppm) AQUEOUS Th-232	
EASTGATE 3.01g (<150 $\mu$ m)	DEIONIZED WATER	Th <sup>4+</sup> (999ppm) AQUEOUS Th-232	

## 6.2 ISOTHERM EXPERIMENTS : THORIUM

Zeolites used in these experiments were previously exchanged to the homoionic cation form i.e.  $K^+$  or  $Na^+$  depending on whether the cation stock solution in the experiment was  $K^+$  or  $Na^+$ .

e.g. for the binary mixture  $Th^{4+}/K^+$  being used on clinoptilolite the zeolite must be in the  $K^+$  - Clinoptilolite form.

All isotherm experiments were conducted at 18°C.

### METHOD

A set of thorium stock solutions (0.1N, 0.01N, 0.001N) were prepared using AnalaR-grade thorium nitrate. 0.1N, 0.01N and 0.001N stock solutions of  $K^+$  and  $Na^+$  were also prepared from their nitrate salts (AnalaR).

For each different isotherm experiment, 22 polyethylene vials were used. Approximately 0.2g, homoionic zeolite (weighed accurately) was placed in each of 11 vials. The following proportions of stock solution of thorium and metal cation (of equal normality) were added, from a burette, to the zeolite so that the total normality and total volume remained the same:

VIAL NUMBER	VOLUME OF Th <sup>4+</sup> /CC	VOLUME OF CATION/CC
1	20.0	0.0
2	18.0	2.0
3	16.0	4.0
4	14.0	6.0
5	12.0	8.0
6	10.0	10.0
7	8.0	12.0
8	6.0	14.0
9	4.0	16.0
10	2.0	18.0
11	0.0	20.0

The remaining 11 vials contained the same proportions of liquid but no zeolite was added and these were used as controls for counting and colourimetry standards.

Each vial was sealed with PTFE tape, capped and placed in a drum on a mineralogical roller. The vials were thus agitated for 2 weeks. The vials were then centrifuged, a portion of the supernatant taken for thorium analysis (and in some cases metal cation analysis) and in other cases the solids were filtered off and a wet chemical analysis conducted on them.

TABLE 24 lists the various conditions peculiar to each experiment conducted and also lists the type of analysis conducted to obtain results.

#### 6.2.1 REPEATED AND REVERSIBLE EXCHANGES

A selected number of samples were taken for further experimentation to see if the ion-exchange process was reversible and also to observe what the maximum exchange was. The first vial which contained thorium solution (20.0cc) after centrifugation was selected in order to observe further exchange. The supernatant was decanted from the solid and a further 20.0cc portion of thorium solution was added. The vial was re-sealed, shaken and placed in a drum on a mineralogical roller for a further 2 week equilibration period.

Vials 3, 7 and 9 were selected for reversibility experiments after removing aliquots of the supernatant for analysis at the end of the first two week equilibration period. The remaining supernatant from each vial was decanted and 20.0cc of the relevant cation solution was added to each vial. The vials were re-sealed, shaken and placed in a drum on a mineralogical roller for a period of two weeks. The vials containing the repeated exchange and reversibility samples were then centrifuged and portions of supernatant removed for analysis of thorium by colourimetry using Morin as the reagent and thorium daughters by the Čerenkov counting technique.

TABLE 24  
EXPERIMENTAL CONDITIONS FOR THORIUM ISOTHERM EXPERIMENTS

ZEOLITE	Th <sup>4+</sup> /N	Na <sup>+</sup> /N	K <sup>+</sup> /N	ANALYSIS FOR
Na-Clinoptilolite	0.100	0.100	—	Th-232 Th-DAUGHTERS*
Na-Clinoptilolite	0.010	0.010	—	Th-232 Th-DAUGHTERS
Na-Clinoptilolite	0.001	0.001	—	Th-232 Th-DAUGHTERS
K-Clinoptilolite	0.100	—	0.10	Th-232 Th-DAUGHTERS
K-Clinoptilolite	0.010	—	0.01	Th-232 Th-DAUGHTERS
K-Clinoptilolite	0.001	—	0.001	Th-232 Th-DAUGHTERS
NaY	0.01	0.01	—	Th-232 Th-DAUGHTERS
KY	0.01	—	0.01	Th-232 Th-DAUGHTERS
NaZ900	0.01	0.01	—	Th-232 Th-DAUGHTERS
KZ900	0.01	—	0.01	Th-232, K <sup>+</sup> , Th-232, Th-DAUGHTERS
Eastgate	0.01	0.01	—	Th-232 Th-DAUGHTERS

\* The solids from samples 1, 3, 5 and 9 were taken for wet chemical analysis for their thorium-232 and thorium daughter content. Sample 3 was lost during experimentation, see section 6.3



### 6.2.2 ISOTHERM EXPERIMENTS : URANIUM

#### METHOD

The experiments using uranium-238 solutions were conducted in exactly the same way as those for thorium solution isotherms, the only difference being that all normalities of uranium solutions and metal cation stock solutions were fixed at 0.01N. TABLE 25 shows all experimental conditions and analysis methods used to construct the isotherm plot in the case of U-238 determination by colourimetry and a plot of total activity in solid 'vs' total activity in solution determined by liquid scintillation counting results.

Repeated exchange and reversibility experiments were conducted as for the thorium experiments [SEE SECTION 6.2.1].

### 6.3 WET CHEMICAL ANALYSIS OF THE SOLIDS FROM ISOTHERM EXPERIMENTS

These experiments used approximately 0.2g of zeolite.

#### METHOD

Isotherm experiments were conducted as in section 6.2. After the removal of aliquots of supernatant for thorium-232, thorium daughter and metal cation analysis, the solid was filtered from the solution and briefly washed with 3 x 1 ml portions of deionized water. The solids and filter papers were allowed to dry in air. When dry the solids were carefully

TABLE 25  
EXPERIMENTAL CONDITIONS FOR URANIUM ISOTHERM EXPERIMENTS

ZEOLITE	BINARY MIXTURE TESTED (ALL FIXED AT 0.01N)	ANALYSIS METHOD FOR SOLUTION	
		COLOURIMETRY (U-238)	LSC (TOTAL ACTIVITY)
K-CLINOPTILOLITE	$\text{UO}_2^{2+} / \text{K}^+$	✓	✓
Na-CLINOPTILOLITE	$\text{UO}_2^{2+} / \text{Na}^+$	✓	✓
K-Z900	$\text{UO}_2^{2+} / \text{K}^+$	✓	✓
Na-Z900	$\text{UO}_2^{2+} / \text{Na}^+$	✓	✓
K-Y	$\text{UO}_2^{2+} / \text{K}^+$	✓	✓
NaY	$\text{UO}_2^{2+} / \text{Na}^+$	✓	✓

removed from the filter papers in a fume cupboard equipped to deal with particulate radioisotope materials and were then placed in a desiccator containing saturated sodium chloride, for two weeks, prior to chemical analysis.

The water equilibrated solids were then removed from the desiccator and were carefully placed in porcelain evaporating dishes which had been pre-weighed. The evaporating dishes were then reweighed to obtain the weight of each of the solids. Hydrochloric acid (AnalaR, 30 ml, 50%) was added to each evaporating dish. The dishes were placed on a sand bath in a fume cupboard and the hydrochloric acid was allowed to boil for 5 hours, after large watch-glasses had been placed over the evaporating dishes. After this time the concave surfaces of the watch-glasses were carefully washed into the evaporating dishes with deionized water. The hydrochloric acid was then allowed to evaporate overnight. This procedure of boiling and evaporation was repeated three times. After the final evaporation, hydrochloric acid (AnalaR, 50 ml, 5%) was added to each dish. A pale yellow solution above some white solid was noted. This was then filtered through a 541 WHATMAN filter paper into a 100 ml volumetric flask. The evaporating dish was then thoroughly washed into the filter paper with several portions (3 x 10 ml) of deionized water. The filtrate was then made up to the mark with deionized water. The solution was then analysed for thorium-232 by colourimetry using Morin as the colourimetric reagent.

#### 6.4 STRIPPED RAFFINATE SOLUTIONS

The plant raffinate (supplied by BNF plc, Springfields) had been solvent extracted to remove Th-234 and Th-232. The composition of this solution, which was a clear, brown colour is shown in FIGURE 27, where FREE ACID represents the nitric acid concentration.

Batch experiments were conducted on this solution and a Th-232-spiked form of the plant raffinate. The solution contained fluoride ions which are known to complex with thorium. A fluoride determination was carried out on some samples in order to show whether thorium had precipitated as  $\text{ThF}_4$ .

##### 6.4.1 EXPERIMENTAL

###### a) BATCH EXPERIMENTS

Thorium nitrate hexahydrate (0.999g) was dissolved in stripped plant raffinate (~100 ml) and was made up to 500 ml in a volumetric flask with the stripped plant raffinate. This solution was designated R1. From this solution, several raffinate solutions were prepared with varying pH by the addition of alkaline reagents. These solutions, their pH and the reagents used to prepare them are shown in TABLE 26.

Batch experiments were conducted, as in section 5.8.1, predominantly on clinoptilolite and NaY (about 0.1g or 0.2g, weighed accurately) using the solutions R1-R7 (10.0 or 20.0 ml respectively). After an equilibration period of between 1 week and 60 days, the vials were centrifuged and aliquots of supernatant were analysed by Čerenkov counting, liquid scintillation counting, taking care to use standards to be able to account for colour quenching, and some samples were taken for  $\gamma$ -spectroscopy.

## Stripped Raffinate Composition.

Composition supplied by H. Greenwood of BNF plc (Springfield).

ION	COMPOSITION/ $\mu\text{g ml}^{-1}$
U	<1
Th	75
Fe	660
Ca	640
Mg	840
Al	540
Mo	5.7
Zr	5.7
Pb	19
F	200
Cl	30
PO <sub>4</sub>	50
ION	COMPOSITION/g 100 ml <sup>-1</sup>
SO <sub>4</sub>	0.63
NO <sub>3</sub>	6.10
FREE ACID	0.08

Fig. 27.

TABLE 26

## VARIOUS RAFFINATE SOLUTIONS

SOLUTION	pH	REAGENT USED	APPEARANCE OF SOLUTION AFTER:	
			24 HOURS	2 WEEKS
R1	0	-	CLEAR BROWN	CLEAR BROWN
R2	1.5	SOLID HEXAMINE 3.0g	CLEAR BROWN	CLOUDED BROWN SOLUTION
R3	3.0	SOLID HEXAMINE 5.0g	CLOUDY BROWN	BROWN PRECIPITATE
R4	1.0	SOLID HEXAMINE 1.0g	CLOUDY BROWN	BROWN PRECIPITATE
R5	1.5	NaOH (1M, 16 ml)	CLOUDY BROWN	BROWN PRECIPITATE
R6	1.5	Na <sub>2</sub> CO <sub>3</sub>	CLOUDY BROWN	BROWN PRECIPITATE
R7	2.0	NaOH (1M, 19 ml)	CLOUDY BROWN	BROWN PRECIPITATE

#### 6.4.2 FLUORIDE DETERMINATION

b) The use of a 940900 ORION fluoride electrode and reference electrode in conjunction with an ORION MODEL 901 ion analyser will not be explained here but it is necessary to say that due to the nature of the solutions to be analysed, a Total Ionic Strength Adjustment Buffer was used with all standards and samples. Samples tested for the fluoride ion in solution were as follows:

- A. Raffinate (stripped, as received).
- B. Clinoptilolite (1.0g) with Raffinate (50.0 ml).
- C. NaY (1.0g) with Raffinate (50.0 ml).
- D. Clinoptilolite (1.0g) with R1 solution (50.0 ml).
- E. NaY (1.0g) with R1 solution (50.0 ml).

(These samples had been equilibrated for two weeks).

## 6.5 X-RAY POWDER DIFFRACTION (XRD)

X-Ray powder diffractograms were obtained for several purposes:

- a) to characterize some of the natural and synthetic zeolites used in this work.
- b) to observe losses in crystallinity created by contact with thorium solutions and/or acidic solutions.
- c) to observe any peaks due to the presence of  $\text{ThO}_2$  or other unidentified peaks with respect to the zeolite itself.

The X-ray powder diffractograms were obtained on two machines:

A SIEMENS D500 X-RAY DIFFRACTOMETER (British Alcan)

PHILIPS PW SERIES

(University of Salford)

Both machines used  $\text{Cu K } \alpha$  radiation.

The following X-ray diffractograms of zeolites were obtained.

TABLE 27

ZEOLITE	COMMENTS
Eastgate	Natural zeolite, background subtracted.
Th-Eastgate	Eastgate treated with 1000ppm $\text{Th}^{4+}$ . Background subtracted (column zeolite).
Clinoptilolite	Natural Zeolite.
Th-Clinoptilolite	Clinoptilolite treated with 1000ppm $\text{Th}^{4+}$ (column zeolite).
Na Z900	Synthetic zeolite
Th Z900	Z900 treated with 1000ppm $\text{Th}^{4+}$ (column zeolite).
NaY	Synthetic zeolite.
Erionite	Natural zeolite.
Mordenite	Natural zeolite.
Ferrierite	Natural zeolite.



## 6.6 ELECTRON PROBE MICROANALYSIS (EPMA)

### EXPERIMENTAL CONDITIONS

A JEOL 733 Electron Probe Microanalyser was used which was equipped with a Link Analytical energy dispersive X-ray detector. The electron beam conditions used to obtain X-ray spectra was 15kV with a probe current of  $3 \times 10^{-9}$  A.

Secondary electron images were obtained using a beam voltage of 15kV and a lower current  $\sim 10^{-10}$  A.

TABLE 28

<u>SAMPLES: (X-RAY SPECTRA)</u>	<u>COMMENTS</u>
1) Clinoptilolite treated with Th-232 on a column. (Column unwashed).	Analysis of the area of a typical particle.
2) Clinoptilolite treated with Th-232 on a column. (Column unwashed).	Analysis of the bright area on a particle.
3) Eastgate treated with Th-232 on a column. (Column acid-washed).	
4) Z900 treated with Th-232 on a column. (Column acid-washed).	
5) CaY treated with Th-232, in nitric acid, on a column. (Column unwashed)	
6) Clinoptilolite treated with Th-232 (0.1N) batch and unwashed.	
7) Clinoptilolite treated with Th-232 (0.1N) batch and unwashed.	Scales Expanded.

## 6.7 DIFFERENTIAL THERMOGRAVIMETRIC ANALYSIS (DTG)

The method of DTG was used to evaluate the equilibrated water content of a zeolite as mentioned in section 5.1.6. Several samples were run on the DTG machine in order to evaluate any changes, with respect to water content of the zeolite, that treatment with thorium solutions may have brought about.

### METHOD

Approximately 25 mg of zeolite sample was placed in a small pre-weighed, silica crucible. This was then placed on a balance pan, attached to a METTLER TG50 Thermobalance, which was then surrounded with a tube furnace. The furnace and thermobalance were linked to a METTLER TC 10A TA processor which allowed the user to programme experimental conditions such as heating rate of the furnace, start and end temperatures etc., which may be seen in the following table. A thermogram and differential thermogravimetric plot were obtained.

### CONDITIONS OF USE

STARTING TEMPERATURE:	(298K)
END TEMPERATURE:	(1023K - 1173K)
HEATING RATE PER MINUTE:	( 20K)

TABLE 29

LIST OF SAMPLES RUN ON DTG MACHINE

SAMPLE	WATER EQUILIBRATION METHOD PRIOR TO ANALYSIS
EASTGATE 2020 - UNTREATED	NaCl (2 WEEKS)
NaCLINOPTILOLITE - HOMOIONIC FORM	NaCl (2 WEEKS)
CLINOPTILOLITE	NaCl (2 WEEKS)
K CLINOPTILOLITE - HOMOIONIC FORM	NaCl (2 WEEKS)
Th(OH) <sub>4</sub> - PREPARED IN THE LABORATORY	NONE
CLINOPTILOLITE TREATED WITH THORIUM NITRATE SOLUTION (1000ppm)	NONE
CLINOPTILOLITE PHASE A*(powdery phase)	NONE
CLINOPTILOLITE PHASE B*(caked sample)	NONE
NaY REPEATEDLY TREATED WITH 0.1N THORIUM SOLUTION	NONE
NaY	NONE

- \* A Thorium-treated Clinoptilolite sample was observed to produce two physical phases on drying in an oven at 100°C for 3 hours. The powdery phase and the caked phase were separated. A sample of each was run on the DTG machine.

## 6.8 $\gamma$ -SPECTROMETRY

$\gamma$ -Spectrometry was used to analyse both solid and liquid samples for the qualitative presence of Th-232, Th-234 and their respective daughters.

### METHOD

The sample was contained in a low-background polyethylene vial. This was placed in the centre of the base of a PRINCETON GAMMATECH lead castle. The lid was placed on the castle. A GeLi semiconductor crystal was used as the detector. The detector was linked to a CANBERRA PACKARD SERIES 35 Multichannel Analyser. The energy scale of the multichannel analyser had to be calibrated [SEE APPENDIX I] using a  $^{22}\text{Na}$  sealed source prior to each sample run to minimize drift, as the samples required long running times of the order of 14 - 25 hours each.

A background  $\gamma$ -spectrum was also taken and the results subtracted from any sample spectrum run.

### TABLE 30 SAMPLES ANALYSED FOR $\gamma$ -PEAKS

#### SOLUTIONS

Th-234 Extracted from U-238.

Th-232 Extracted from its daughters.

Th-232-DAUGHTERS Extracted from Th-232.

Solution R1.

Control Solution  $\text{Na}^+:\text{Th}^{4+}$  (0.1N) from isotherm:Na Clinoptilolite.

Equilibration solution  $\text{Na}^+:\text{Th}^{4+}$  (0.1N) isotherm solution.

SAMPLES ANALYSED FOR  $\gamma$ -PEAKS (continued)SOLIDS

Acid Washed Eastgate (column)	Th-232
Clinoptilolite : Acid Washed (column)	Th-232
Clinoptilolite : Acid Washed (column)	Th-234
Raffinate-Treated Zeolite	Th-232/Th-234
Isotherm Solid Th-Clinoptilolite	Th-232

## 6.9 $\beta$ -SPECTROMETRY

$\beta$ -Spectrometry involved modifications to the use of a CANBERRA PACKARD SERIES 35 Multichannel Analyser in conjunction with an SL30 Intertechnique Automatic Liquid Scintillation Counting system. No automatic calibration was possible and the full procedure of determining end channels and their conversion to energies is shown in APPENDIX II.

### METHOD

The sample solution (10.0 ml) was pipetted into a counting vial and placed in the liquid scintillation counter. The sample was lowered into the detector well. A spectrum of the sample was collected and displayed on the multichannel analyser screen. A background spectrum of each respective vial containing sample solution but no thorium, was taken and subtracted from the spectrum of the sample.

The samples used and the operating conditions used are listed below.

TABLE 31

ISOTOPE	COUNTING TIME/S	COUNTING MEDIUM	VIAL TYPE	$E_{\max}$ /keV.	COUNTING CHANNEL
C-14	1500	COCKTAIL	GLASS	146.0	C-14
H-3	1500	COCKTAIL	GLASS	18.6	C-14
Tl-204	1000	WATER	PLASTIC	763.5	H-3
Th-234	1000	WATER	PLASTIC	191.0	H-3

#### 6.10 SCANNING ELECTRON MICROSCOPY (SEM)

Scanning electron micrographs were obtained as a direct result of the use of EPMA [See Section 6.6]. Scanning electron micrographs were obtained of samples 1-6 in TABLE 28 and the results may be seen in the photographic plates 1-3 at the end of Chapter 7.

## CHAPTER 7

### RESULTS



TABLE 32

ZEOLITE WET CHEMICAL ANALYSIS

OXIDE	% OXIDE:		MOLES/100g ZEOLITE:	
	EASTGATE	CLINOPTILOLITE	EASTGATE	CLINOPTILOLITE
SiO <sub>2</sub>	58.43	64.23	0.9726	1.0990
Al <sub>2</sub> O <sub>3</sub>	13.78	10.61	0.1353	0.1030
Na <sub>2</sub> O	1.49	2.71	0.0240	0.0524
K <sub>2</sub> O	2.46	2.84	0.0261	0.0192
CaO	5.45	2.42	0.0972	0.0280
Fe <sub>2</sub> O <sub>3</sub>	1.97	0.72	0.0332	0.0070
MgO	2.45	0.16	0.0607	0.0140
TiO <sub>2</sub>	-	-	-	-
MnO	-	0.02	-	0.0038

TABLE 33

EXCHANGE CAPACITIES OF TESTED ZEOLITES

ZEOLITE	EXCHANGE CAPACITY/meq g <sup>-1</sup>			REFERENCE
	KJELDHAL: NH <sub>4</sub> <sup>+</sup> PROBE ION	AlO <sub>2</sub> <sup>-</sup> CONTENT: WET CHEMICAL ANALYSIS	LITERATURE VALUE	
CLINOPTILOLITE	1.68	1.78	1.65	[REF.104]
Z900	2.29	2.17	2.30	[REF.105]
NaY	2.59	3.72	NOT AVAILABLE	[REF.106]
CaY	2.13	[REF.107]	NOT AVAILABLE	[REF.107]

TABLE 34

LEACHING EFFECT OF WATER ON SELECTED ZEOLITES

ZEOLITE	LEACHED ION CONCENTRATIONS/meq g <sup>-1</sup>		
	K <sup>+</sup>	Na <sup>+</sup>	Al <sup>3+</sup>
SODIUM Y	0	3.57x10 <sup>-3</sup>	0
SODIUM Z900	0	1.74x10 <sup>-3</sup>	0
CLINOPTILOLITE	6.50x10 <sup>-4</sup>	3.15x10 <sup>-3</sup>	6.67x10 <sup>-2</sup>
EASTGATE	1.65x10 <sup>-3</sup>	2.83x10 <sup>-3</sup>	6.11x10 <sup>-2</sup>

TABLE 35

LEACHING EFFECT ON ZEOLITES TREATED WITH ACID SOLUTION

ZEOLITE	[HNO <sub>3</sub> ] /N	[K <sup>+</sup> ] /meq	[Na <sup>+</sup> ] /meq
Z900	0.1	0	0.135
	0.5	0	0.143
EASTGATE	0.1	2.5x10 <sup>-3</sup>	0.087
	0.5	0	0.130
CLINOPTILOLITE	0.1	5.0x10 <sup>-3</sup>	0.087
	0.5	1.5x10 <sup>-2</sup>	0.096
NaY	0.1	0	0.326
	0.5	0	0.326

TABLE 36

LEACHING EFFECT ON ZEOLITES TREATED WITH THORIUM SOLUTIONS

ZEOLITE	[Th]/ppm	[K <sup>+</sup> ] /meq	[Na <sup>+</sup> ] /meq
Z900	5	-	$1.08 \times 10^{-3}$
EASTGATE	5	-	-
CLINOPTILOLITE	5	-	-
NaY	5	-	-
Z900	100	0	0.017
EASTGATE	100	$1.15 \times 10^{-3}$	0.040
CLINOPTILOLITE	100	0	0.047
NaY	100	0	0.020

TABLE 37

LEACHING EFFECTS ON ZEOLITES TREATED WITH THORIUM SOLUTIONS

ZEOLITE	INITIAL[Th] /ppm	MILLIEQUIVALENT RATIOS:	
		K : Th	Na : Th
Z900	5	-	1.2
EASTGATE	5	0.2	-
CLINOPTILOLITE	5	0.7	-
NaY	5	-	-
Z900	100	-	1.0
EASTGATE	100	0.1	2.4
CLINOPTILOLITE	100	-	2.8
NaY	100	-	1.2

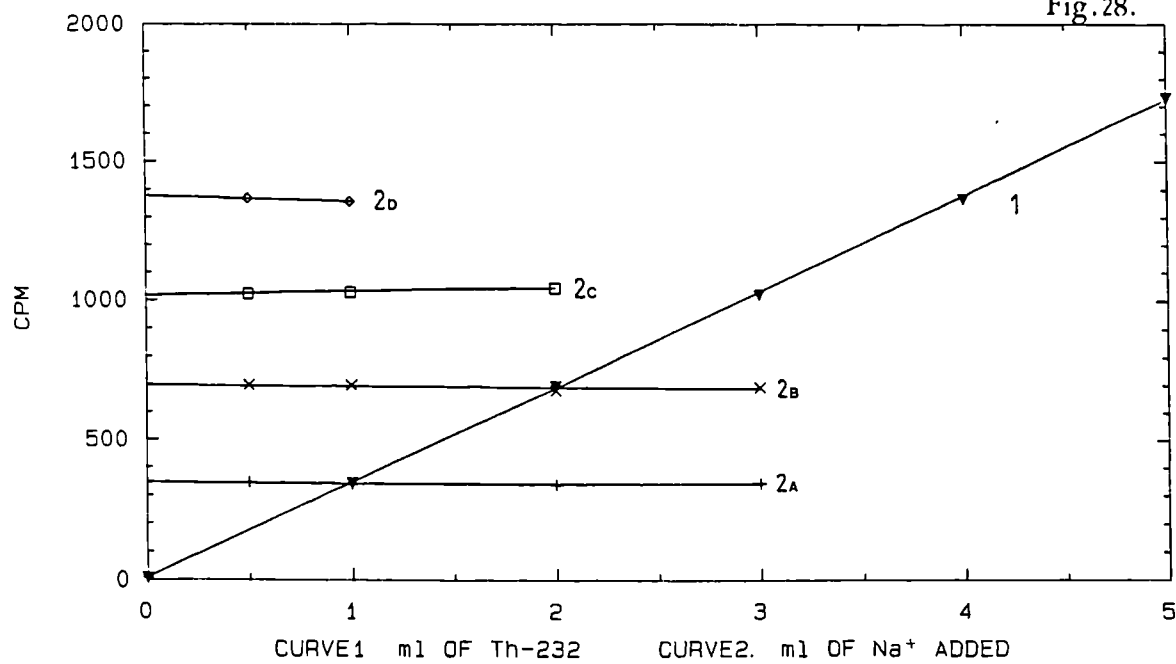
TABLE 38

ANALYSIS FOR  $\text{Na}^+$ ,  $\text{K}^+$  RELEASE AND  $\text{Th}^{4+}$  UPTAKE CONCERNING ZEOLITES CONTACTEDWITH A  $10^3$  ppm  $\text{Th}^{4+}$  SOLUTION

ZEOLITE	MASS OF ZEOLITE/g	% $\text{Th-232}$ REMOVAL FROM SOLUTION	$[\text{Th}^{4+}]$ IN ZEOLITE/meq	$[\text{Na}^+]$ REMOVED FROM ZEOLITE/meq	$[\text{K}^+]$ REMOVED FROM ZEOLITE/meq
CLINOPTILOLITE	1.0802	19.1	0.329	0.743	0.01
NaY	0.9915	100.0	1.724	1.70	0.00

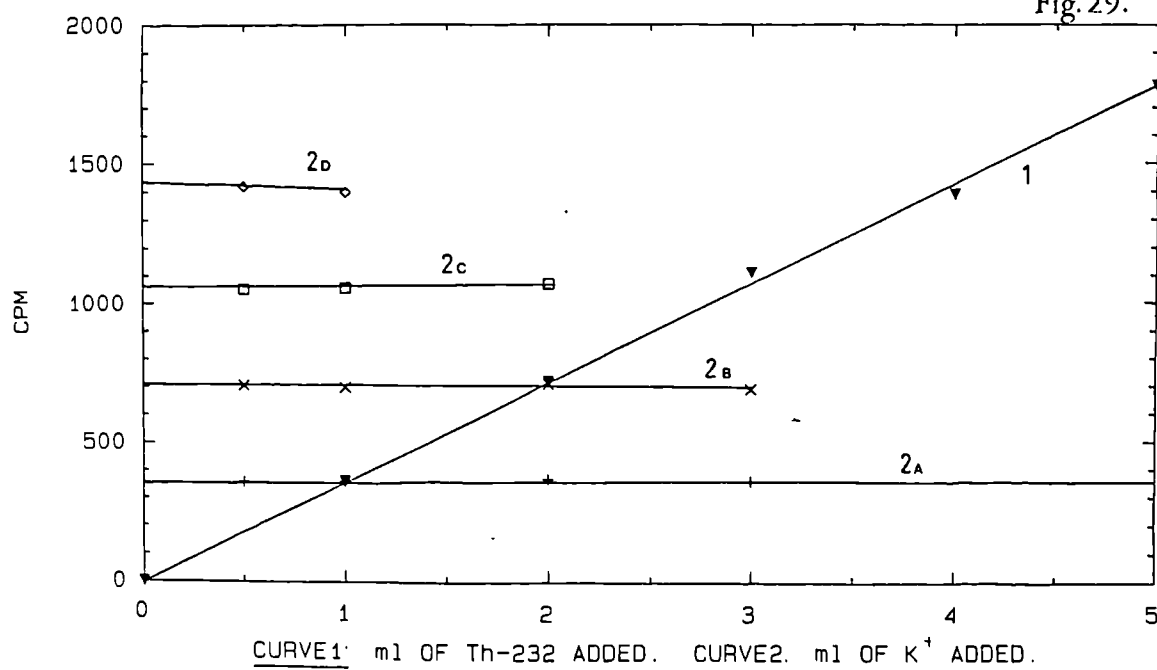
CURVE1. [Ac-228/Ra-228] 'VS' CPM CERENKOV CURVE2. Na<sup>+</sup> QUENCH CURVE.

Fig.28.

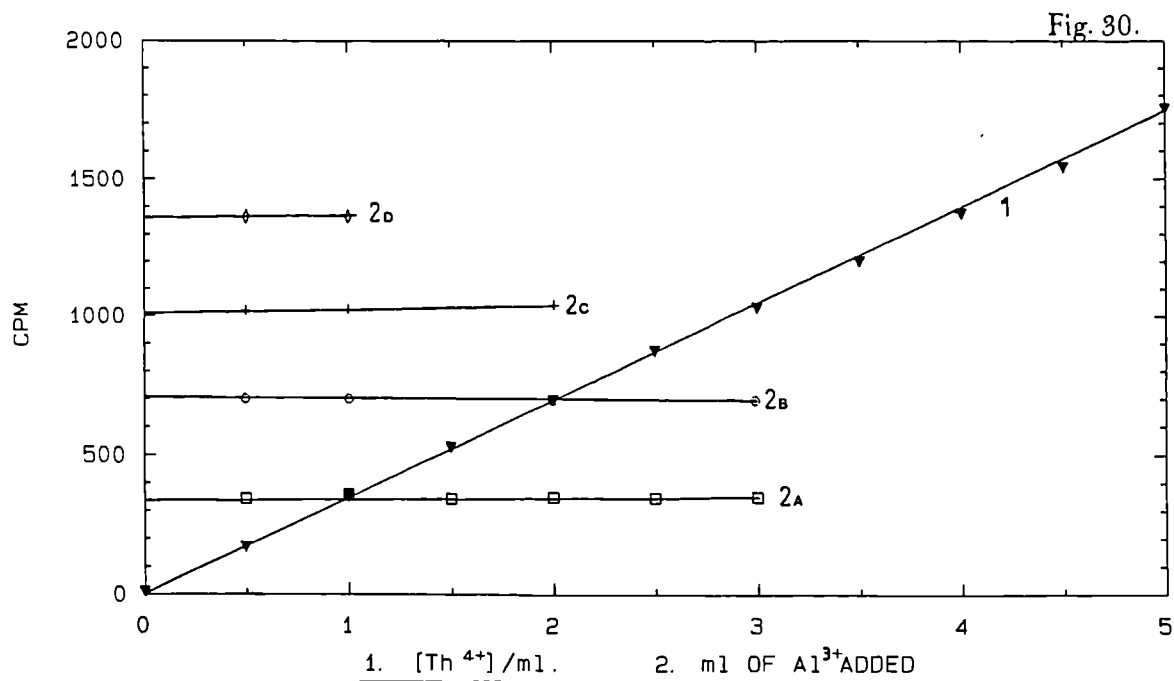


CURVE1 [Ac-228/Ra-228] 'VS' CPM CERENKOV CURVE2. K<sup>+</sup> QUENCH CURVE

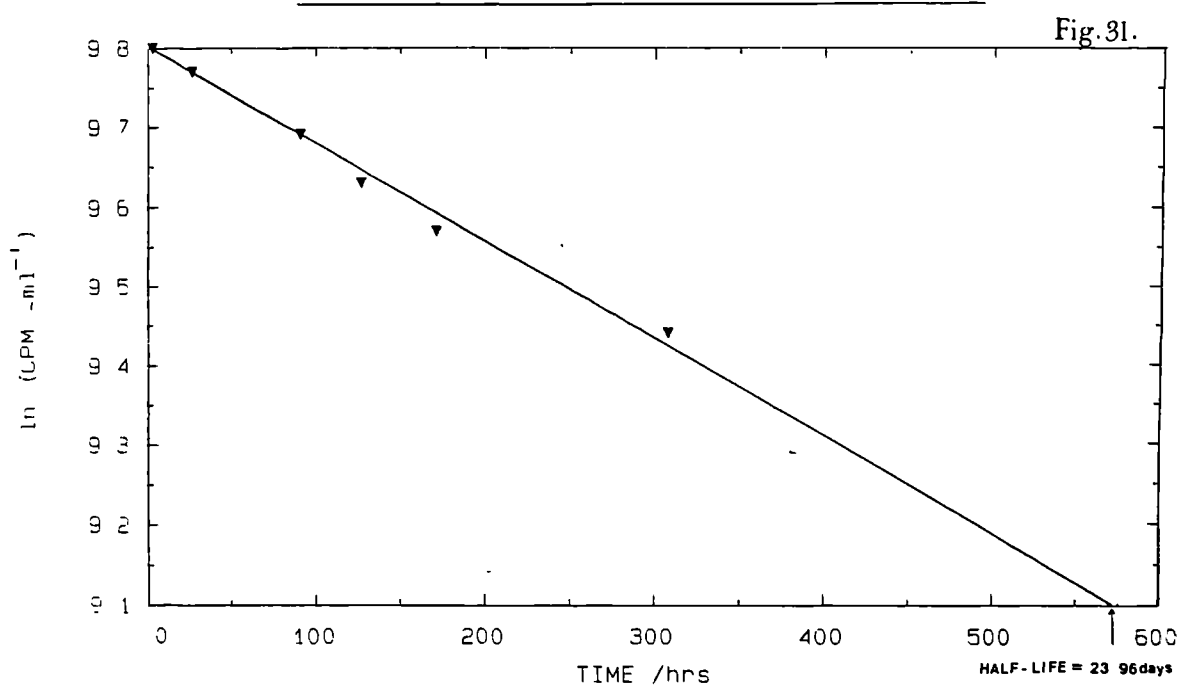
Fig.29.



CURVE 1. [Ac-228/Ra-228] 'VS' CPM. CURVE 2.  $Al^{3+}$  QUENCH  
CURVE. ČERENKOV



HALF-LIFE CURVE FOR SOLVENT-EXTRACTED Th-234





RESULTS OF NATURAL ZEOLITE SCREENING. (FINAL UPTAKE VALUES)

TABLE 39

0.01N Thorium nitrate, 20°C. (EQUILIBRIUM VALUES)

ZEOLITE	meq Th in solution	meq Th in solid	K <sub>d</sub>
CLINOPTILOLITE	0.050	0.050	102.2
CHABAZITE 1	0.008	0.090	212.5
CHABAZITE 2	0.032	0.068	215.1
MORDENITE	0.053	0.047	109.3
EASTGATE	0	0.100	TOTAL REMOVAL ( $\infty$ )
FERRIERITE	0.068	0.032	48.5
PHILLIPSITE	0.024	0.076	321.8
CHABAZITE 3	0.010	0.090	900.0
1010A	0.070	0.030	43.1
ANALCIME	0.100	0	NO REMOVAL
ERIONITE	0.064	0.036	56.3

TABLE 400.1N thorium nitrate, 20°C

ZEOLITE	meq Th in solution	meq Th in solid	K <sub>d</sub>
CLINOPTILOLITE	0.686	0.414	60.3
CHABAZITE 1	0.898	0.205	22.8
CHABAZITE 2	1.100	0.003	0.3
MORDENITE	0.960	0.150	16.1
EASTGATE	0.370	0.730	195.9
FERRIERITE	1.040	0.060	6.1
PHILLIPSITE	0.870	0.230	26.3
CHABAZITE 3	0.860	0.240	27.4
1010A	0.780	0.220	26.4
ANALCIME	1.050	0.050	4.8
ERIONITE	0.462	0.538	119.4

TABLE 41

SYNTHETIC ZEOLITE SCREENING  $K_d$  VALUES0.01N Thorium nitrate, 20°C, equilibrium:

ZEOLITE	[Th]/meq in solution	[Th]/meq in solid	$K_d$
4A	0	0.100	TOTAL UPTAKE
NaY	0	0.100	TOTAL UPTAKE
NaZ900	0.088	0.012	14.5
0.1N Thorium nitrate, 20°C, equilibrium			
ZEOLITE	[Th]/meq in solution	[Th]/meq in solid	$K_d$
4A	SAMPLE DISSOLVED		
NaY	0.683	0.317	48.9
NaZ900	1.000	0.000	NO UPTAKE

TABLE 42

TOTAL ACTIVITY REMOVAL BY VARIOUS ZEOLITES TREATED WITH A  
0.01N Th<sup>4+</sup> SOLUTION AT EQUILIBRIUM

ZEOLITE	PERCENTAGE REMOVAL OF TOTAL ACTIVITY BY LIQUID SCINTILLATION COUNTING
Clinoptilolite	39
Chabazite 1	43
Chabazite 2	40
Mordenite	28
Eastgate	79
Ferrierite	25
Phillipsite	29
Chabazite 3	50
Analcime	0

Approximate mass of zeolite = 0.1g

Thorium solution normality = 0.01N (10.0 ml per sample)

Equilibration time = 1 week

TABLE 43

## RESULTS OF SCREENING OF ZEOLITES FOR

Ac-228/Ra-228, 0.01N Th-232

ZEOLITE	AT EQUILIBRIUM		AFTER 1 HOUR
	Ac-228/Ra-228 /% in solution	Ac-228/Ra-228 /% in solid	Ac-228/Ra-228 /%
CLINOPTILOLITE	5.9	94.1	72.5
APATITE	UNSTABLE	-	-
CHABAZITE 2	11.2	88.8	54.7
EASTGATE 2020	16.3	83.7	71.7
CHABAZITE 3	7.3	92.7	<87.1
FERRIERITE	7.8	96.2	77.3
MORDENITE	32.5	67.5	51.2
PHILLIPSITE	4.8	95.2	72.3
ERIONITE	2.7	97.3	72.2
ANALCIME	62.9	37.1	<22.0
CHABAZITE 1	3.6	96.4	71.1
PALAGONITE	52.8	47.2	41.8
COWLESITE	71.6	28.4	19.4
NATROLITE	UNSTABLE	-	-
BREWSTERITE	74.7	25.3	15.3
LAVA ASH	8.3	91.7	57.3
HEULANDITE	26.8	73.2	18.8
5050L	7.1	92.9	73.2
5050F	4.2	95.8	66.0
1010A	3.3	96.7	67.8

TABLE 44

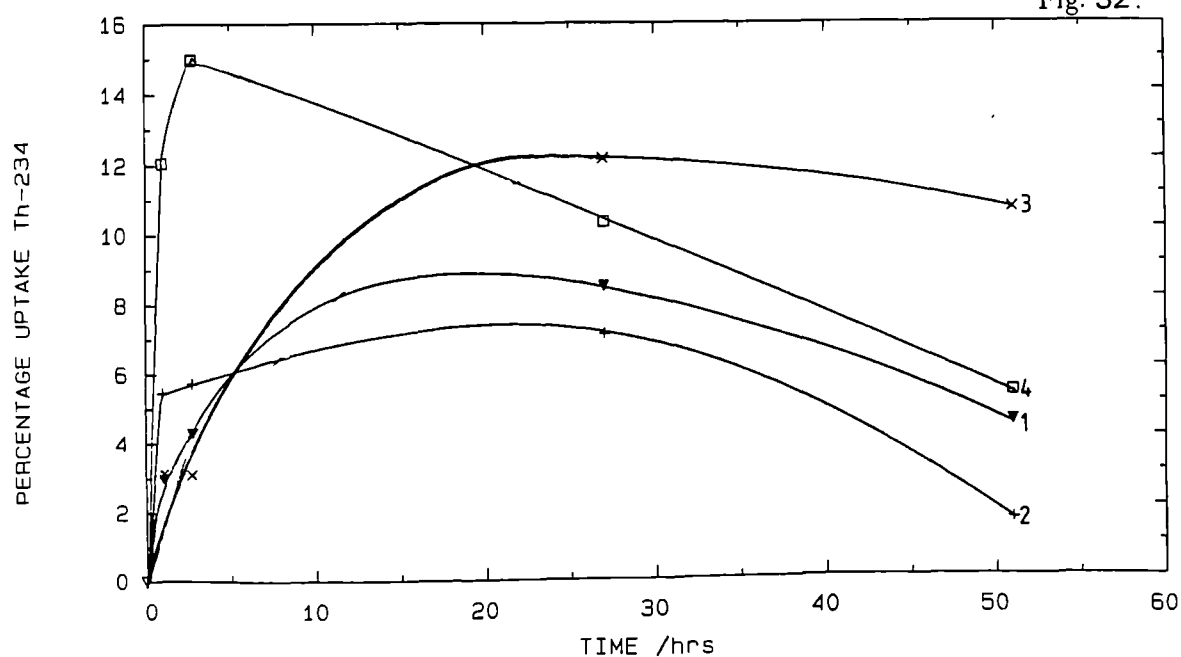
## RESULTS OF SYNTHETIC ZEOLITE TRIALS FOR

Ac-228/Ra-228 20°C. [Th-232] = 0.01N

ZEOLITE	% $^{228}\text{Ra}/^{228}\text{Ac}$ in solution	% $^{228}\text{Ra}/^{228}\text{Ac}$ in solid	% UPTAKE AFTER 1 HOUR
	AT EQUILIBRIUM		
NaY	10.7	89.3	77.1
13X	42.5	57.5	50.6
Z900	4.4	95.6	62.8
4A (POWDER)	70.6	29.4	18.5
K-L	35.2	64.8	65.6
5A (BOUND)	78.9	21.1	2.3
5A (POWDER)	UNSTABLE.		

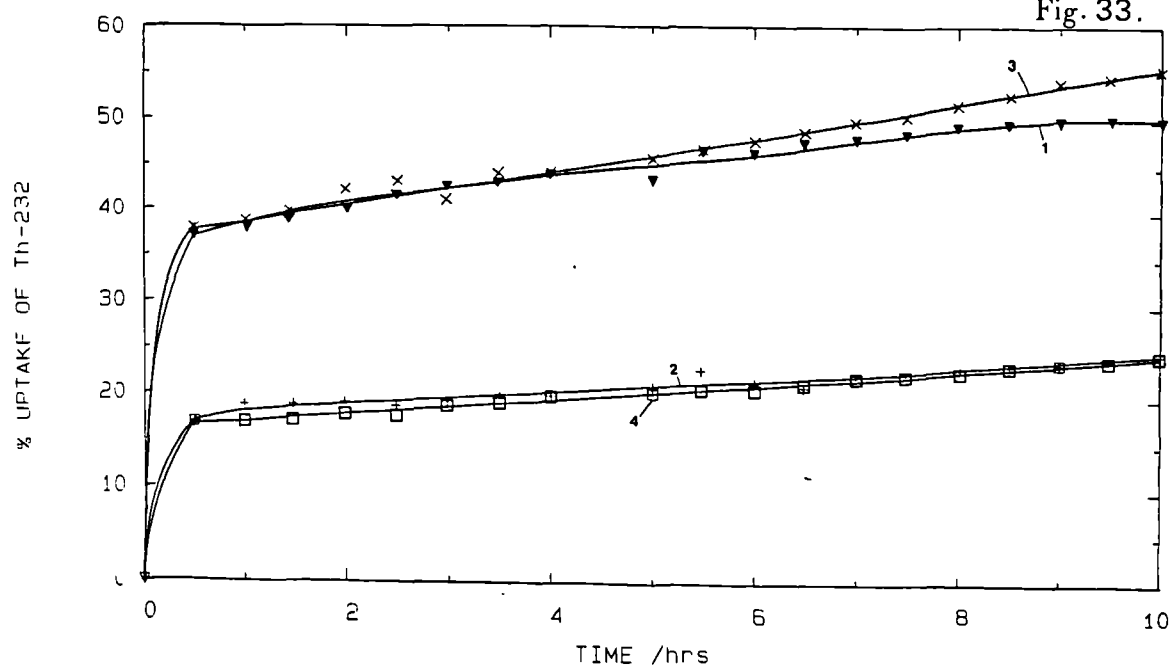
Th-234 UPTAKE CURVES 1) CLINOPTILOLITE 106 $\mu$ m 2) PHILLIPSITE  
3) CHABAZITE-3 4) CLINOPTILOLITE

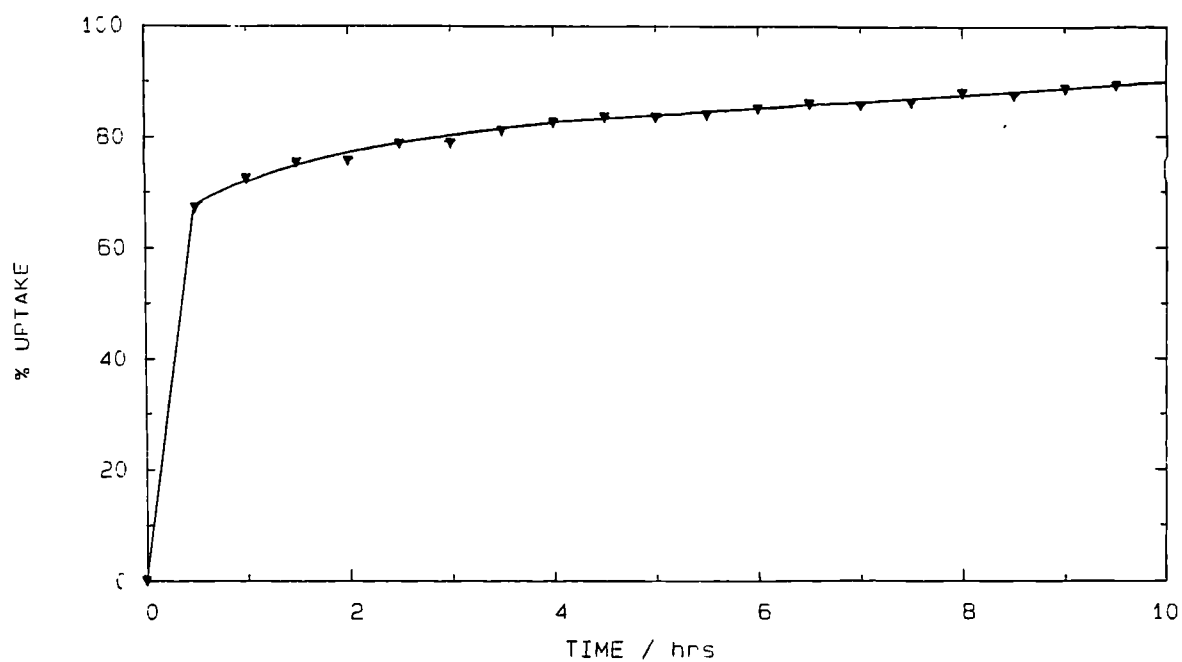
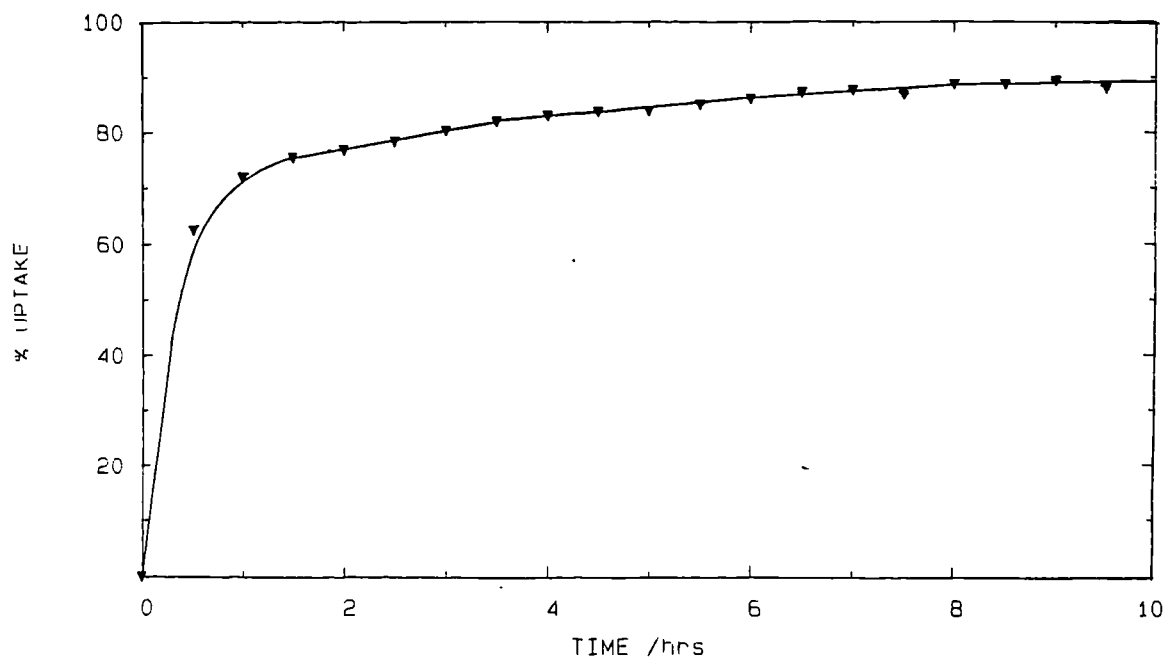
Fig. 32.



TEN HOUR UPTAKE CURVE (Th-232) 1) CLINOPTILOLITE  
2) CHABAZITE-3 3) ERIONITE 4) PHILLIPSITE

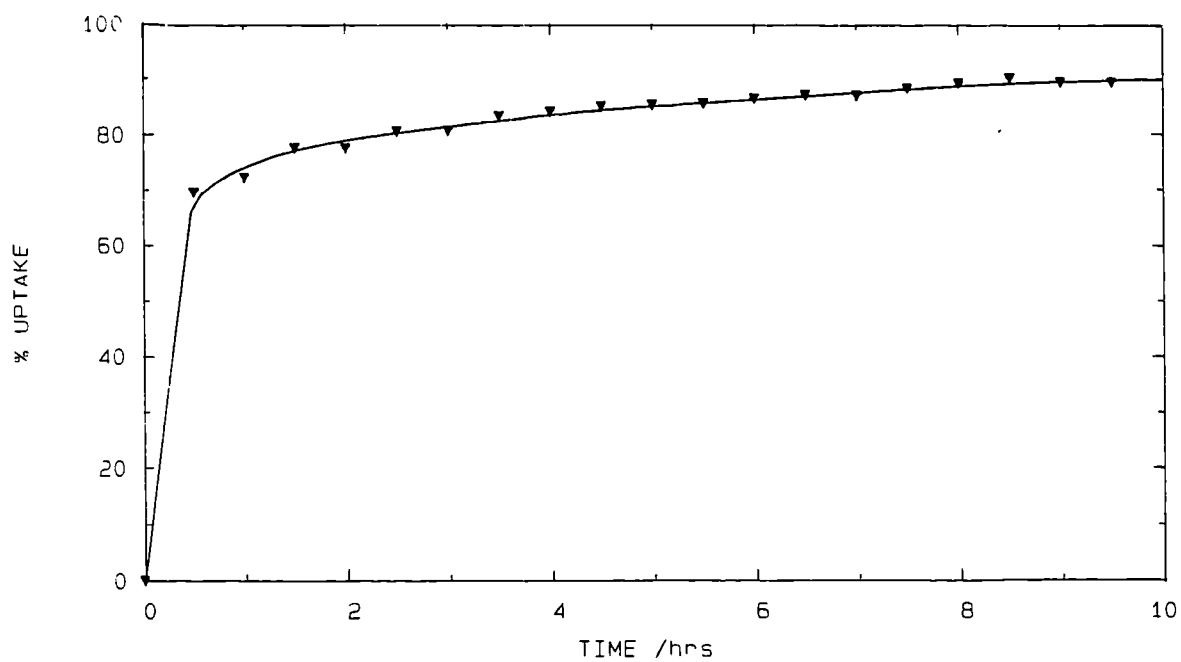
Fig. 33.



TEN-HOUR UPTAKE CURVE PHILLIPSITE Ac-228/Ra-228 **Fig.34.**TEN-HOUR UPTAKE CURVES CHABAZITE-3 Ac-228/Ra-228 **Fig.35.**



TEN-HOUR UPTAKE CURVE ERIONITE Ac-228/Ra-228 Fig.36.



TEN HOUR UPTAKE CURVE FOR CLINOPTILOLITE (Ac-228/Ra-228) Fig.37.

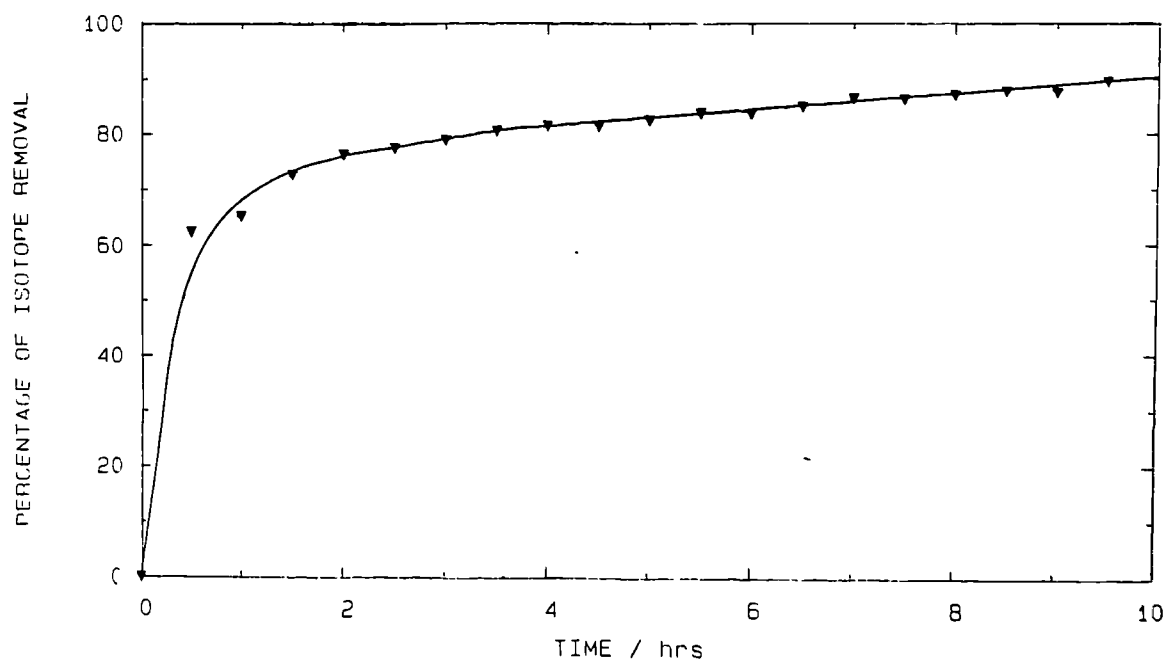


TABLE 45

EFFECT OF TEMPERATURE AND CONCENTRATION CHANGES ON SELECTED  
ZEOLITES CONCERNING THE UPTAKE OF Th-232

ZEOLITE	[Th-232]/M INITIAL	TEMPERATURE /°C	Th-232 UPTAKE ON ZEOLITE/%
CLINOPTILOLITE	0.0418	20	14.3
	0.0418	36	14.0
	0.0418	57	13.8
	0.0418	75	13.7
	0.0209	20	15.2
	0.0042	20	19.0
	0.0021	20	50.0
FERRIERITE	0.0418	20	3.0
	0.0209	20	5.5
EASTGATE	0.0418	20	47.0
	0.0209	20	66.4
	0.0021	20	100.0
CHABAZITE 3	0.0418	20	13.2
	0.0209	20	22.0
	0.0042	20	57.0

TABLE 46

EFFECT OF TEMPERATURE AND CONCENTRATION CHANGES ON SELECTED  
ZEOLITES FOR THE UPTAKE OF THORIUM DAUGHTER  $\beta$ -EMITTERS

ZEOLITE	CONCENTRATION OF Th-232/M	TEMPERATURE /° C	% $\beta$ -ACTIVITY IN ZEOLITE
CLINOPTILOLITE	0.0418	20	94.1
	0.0418	36	94.0
	0.0418	57	88.9
	0.0418	75	88.9
	0.0209	20	97.8
	0.0042	20	91.6
	0.0021	20	94.7
	0.0418	36	94.0
FERRIERITE	0.0418	20	96.2
	0.0209	20	96.0
EASTGATE	0.0418	20	83.7
	0.0209	20	96.2
	0.0021	20	100.0
CHABAZITE 3	0.0418	20	92.1
	0.0209	20	92.0
	0.0042	20	93.0

TABLE 47

RESULTS OF NATURAL ZEOLITE UPTAKES OF  $\text{UO}_2^{2+}$  (U-238) $[\text{U}] = 0.01\text{N}$ ,  $20^\circ\text{C}$ 

ZEOLITE	EQUILIBRIUM VALUE OF U-238 UPTAKE		$K_d$
	% U-238 REMOVED BY THE ZEOLITE	[U] REMOVED /mg	
Clinoptilolite	19.3	2.6	22.9
Chabazite 1	25.9	3.5	33.3
Chabazite 2	25.9	3.5	36.3
Mordenite	22.2	3.0	28.0
Eastgate	63.0	8.5	168.2
Ferrierite	17.0	2.3	20.8
Phillipsite	17.0	2.3	20.5
Chabazite 3	31.1	4.2	43.9
Analcime	7.4	1.0	7.6

TABLE 48

RESULTS OF SELECTED SYNTHETIC ZEOLITE UPTAKES OF  $\text{UO}_2^{2+}$  (U-238) $[\text{U-238}] = 0.01\text{N}$ ,  $20^\circ\text{C}$ 

ZEOLITE	EQUILIBRIUM VALUE OF U-238 UPTAKE		$K_d$
	% U-238 REMOVED BY THE ZEOLITE	[U] REMOVED /mg	
NaY	94.1	12.7	1594.7
NaZ900	25.2	3.4	33.9

TABLE 49PERCENTAGE UPTAKE OF U-238  $\beta$ -EMITTER DAUGHTERS ON ZEOLITES

ZEOLITE	MAXIMUM PERCENTAGE REMOVAL OF WEAK $\beta$ -EMITTER DAUGHTERS OF U-238/%
Clinoptilolite	96.7
NaZ900	97.2
NaY	93.8

Contact time = 52 hours. [U-238] = 500 ppm.

TABLE 50

MAXIMUM PERCENTAGE UPTAKE OF U-238  $\beta$ -EMITTER DAUGHTERS  
ON ZEOLITES IN THE PRESENCE OF NITRIC ACID

ZEOLITE	MAXIMUM PERCENTAGE REMOVAL OF WEAK $\beta$ -EMITTERS OF U-238 DECAY SERIES IN:		
	0.01N HNO <sub>3</sub>	0.10N HNO <sub>3</sub>	0.50N HNO <sub>3</sub>
Clinoptilolite	96.7	24.3	0.0
NaZ900	97.2	28.6	0.0
NaY	93.8	93.2	0.0

TABLE 51

## EFFECT OF COMPETING CATIONS ON THE UPTAKE OF Th-232

 $\beta$ -EMITTER DAUGHTERS : Ra-228, Ac-228

ZEOLITE	[Th]/N	CATION	[CATION] /ppm	% UPTAKE AFTER 1 HOUR	
				WITHOUT CATION	WITH CATION
CLINOPTILOLITE	0.168	Na <sup>+</sup>	10 <sup>4</sup>	65.2	37.8
CHABAZITE 3	0.168	Na <sup>+</sup>	10 <sup>4</sup>	<87.1	56.2
CHABAZITE 1	0.168	Na <sup>+</sup>	10 <sup>4</sup>	71.1	57.5
5050L	0.168	Na <sup>+</sup>	10 <sup>4</sup>	73.2	50.5
FERRIERITE	0.168	Na <sup>+</sup>	10 <sup>4</sup>	52.1	15.4
1010A	0.168	Na <sup>+</sup>	10 <sup>4</sup>	67.8	43.1
ERIONITE	0.168	Na <sup>+</sup>	10 <sup>4</sup>	72.2	35.6
PHILLIPSITE	0.168	Na <sup>+</sup>	10 <sup>4</sup>	72.2	61.5
EASTGATE	0.168	Na <sup>+</sup>	10 <sup>4</sup>	71.7	42.1

TABLE 52

EFFECT OF SODIUM ON THE UPTAKE OF  $^{228}\text{Ac}$  and  $^{228}\text{Ra}$  $0.168\text{N Th}^{4+}$ ,  $\sim 10^3$  ppm  $\text{Na}^+$ ,  $20^\circ\text{C}$  AT EQUILIBRIUM

ZEOLITE	$[\text{Na}^+]/\text{ppm}$	% UPTAKE	
		WITHOUT CATION PRESENT	WITH CATION PRESENT
CLINOPTILOLITE	$10^4$	94.1	81.7
CHABAZITE 3	$10^4$	92.7	63.1
CHABAZITE 1	$10^4$	96.4	63.8
FERRIERITE	$10^4$	96.2	77.2

TABLE 53

EFFECT OF POTASSIUM ON THE UPTAKE OF  $^{228}\text{Ac}$  and  $^{228}\text{Ra}$  $0.168\text{N Th}^{4+}$ ,  $4 \times 10^2$  ppm  $\text{K}^+$ ,  $20^\circ\text{C}$ , AT EQUILIBRIUM

ZEOLITE	% UPTAKE OF $^{228}\text{Ra}$ and $^{228}\text{Ac}$			
	AFTER 1 HOUR		AT EQUILIBRIUM	
	WITHOUT CATION	WITH CATION	WITHOUT CATION	WITH $\text{K}^+$
CLINOPTILOLITE	72.5	43.0	94.1	90.4
CHABAZITE 3	<87.1	70.5	92.7	95.4
CHABAZITE 1	71.1	65.5	96.4	93.4
EASTGATE	71.7	53.1	83.7	81.7

TABLE 54

EFFECT ON THE UPTAKE OF Th-232 BY VARYING THE CONCENTRATIONS  
OF COMPETING CATIONS

ZEOLITE	% UPTAKE OF Th-232					
	1:1 Na/Th	2:1 Na/Th	1:1K/Th	2:1/Th	0.1N H <sup>+</sup>	0.5N H <sup>+</sup>
NaY	100.0	100.0	100.0	100.0	41.2	-
EASTGATE	92.7	93.9	93.9	87.9	-	-
CLINOPTIL- OLITE	27.3	15.2	15.2	3.0	8.8	-
Z900	-	3.0	3.0	-	-	-



TABLE 55

COMPETING ION EFFECTS OF  $\text{Na}^+$ ,  $\text{K}^+$ ,  $\text{Mg}^{2+}$ ,  $\text{Ca}^{2+}$ ,  $\text{Al}^{3+}$  ON  
 $\text{Th}^{4+}$  UPTAKES ONTO CLINOPTILOLITE AND Z900

SAMPLE	% UPTAKE OF THORIUM									
	CLINOPTILOLITE					Z900				
	Na	K	Mg	Ca	Al	Na	K	Mg	Ca	Al
1	-	-	-	-	-	-	-	-	-	-
2	9	-	39	40	14	-	-	26	-	-
3	-	-	42	34	-	-	-	36	35	5
4	-	-	44	32	9	-	-	31	40	9
5	2	-	41	36	-	-	-	29	48	13
6	-	-	40	41	9	-	-	32	29	-
7	-	-	47	42	-	-	-	30	41	-
8	-	-	37	47	-	-	-	36	30	-
9	8	-	64	36	-	-	-	-	30	-
10	20	-	64	60	-	-	-	-	60	-


Decreasing  $\text{H}^+$  and  $\text{Th}^{4+}$  concentration  


TABLE 56

Th-232 UPTAKES FOR ZEOLITES CONTACTED WITH SOSIM SOLUTIONS

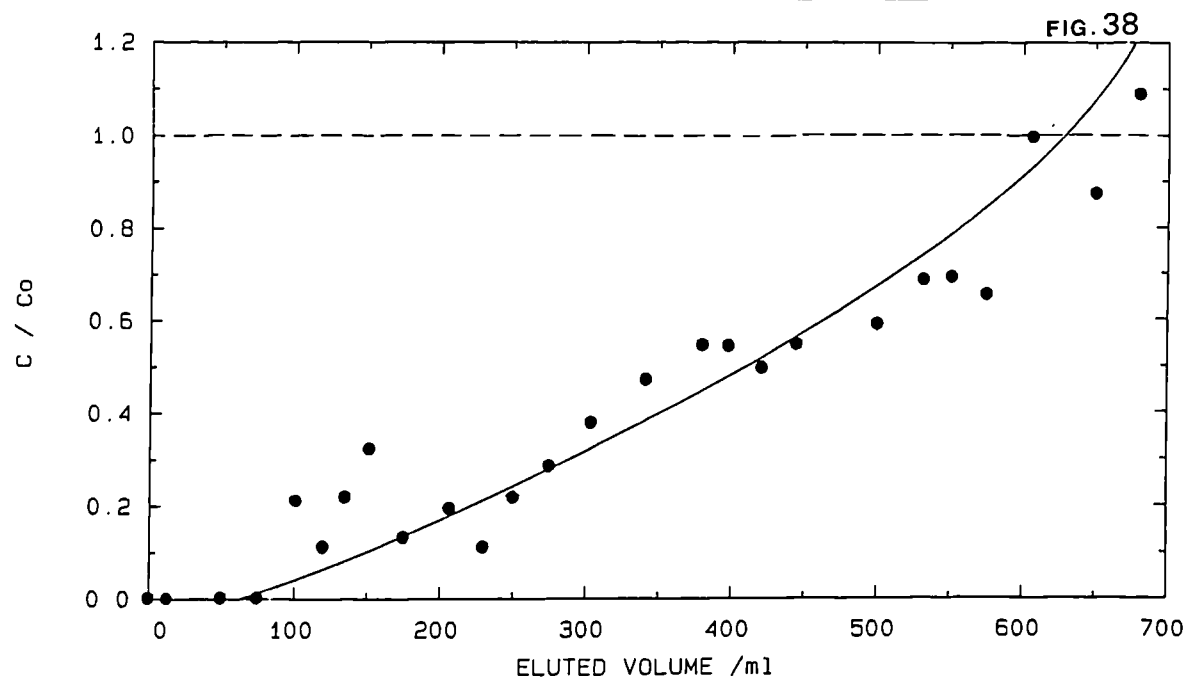
ZEOLITE	Th-232 UPTAKE/mg per 0.1g zeolite (% REMOVAL)		
	SOSIM 1	SOSIM 2	SOSIM 3
EASTGATE	0.9 (42.0)	-	1.61 (34.0)
CLINOPTILOLITE	0.1 ( 6.5)	-	0.24 ( 5.1)
Z900	-	-	-
4A	SAMPLE DISSOLVED		
NaY	-	-	-

TABLE 57

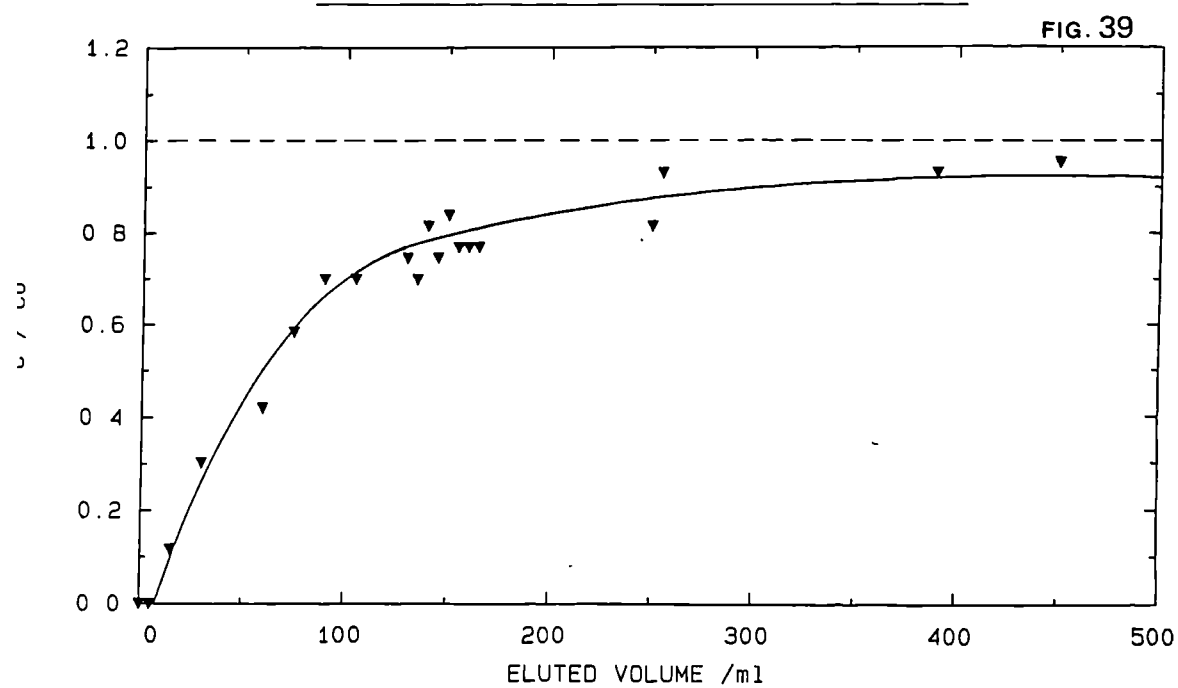
FREE COLUMN VOLUME DETERMINATION OF ZEOLITES

ZEOLITE	FREE COLUMN VOLUME /cc.	MASS OF ZEOLITE /g
CLINOPTILOLITE	4.50	3.01
NaZ900	4.80	3.02
CaY	4.90	3.00
EASTGATE	4.65	3.01

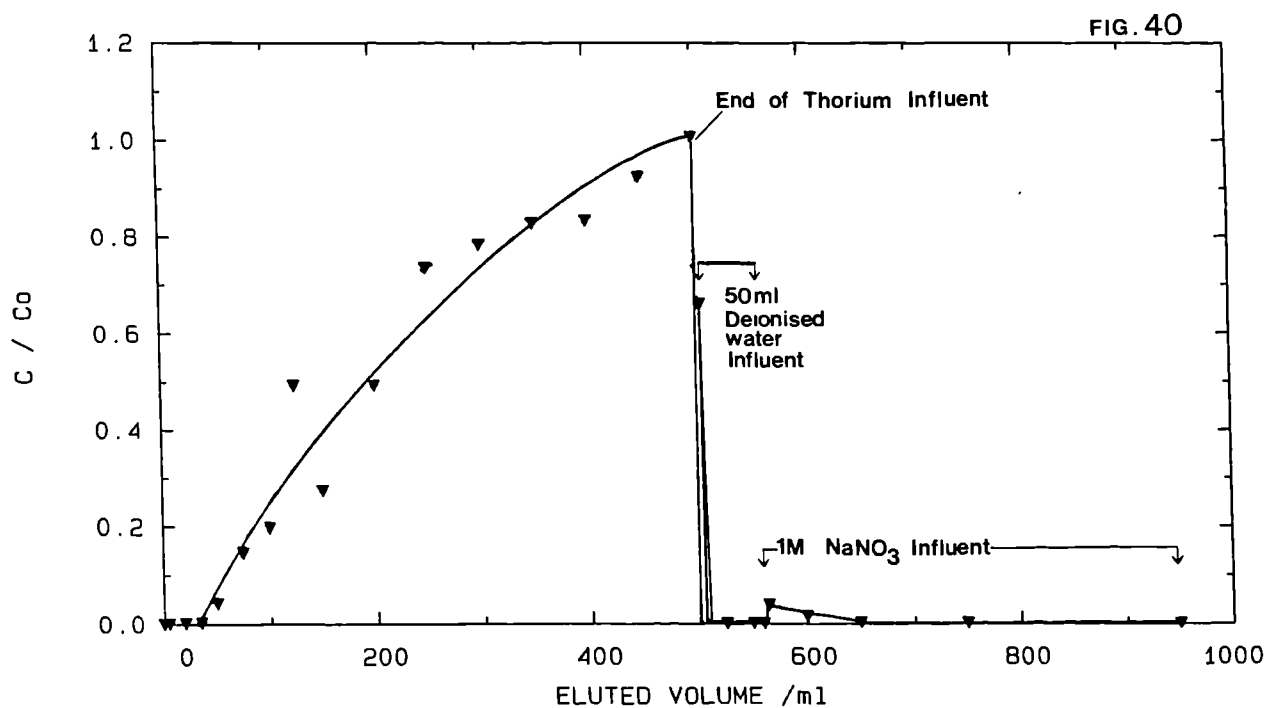
BREAKTHROUGH CURVE EASTGATE Th-232.



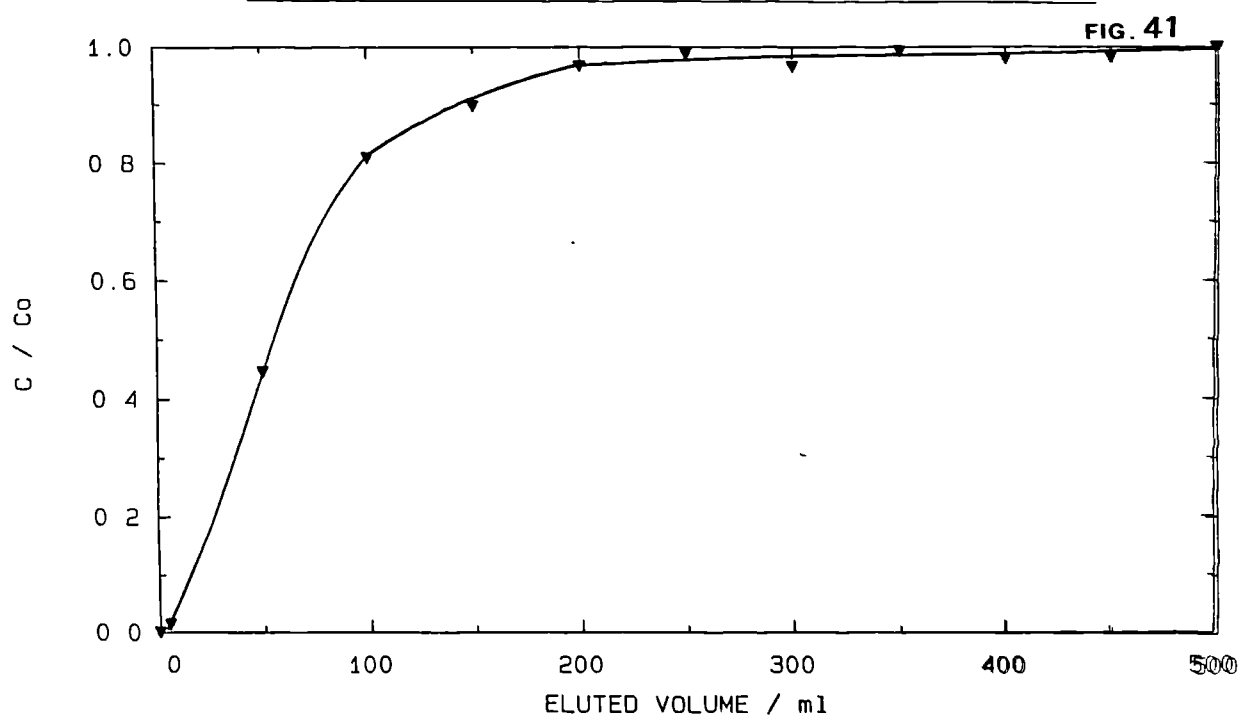
BREAKTHROUGH CURVE CLINOPTILOLITE. Th-232.



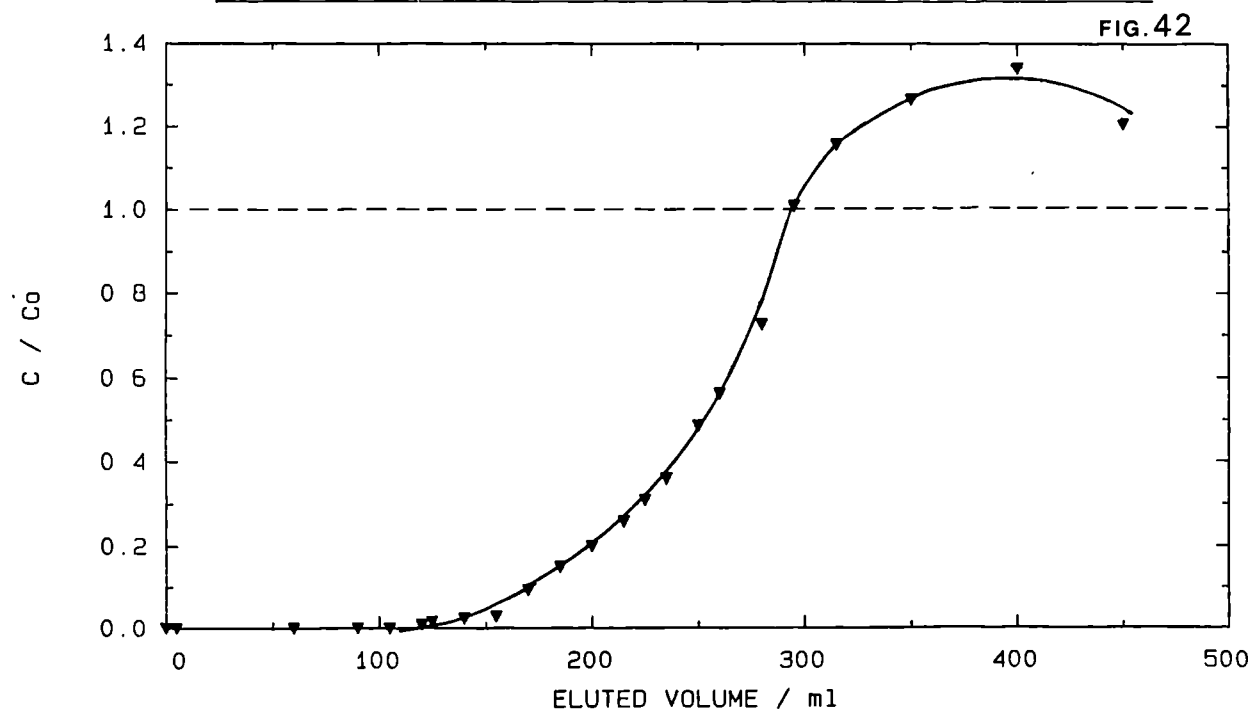
BREAKTHROUGH CURVE: CLINOPTILOLITE. Th-234 IN 0.5M NITRIC  
ACID.



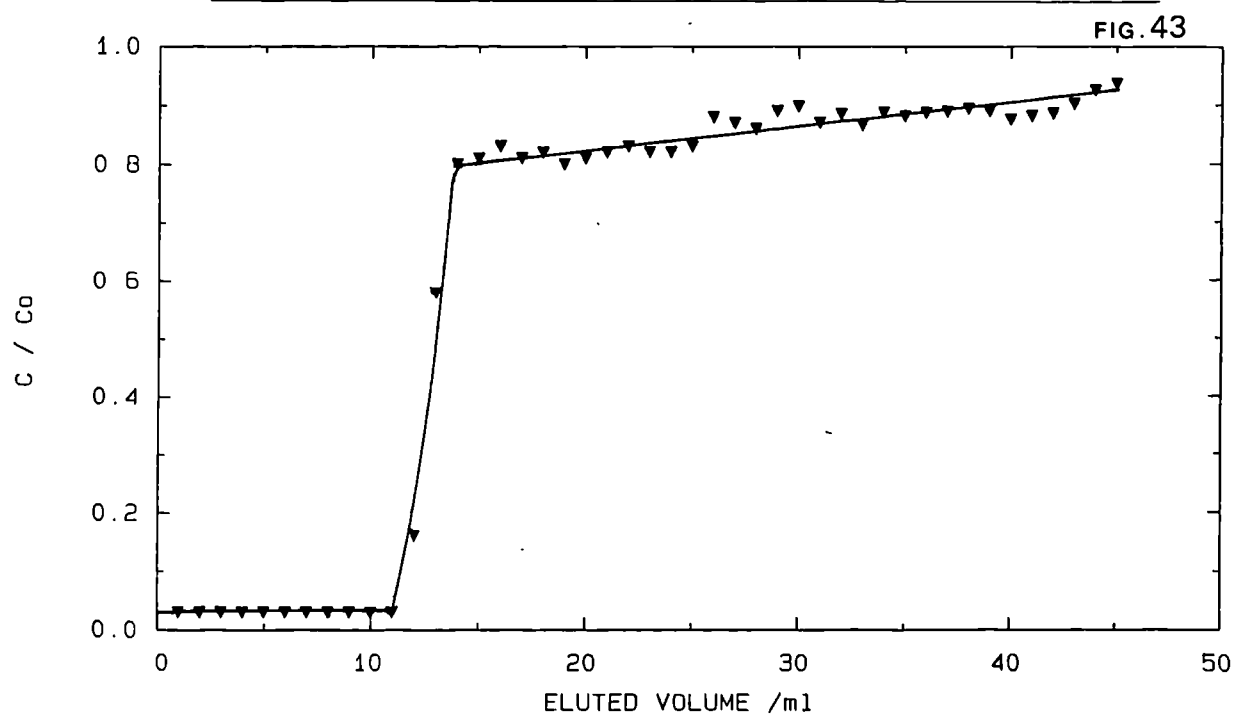
BREAKTHROUGH CURVE: Z900 Th-234 IN 0.5M NITRIC ACID.



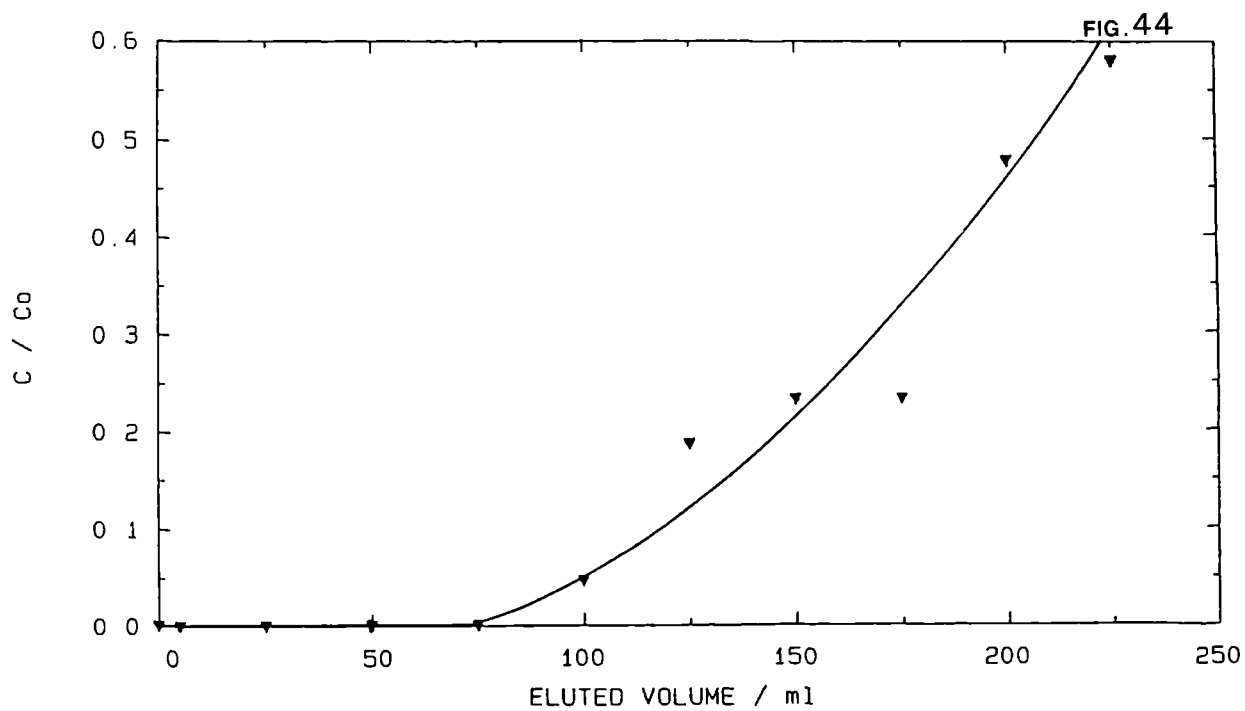
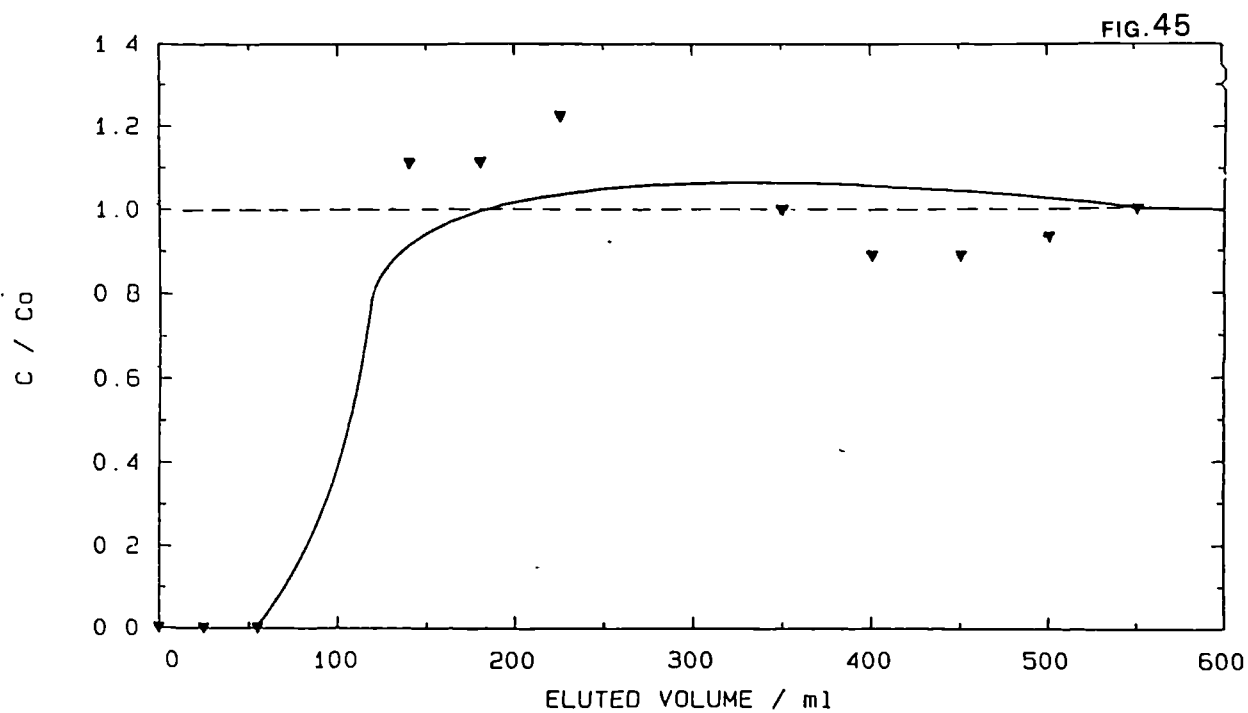
BREAKTHROUGH CURVE. CaY. Ac-228/Ra-228 IN 0.1M NITRIC ACID



BREAKTHROUGH CURVE: Z900. Ac-228/Ra-228 IN 0.1M NITRIC ACID.

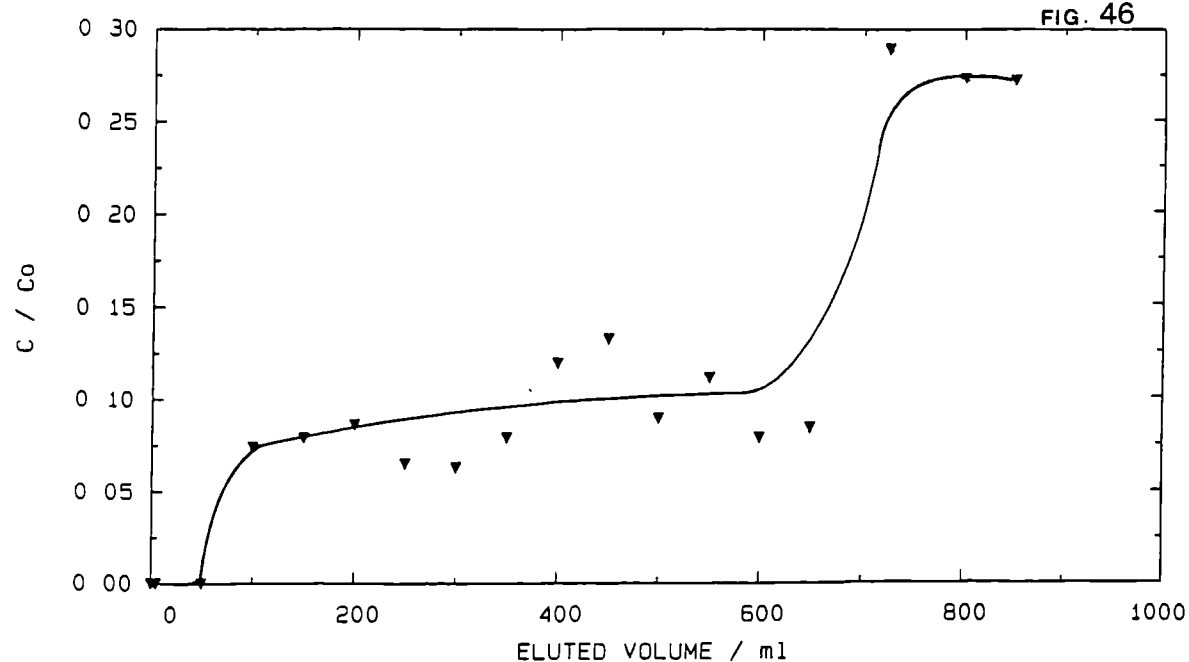


BREAKTHROUGH CURVE. Z900 Th-232 IN 0.1M NITRIC ACID

BREAKTHROUGH CURVE CLINOPTILOLITE Th-232 IN 0.5M NITRIC  
ACID

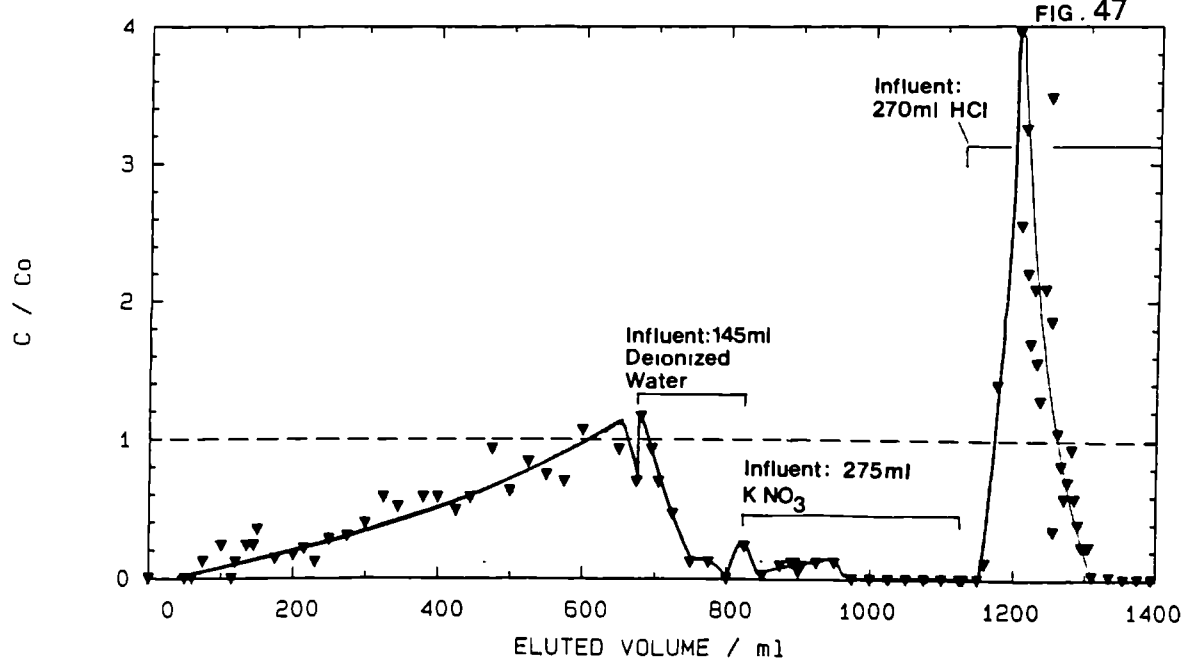
BREAKTHROUGH CURVE CLINOPTILOLITE Ac-228/Ra-228 IN 0.5M  
NITRIC ACID

FIG. 46

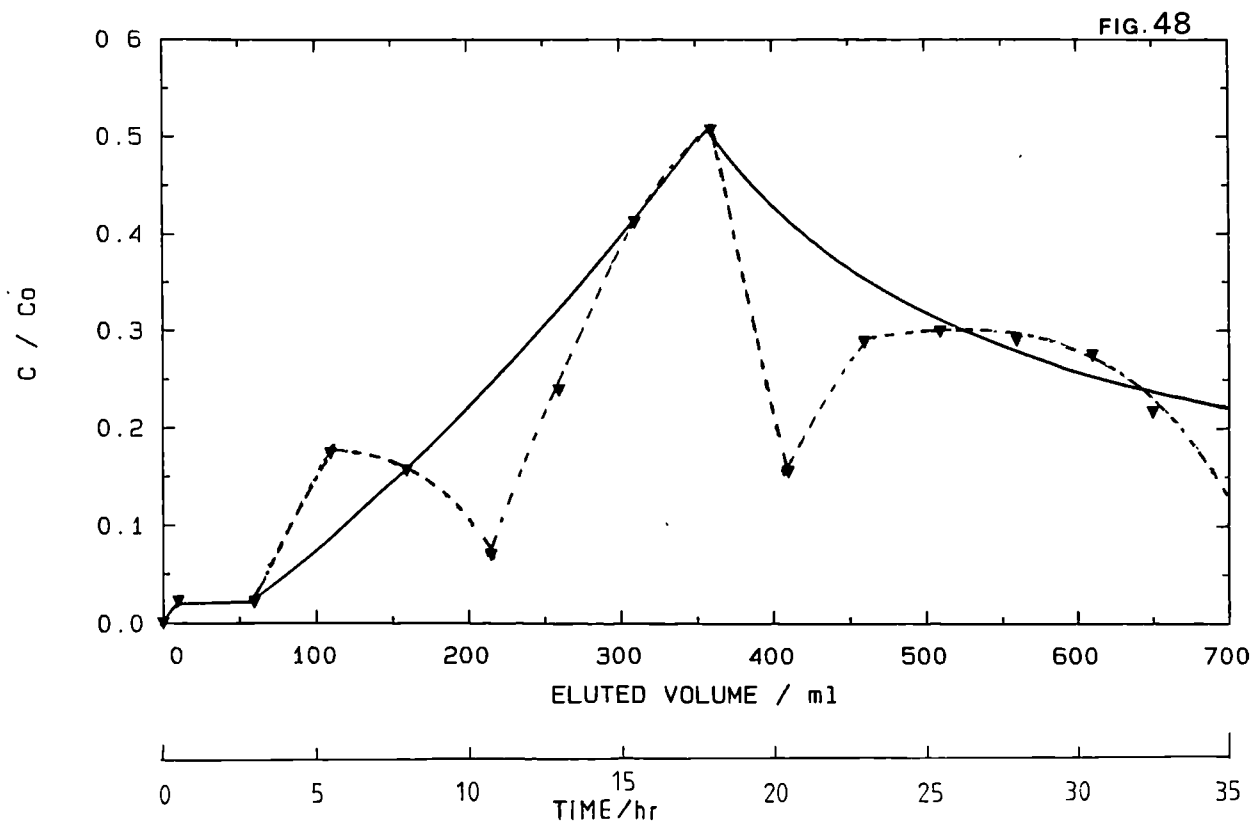


BREAKTHROUGH CURVE EASTGATE Th-232/H<sub>2</sub>O/K<sup>+</sup>/HCl.

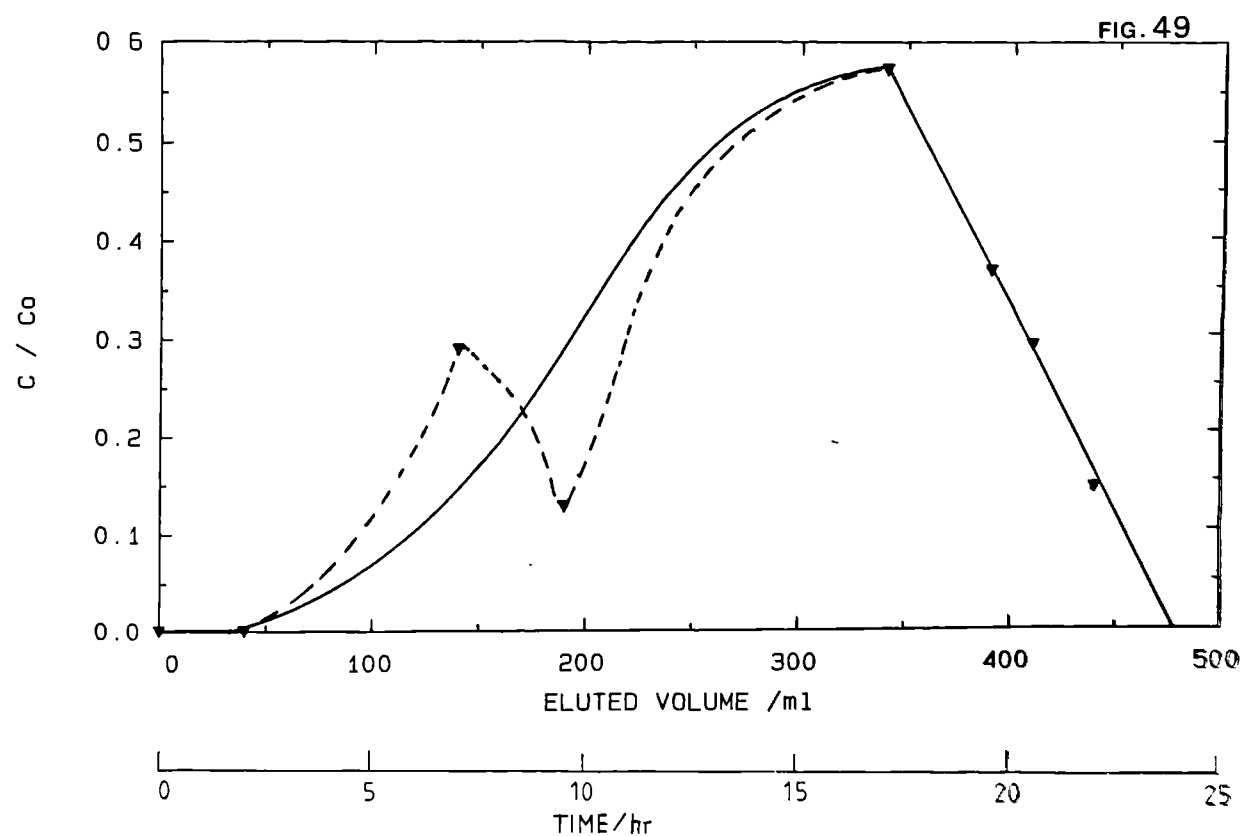
FIG. 47



BREAKTHROUGH CURVE: EASTGATE. Ac-228/Ra-228.



BREAKTHROUGH CURVE: EASTGATE. TOTAL ACTIVITY.





ISOTHERM. CLINOPTILOLITE  $K^+ / Th^{4+}$  (0.01N)

Fig. 50

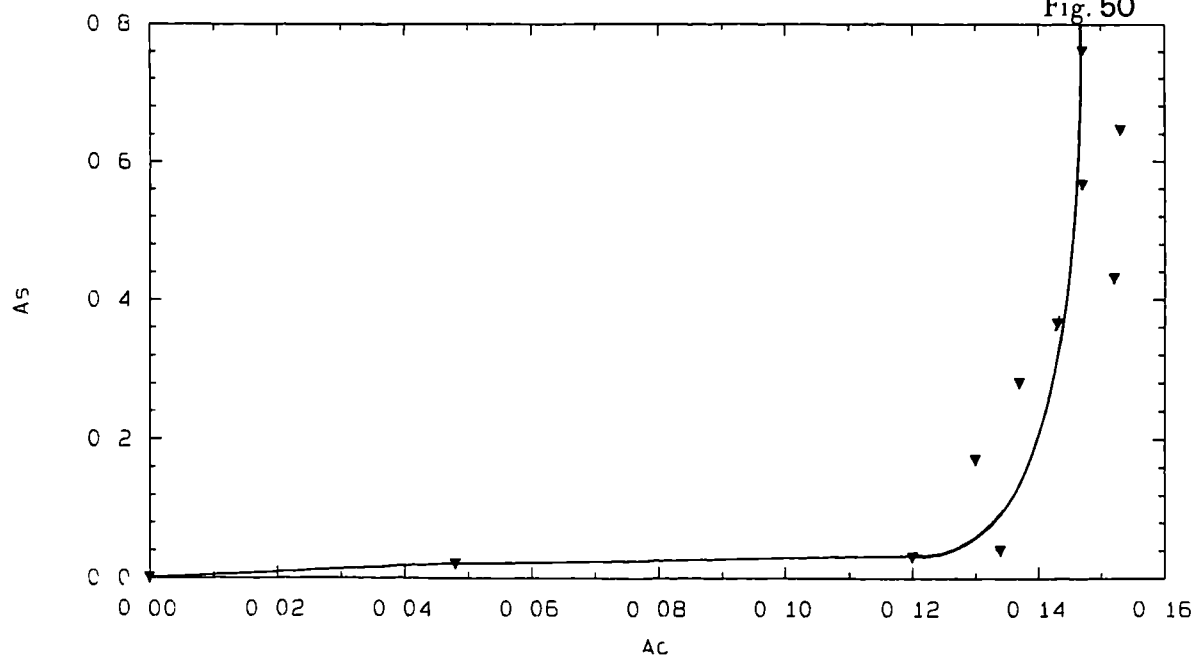
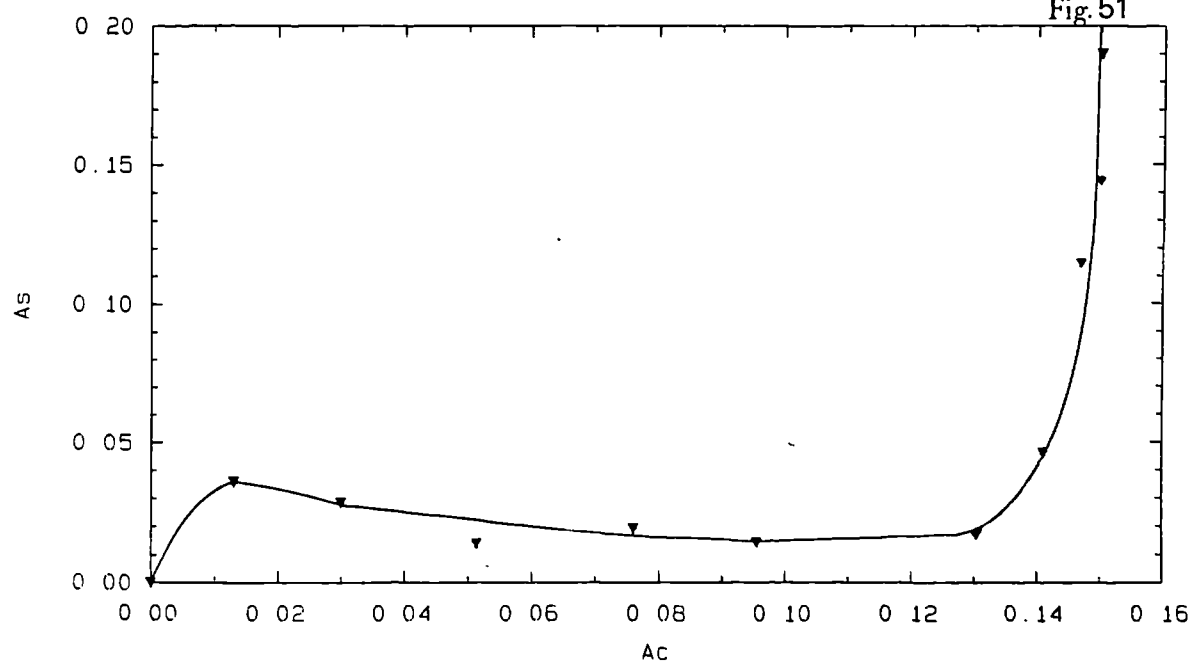
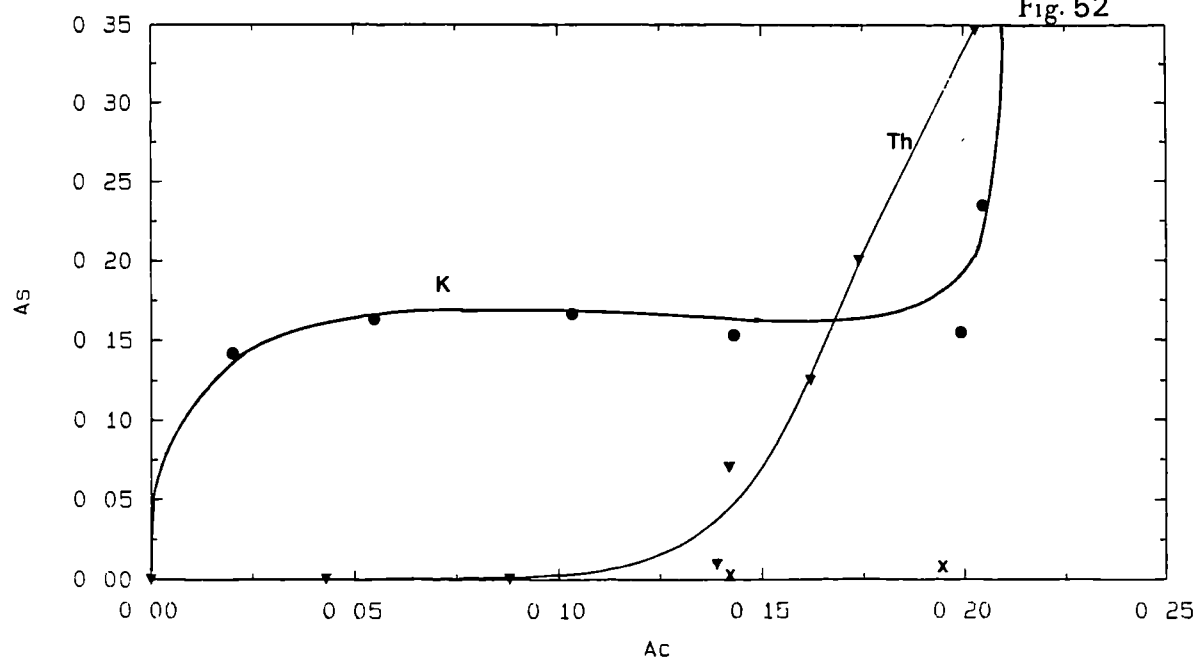
ISOTHERM CLINOPTILOLITE  $K^+ / Th^{4+}$  (0.001N)

Fig. 51



ISOTHERM. Z900  $K^+ / Th^{4+}$  (0.01N)

Fig. 52



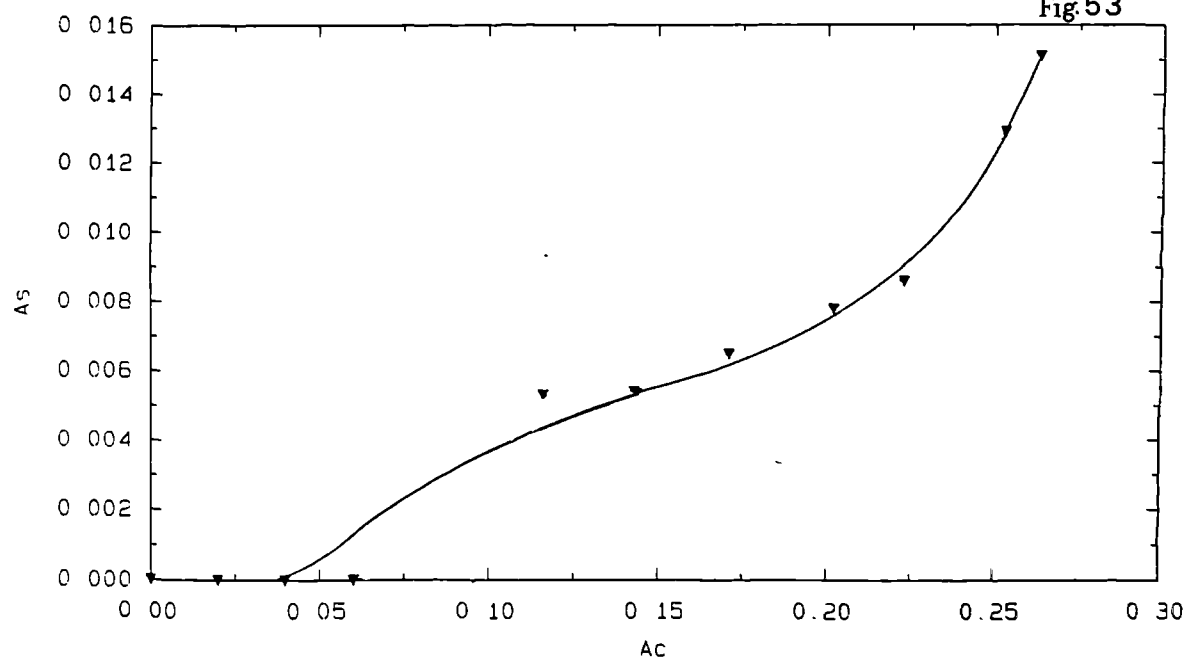
Where: 'x' denotes Reversibility points for Thorium

● represents  $K^+$  Isotherm

▼ represents  $Th^{4+}$  Isotherm

ISOTHERM NaY  $Na^+ / Th^{4+}$  (0.01N)

Fig. 53



ISOTHERM: CLINOPTILOLITE.  $\text{Na}^+ / \text{Th}^{4+}$  (0.1N)

Fig. 54

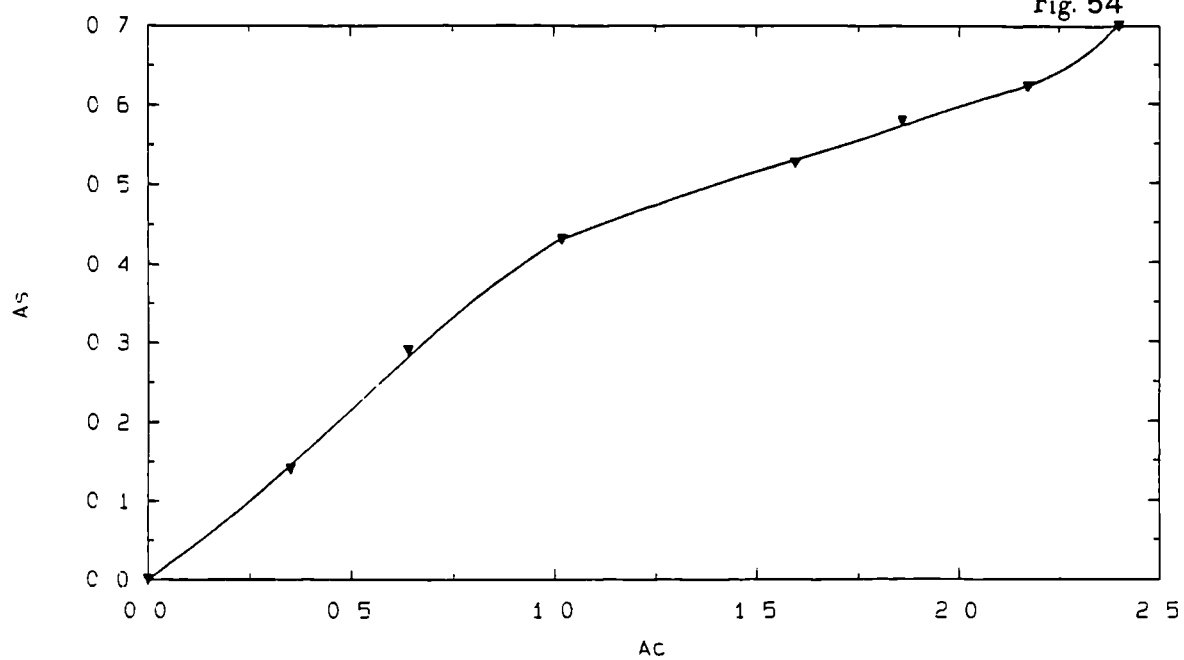
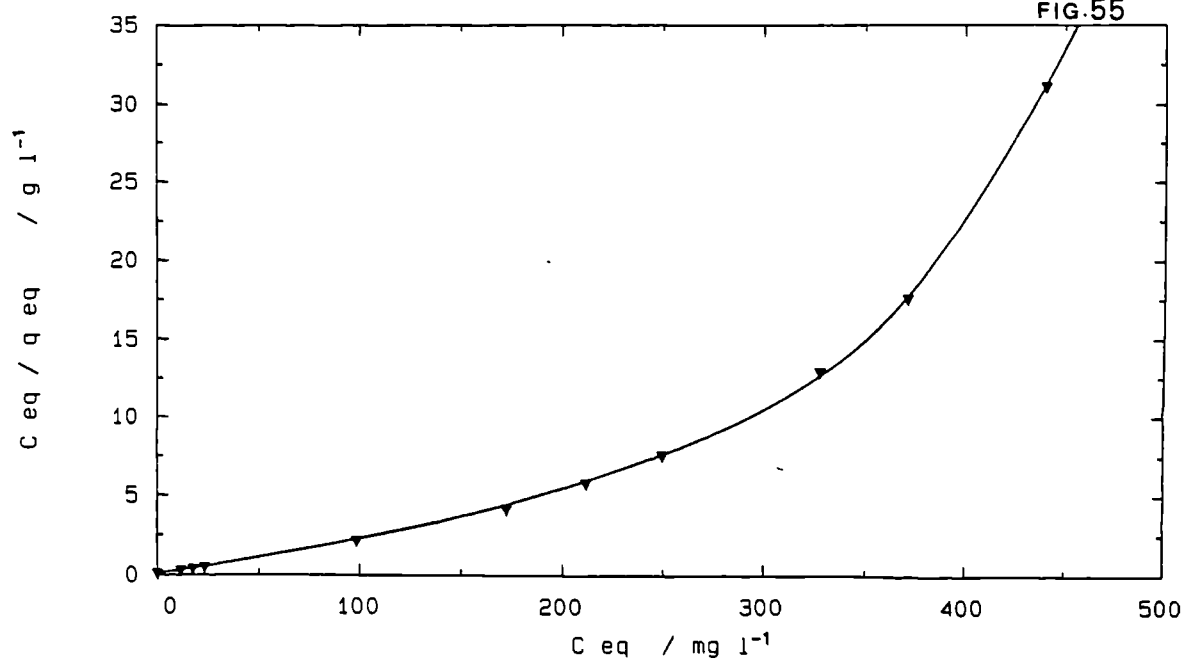
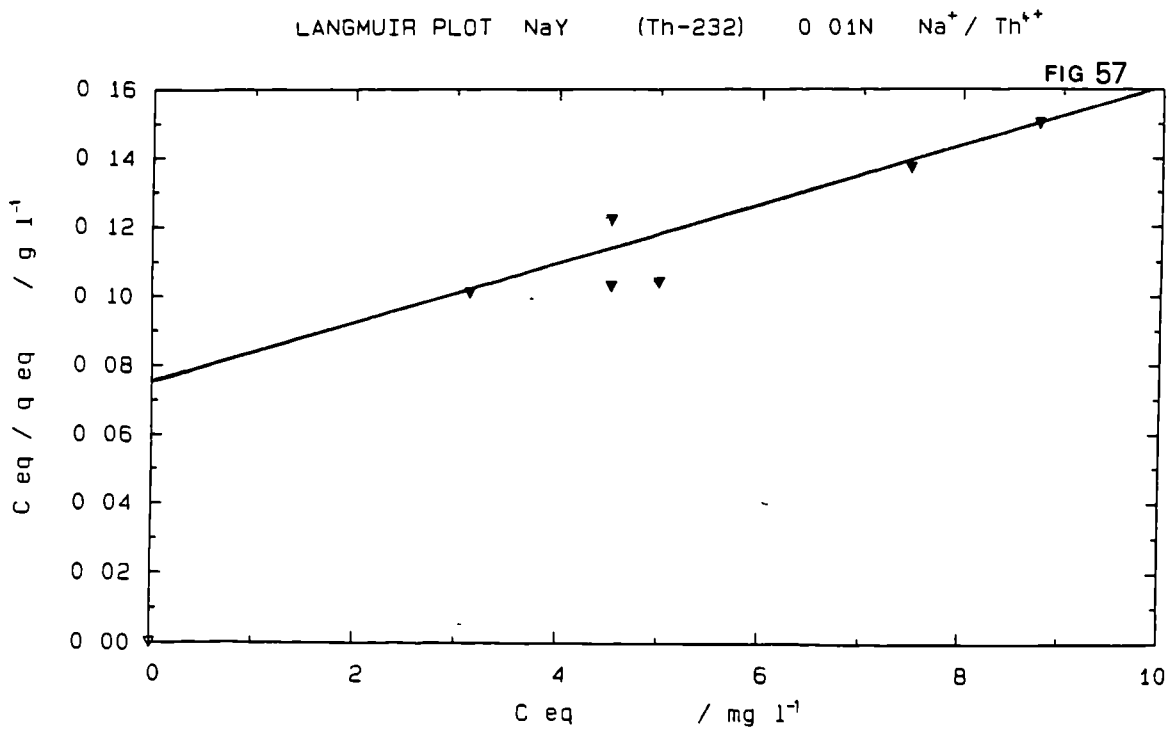
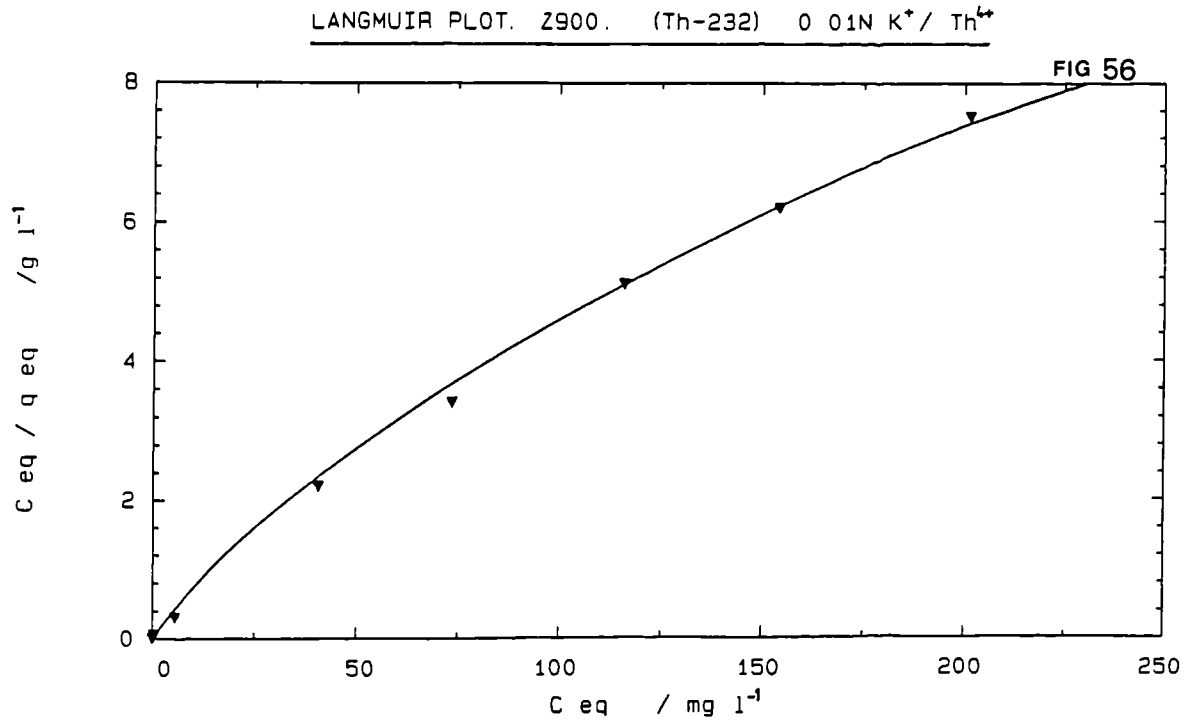
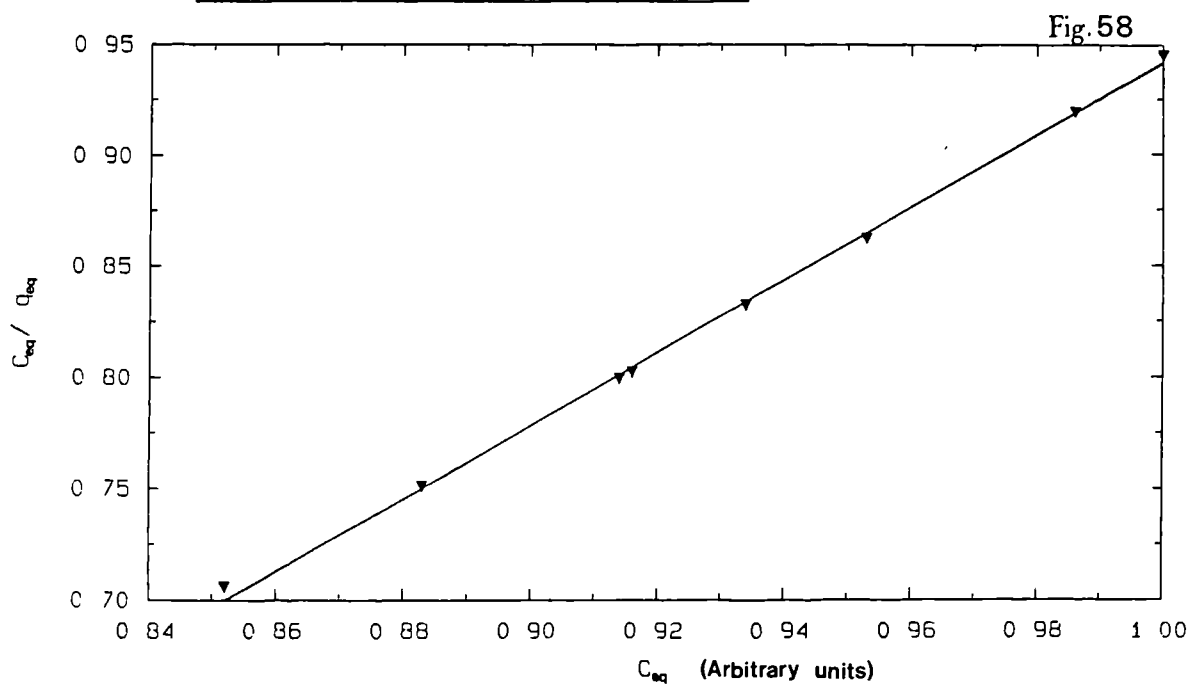
LANGMUIR PLOT CLINOPTILOLITE (Th-232) 0.01N  $\text{K}^+ / \text{Th}^{4+}$ 

FIG. 55

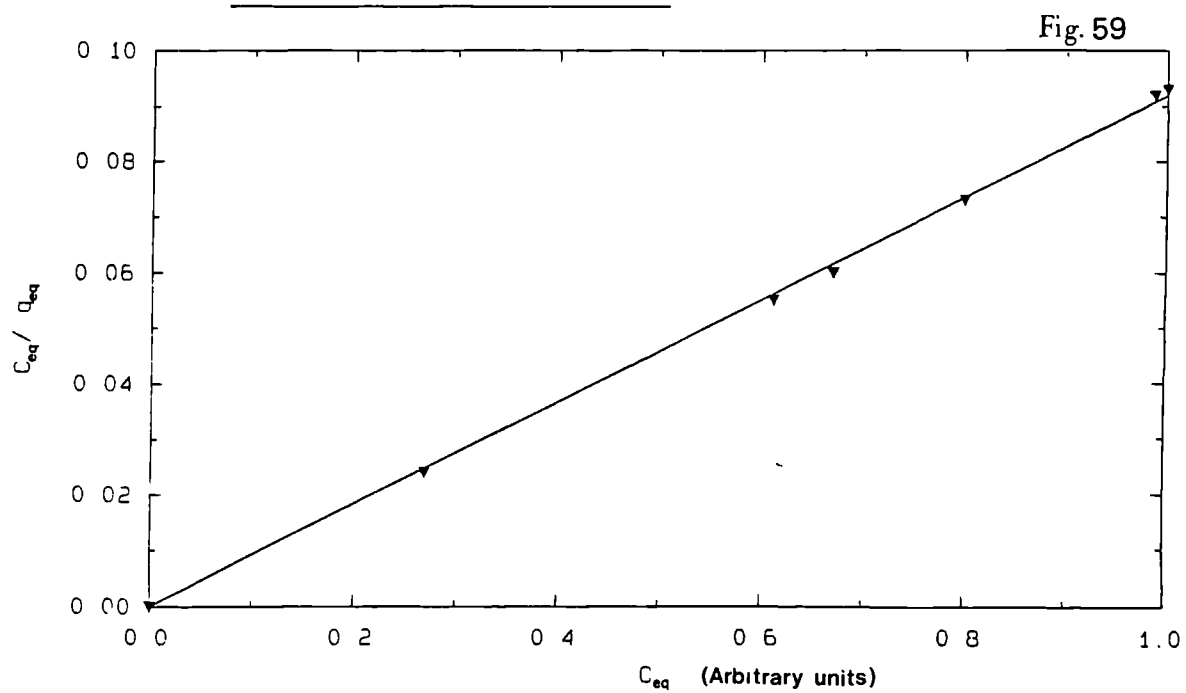




LANGMUIR PLOT CLINOPTILOLITE  $K^+$  / (TOTAL ACTIVITY) 0.1N  
Th-232. X-AXIS NORMALISED

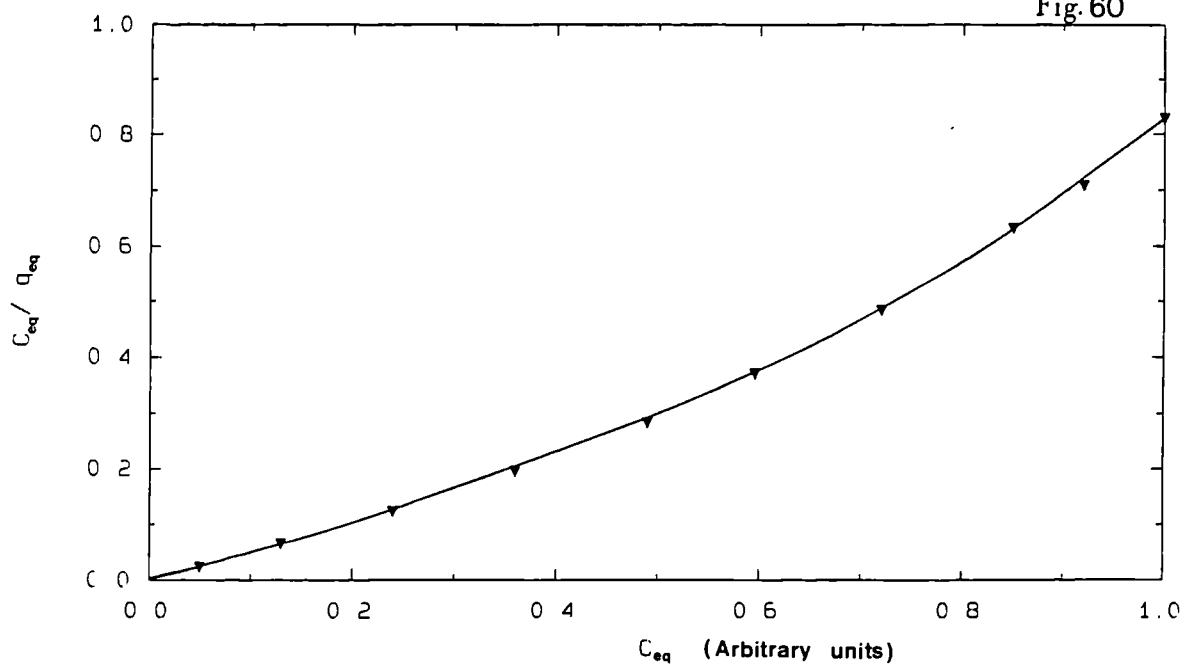


LANGMUIR PLOT. Z900  $K^+$  / (Ac-228/Ra-228) 0.01N Th-232  
X-AXIS NORMALISED



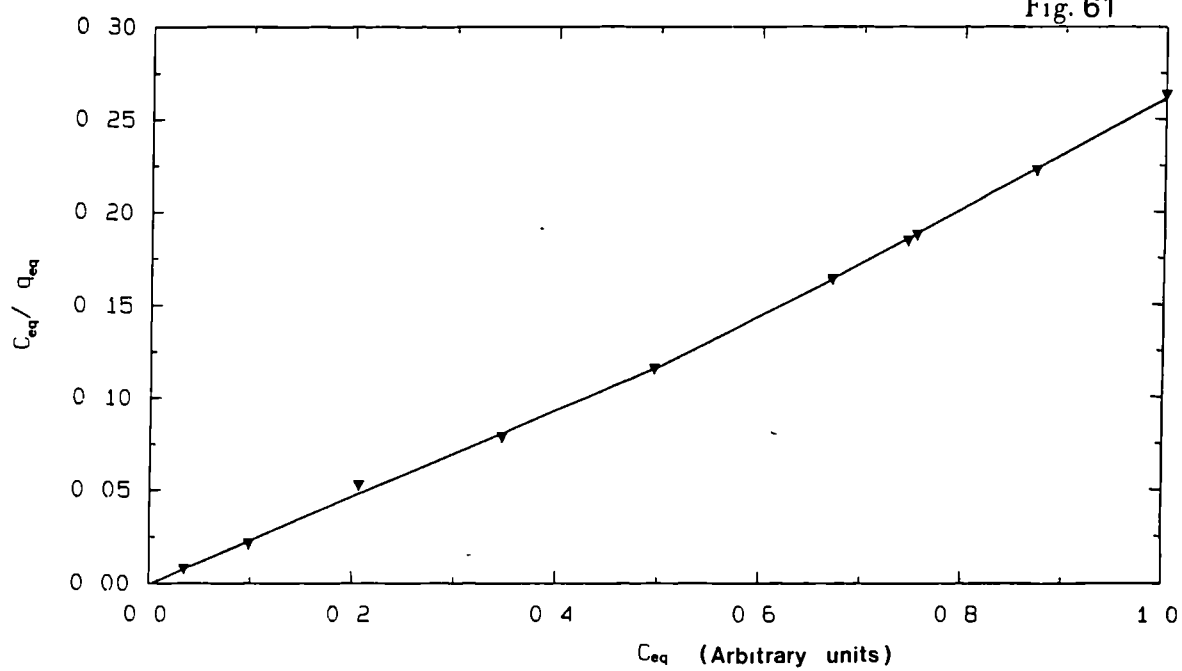
LANGMUIR PLOT CLINOPTILOLITE  $K^+$  / (Ac-228\Ra-228) 0 1N  
Th-232 X-AXIS NORMALISED

Fig. 60



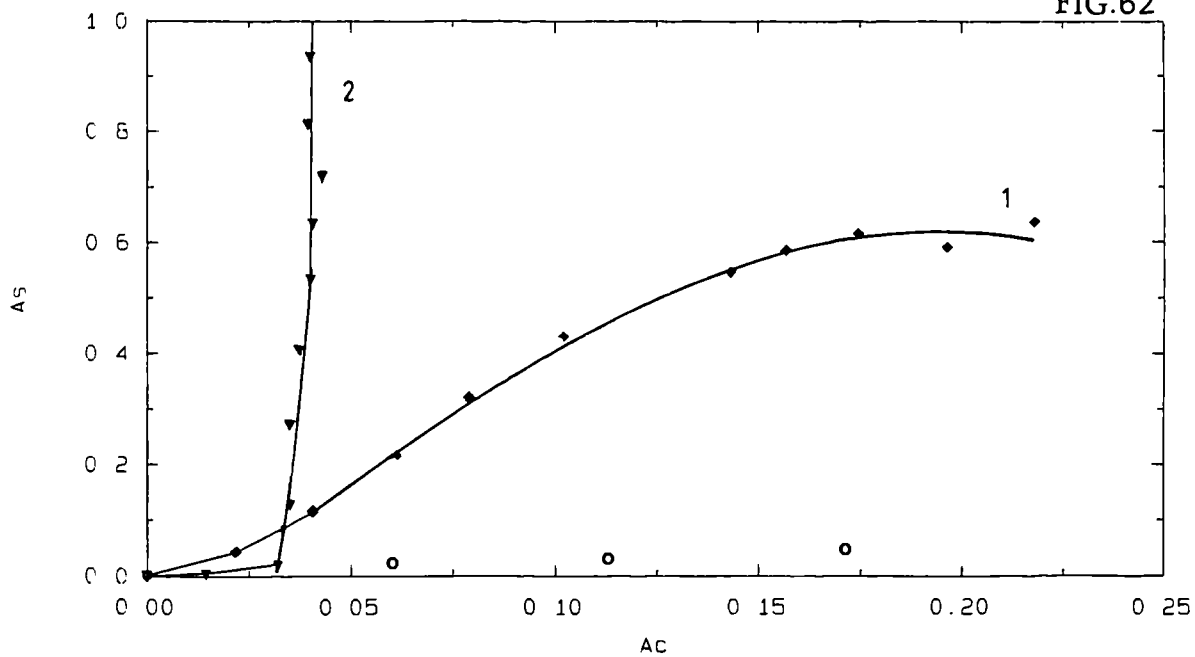
LANGMUIR PLOT CLINOPTILOLITE  $Na^+$  / (Ac-228\Ra-228) 0 1N  
Th-232. X-AXIS NORMALISED

Fig. 61



ISOTHERM CLINOPTILOLITE 1)  $\text{Na}^+ / \text{UO}_2^{2+}$  2)  $\text{K}^+ / \text{UO}_2^{2+}$

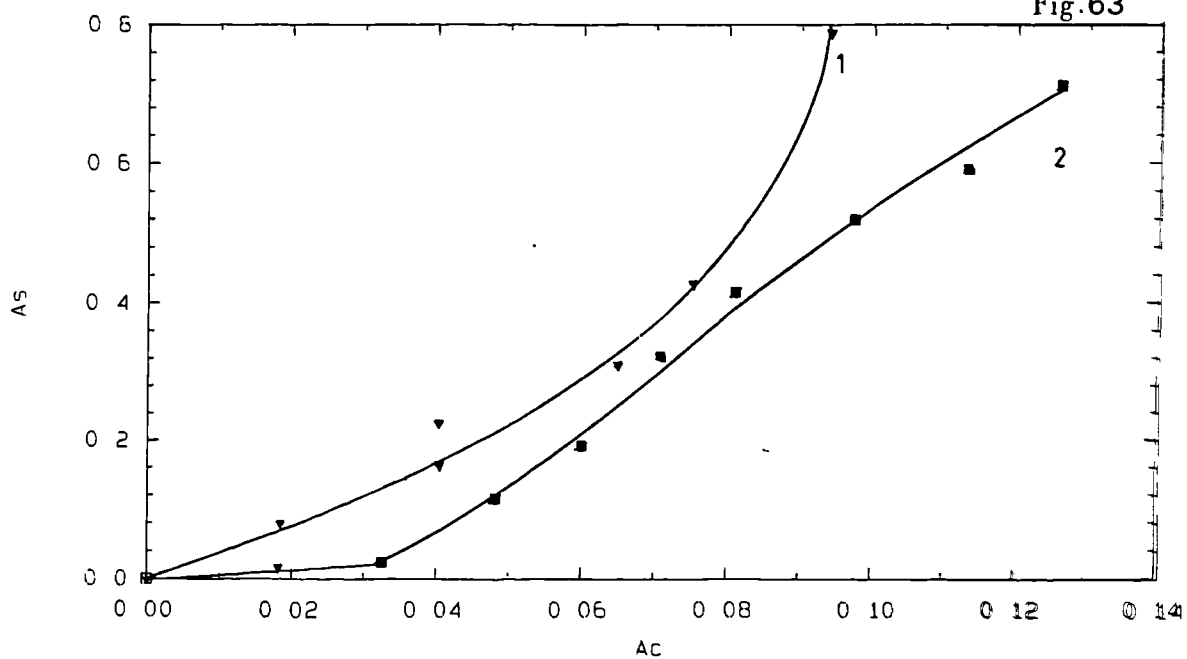
FIG.62



Curve 1: ○ Indicate Reversibility Points

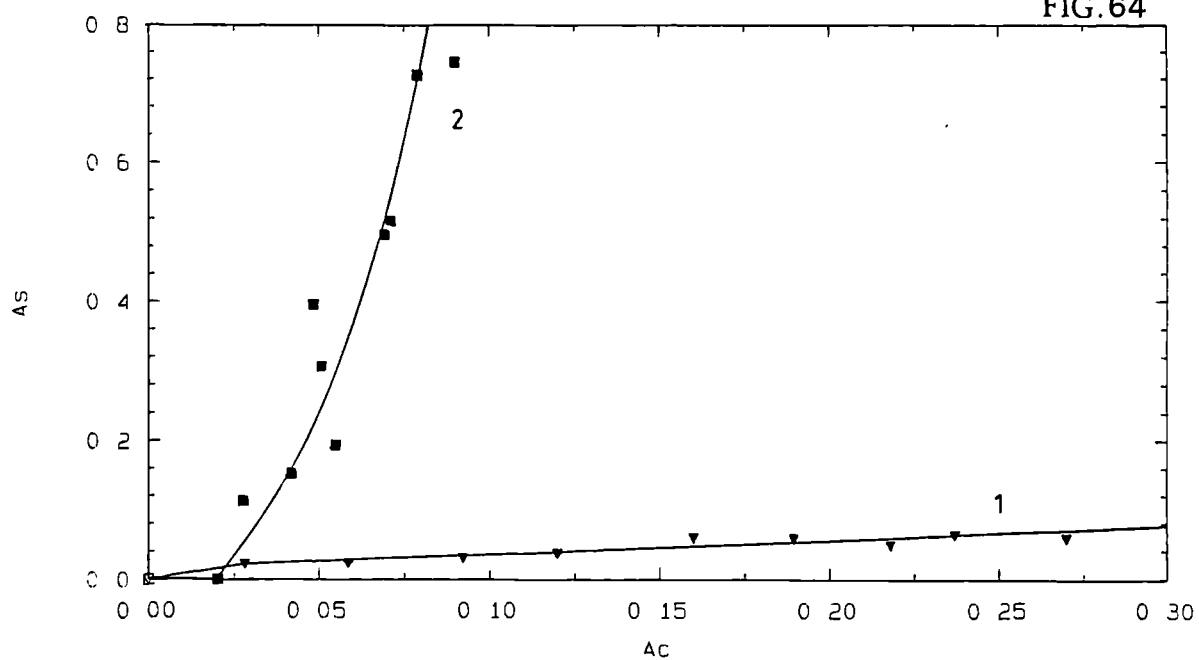
ISOTHERM Z900 1)  $\text{Na}^+ / \text{UO}_2^{2+}$  2)  $\text{K}^+ / \text{UO}_2^{2+}$

Fig.63



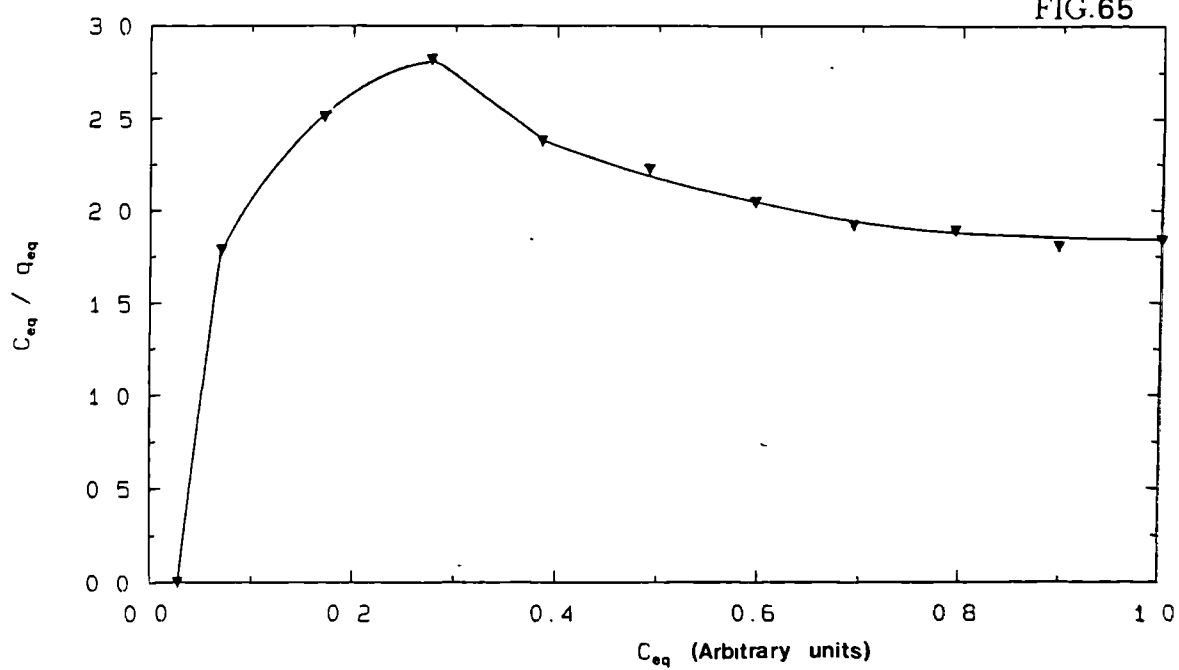
ISOTHERM ZEOLITE Y. 1)  $\text{Na}^+ / \text{UO}_2^{2+}$  2)  $\text{K}^+ / \text{UO}_2^{2+}$

FIG.64

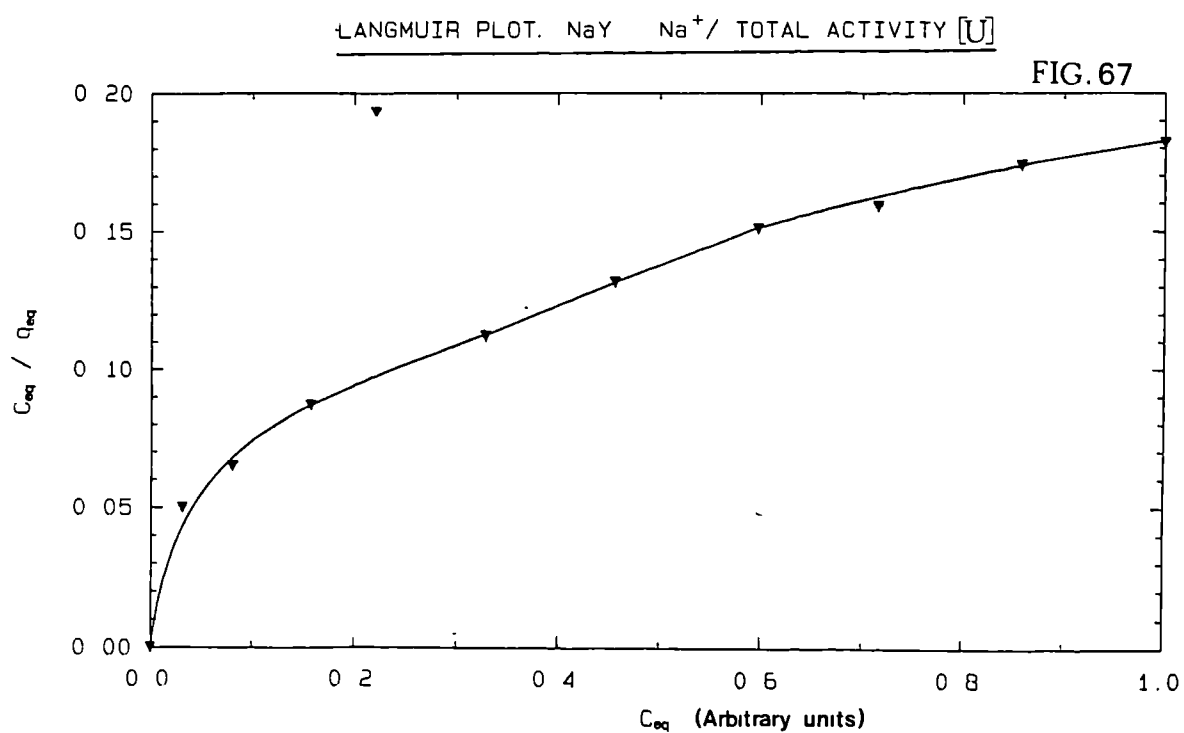
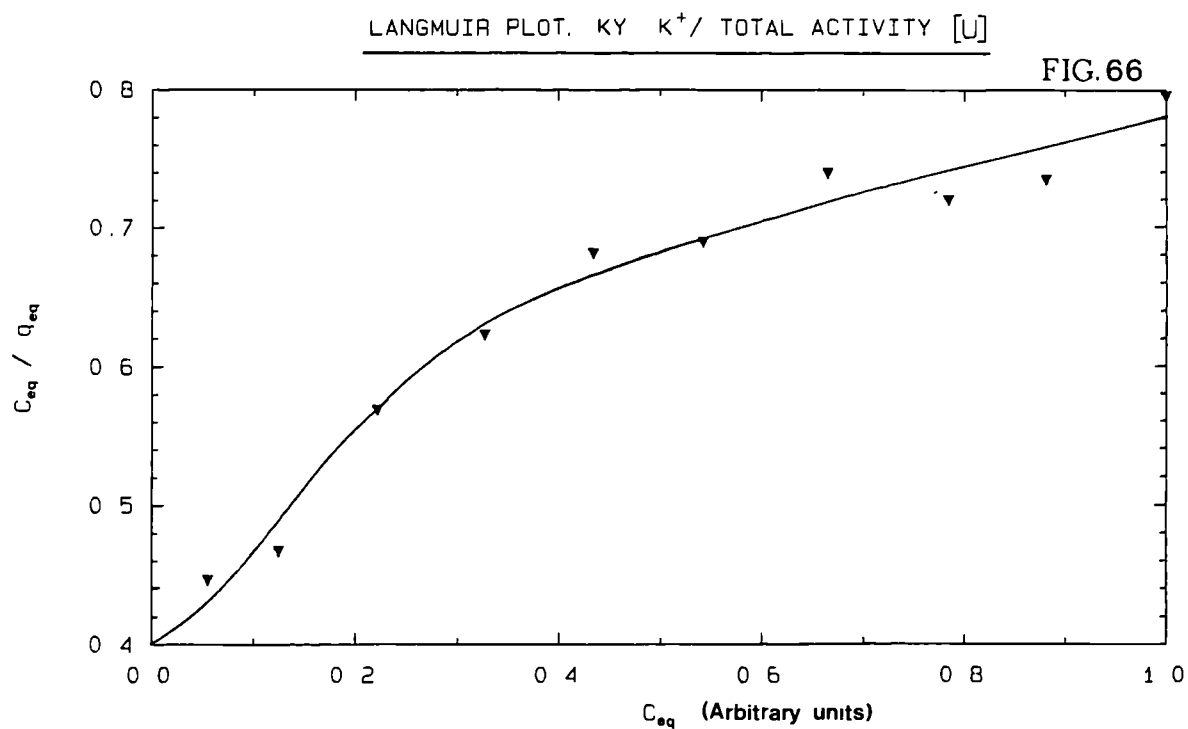


LANGMUIR PLOT CLINOPTILOLITE  $\text{Na}^+ / \text{TOTAL ACTIVITY [U]}$

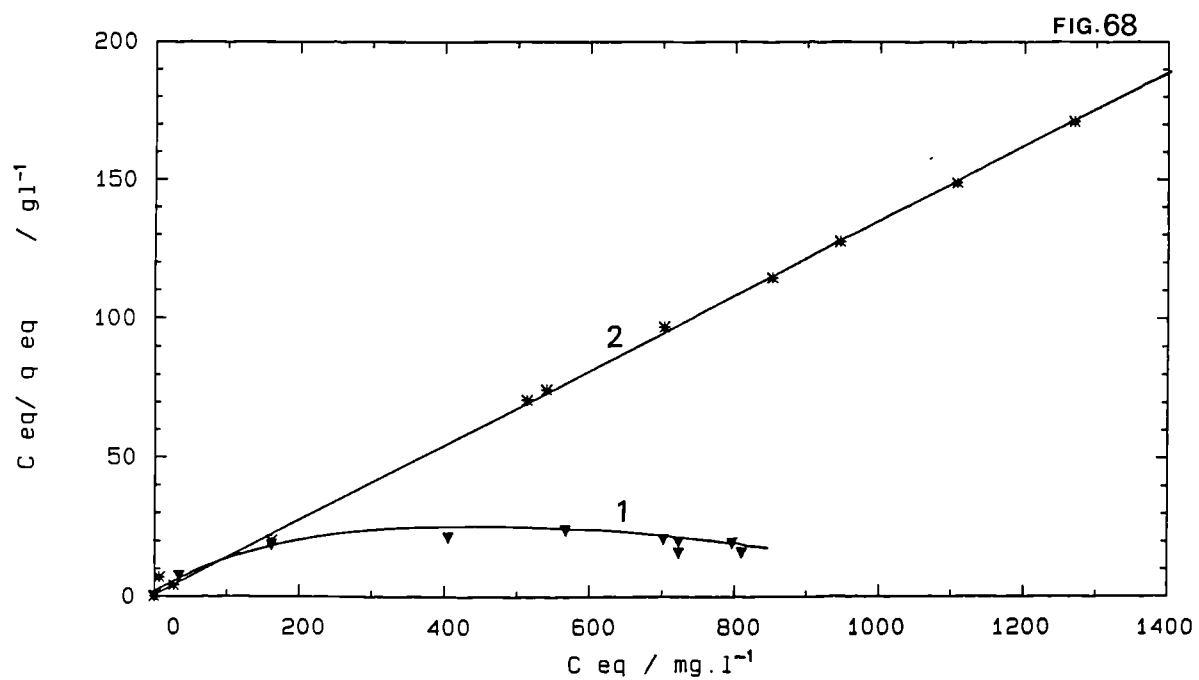
FIG.65



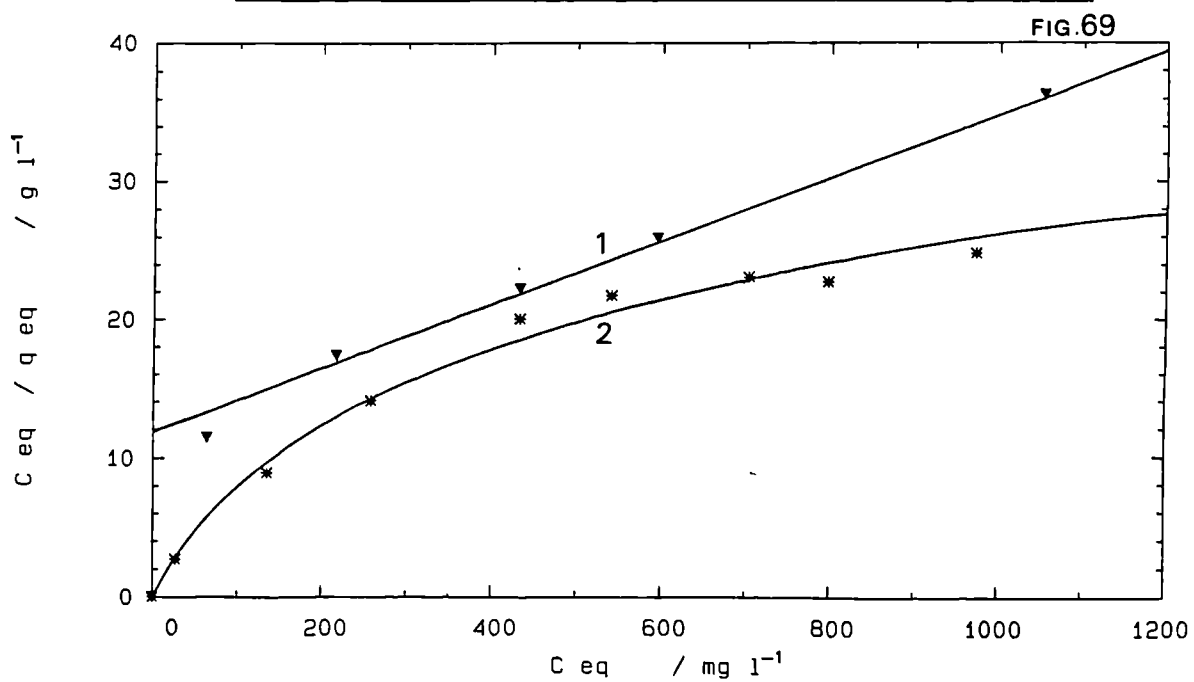




LANGMUIR PLOT. CLINOPTILOLITE CURVE1=  $\text{Na}^+/\text{UO}_2^{2+}$  CURVE2=  $\text{K}^+/\text{UO}_2^{2+}$



LANGMUIR PLOT. Z900 CURVE1=  $\text{Na}^+/\text{UO}_2^{2+}$  CURVE2=  $\text{K}^+/\text{UO}_2^{2+}$



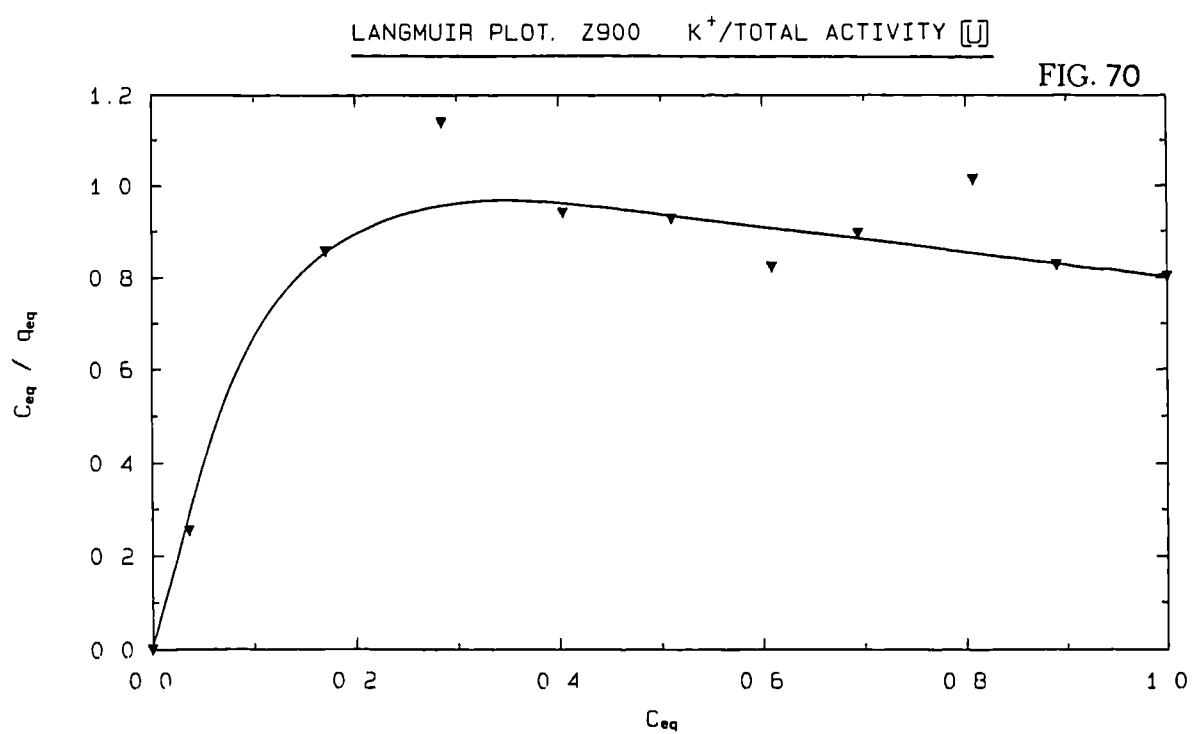


TABLE 58

REPEAT EXCHANGE VALUES OF THORIUM AND URANIUM/meq  
OF FURTHER EXCHANGE ON SELECTED ZEOLITES

ZEOLITE	ISOTHERM TYPE	meq REMOVAL OF THORIUM OR URANIUM SPECIES
Z900	$K^+ / Th^{4+}$	0.025
CLINOPTILOLITE	$Na^+ / UO_2^{2+}$	0.043
NaY	$Na^+ / UO_2^{2+}$	0.080

TABLE 59

ISOTHERM SOLID ANALYSIS :  $\text{Na}^+/\text{Th}^{4+}$  0.1N  
(Na-Clinoptilolite)

SAMPLE VIAL NUMBER	ANALYSED MASS OF ZEOLITE/g	ANALYSED MASS OF Th-232/mg	ORIGINAL MASS OF Th-232/mg	ORIGINAL MASS OF ZEOLITE/g
1	0.1222	1.23	116.0	0.1984
5	0.1445	1.58	69.6	0.1897
9	0.1247	1.23	23.2	0.1942

TABLE 60

ZEOLITES WHICH EXPERIENCED TOTAL UPTAKES OF Th-232  
IN ISOTHERM EXPERIMENTS

ZEOLITE	MAXIMUM TOTAL UPTAKE /meq THORIUM	ISOTHERM
EASTGATE	0.20	0.01N/Na/Th
EASTGATE	0.20	0.01N/K/Th
CLINOPTILOLITE	0.02	0.001N/Na/Th

TABLE 61FLUORIDE DETERMINATIONS IN RAFFINATE

SAMPLE	FLUORIDE CONCENTRATION /mg per 100 ml
RAFFINATE (STRIPPED)	280
CLINOPTILOLITE + STRIPPED RAFFINATE	200
CLINOPTILOLITE + R1 SOLUTION	200
NaY + STRIPPED RAFFINATE	170
NaY + R1 SOLUTION	170

# X-Ray Powder Diffractograms.

Fig. 71

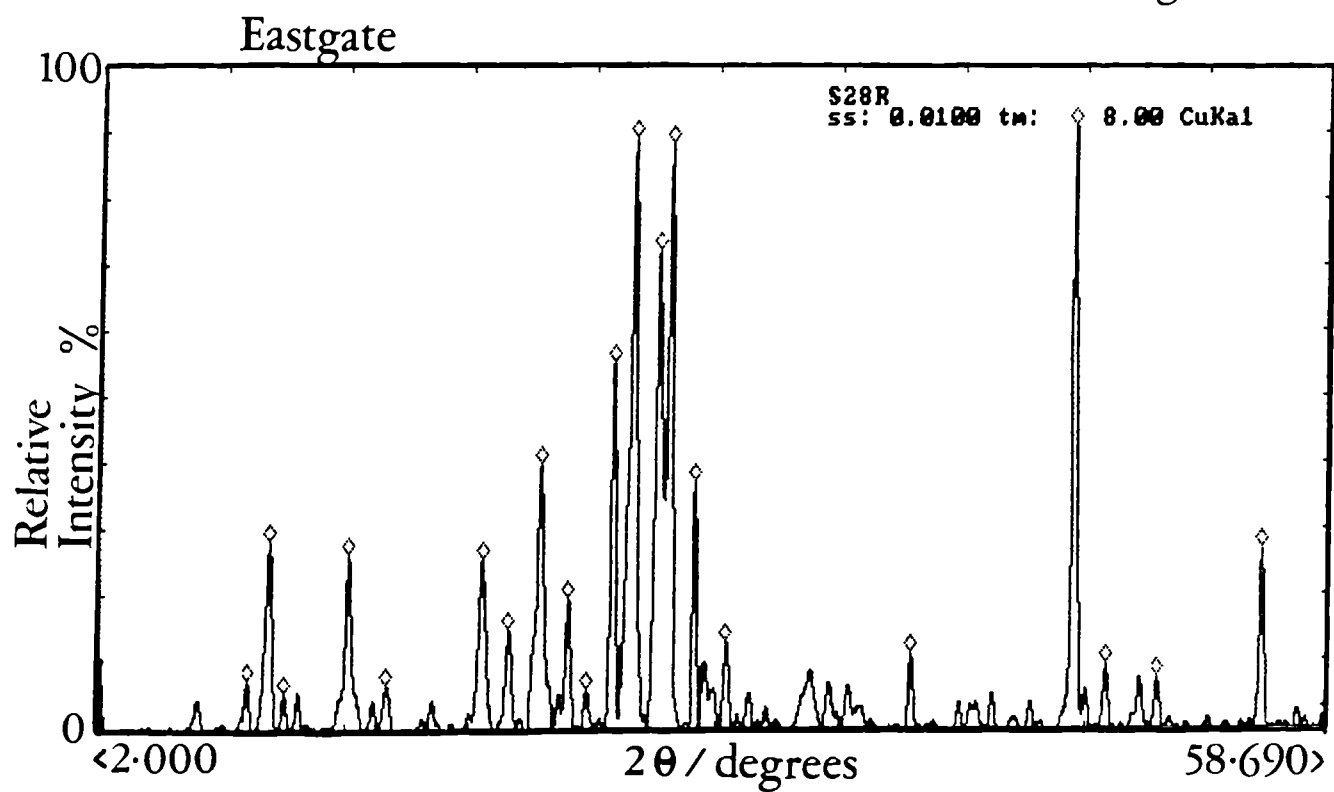
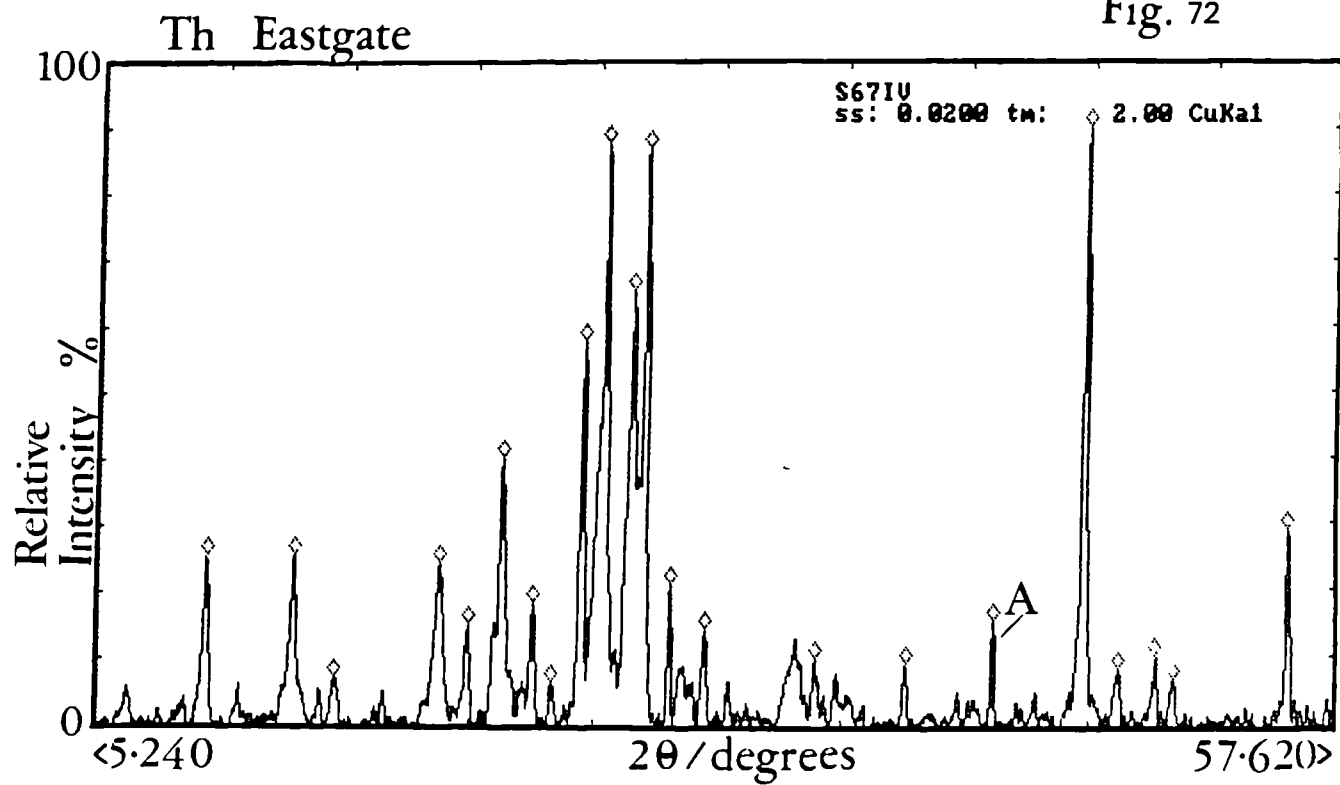


Fig. 72



# X-Ray Powder Diffractograms.

Fig. 73

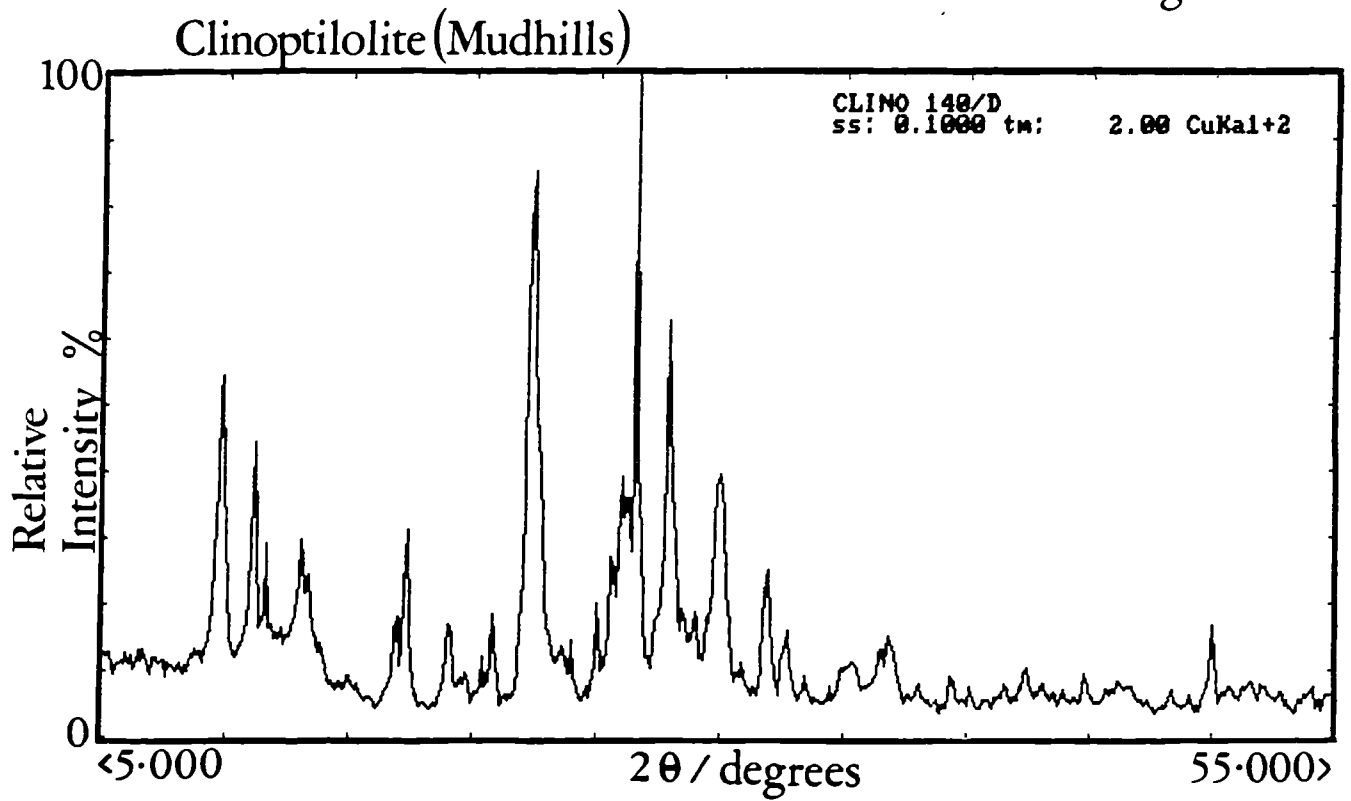
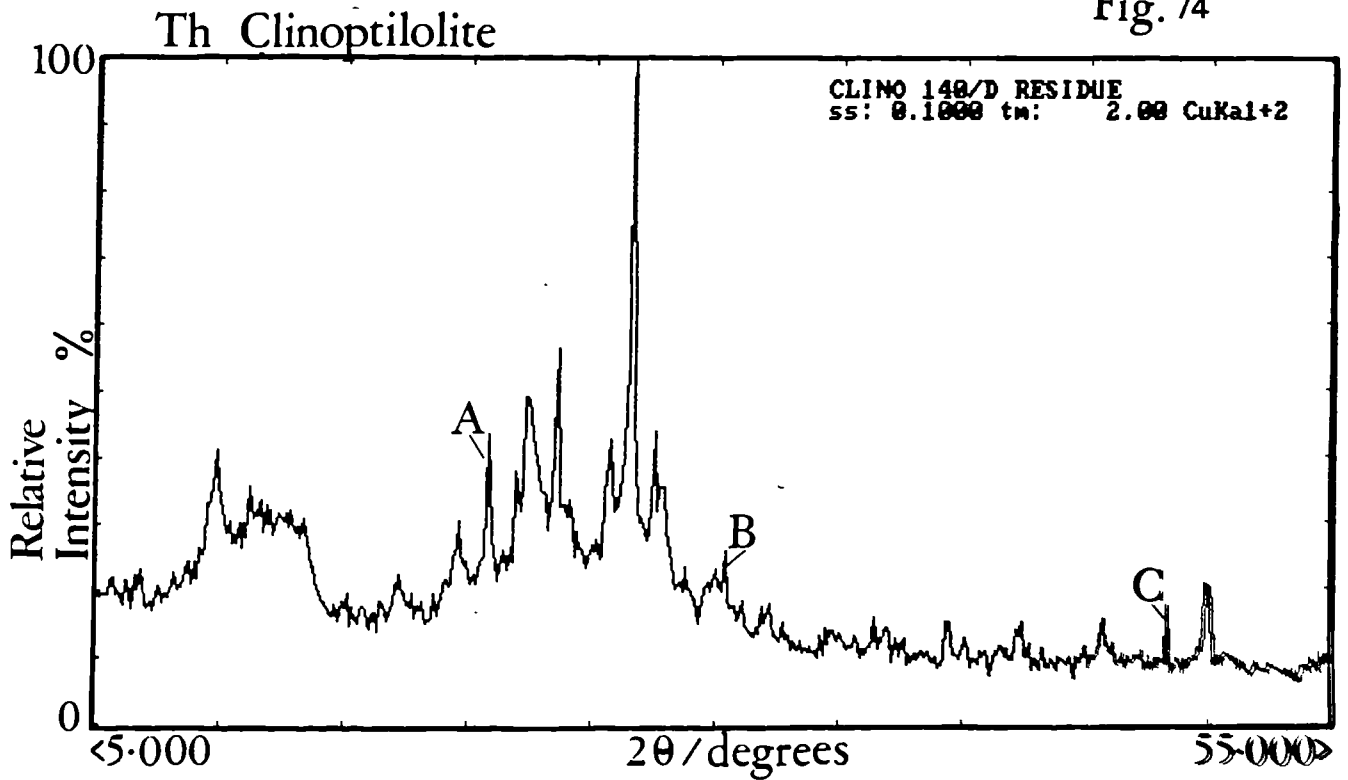
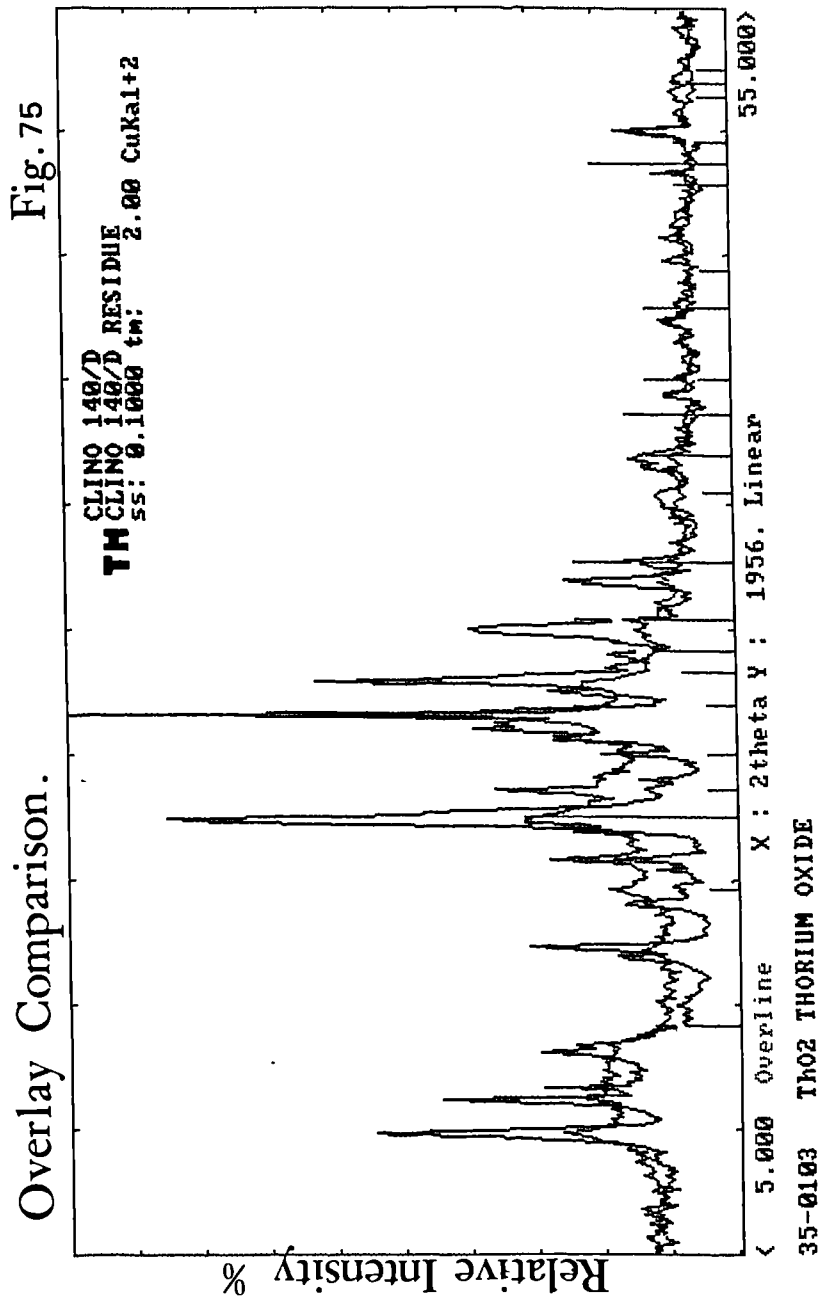


Fig. 74





## X-Ray Powder Diffractograms.



## X-Ray Powder Diffractograms.

Fig. 76

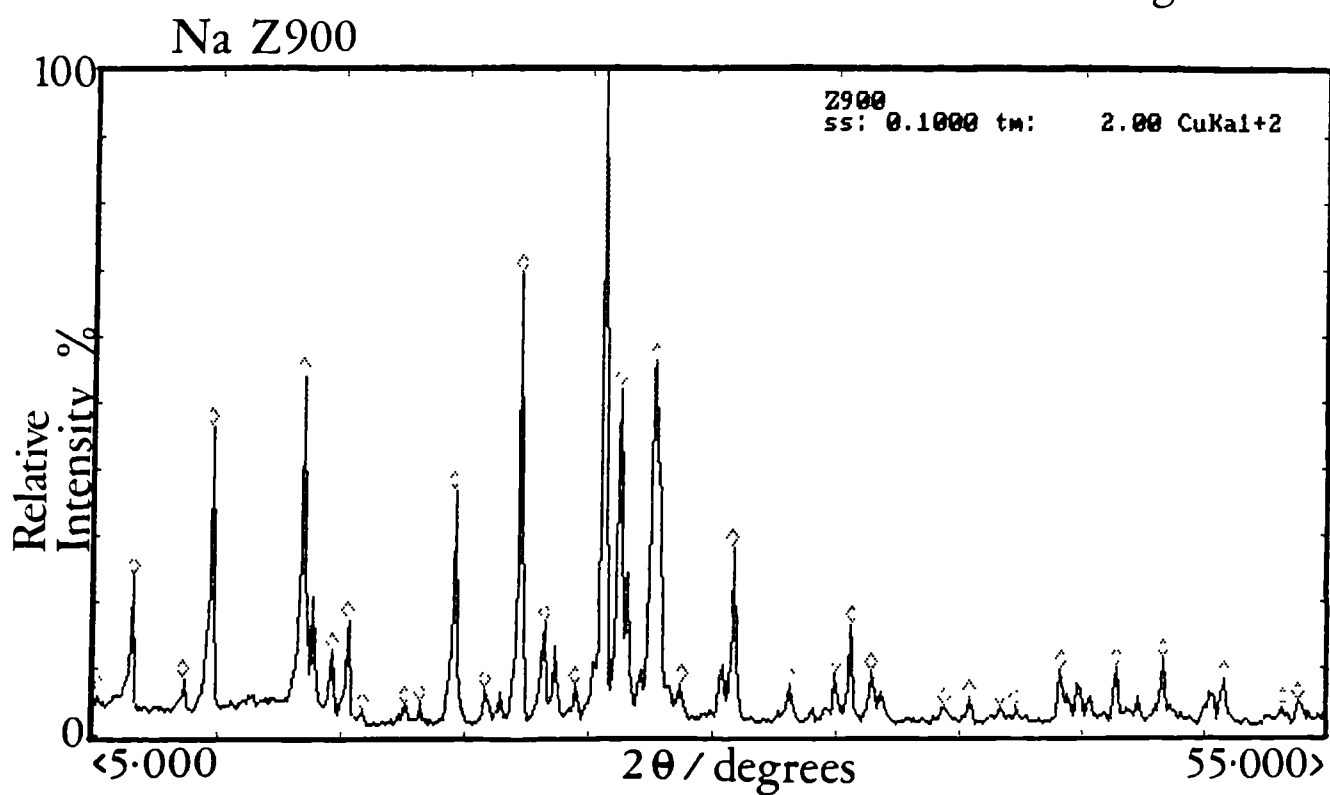
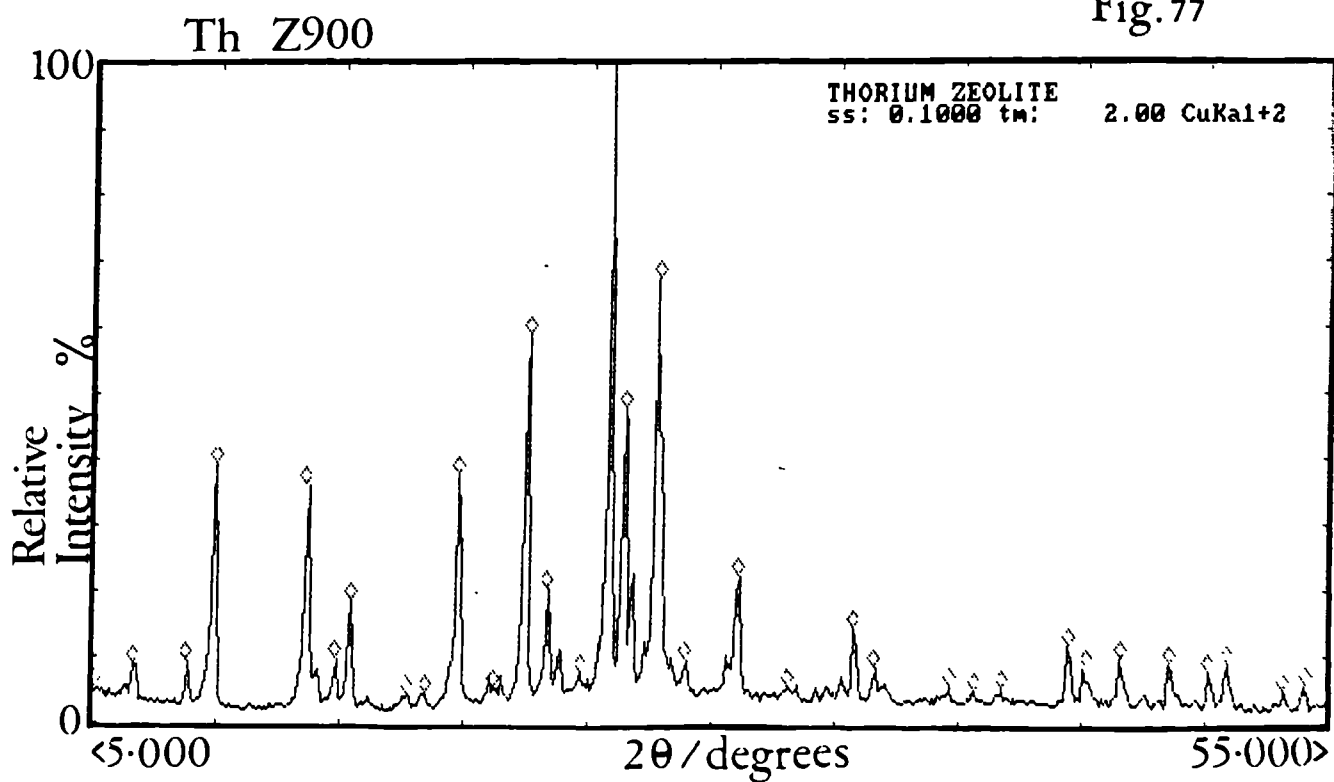


Fig. 77



# X-Ray Powder Diffractograms.

Fig. 78

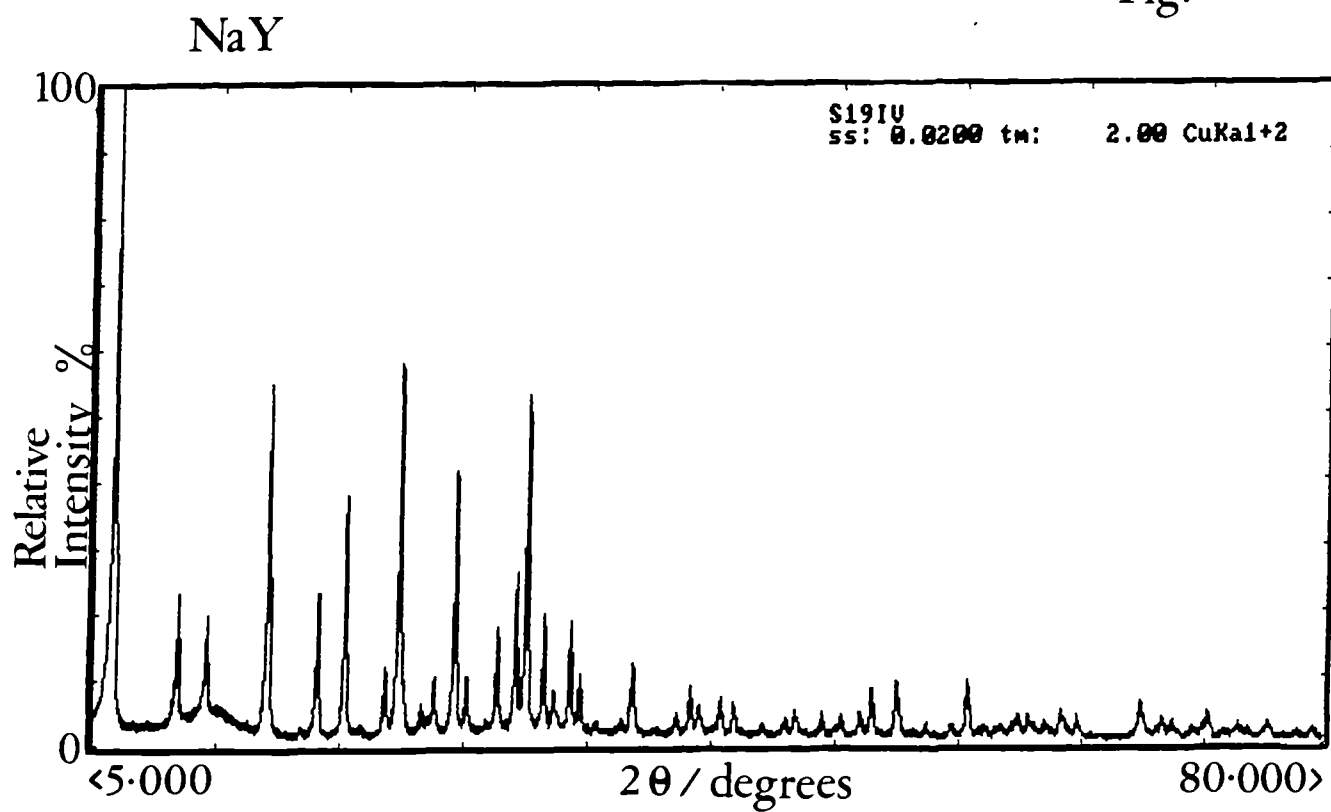
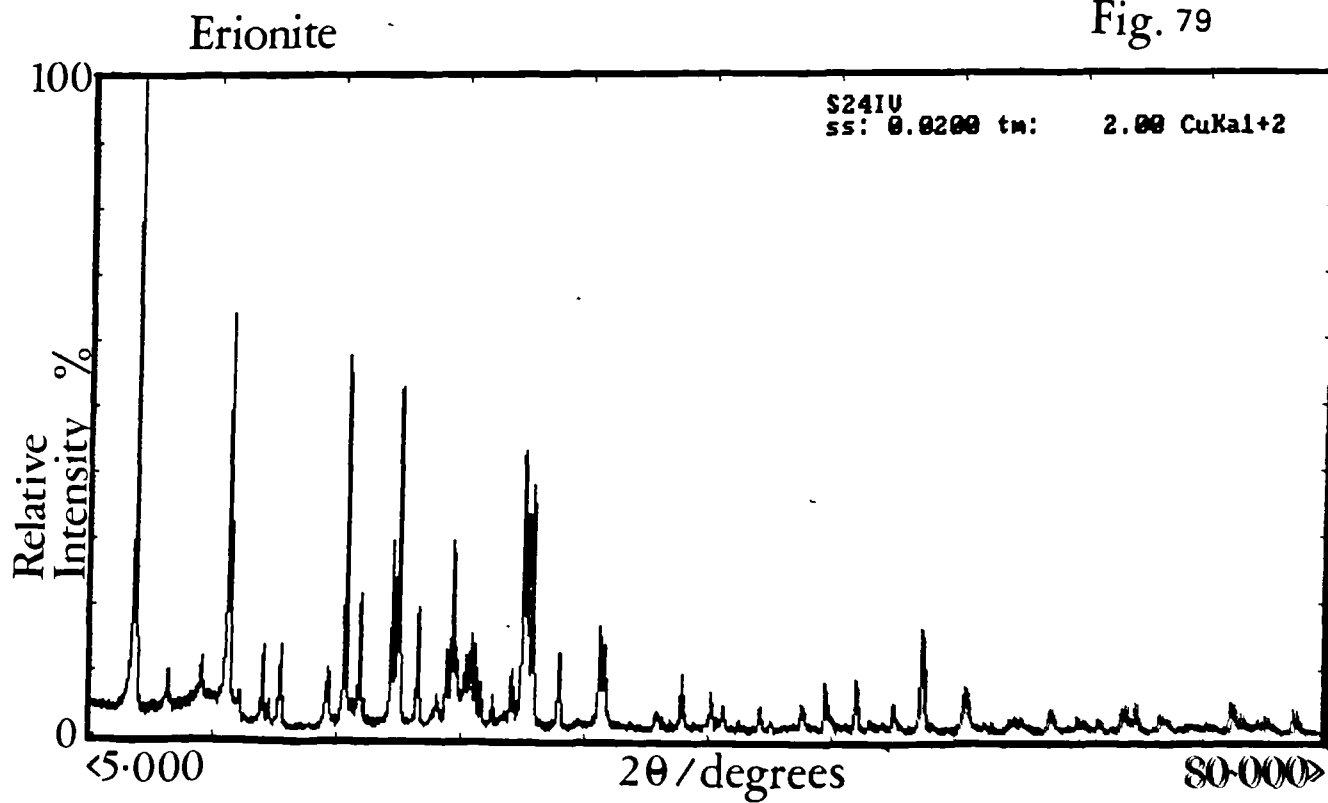


Fig. 79



# X-Ray Powder Diffractograms.

Fig. 80

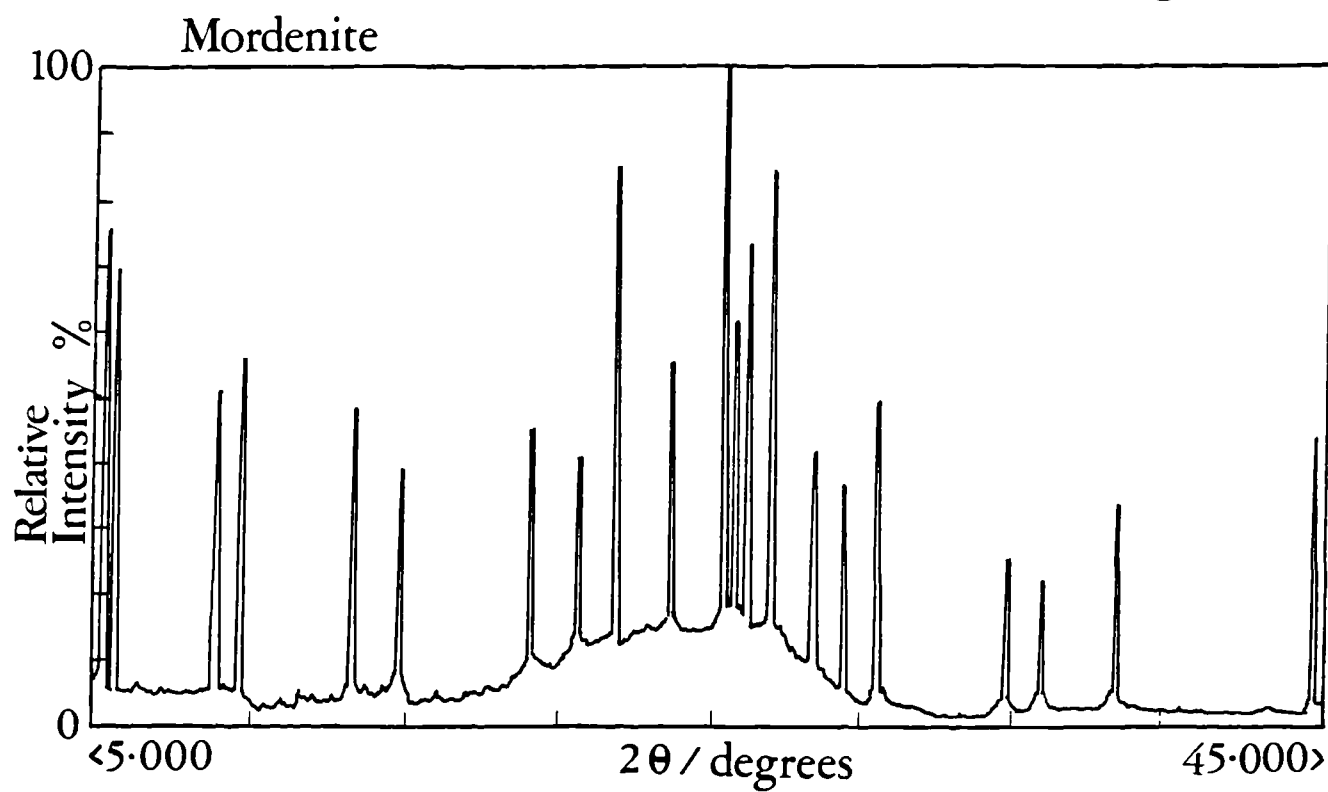
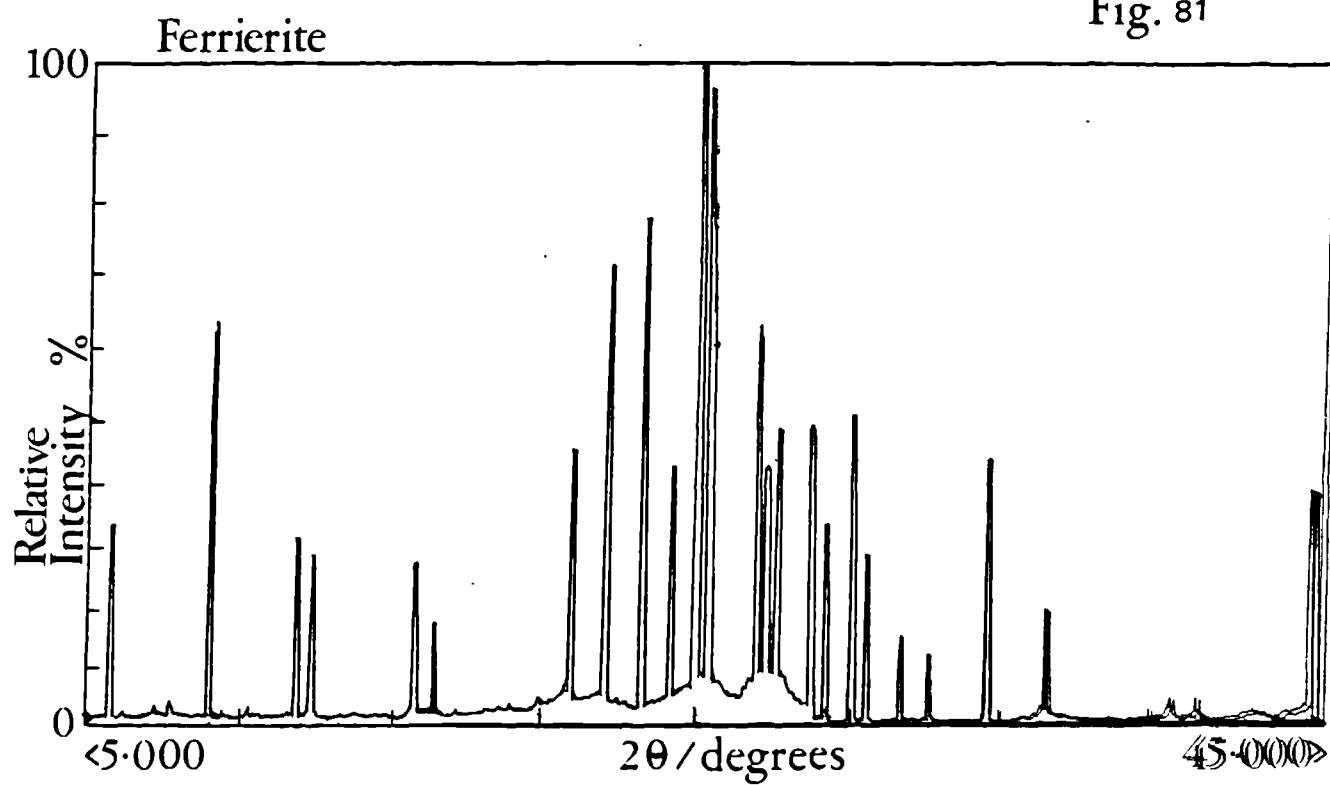


Fig. 81



X-Ray Spectrum of Clinoptilolite treated  
with Thorium. (Column unwashed.) EDX

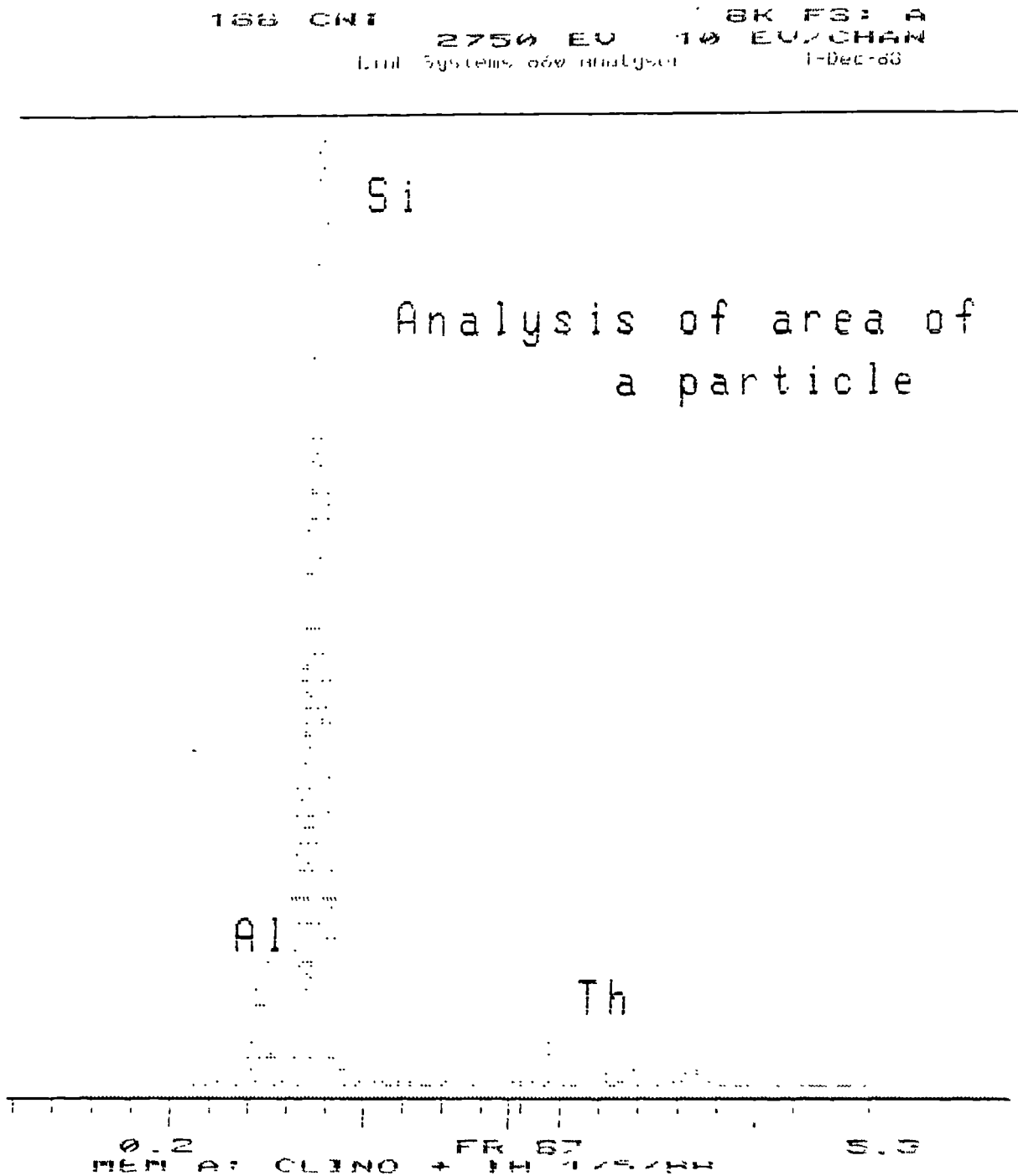


Fig. 82

X-Ray Spectrum of Clinoptilolite treated  
with Thorium. (Column unwashed.) EDX

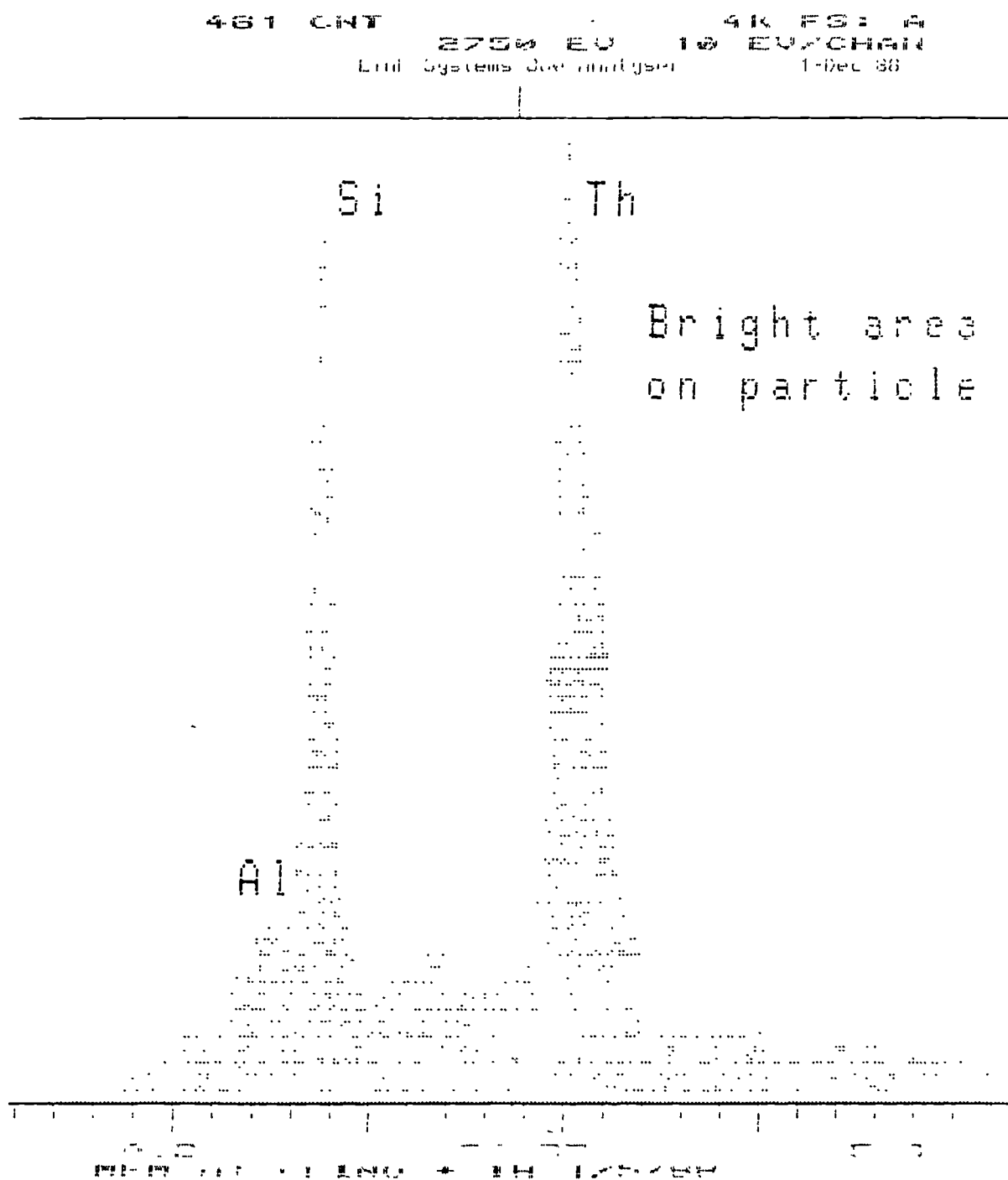


Fig. 83

X-Ray Spectrum of Eastgate treated  
with Thorium. (Acid-washed column.) EDX

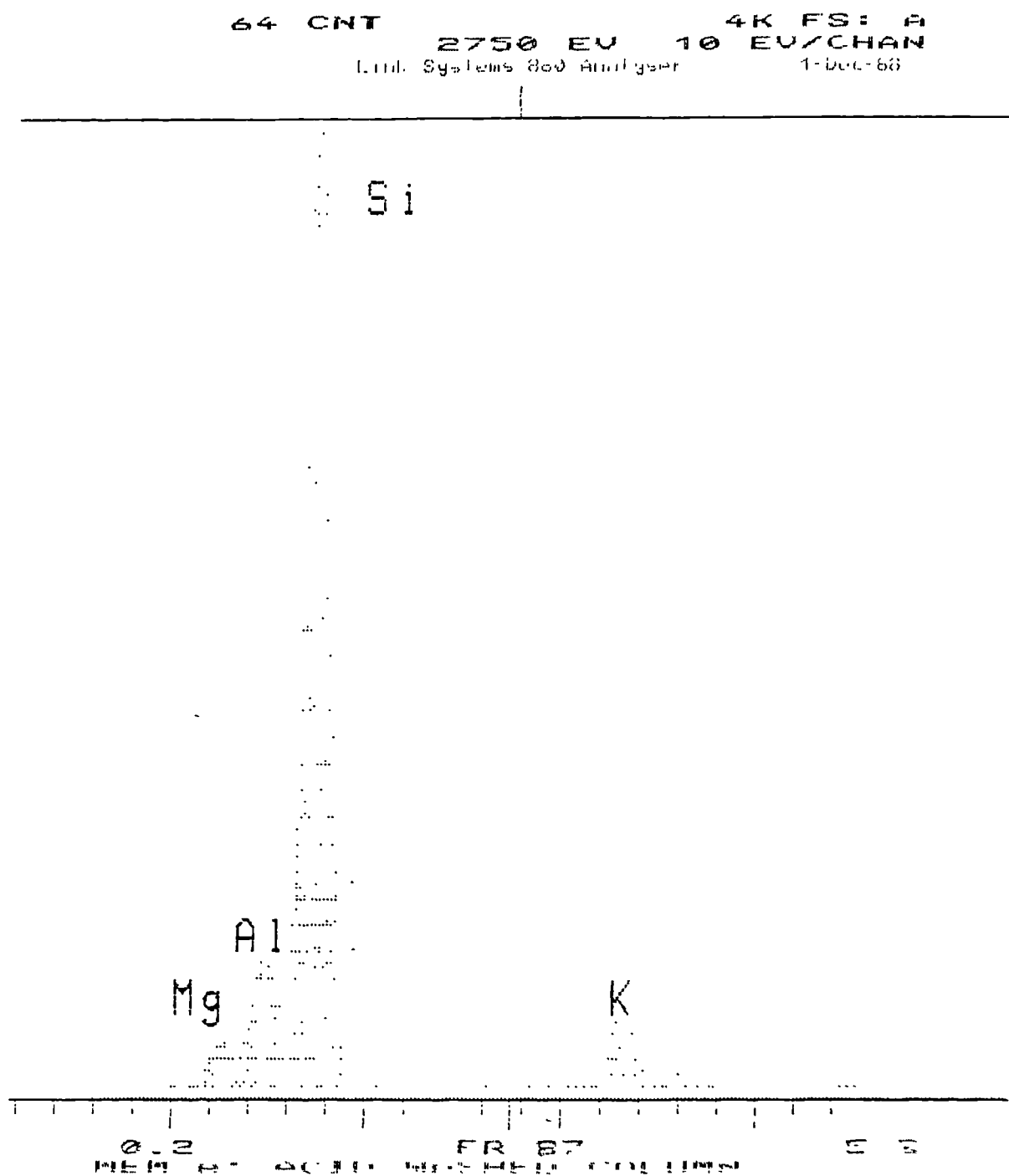


Fig. 84

X-Ray Spectrum of Z900 treated with  
Thorium. (Acid-washed column.) EDX

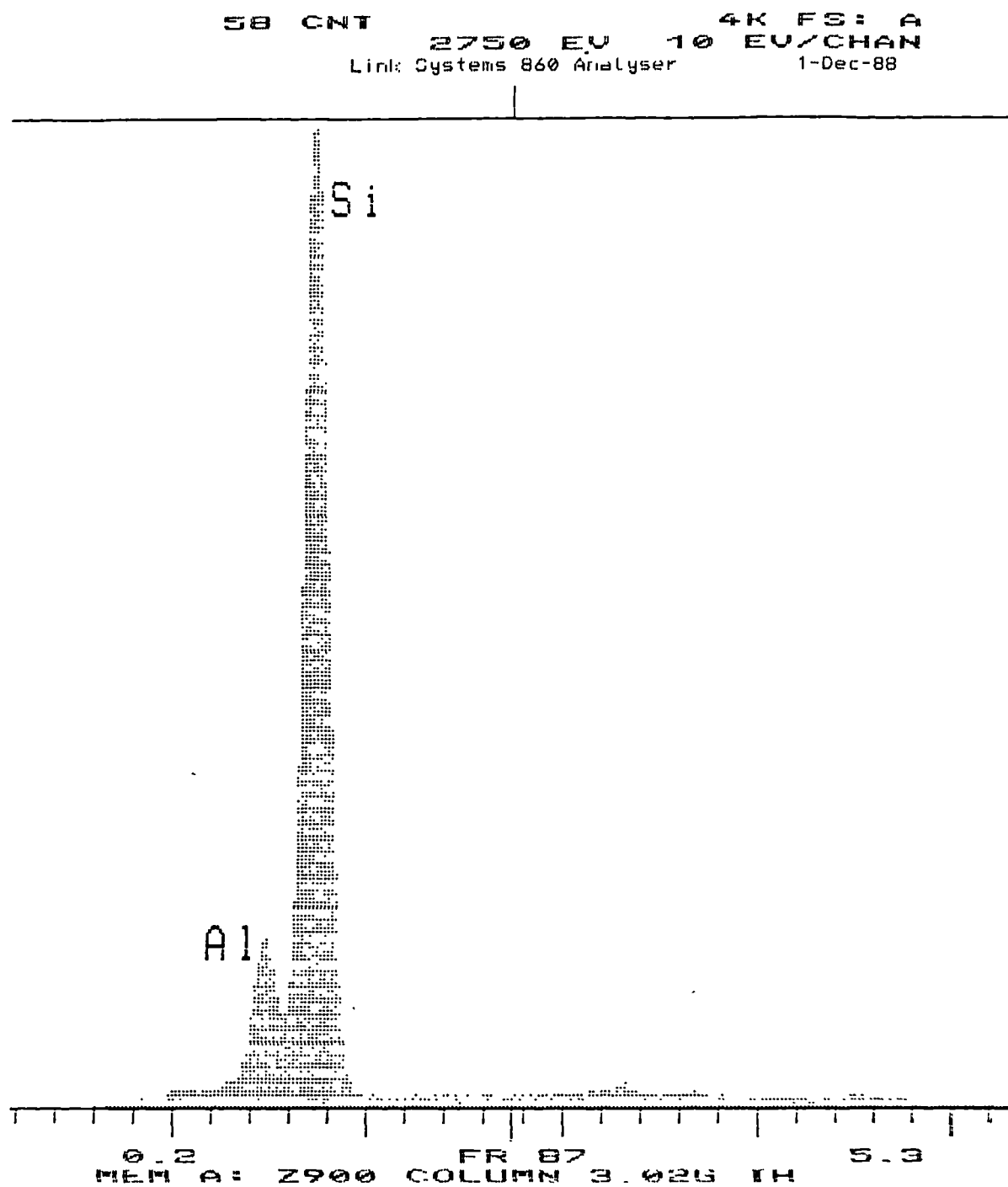


Fig. 85



X-Ray Spectrum of CaY treated with HNO<sub>3</sub>/  
Thorium. (Column unwashed.) EDX

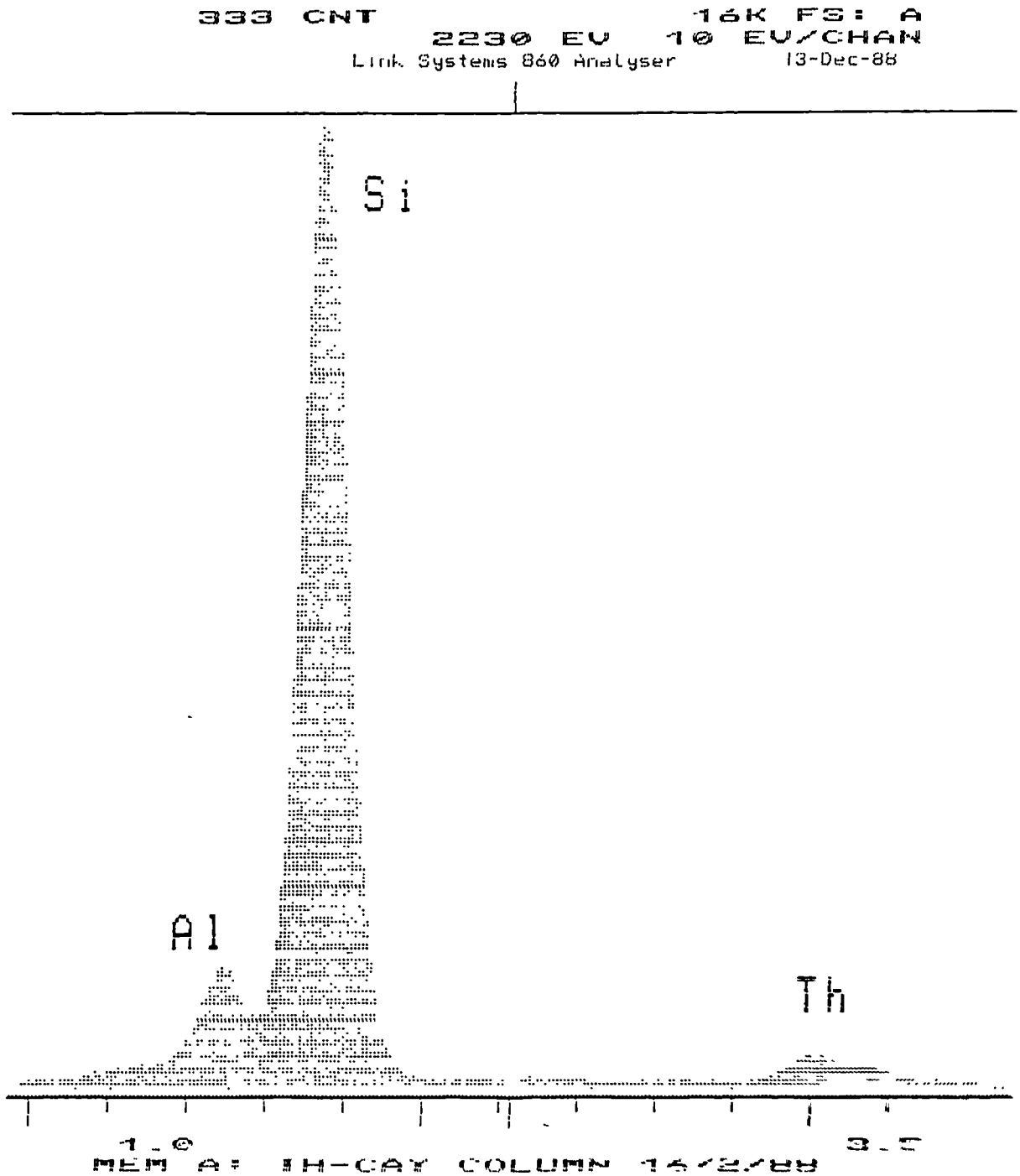


Fig. 86

X-Ray Spectrum of Clinoptilolite treated  
with Thorium. (Batch, unwashed.) EDX

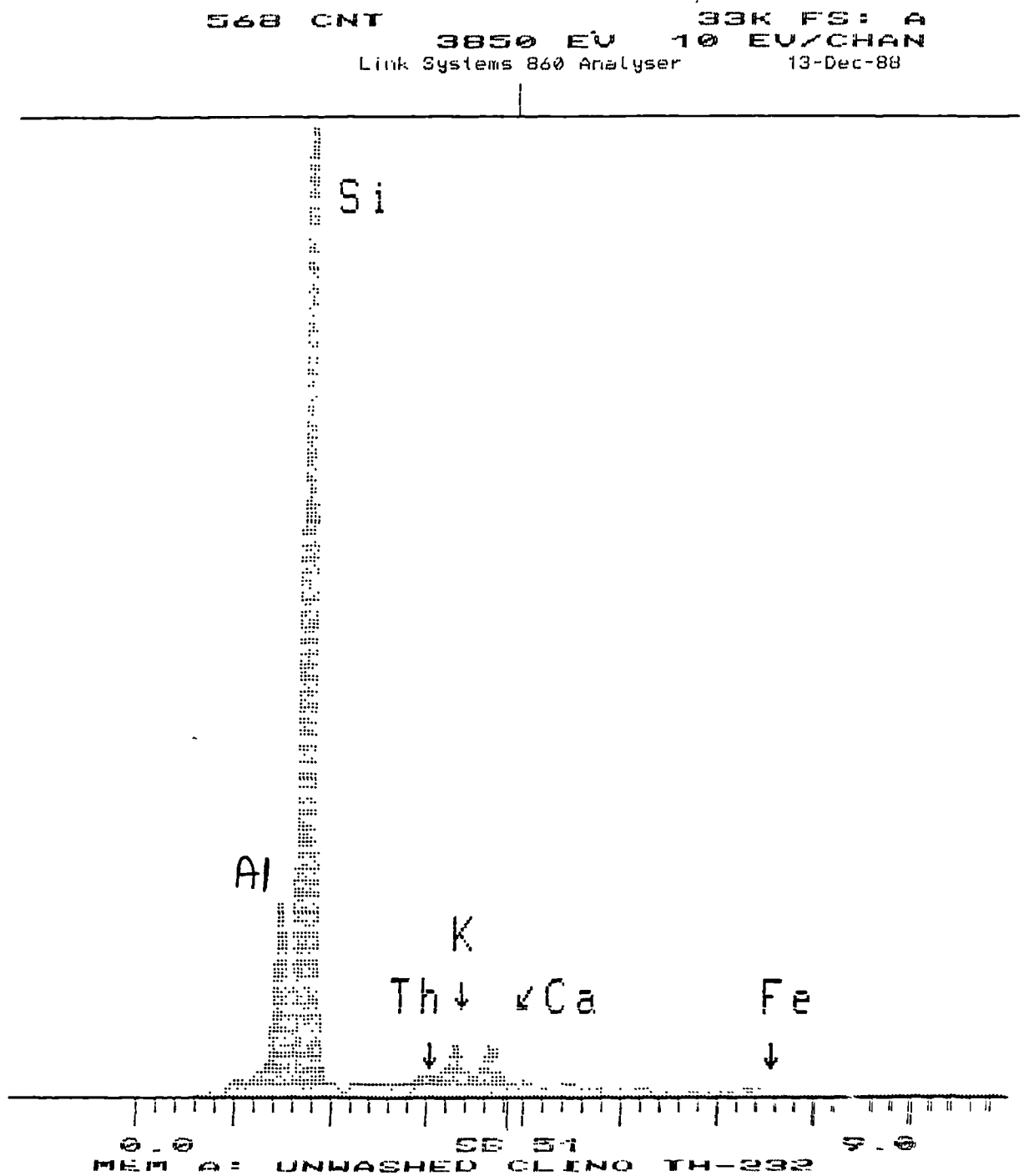


Fig. 87

# X-Ray Spectrum of Clinoptilolite treated with Thorium. (Batch.) Axes Expanded.

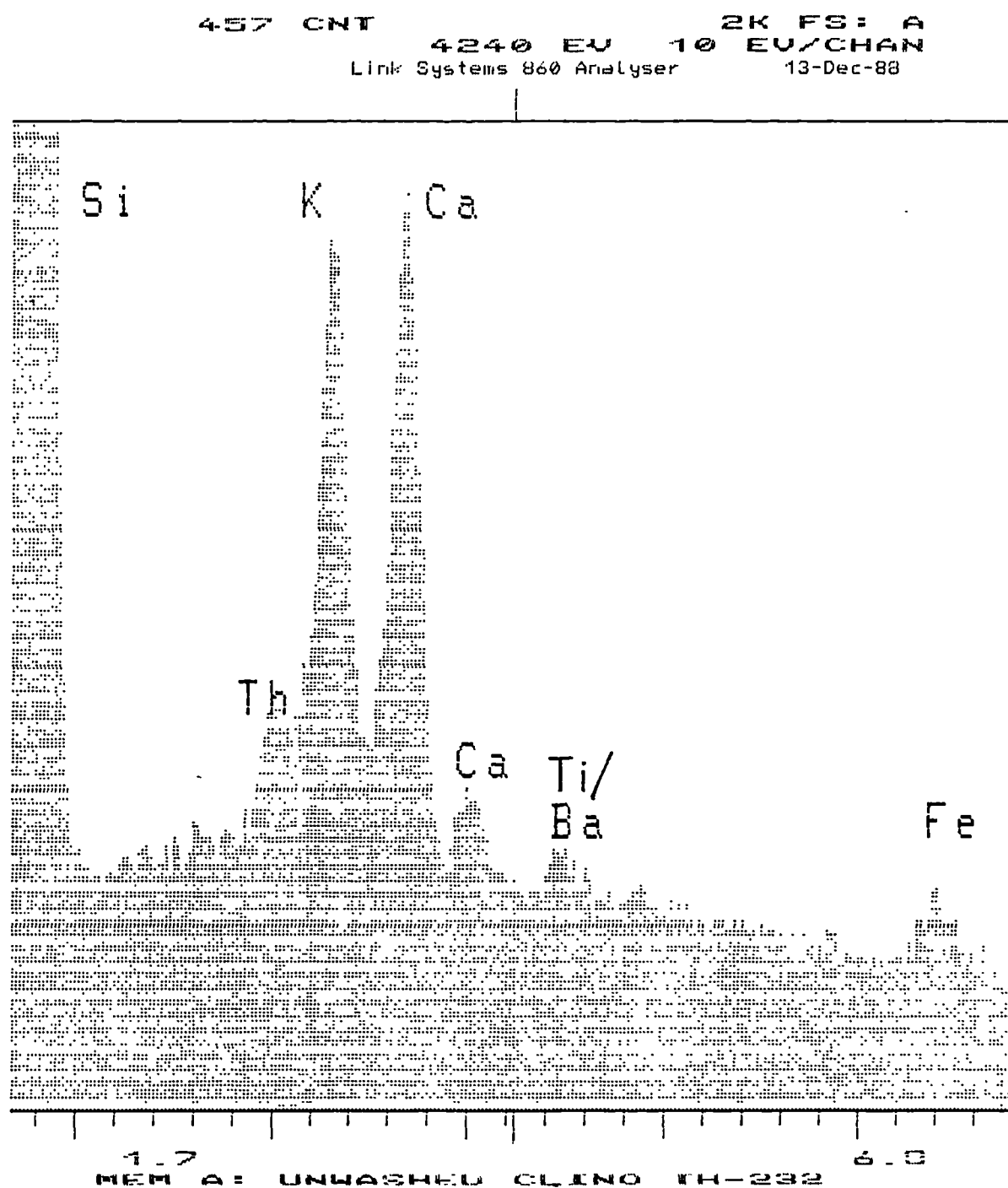


Fig. 88

## Differential Thermal Gravimetry.

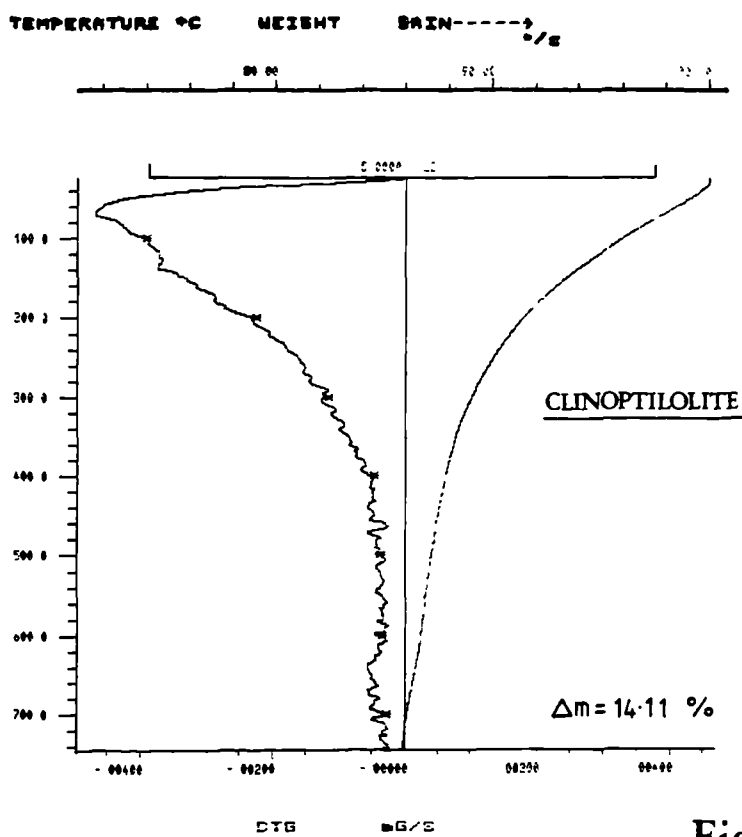


Fig. 89

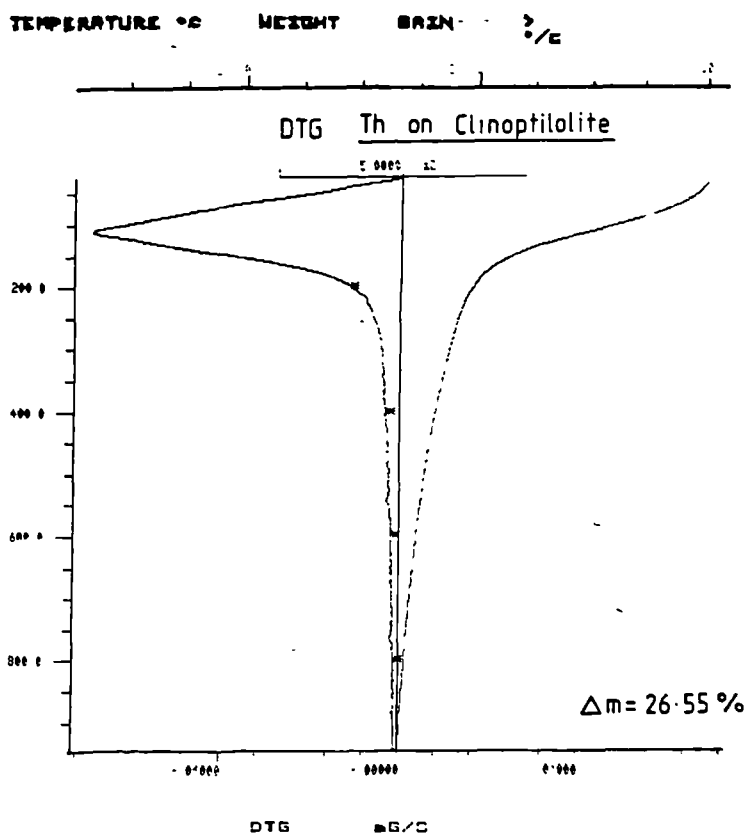


Fig. 90

# Differential Thermal Gravimetry.

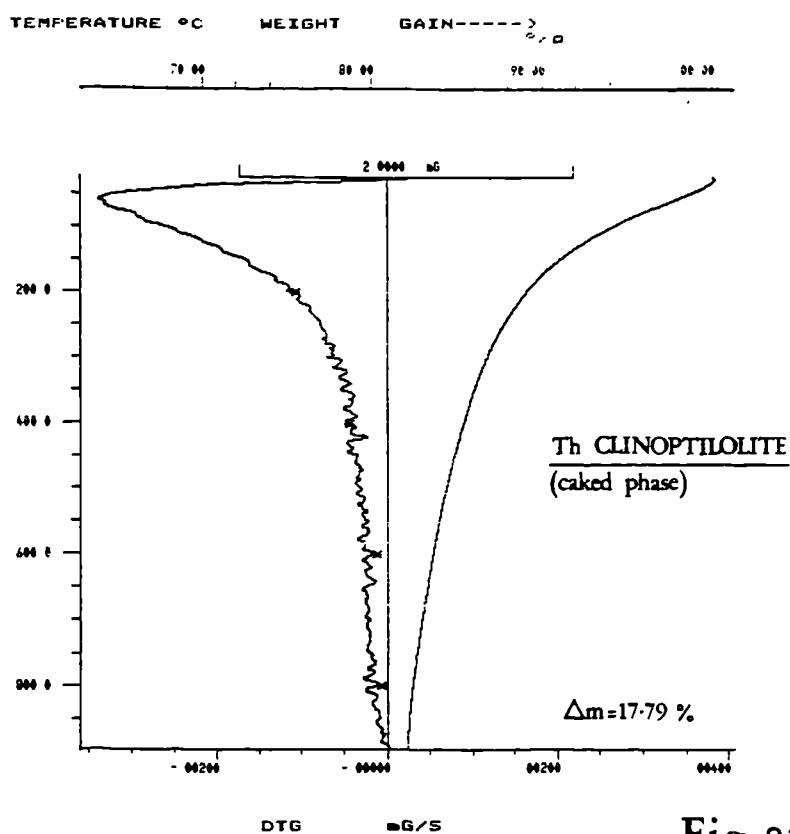


Fig. 91

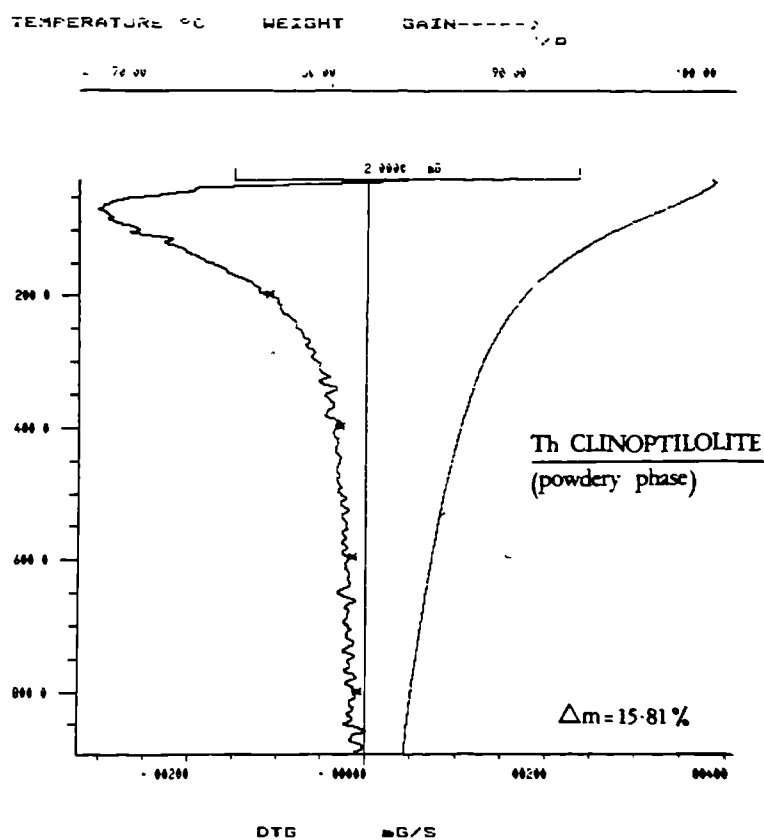


Fig. 92

# Differential Thermal Gravimetry.

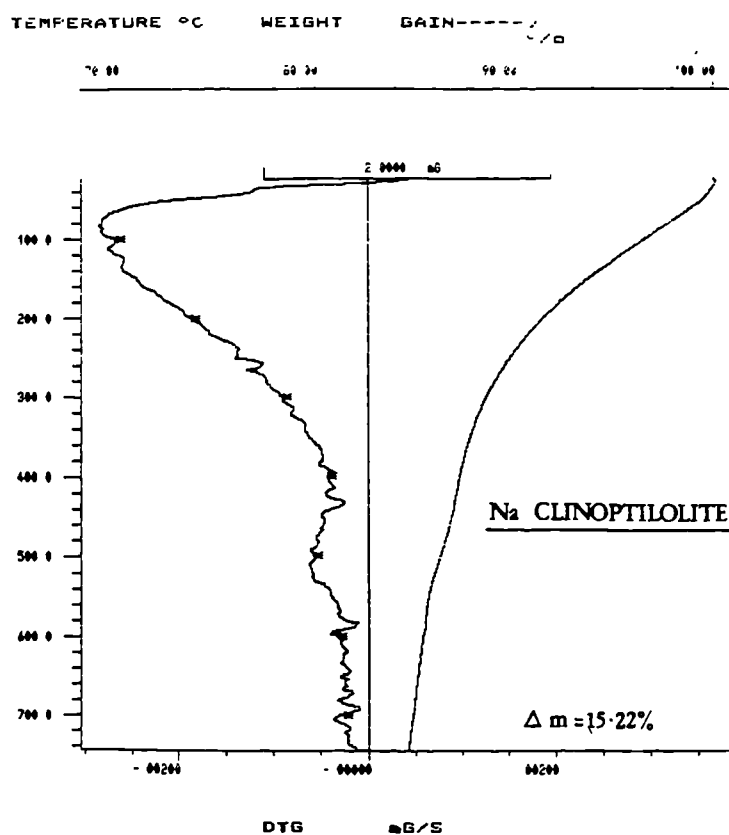


Fig. 93

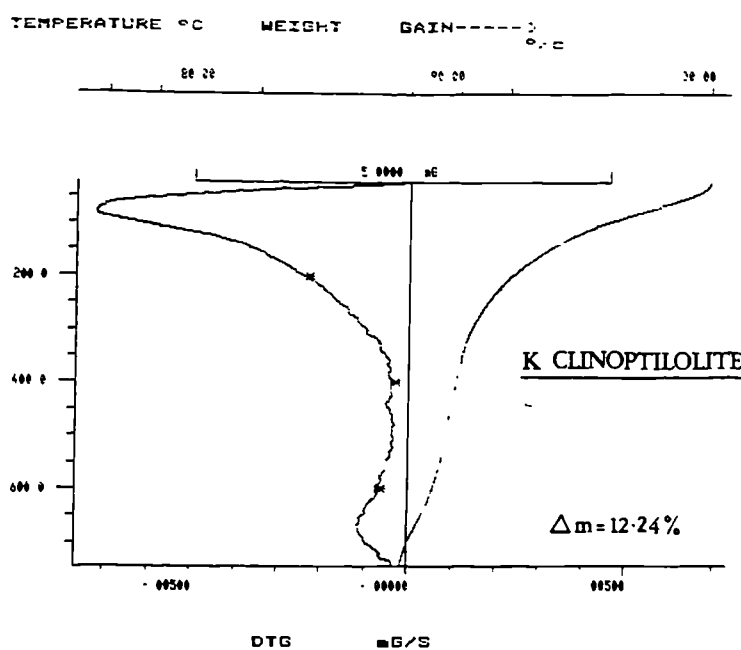


Fig. 94

# Differential Thermal Gravimetry.

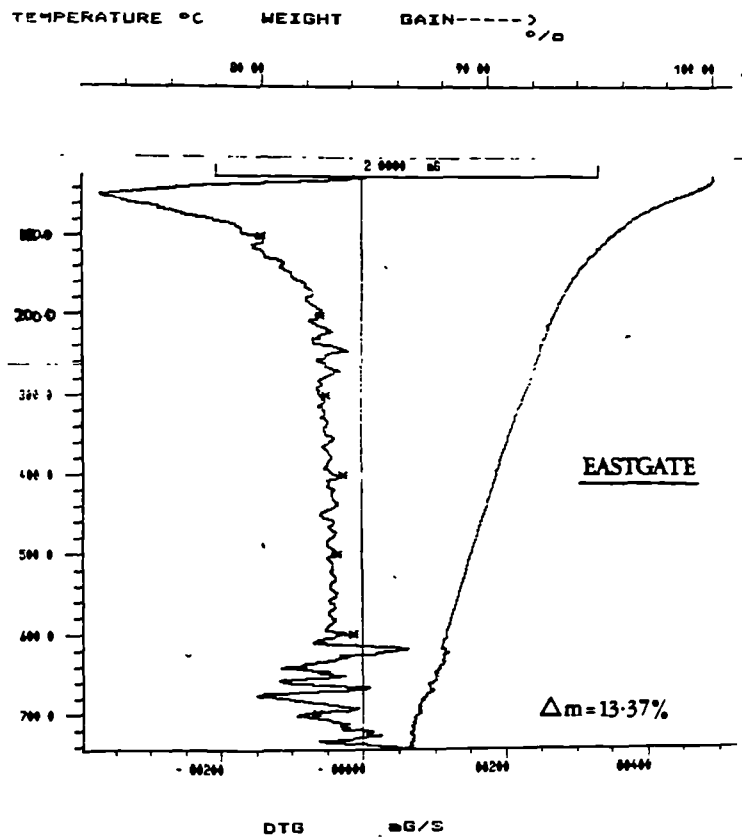


Fig. 95

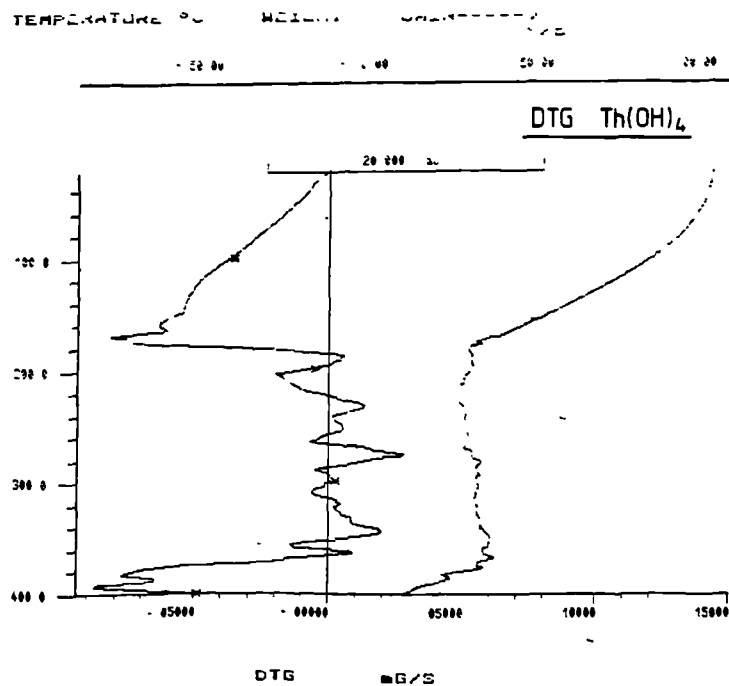


Fig. 96

# Differential Thermal Gravimetry.

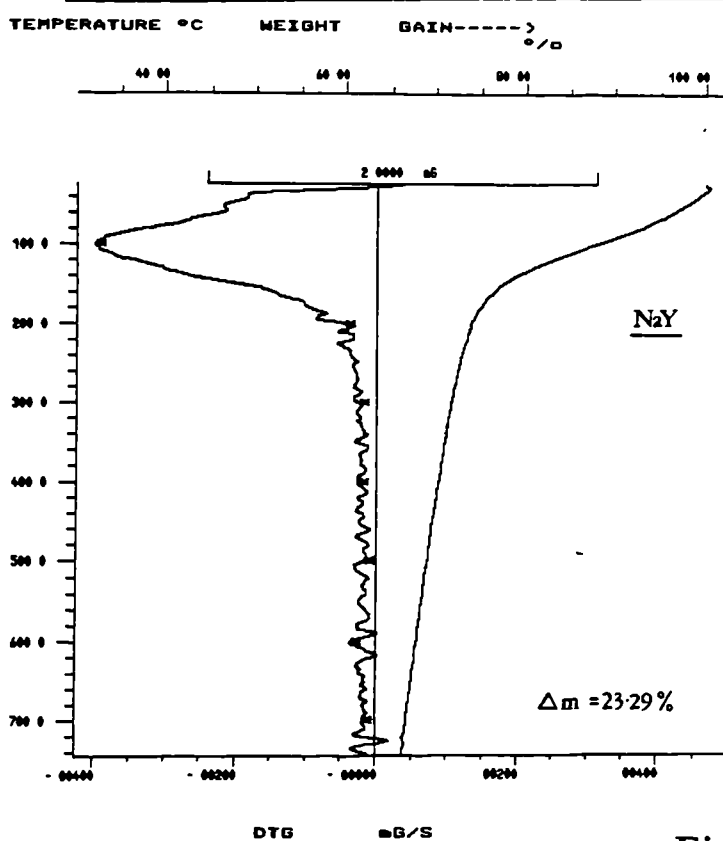


Fig. 97

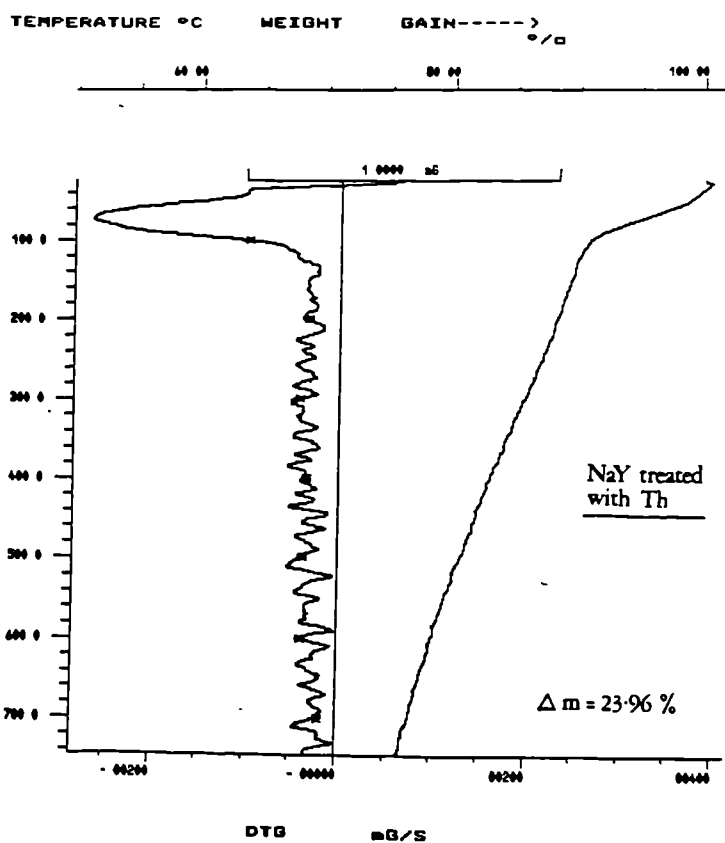


Fig. 98



# $\gamma$ -Spectrometry.

Fig. 99

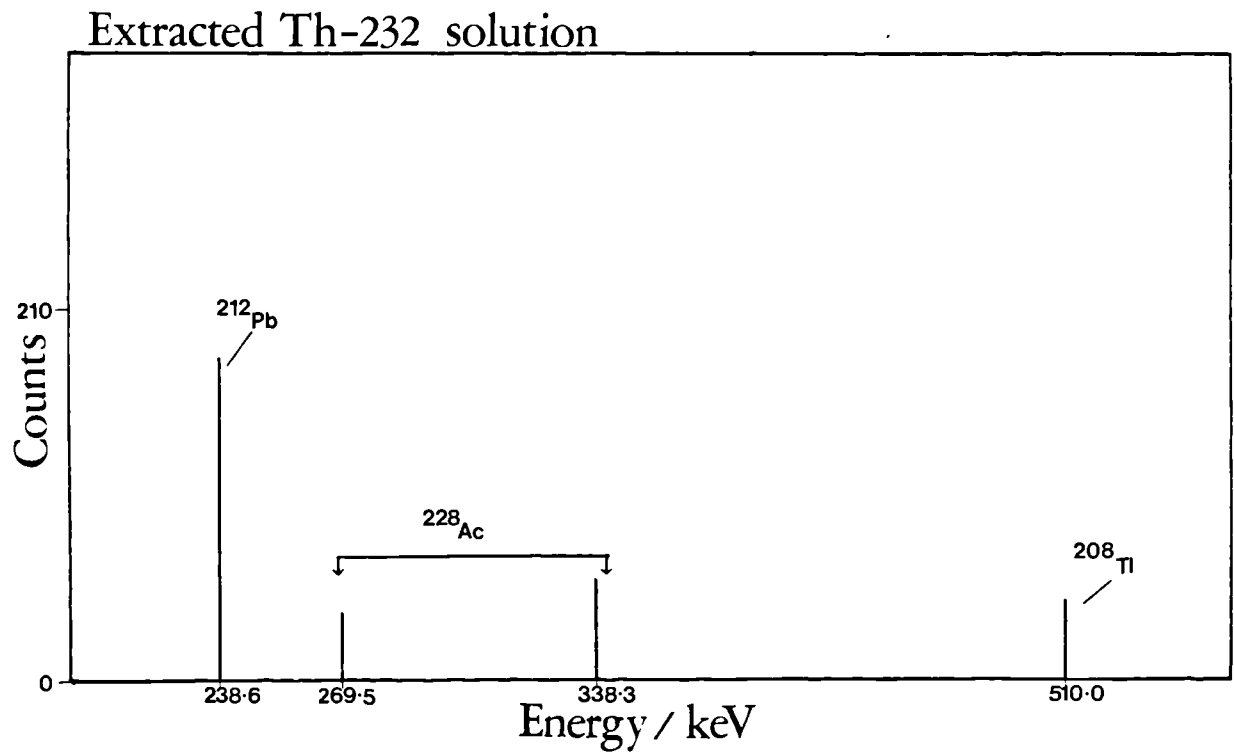
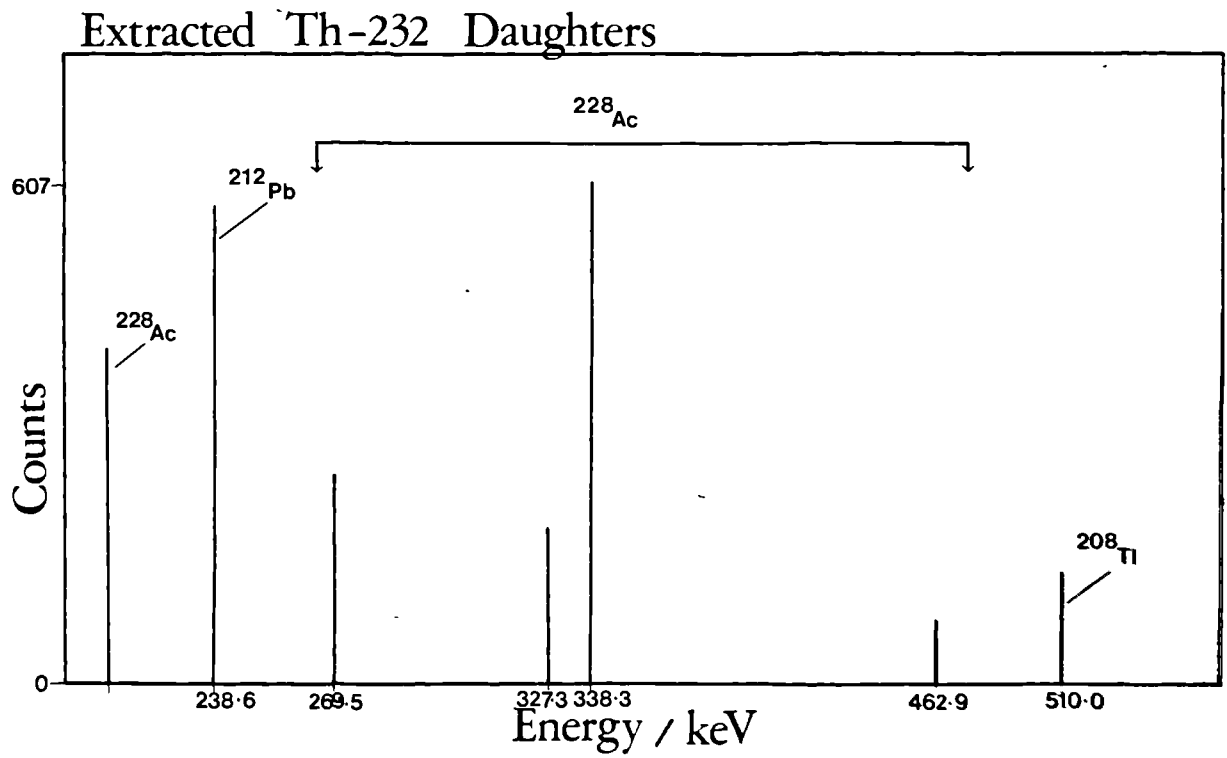
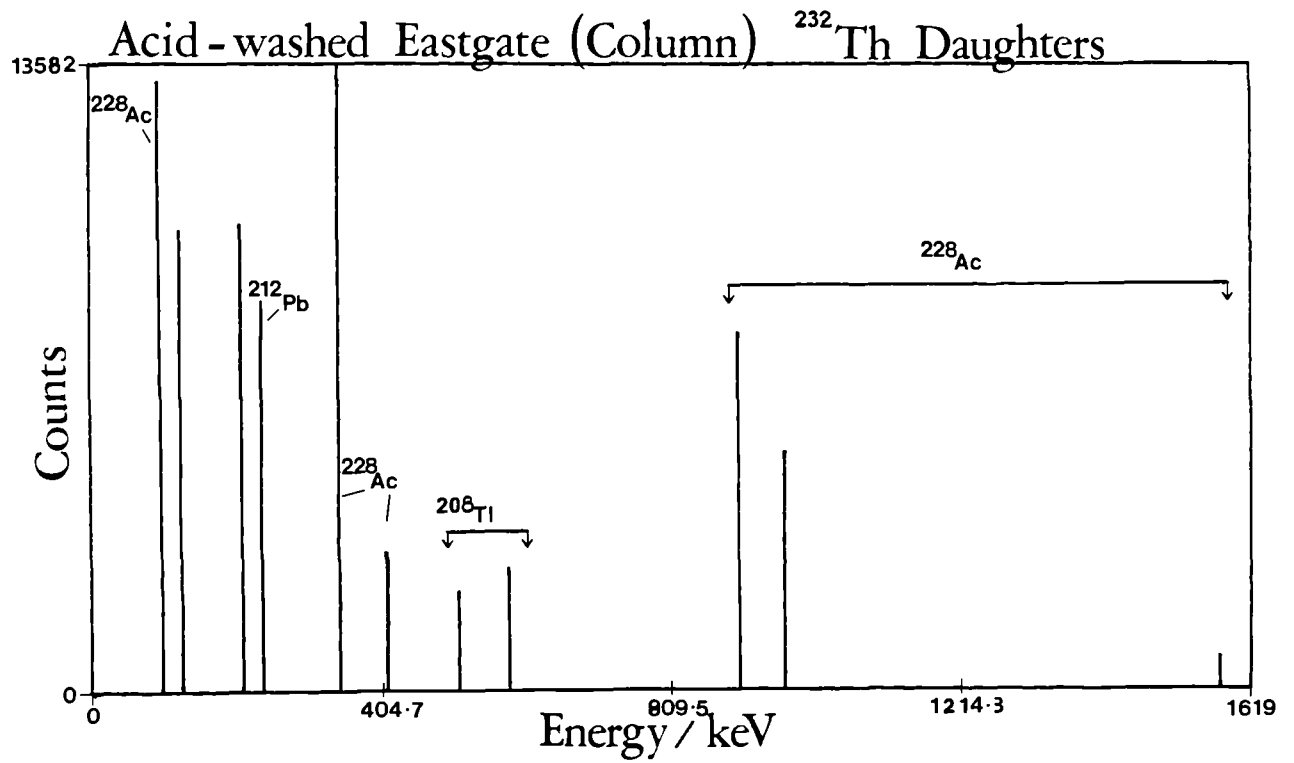


Fig. 100

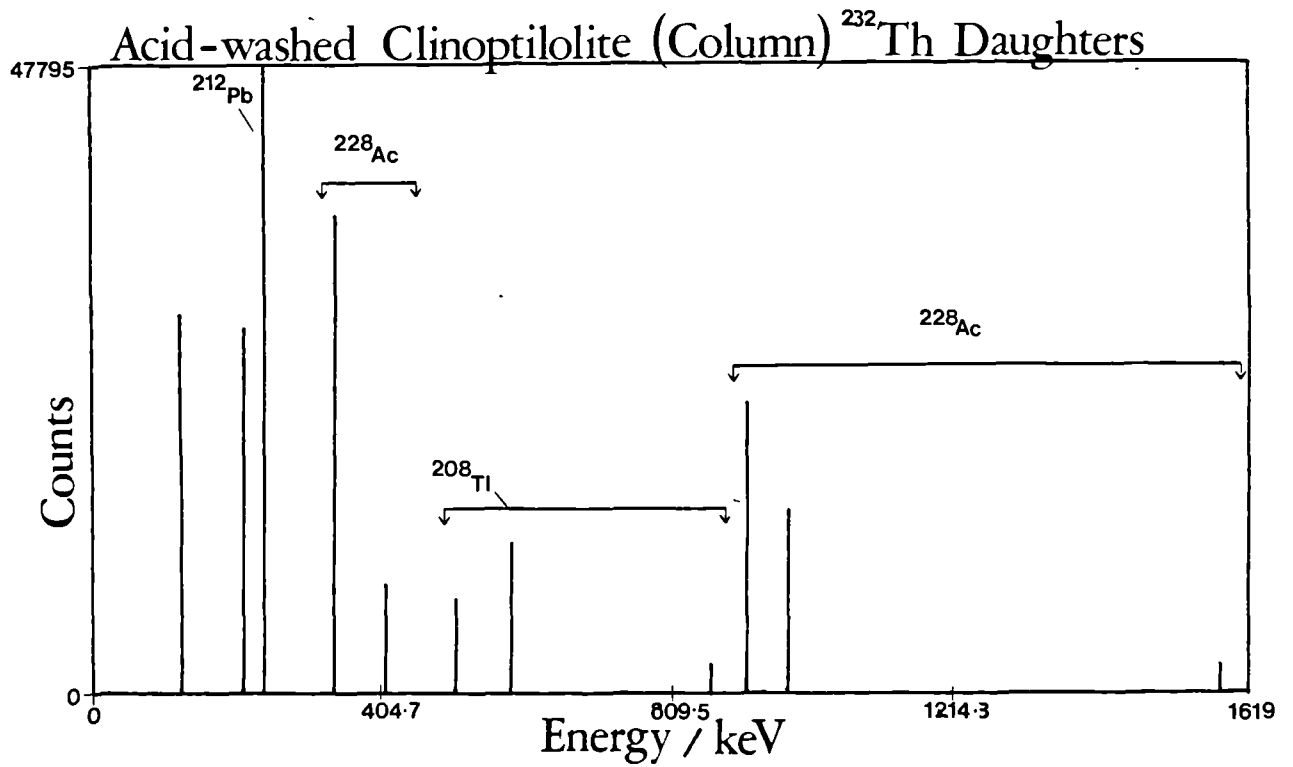


# $\gamma$ -Spectrometry.

## Fig. 101

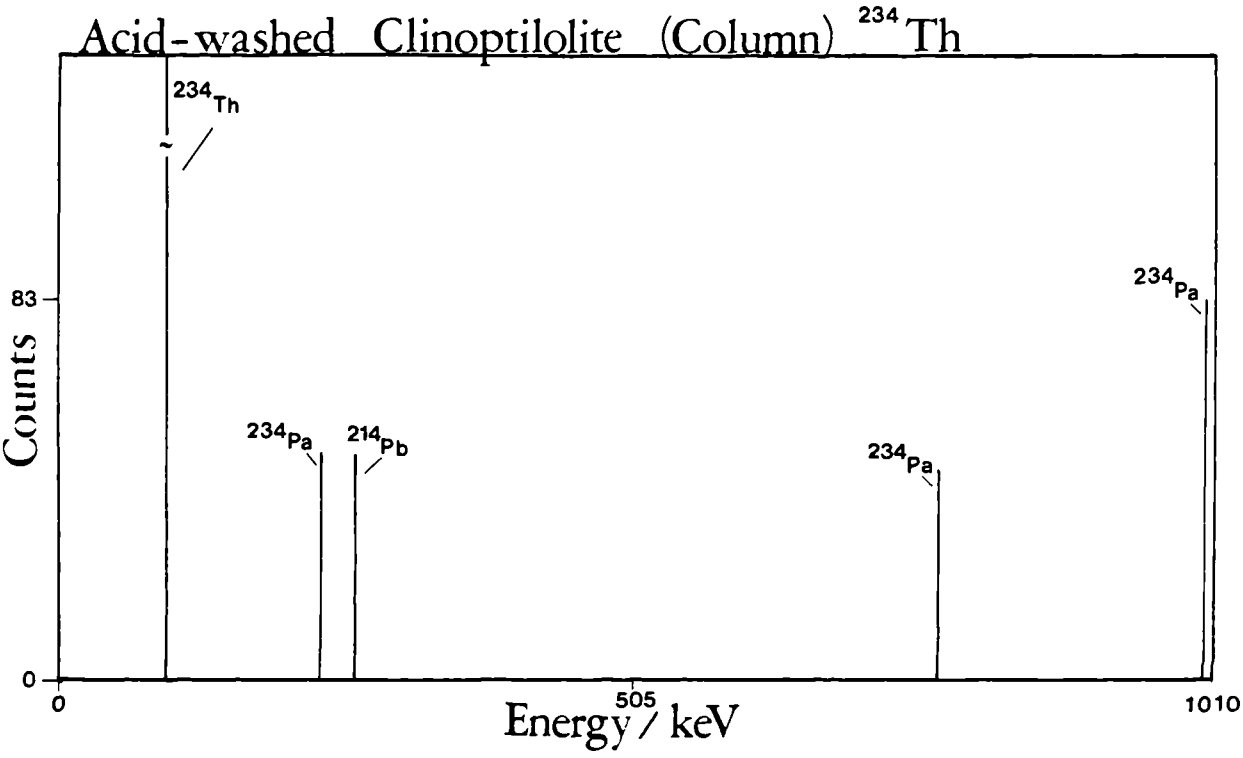


## Fig. 102



$\gamma$ - Spectrometry.

Fig. 103



# $\gamma$ -Spectrometry.

Fig. 104

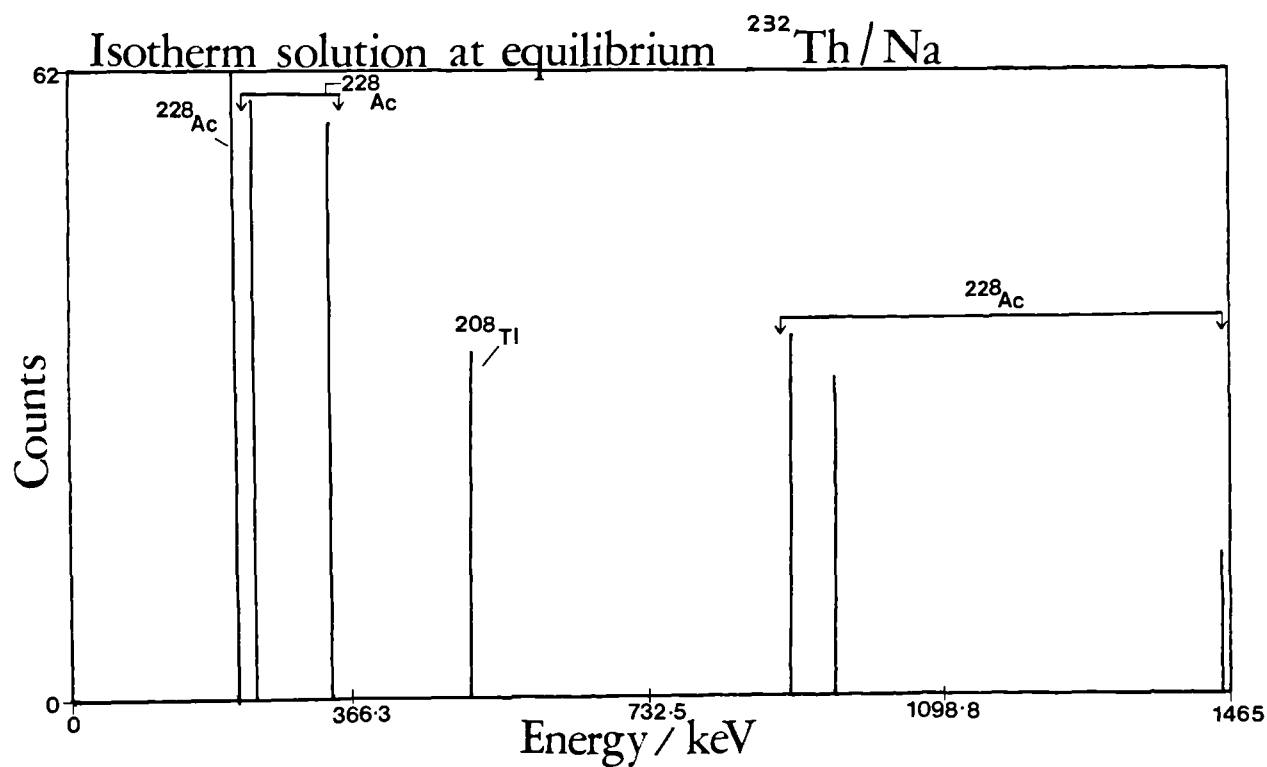
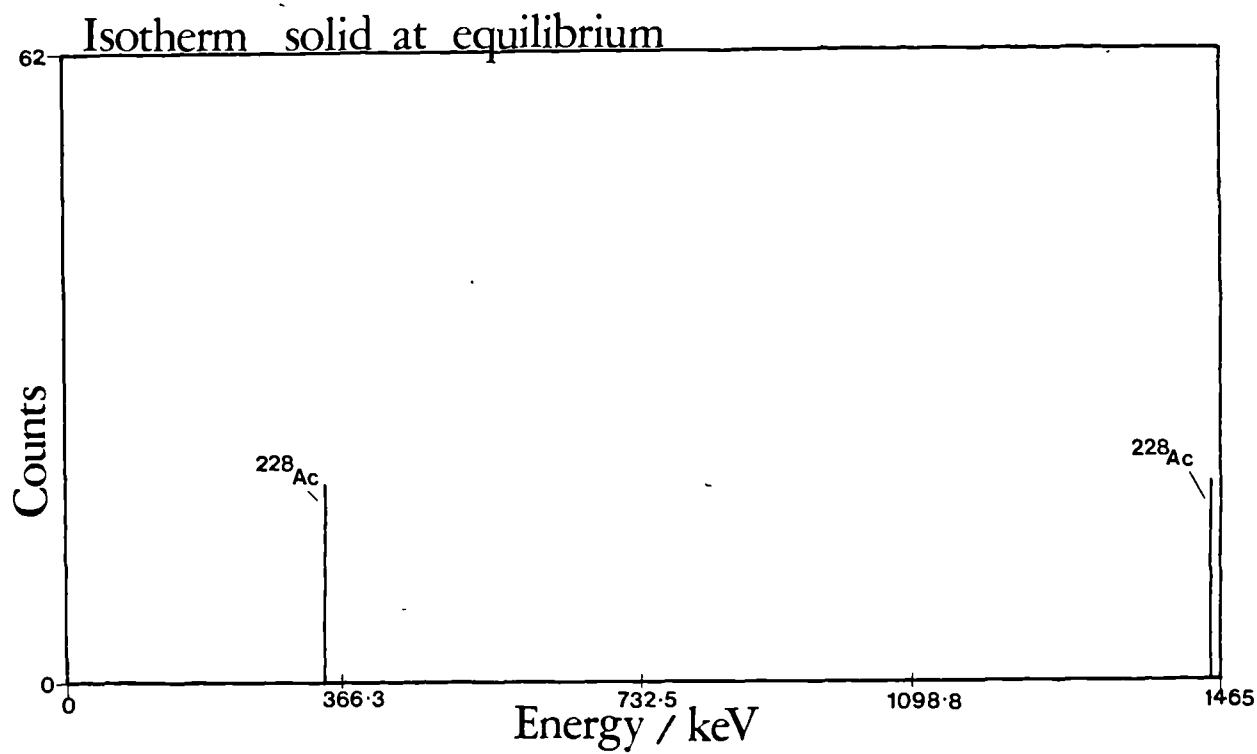


Fig. 105



$\gamma$ -Spectrometry.

Fig. 106

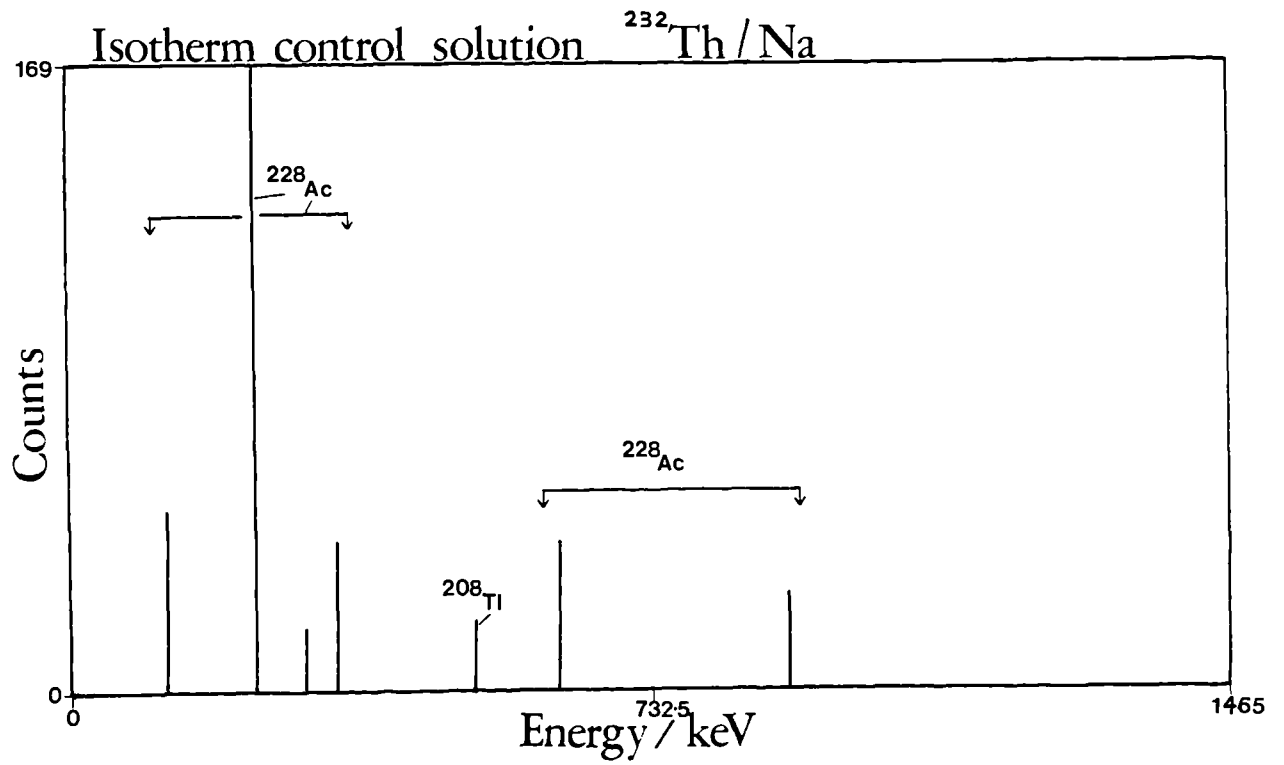
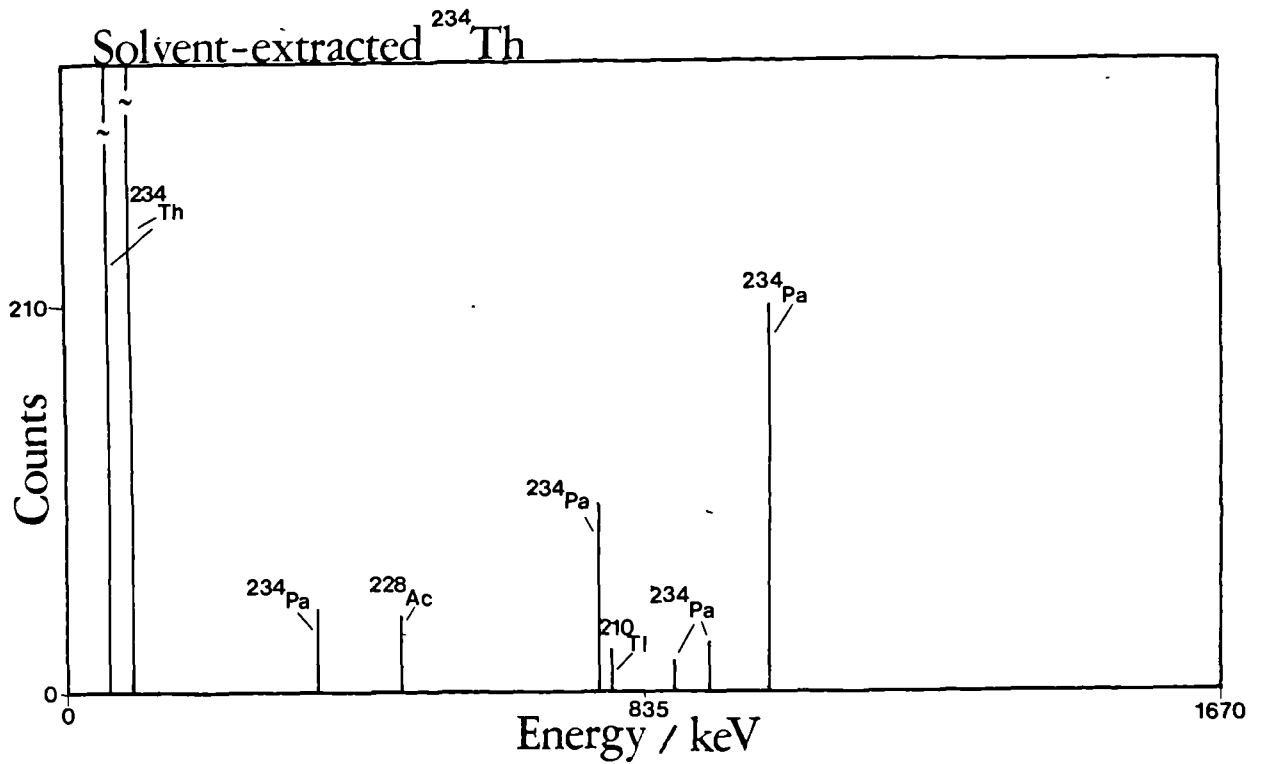
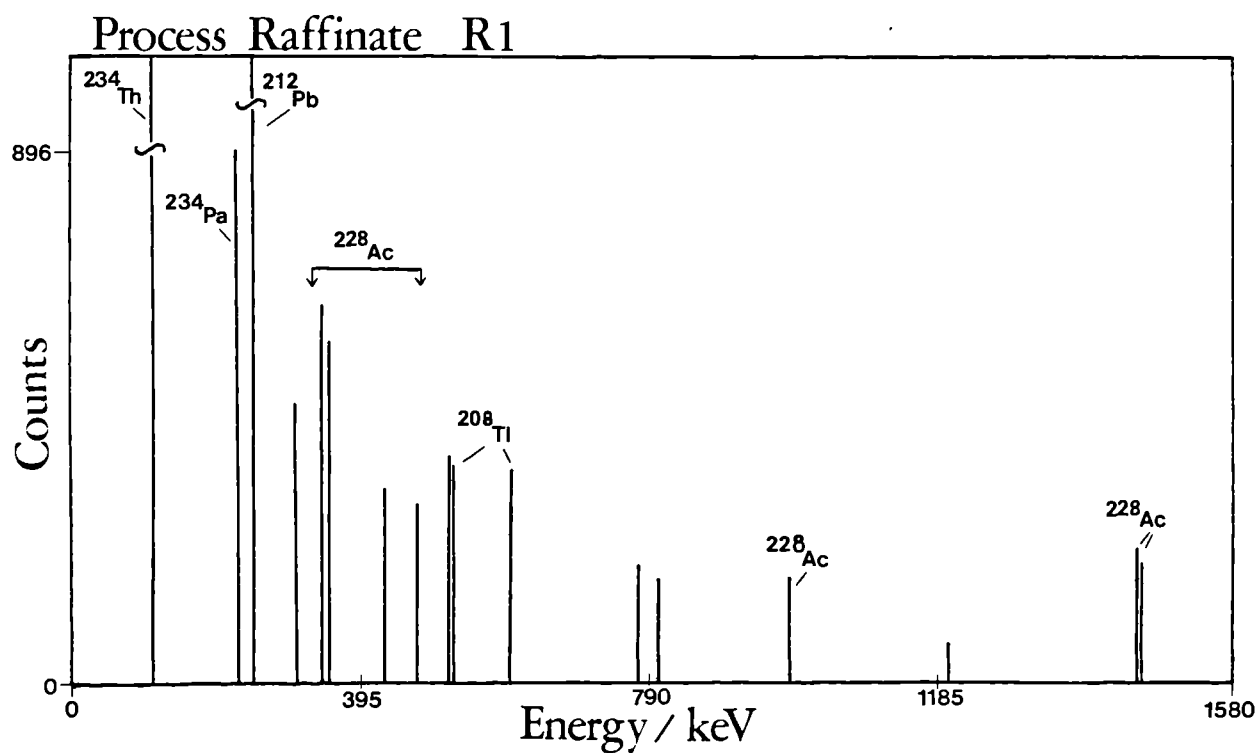


Fig. 107

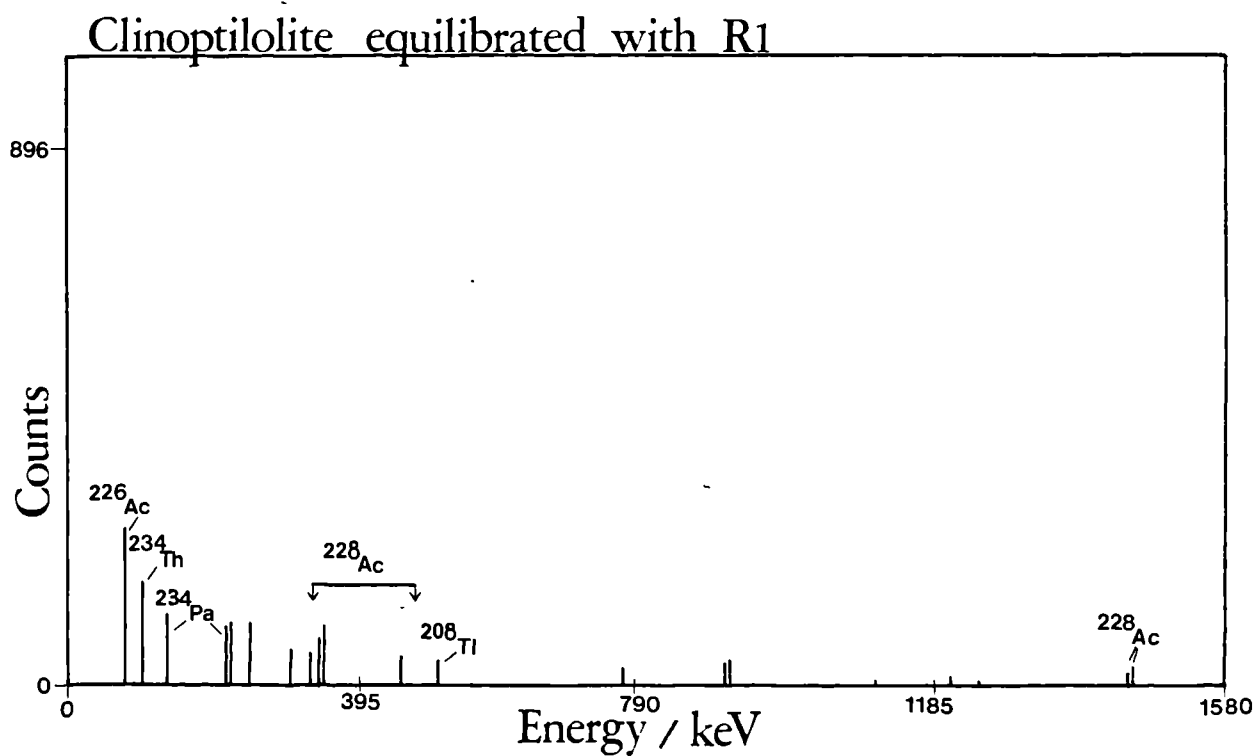


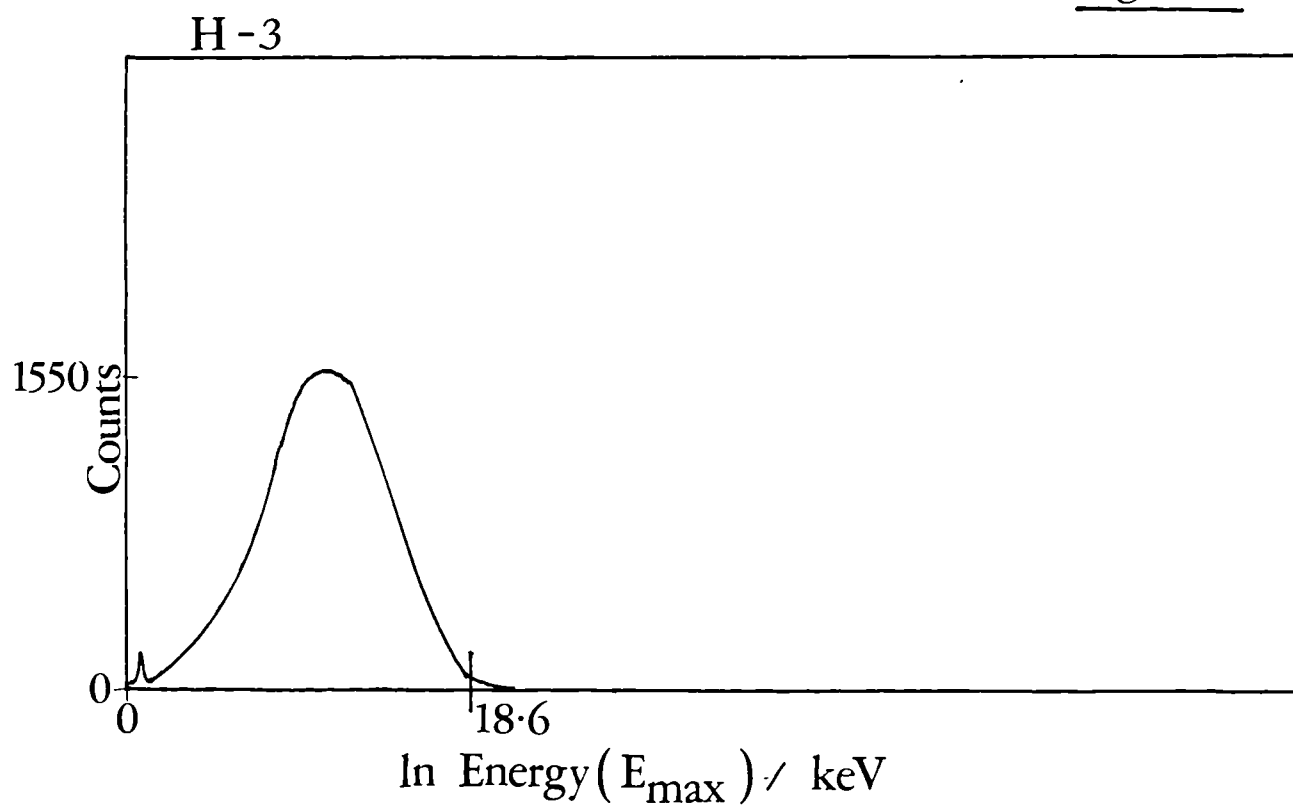
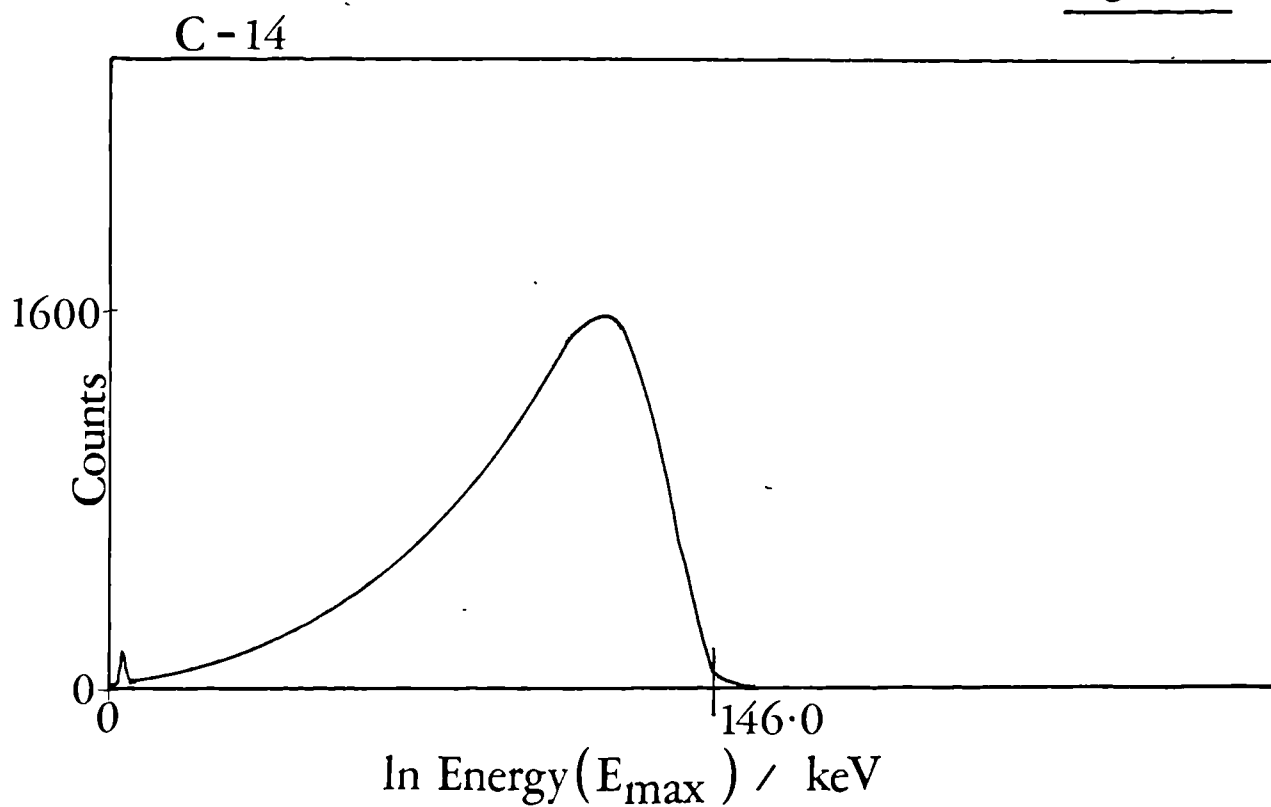
# $\gamma$ -Spectrometry.

## Fig. 108



## Fig. 109



$\beta$ - Spectrometry.Fig. 110Fig. 111

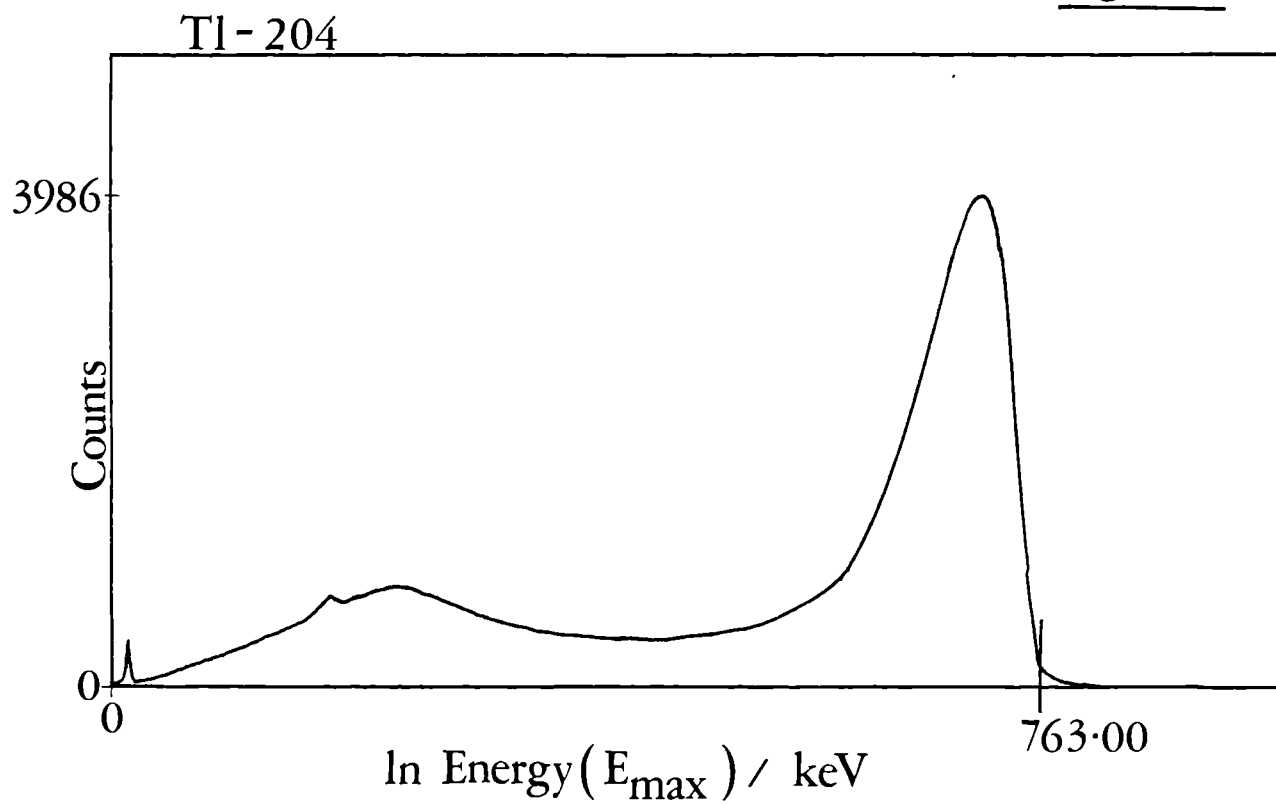
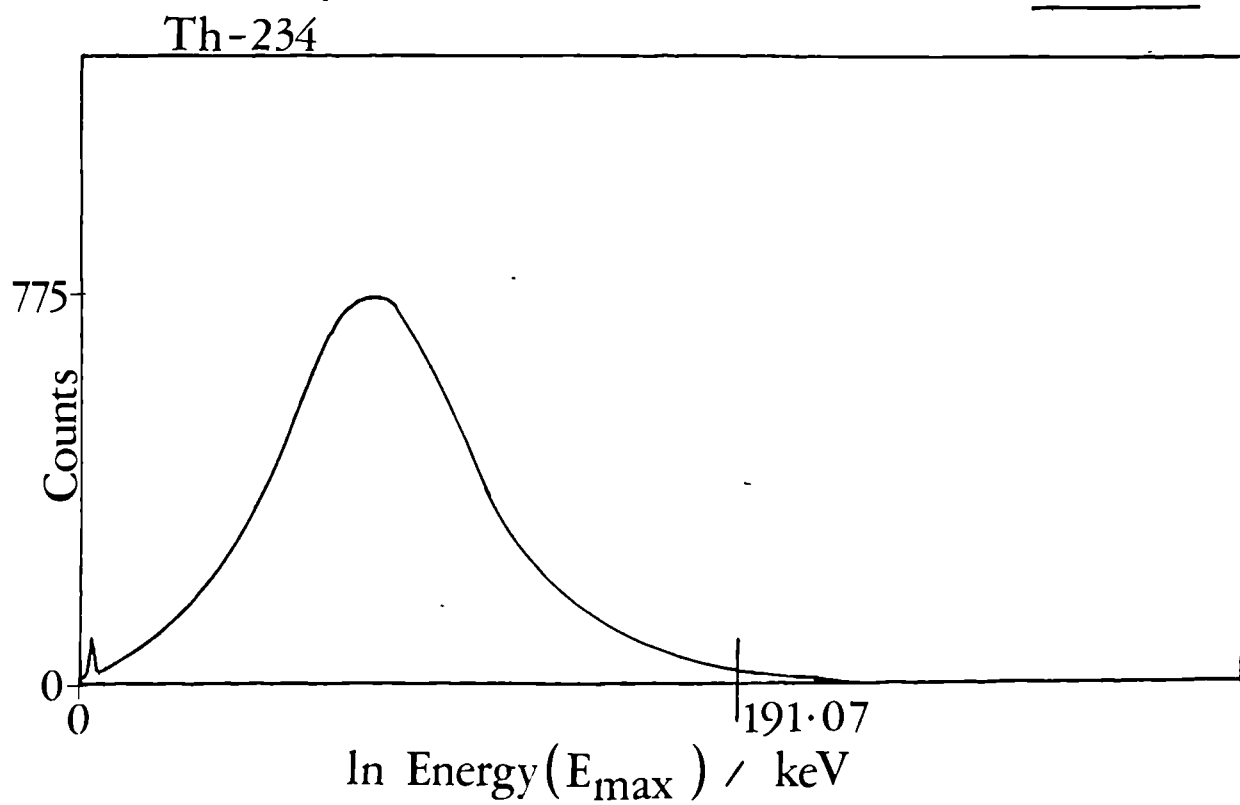
$\beta$ - Spectrometry.Fig. 112Fig. 113



TABLE 62

 $\beta$ -SPECTROMETRY

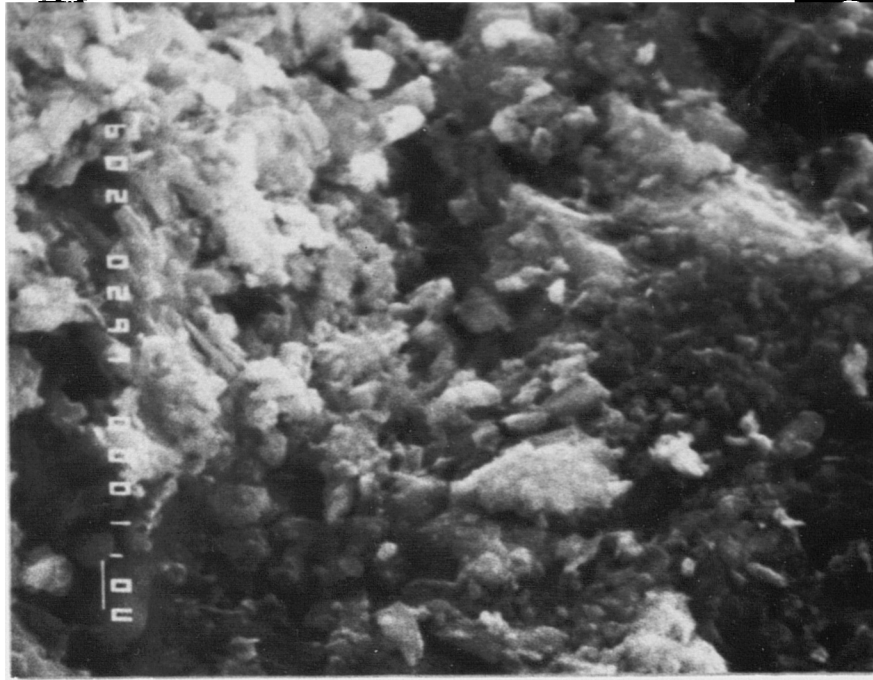
ISOTOPE	REASON FOR USE	END CHANNEL NUMBER	COUNTS AT MAXIMUM PEAK HEIGHT	E <sub>max</sub> /keV
C-14	Calibration	2933	1600	146.0
H-3	Calibration	2262	1550	18.6
Tl-204	Calibration check	3255	3986	763.0
Th-234	Sample determination	2576	775	191.07

### Scanning Electron Micrographs.

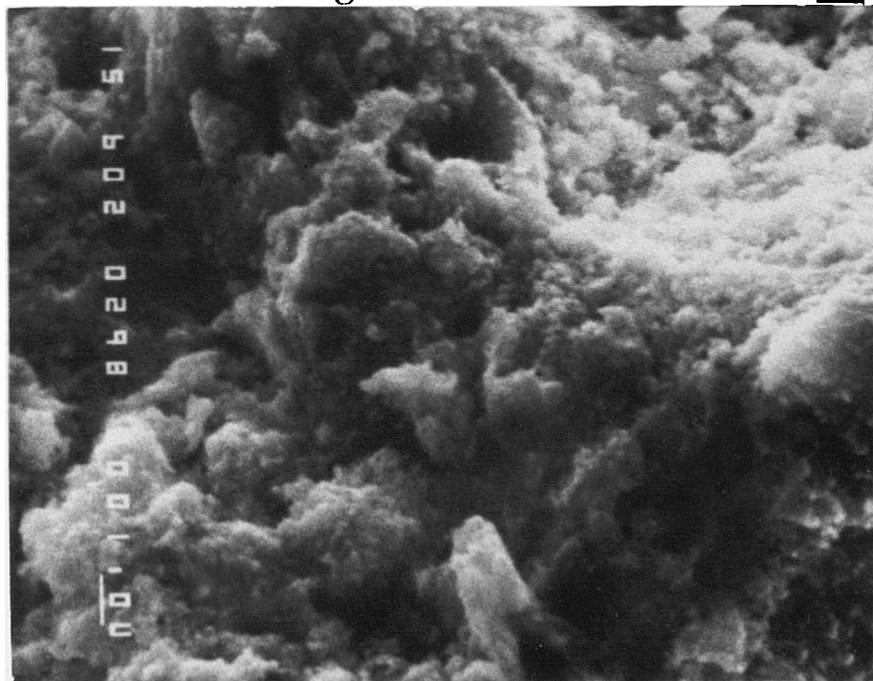
**PLATE 1.**

**Clinoptilolite-Th [Secondary Electron]**

### (1) Typical Particle



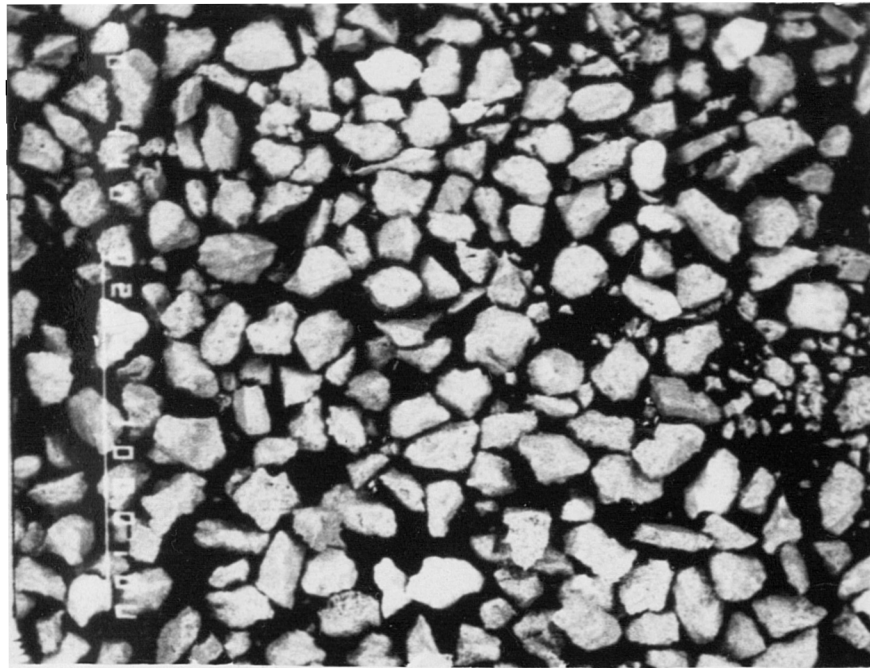
(2) Particle with high Thorium content 1μ



Scanning Electron Micrographs. **PLATE 2.**

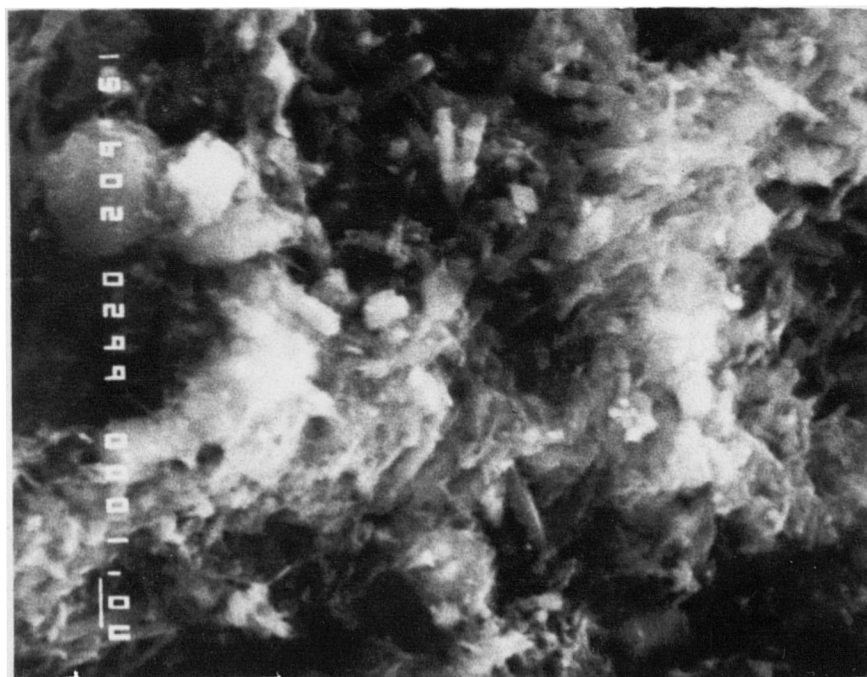
(1) Th Clinoptilolite

200  $\mu$



(2) Acid-washed Th Eastgate

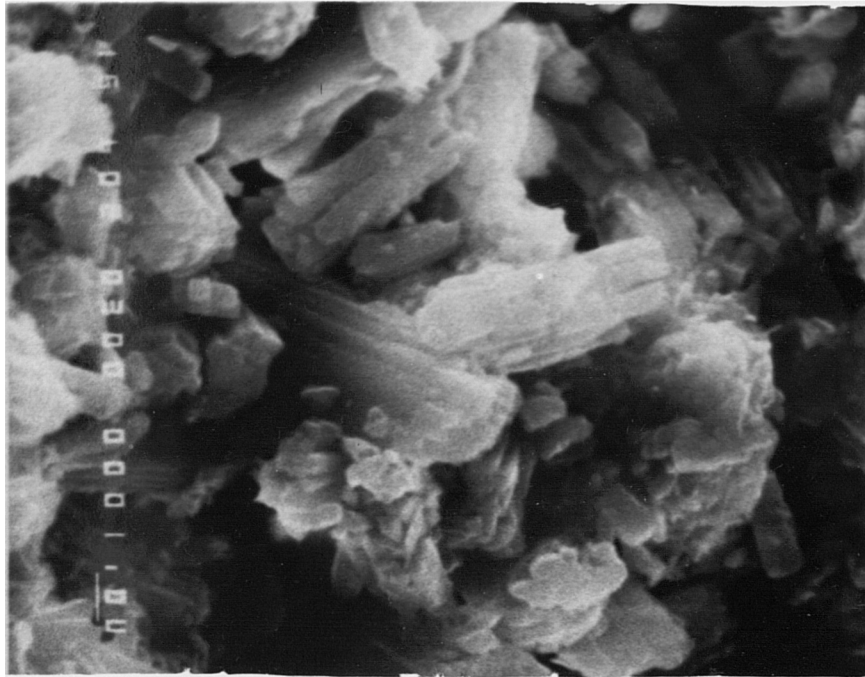
1  $\mu$



Scanning Electron Micrographs. **PLATE 3.**

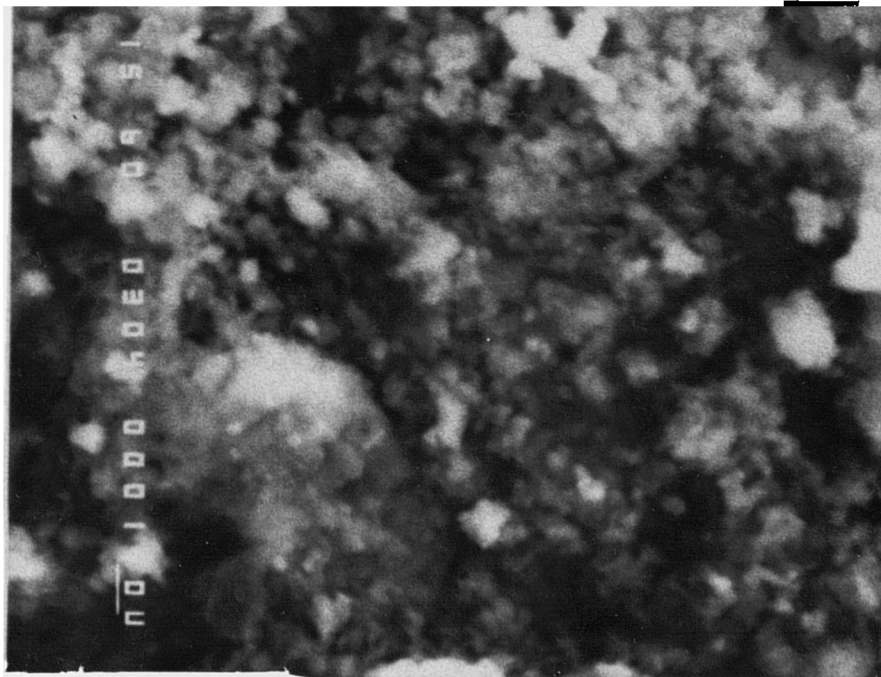
(1) Acid-washed Th Z900

1 $\mu$



(2) Acid-washed, Th-treated CaY

1 $\mu$



## CHAPTER 8

### DISCUSSION OF RESULTS

## DISCUSSION OF RESULTS

### 8.1 WET CHEMICAL ANALYSIS OF CLINOPTILOLITE AND EASTGATE

The analysis of clinoptilolite agreed with that of the data sheet supplied by the zeolite company from which the clinoptilolite was obtained. The  $\text{SiO}_2:\text{Al}_2\text{O}_3$  ratio was calculated to be 5.16 and the differential thermogram of clinoptilolite [FIGURE 89] was found to be 14.75%. The percentage composition of oxides may be seen in TABLE 32.

The Eastgate sample was found to have a calculated  $\text{SiO}_2:\text{Al}_2\text{O}_3$  ratio of 3.60 and contained reasonable amounts of  $\text{Mg}^{2+}$  which was unusual for erionite. The main constituents of Eastgate were thought to be erionite and chabazite. The  $\text{SiO}_2:\text{Al}_2\text{O}_3$  ratio confirmed this, but the X-ray powder diffraction pattern of Eastgate showed little resemblance of erionite and a greater similarity to a mordenite pattern [FIGS.79 AND 80]. This Eastgate sample may therefore contain a mixture of erionite, mordenite and clinoptilolite and there is evidence [REF. 95] that such deposits exist. The oxide composition of Eastgate may be seen in TABLE 32. The water content of the Eastgate sample was found to be 13.37% [FIGURE 95].

### 8.2 CATION EXCHANGE CAPACITY

The cation exchange capacity (CEC) used in the isotherm experiments was calculated from the theoretical ion-exchange capacity, which was based on the aluminium content of the zeolite concerned.

Experiments were conducted to observe the amount of possible exchange of a selected probe ion, in this case  $\text{NH}_4^+$ , and the results shown by this method were compared with the capacities given by the  $\text{AlO}_2^-$  content of each zeolite [TABLE 33]. The  $\text{Th}^{4+}$  ion was not chosen as a probe ion as over-exchange was suspected after preliminary  $\text{Th}^{4+}$ -uptake experiments.

#### 8.2.1 LEACHING EFFECTS OF SOLUTIONS ON ZEOLITES

Since much of this work involved the natural zeolites, it was important to determine losses of zeolitic cations on treatment with aqueous solutions i.e. water, nitric acid solutions and pure thorium nitrate solutions. In most of the experiments, two natural (clinoptilolite and Eastgate) and two synthetic (NaY, NaZ900) zeolites were chosen to compare the leaching of zeolitic cations:

#### 8.2.2 LEACHING EFFECT OF WATER

The natural zeolites were found to leach  $\text{K}^+$ ,  $\text{Na}^+$  and  $\text{Al}^{3+}$ . This was due to occluded soluble species within the zeolite itself. The unpurified natural zeolites may often contain soluble salts, such as NaCl, which would readily leach from the zeolite on contact with water. The synthetic zeolites gave no leaching effects involving the removal of  $\text{K}^+$  or  $\text{Al}^{3+}$ , however there was a slight removal of  $\text{Na}^+$ , due to the fact that homoionic sodium - forms of the zeolites had been used. The amount of  $\text{Na}^+$  removed was of the order of  $10^{-3} \text{ meq g}^{-1}$  of zeolite and may have been due to some  $\text{H}_3\text{O}^+$  or  $\text{H}^+$  exchange for the  $\text{Na}^+$  within the zeolite [TABLE 34].

### 8.2.3 LEACHING EFFECT OF NITRIC ACID

Two normalities of nitric acid were chosen as these would be the concentrations most frequently used in further experiments. Both of the synthetic zeolites lost  $\text{Na}^+$  but no  $\text{K}^+$  and NaY lost  $2\frac{1}{2}$  times its  $\text{Na}^+$  content than did NaZ900. There appeared to be little correlation between the normality of nitric acid used and the amount of  $\text{Na}^+$  lost, and both normalities of acid had the effect of removing similar amounts of  $\text{Na}^+$  from the zeolite.

The natural zeolites suffered losses of both  $\text{K}^+$  and  $\text{Na}^+$  from their frameworks and more  $\text{Na}^+$  was lost, in terms of milliequivalents than  $\text{K}^+$ . Unlike the synthetic zeolites, the natural zeolites showed a dependence on acid normality in relation to the amount of cations leached. More  $\text{Na}^+$  and  $\text{K}^+$  was leached as the acid normality was increased from 0.1N to 0.5N [TABLE 35].

The leaching effect of water had been taken into account in determining these results. It was most probable that all of these zeolites experienced ion-exchange of such alkali metals with  $\text{H}^+$ , as well as dissolution of occluded species within the zeolite framework [REFS. 34,96,97].

### 8.2.4 LEACHING EFFECTS OF PURE THORIUM NITRATE SOLUTIONS

Two different concentrations of thorium-232 were used in these experiments a) 5ppm solutions and b) 100ppm solutions [TABLE 36].



The zeolites tested with the 5ppm thorium solutions released no potassium into solution that was not deemed due to the action of  $H^+$ . (The potassium released due to water was subtracted from any results obtained). NaZ900 was the only zeolite to release  $Na^+$  that was not deemed due to  $H^+$  exchange on contact with thorium solutions. However this was classed as a spurious result and will not be considered further.

TABLE 37 shows the numbers of milliequivalents of cations removed from the zeolite, expressed as ratios, with the numbers of milliequivalents of thorium sorbed onto the zeolite. Z900 showed a 1:1 milliequivalent ratio for the 100ppm thorium solution. The zeolites Eastgate and clinoptilolite showed ratios of between 2 and 3 for  $Na^+:Th^{4+}$ , showing an approximate 2 or 3  $Na^+$  cation release per thorium ion sorbed. NaY showed an approximate 1:1 milliequivalent ratio of  $Na^+:Th^{4+}$ . No potassium, due to thorium solution contact appeared to be released.

#### 8.2.5 LEACHING EFFECT OF A 1000ppm $Th^{4+}$ SOLUTION

Clinoptilolite and NaY were chosen to be representative of a natural and synthetic zeolite respectively. NaY showed a 1:1 ratio of milliequivalents of thorium sorbed onto the zeolite to milliequivalents of  $Na^+$  removal from the zeolite. This corresponded to 43% removal of the original  $Na^+$  content of NaY. No  $K^+$  was released from the zeolite [TABLE 38].

Clinoptilolite showed a 2.3:1.0 ratio of milliequivalents of  $\text{Na}^+$  removed from the zeolite to milliequivalents of thorium sorbed onto the zeolite, with a loss of 79% of the original  $\text{Na}^+$  component of the clinoptilolite. Approximately 0.01 meq of  $\text{K}^+$  was released into solution.

All leaching effect analysis experiments were conducted at equilibrium.

The 1:1 milliequivalent ratios of Th:Na for NaY has also been observed by A.P. Bolton [REF. 46]. The  $7.4\text{\AA}$  aperture of the NaY zeolite was adequate to allow the hydrated  $\text{Th}^{4+}$  ion into the zeolite structure.

The clinoptilolite pore size was  $4.0\text{\AA}$ . These results are discussed in more detail in Chapter 9.

### 8.3 QUENCHING EFFECTS OF $\text{Na}^+$ , $\text{K}^+$ AND $\text{Al}^{3+}$ ON ČERENKOV COUNTING

FIGS. 28-30 show no appreciable quenching effects. In each case CURVE 1 shows a linear calibration curve of concentration of Th-232 'vs' counts per minute (CPM). CURVE 2 shows the various effects of the addition of increasing volumes of ion, on a particular count rate exhibited by Ac-228/Ra-228 daughters of Th-232. The curves at each particular count rate show horizontal lines. The lines would have had positive or negative slopes if the ion was acting as a quencher.

The same result was also true for nitric acid quenching up to 8M nitric acid.

### 8.3.1 QUENCHING EFFECT OF $\text{Na}^+$ , $\text{K}^+$ , $\text{Al}^{3+}$ ON LSC (Th-232 AND U-238)

No quenching effects were displayed either by the addition of these cations to the Th-232 liquid scintillation counting system or to that of U-238.

The effects of  $\text{H}^+$  on these counting systems were not studied because no acid/U-238 experiment necessitated counting by LSC.

### 8.4 CHARACTERIZATION OF SOLVENT-EXTRACTED Th-234 SOLUTION

Th-234 aqueous solution that had been solvent extracted from U-238 was characterized by 2 methods.

- a) A half-life curve was constructed [FIG. 31] and was found to be linear. This straight line was extrapolated to the abscissa to the point where half the original activity of the solution occurred on the ordinate axis. The extrapolation produced a time of 23.96 days and agreed, within experimental error, with a half-life of 24.1 days for Th-234 [REF. 51].
- b)  $\beta$ -spectrometry was used to produce a  $\beta$ -spectrum of the sample solution (SEE APPENDIX II). The  $E_{\text{max}}$  of this spectrum occurred at 191.07 keV [FIG. 113].

### 8.5 CHARACTERIZATION OF SOLVENT-EXTRACTED Th-232 SOLUTION

The  $\gamma$ -spectra of the aqueous Th-232 solution and the aqueous solution of its daughters were taken and the Th-232 spectrum showed a greatly reduced number of daughter products although some of the highly active Ac-228 was present. The

short half-life of 6.13 hrs for Ac-228 explained its high activity and rapid regrowth into the solvent-extracted Th-232 solution [SEE SECTION 8.18 and FIGURES 104 AND 105].

#### 8.6 UPTAKES OF Th-232 AND TOTAL ACTIVITY ONTO A RANGE OF NATURAL AND SYNTHETIC ZEOLITES

TABLES 39-44 show the results of Th-232 uptakes onto zeolites, total activity uptakes i.e. Th-232 and its daughters and also Ac-228/Ra-228 uptakes.

Th-232 uptakes were studied at 2 normalities of Th-232 (0.01N and 0.1N) at 20°C. TABLES 39-41 show the equilibrium concentrations of Th-232, in terms of milliequivalents, in solid and solution.  $K_d$  values are also shown [SEE SECTION 2.19] Eastgate showed total removal of Th-232 from solution at 0.01N concentrations and a 73% removal when the initial normality of Th-232 was increased to 0.1N. All other zeolites tested showed at least a 30% removal of Th-232 (initially 0.01N) except for analcime which shows no uptake of Th-232 at all. The chabazites, phillipsite and clinoptilolite each removed >50% of the 0.01N Th-232 solution and ferrierite and erionite removed the least amount of Th-232.

Any  $\text{Th}^{4+}$  will be hydrated with an approximate hydrated ionic radius of  $\sim 4\text{\AA}$  comparing with the hydrated ionic radius of radium, which is  $3.98\text{\AA}$  [REF. 100]. If the thorium were to penetrate the structure of zeolites it would be necessary to shed its hydration shell. The pore size of the Mudhills [REF. 104] clinoptilolite is  $4\text{\AA}$ . Entry into the chabazite 20-hedron cage

is governed by the  $3.7 \times 4.2\text{\AA}$  channel aperture. Chabazite 1 and 3 removed larger amounts of Th-232 than chabazite 2. This is probably due to the different cation contents corresponding to the geological occurrences of the chabazites. Erionite, having twisted channel systems experienced difficulty in removing Th-232 even though it contained a large 23-hedron cage.

At 0.1N solutions of Th-232,  $K_d$  values decreased greatly with respect to those exhibited for 0.01N solutions, with the exception of Eastgate which removed 0.730 meq of Th-232.

In the case of the synthetic zeolites [TABLE 41], NaY removed all of the Th-232 from a 0.01N solution, as did 4A. The large  $7.4\text{\AA}$  aperture of NaY allows for the entry of Th-232 but uptakes were greatly reduced at 0.1N thorium concentrations. The  $4.2\text{\AA}$  apertures of 4A may be allowing Th-232 exchange but this was doubtful and the uptakes were more likely to be surface adsorption, especially when the 4A result is considered for 0.1N thorium solution, because the 4A sample dissolved in the solution. NaZ900 experienced no uptake of Th-232 at 0.1N thorium solutions and only 12% uptakes at the lower normality.

Total activity uptakes (Th-232 and its daughters) for selected zeolites at 0.01N Th-232 concentrations [TABLE 42] revealed approximate similarities to the Th-232 uptakes at this normality. Eastgate removed 78% of total activity. The chabazites and clinoptilolite were comparable in terms of uptakes.

#### 8.6.1 UPTAKES OF Ac-228/Ra-228 ONTO NATURAL AND SYNTHETIC ZEOLITES (0.01N, Th-232)

At equilibrium, all the natural zeolites showed between 80 and 90%  $\beta$ -emitter daughter uptakes [TABLE 43].  
 Analcime showed little uptake as did some of the more obscure materials such as cowlesite, brewsterite and the palagonite tuff [REF 101]. These daughter isotopes are most realistically undergoing an adsorption process. All uptakes are  $\sim$  70% complete after 1 hour in contact with the zeolites.

The synthetic zeolites experienced lower uptakes of the Ac-228/Ra-228 daughters of Th-232 except for Z900 which was the zeolite which removed the least Th-232 from 0.01N solutions and the most Ac-228/Ra-228 of the synthetic zeolites [TABLE 44].

Uptake curves for the natural and synthetic zeolites may be seen in APPENDIX IV and show uptakes for Ac-228/Ra-228 and Th-232.

#### 8.6.2 Th-234 UPTAKES ONTO SELECTED ZEOLITES

The Th-234 was in approximately 0.5M nitric acid due to the nature of the solvent extraction procedure used to obtain it. Uptakes of thorium onto clinoptilolite, chabazite 3 and phillipsite were considerably reduced compared with uptakes of Th-232 in non-acid solution [FIG. 32]. Clinoptilolite experienced the highest uptakes of Th-234 in nitric acid due to its greater resistance to acid attack than the other zeolites. Two particle sizes were used and the larger particle-sized clinoptilolite experienced uptakes of about 14% Th-234.

### 8.6.3 TEN HOUR UPTAKES OF Th-232 ONTO ZEOLITES

FIGS. 34-37 show the uptakes of Ac-228/Ra-228 onto various zeolites. The curves were similar and all show a fast uptake occurring within the first 30 minutes of the experiment. FIG. 33 shows the uptake of Th-232 in the first 10 hours of the experiment. Again most uptake of Th-232 has occurred in the first 30 minutes of the experiment.

### 8.7 VARIATIONS OF TEMPERATURE AND CONCENTRATION ON THE Th-232 UPTAKES

A very clear increase in uptakes (percentage-wise) were shown for all zeolites as the initial Th-232 concentration for each experiment was reduced [TABLE 45].

#### 8.7.1 VARIATIONS OF TEMPERATURE AND CONCENTRATION: EFFECTS ON THE UPTAKES OF Th-232 DAUGHTERS

Only the Eastgate sample showed any relationship of change in concentration with uptakes (uptakes increased as concentration decreased). Clinoptilolite showed little decrease in the uptakes experienced at different temperatures but keeping the normality of Th-232 constant [TABLE 46].

### 8.8 UPTAKES OF U-238 ON ZEOLITES

Uptake percentages of U-238 corresponded to those of Th-232 on the same zeolites. [TABLES 47 and 48]. Eastgate and NaY removed the most  $\text{UO}_2^{2+}$ . Since the  $\text{UO}_2^{2+}$  ion is linear it must enter any zeolite aperture "end-on". The equilibrium value of  $\text{UO}_2^{2+}$  uptake onto clinoptilolite was 0.0193 meq.

### 8.9 UPTAKES OF U-238 ( $\beta$ -emitter daughters) ONTO SELECTED ZEOLITES

Large uptakes of the order of 90% were experienced by the three zeolites tested i.e. clinoptilolite, NaZ900 and NaY. In the presence of 0.1N and 0.5N nitric acid, these uptakes decreased. No adsorption occurred at 0.5N acid concentrations and uptakes of U-238  $\beta$ -emitter daughters were reduced in clinoptilolite and NaZ900 at 0.1N nitric acid concentrations. NaY was not severely affected in its uptake ability at this concentration of acid [TABLES 49 AND 50].

### 8.10 COMPETING ION EFFECTS OF $K^+$ AND $Na^+$ ON Th-232 DAUGHTER UPTAKES

TABLE 51 shows the competing ion effect of  $Na^+$  on the uptakes of Ac-228/Ra-228 after 1 hour.  $10^3$  ppm  $Na^+$  had a reducing effect on the uptakes of thorium  $\beta$ -emitter daughters for clinoptilolite, chabazite, erionite and Eastgate and the largest reduction in uptake was experienced by ferrierite.

TABLES 52 AND 53 show the total effect of  $Na^+$  and  $K^+$  (400ppm) on the equilibrium uptakes for selected zeolites. It was Eastgate that was the most affected by the presence of  $K^+$ .

#### 8.10.1 COMPETING ION EFFECTS OF $K^+$ , $Na^+$ and $H^+$ ON Th-232 UPTAKES

TABLE 54 reveals the difference between the abilities of NaY and Z900 to remove Th-232 from solution in the presence of competing cations. Z900 took up virtually no thorium but in contrast, NaY removed all thorium from solution where  $Na^+$  and  $K^+$



were competing, but was restricted by the presence of 0.1N nitric acid where uptakes dropped from 100% to 41%. No uptake of Th-232 occurred in NaY at 0.5N nitric acid concentrations.

Eastgate was little affected by the presence of  $\text{Na}^+$  even when  $\text{Na}^+$  is present at twice the concentration of that of thorium. There was a very slight reduction in uptakes of Th-232 in the presence of a 2:1 ratio of  $\text{K}^+:\text{Th}^{4+}$ .

Clinoptilolite was severely restricted in its uptake of Th-232 in the presence of  $\text{K}^+$  but less in the presence of  $\text{Na}^+$ . All zeolites tested had no uptakes or very limited uptakes of Th-232 in acid solutions [TABLE 54].

#### 8.10.2 COMPETING ION EFFECTS $\text{Na}^+$ , $\text{K}^+$ , $\text{Mg}^{2+}$ , $\text{Ca}^{2+}$ , $\text{Al}^{3+}$ ON THE UPTAKE OF THORIUM IN NITRIC ACID SOLUTION BY CLINOPTILOLITE AND Z900

TABLE 55 shows that as thorium, 0.1N, and nitric acid, 0.5N, concentrations decreased, even though the competing cation solution concentrations were increasing, uptakes of thorium were generally increased. In the case of clinoptilolite, the presence of magnesium and calcium had little competing ion effect. Potassium allowed no uptakes of thorium in acid solution. From the literature [REF. 114] clinoptilolite has a large selectivity for  $\text{K}^+$  and also for  $\text{Na}^+$  and sodium also interfered with thorium uptakes in the presence of nitric acid, as did aluminium.

The results for Z900 showed no uptakes of thorium in the presence of acid where the counter ions were sodium and potassium. Calcium and magnesium ions had little effect on the uptakes of thorium in nitric acid [TABLE 55].

8.11      Th-232 UPTAKES FROM SIMULATED RAFFINATE SOLUTIONS  
            "SOSIM" SOLUTIONS

TABLE 56 shows that only the natural zeolites Eastgate and clinoptilolite removed any of the Th-232 in the simulated raffinate solutions. The synthetic zeolites removed no thorium. 4A dissolved in those solutions which were of very low pH ( $\sim 0.5$ ). Eastgate removed Th-232 in the two solutions containing the lowest amounts of nitric acid, the uptakes decreased with increasing nitric acid concentration. Clinoptilolite removed  $\sim 5\%$  of Th-232 from the solutions. SOSIM 2 which had the highest total ionic concentration, including free acid had no thorium removed by any zeolite.

None of the synthetic or natural zeolites removed any Th-232  $\beta$ -emitter daughters from solution and this was due to the acid and the presence of  $\text{Na}^+$  and  $\text{K}^+$ , which severely limited adsorption.

As has been seen in the previous sections, the effect of  $\text{H}^+$  on the uptake of Th-232 by zeolites was greater and this was shown in the simulated raffinate.

## 8.12 COLUMN EXPERIMENTS

### FREE COLUMN VOLUME

The synthetic zeolites exhibited the greatest free column volumes [TABLE 57]. These zeolites have more open structures therefore allowing for the sorption of larger amounts of water into the zeolite structure. The natural zeolites showed lower free column volumes due to their less open structures. This was also due to the expected presence of occluded species and extra-framework compounds, which may block access to channels and cavities.

#### 8.12.1 BREAKTHROUGH CURVES

FIGURES 39-46 represent column experiment breakthrough curves where  $C$  was the concentration of the species being analysed and  $C_0$  was the initial concentration value.

FIGS. 38 AND 39 represent the breakthrough curves obtained for Th-232 on Eastgate and clinoptilolite respectively. Eastgate gave a 50% breakthrough of Th-232 at 360 ml eluted volume. The Th-232 reservoir solution was at a set concentration of 1000ppm in both the columns shown in these figures. The clinoptilolite column showed a 50% breakthrough at 60 ml eluted volume. Both columns showed some Th-232 being eluted at a  $C/C_0$  value greater than 1.0, this may be attributable to some of the sorbed thorium being removed from the column at these points.

FIGS. 40 AND 41 represent the breakthrough curves for Z900 and clinoptilolite treated with a reservoir solution of Th-234 in 0.5M nitric acid. Clinoptilolite [FIG. 40] showed a 50% breakthrough at 200 ml eluted volume. It may seem odd that the Th-232 and Th-234 50% breakthrough values should differ by so much, especially when the Th-234 is in 0.5M nitric acid. It has been shown that pre-conditioning of the natural zeolites with acid, prior to ion-exchange, improved the capacity of the zeolite [REF. 98] by removing occluded species and impurities. At a 100% breakthrough value the Th-234 influent reservoir was removed and replaced by deionised water. A small, immediate elution peak was obtained which accounted for some surface removal of Th-234. The activity of the effluent quickly dropped to background values and after 50 ml of deionised water had been pumped through the column, the influent was changed to 1M sodium nitrate solution.

FIG. 40 shows that very little of the Th-234 was removed by the  $\text{Na}^+$  ions and most of the Th-234 was retained on the clinoptilolite column.

FIG. 41 shows that 50% breakthrough of Th-232 on a Z900 acid pre-conditioned column occurred at 60 ml eluted volume, and there was a steady increase of breakthrough upto 100%.

FIGS. 42 AND 43 are the breakthrough curves for CaY and Z900 based on the daughter  $\beta$ -activity of Th-232. For CaY, 50% breakthrough of Ac-228/Ra-228 occurred at 250 ml eluted volume but Z900 gave an eluted volume of only 13 ml at 50% breakthrough. For Z900 the breakthrough was sharp unlike that

for CaY. These breakthrough curves for Ac-228/Ra-228 adsorption were based on thorium solutions in 0.1M nitric acid.

FIGS. 45 AND 46 show the breakthrough curves for clinoptilolite and Th-232 in 0.5M nitric acid and adsorption of Ac-228/Ra-228 in 0.5M nitric acid respectively.

50% breakthrough of Th-232 in 0.5M nitric acid occurred at 110 ml and by comparing this with FIGS 39 and 40, is seemed to be confirmed that pre-conditioning the clinoptilolite with 0.5M nitric acid improved its uptake of Th-232 (or Th-234). It was not possible to produce identical results in any two samples of natural zeolites as these samples may vary greatly in their composition and impurities.

Clinoptilolite sorbed large quantities of  $\beta$ -emitter daughters of thorium, even in 0.5M nitric acid.

FIGS. 48 AND 49 show the breakthrough curves obtained for Eastgate columns with thorium-232  $\beta$ -emitter daughters and total activity (Th-232 and its daughters together). FIG. 48 has a very irregular curve and shows difficulty in sorption of Ac-228/Ra-228 followed by a possible increase in the sorption at  $\sim 500$  ml eluted volume.

Comparing FIGS 48 and 49 (FIG 49 represents the breakthrough curve of Eastgate - total activity i.e. Th-232 and its daughters) it can be seen that there was a sharp drop in activity displayed at similar points on the curve. This was most likely due to a half-life factor. APPENDIX III shows the Th-232 daughters. These half-lives are short and several half-lives

of these daughters had elapsed within the time of the experiment and, due to the complex nature of the decay of the Th-232 chain, was not corrected for. The daughter isotopes which caused this phenomenon were Ac-228 ( $t_{1/2}=6.13\text{h}$ ), Pb-212 ( $t_{1/2}=10.64\text{h}$ ), Bi-212 (60.50min), and Tl-208 ( $t_{1/2}=3.10\text{min}$ ). Even though these daughters were present in small quantities, compared with the parent Th-232, their activities were high. The smaller step-like drops in activity displayed in FIGS 48 and 49 were due to single isotope half-life drops in activity, however the large drop at 17 hours on the time scales of FIGS. 48 and 49 were due to a combined drop in the activity of isotopes at the same time - due to half-life. FIG. 42 also shows a drop in activity on the same time scale.

This may mean that the zeolite was not sorbing some or all of the daughter isotopes, however the  $C_0$  values were obtained using the influent isotope solution and this was prone to the same half-life effects, so presumably, the drops in activity in FIGS. 48 and 49 illustrated some isotope separation as well, with respect to time.

FIGURE 44 shows the breakthrough curve for Z900, treated with Th-232 in 0.1M nitric acid. 50% breakthrough occurred at 210 ml eluted volume, which was better than that obtained for Th-234 in 0.5M nitric acid [FIG. 41].

FIGURE 47 represents the breakthrough curve for the Eastgate column treated with Th-232 (the first part of which, is shown in FIGURE 38). The column was treated with an influent

stream of water, which was replaced by  $\text{KNO}_3$  (0.01N  $\text{K}^+$ ) and finally, this was replaced by hydrochloric acid in a similar way as for the clinoptilolite column the results from which are displayed in FIGURE 40. An elution peak can be seen at 690 ml on FIGURE 47 at the point where the influent was changed to deionized water and this was attributed to some surface thorium being removed from the column. When the influent stream was changed to 0.01N  $\text{K}^+$  solution a small elution peak was observed on FIGURE 47 and 875 ml and this was followed by a drop in thorium elution, then a slow, but steady increase in thorium elution upto 950 ml effluent collection. At this point no more thorium could be eluted. These elutions were assumed to be ion-exchange of thorium for potassium. Exchange with  $\text{K}^+$  was limited and from 975 ml to 1125 ml (eluted volume) no more thorium was displaced. At 1125 ml elution, the influent was changed to 1% hydrochloric acid which rapidly removed most of the thorium on the column.

Despite the way that the acid elution peak was drawn it can be noted that there were three elution peaks due to influx of acid at 1200 ml, 1210 ml and 1245 ml (eluted volume) respectively. It was difficult to say whether this was experimental error or whether the elution peaks were actually due to degree of exchange difficulty of  $\text{H}^+$  for the thorium on the Eastgate perhaps reflecting a site selectivity.

### 8.13 ISOTHERMS

#### 8.13.1 THORIUM

FIGURES 50 AND 51 represent the isotherms plotted for clinoptilolite equilibrated with  $K^+$  and  $Th^{4+}$  binary mixtures (the concentration of each ion initially being set at 0.01N and 0.001N respectively). All of the isotherms were based on  $A_s$  and  $A_c$  values of thorium. The isotherms illustrated that, at low concentrations of thorium, clinoptilolite was selective for thorium ions over potassium ions. There was a distinct concentration dependence shown for the removal of thorium from potassium solutions represented by the sharp turning point in both of the curves in FIGURES 50 AND 51. (The turning point in both curves occurred at  $A_c$  values of 0.13).

FIGURE 52 shows the isotherms for both thorium and potassium with Z900, i.e. the samples were analysed for both thorium and potassium content. The thorium isotherm was a similar square-type of curve to that displayed by clinoptilolite and thorium was selectively removed over potassium from the solution at lower thorium concentrations. Two reversibility points were obtained for this experiment and clearly showed that thorium removal by the zeolite was not fully reversible. The potassium isotherm plotted for Z900 verifies the fact that, at low thorium concentrations, potassium was not selectively removed by the zeolite. It can be seen from FIG. 52 that, at higher thorium concentrations, potassium was selectively removed from the solution by Z900 upto  $A_c$  values of 0.20.



FIGURE 53 shows a slightly different shape of isotherm for 0.01N binary mixtures of sodium and thorium with zeolite NaY. The isotherm of NaY was similar to the previous isotherms mentioned, in the respect that high thorium selectivity was shown by the zeolite. However, a further concentration dependence was shown by NaY and was represented by the plateau region of the curve (between  $A_c$  values of 0.10 and 0.225) and from  $A_c$  values of 0.225 upwards, the curve rose sharply.

FIGURE 54 represents the isotherm clinoptilolite and binary mixtures of thorium and sodium at fixed total concentrations of 0.2N. Within the scope of the experimental points the isotherm showed no preference for thorium at these high concentrations, with respect to ion-exchange.

#### 8.13.2 LANGMUIR PLOTS

FIGURES 55 - 57 represent the Langmuir plots for Th-232 obtained from experimental data produced by the isotherms described in section 8.13.1. The Langmuir plot obtained for clinoptilolite equilibrated with potassium/thorium solutions of total fixed concentration 0.02N [FIG. 55] passed through the origin and no intercept value could be calculated. The lower concentration part of the plot was linear ( $C_{eq}$  values 0-175.0) showing Langmuir adsorption, however at the higher concentration end of the curve, the plot rose smoothly showing that a process other than Langmuir adsorption was occurring with clinoptilolite at higher thorium concentrations. FIGURE 56 shows the respective

Langmuir plot for thorium in the binary isotherm mixture with potassium, equilibrated with zeolite Z900. The plot seemed more linear than the clinoptilolite plot throughout the concentration range of the curve except at the higher  $C_{eq}$  values. The curve passed through the origin and was not linear enough to estimate its slope. FIGURE 57 shows a Langmuir plot of a binary isotherm mixture of sodium and thorium with zeolite NaY. Again, the plot was not linear but it was the only curve which did not pass through the origin. If it was assumed that the lower concentration end of the plot was linear, i.e.  $C_{eq}$  values between 0 and  $9 \text{ mg l}^{-1}$ , a slope of  $6.25 \times 10^{-3}$  may be calculated and  $q_{max} = 160 \text{ mg g}^{-1}$ . The intercept = 0.075 and a value of  $K = 0.083$  can be obtained. This part of the plot showed Langmuir-type adsorption. The rest of the plot, at higher concentrations, was not linear.

In all of these curves, where the plot was non-linear, the zeolites were showing that precipitation of thorium was occurring out of the solution at higher concentrations.

#### 8.13.3 LANGMUIR PLOTS INVOLVING THE THORIUM DAUGHTER ISOTOPES

FIGURES 58 - 61 represent the Langmuir plots of the thorium daughter isotopes and were quite different to plots of this type for Th-232. FIGURE 58 shows the total activity Langmuir plot for the thorium parent-daughter equilibrium solution and potassium (total concentration 0.2N) for clinoptilolite. This plot was entirely linear and showed Langmuir-type adsorption of the parent-daughter radioactive equilibrium solution. It was

difficult to say which of the isotopes were removed from the solution. (The weight fraction of daughter isotopes with respect to unit weight of thorium, at equilibrium, may be seen in the table in APPENDIX V). The curve did not pass through the origin and the X-axis has been normalized because units of percentage of total activity in solution have been used to calculate points. Although an intercept was evident, no calculations to obtain  $q_{\max}$  or K could be made.

FIGURES 59 - 61 illustrated the types of curves obtained for various zeolites, where only the  $\beta$ -emitter daughters of Th-232 were analysed. All of the plots obtained were reasonably linear, apart from that in FIGURE 60.

FIGURE 59 shows the Ac-228/Ra-228 Langmuir plot for Z900 in a binary mixture with potassium. The  $\beta$ -emitter daughter isotopes experienced Langmuir-type adsorption onto Z900 in this particular system. The plot passed through the origin and thus gave no Langmuir constant. A slope, and therefore  $q_{\max}$ , obviously cannot be calculated, due to the presence of more than one isotope and the use of arbitrary units in the calculation of  $C_{eq}$  and  $q_{eq}$  values.

FIGURES 60 AND 61 show the Ac-228/Ra-228  $\beta$ -emitter daughter adsorption onto clinoptilolite, in the presence of potassium and sodium respectively. There was a curvature in the plots at the higher concentration ends of the curves.

These isotherms were not prone to half-life activity as

they had been compensated for by the use of a standard (or control solution) for counting. Counting times also were kept to a minimum by the large count rates displayed by some of these solutions.

#### 8.13.4 ION-EXCHANGE ISOTHERMS : URANYL IONS

FIGURE 62 represents the isotherm curves plotted for clinoptilolite. FIGURE 62(1) was the isotherm obtained for a binary mixture of sodium and uranyl ions. There was little preference for  $\text{UO}_2^{2+}$  ions demonstrated by clinoptilolite except perhaps a slight preference, at low concentrations of uranyl ions. FIGURE 62(2) was the isotherm plotted for a binary mixture of potassium and uranyl ions. This curve was completely different to that exhibited by sodium and uranyl ions. Exchange was not fully complete and showed a marked concentration-dependent preference for uranyl at low concentrations and a very sharp turning point in the curve at an  $A_c$  value of 0.03. At this point in the concentration range the clinoptilolite showed preference for the potassium ions in the solutions.

FIGURE 63(1) represents the isotherm plot obtained for Z900 and a binary mixture of sodium and uranyl ions. Exchange was not complete and the uranyl ion was initially preferred over sodium by Z900. FIGURE 63(2) shows the isotherm plot exhibited for a binary mixture of potassium and uranyl ions with Z900. The zeolite showed initial selectivity for  $\text{UO}_2^{2+}$  at low concentrations of uranyl, followed by no preference for either ion over the rest of the concentration range.

FIGURE 64(1) shows the isotherm produced by data given by NaY in a binary mixture of sodium and uranyl ions. This curve showed that NaY was highly selective for  $\text{UO}_2^{2+}$  ions over the entire concentration range and exchange went to completion. FIGURE 64(2) represents the isotherm of KY equilibrated with a binary mixture of potassium and uranyl ions. The curve was not smooth and thus the KY zeolite exhibited some ion-sieving effects which were concentration dependent. Exchange was not complete at room temperature, but as shown with the majority of zeolites, KY was selective for  $\text{UO}_2^{2+}$  at very low concentrations.

From the isotherm data obtained for both thorium and uranium, cation sitings for zeolites equilibrated with these ions are suggested in Chapter 9.

#### 8.13.5 LANGMUIR ISOTHERMS : URANIUM

FIGURES 65 - 67 AND FIGURE 70, show the Langmuir isotherm plots obtained for total activity of the U-238 radioactive equilibrium solution, i.e. U-238 and all of its daughters. The plots were not linear and it was evident that a half-life phenomenon was affecting the counting procedure and hence, not much information can be obtained from these curves.

More useful information can be obtained from the Langmuir plots obtained for U-238 alone, in FIGURES 68 AND 69. FIGURE 68(1) shows the Langmuir plot for clinoptilolite equilibrated with a solution of sodium and uranyl. The plot was non linear thus illustrating a non Langmuir-type of adsorption. FIGURE 68(2)

however displayed a linear curve for clinoptilolite equilibrated with potassium and uranyl ions. A Langmuir-type of adsorption was occurring with this zeolite and the uranyl ion, under these particular conditions. The curve passed through the origin so  $K$  was 0, but a slope of 0.135 can be calculated, thus giving a  $q_{\max}$  value of  $7.43 \text{ mg g}^{-1}$ .

FIGURE 69(1) shows the Langmuir-type of adsorption for Z900 equilibrated with sodium and uranyl ions. A  $q_{\max}$  value of  $42.8 \text{ mg g}^{-1}$  was calculated. The Langmuir constant,  $K$ , was therefore  $1.9 \times 10^{-3}$ .

FIGURE 69(2) was not linear and showed no Langmuir-type of adsorption for Z900 in equilibrium with potassium and uranyl ions and showed that precipitation of uranyl was occurring.

#### 8.13.6 REPEATED EXCHANGES

It can be seen in TABLE 58, that repeated exchanges were possible. Due to non-reversibility of both thorium and uranium with zeolites and the non-linearity of some of the Langmuir plots, it was reasonable to assume that precipitation of thorium and uranium onto the zeolites was occurring as well as some ion-exchange.

#### 8.13.7 WET CHEMICAL ANALYSIS OF CLINOPTILOLITE TREATED WITH THORIUM

The clinoptilolite that had been equilibrated with 0.1N binary mixtures of sodium and thorium, showed that very little thorium was actually on the zeolite [TABLE 59] and these results agreed with the non-selectivity shown by the zeolite in the

plotted isotherm [FIG. 54]. The quantity of  $\text{Th}^{4+}$  on the clinoptilolite corresponded to 2 mg per 0.2g of zeolite and was not affected by concentration at this high normality of thorium.

#### 8.13.8 TOTAL UPTAKES OF THORIUM IN ISOTHERM SOLUTIONS

Eastgate removed all of the thorium from isotherm equilibrium solutions of total normality 0.02N with both sodium and potassium [TABLE 60]. No isotherm could be plotted for this zeolite and it was evident from these and previous thorium uptake data, that Eastgate was very selective for thorium. Clinoptilolite also removed all of the thorium from a binary mixture of sodium and thorium (fixed total concentration of 0.002N) [TABLE 60] and no isotherm could be plotted for this system.

#### 8.14 STRIPPED RAFFINATE EXPERIMENTS

Uptakes of thorium from stripped raffinate solutions onto clinoptilolite and NaY were negligible and it was believed that the large presence of nitric acid ( $\text{H}^+$ ), in conjunction with other competing ion effects, hindered uptakes of thorium. TABLE 61 shows the fluoride concentrations of initial solutions, and solutions contacted with zeolites. Thorium fluoride was not precipitating, within the timescale of the equilibration experiments.

8.15      X-RAY POWDER DIFFRACTOGRAMS

FIGS. 71 TO 80 show X-ray powder diffractograms of various zeolites and thorium treated zeolites.

FIGS. 71 AND 72 are Eastgate and a thorium treated Eastgate. The Eastgate sample was believed to be a mixture of zeolites (including erionite) and comparison with an X-ray diffractogram of erionite [FIG. 79] shows that the Eastgate sample bears little resemblance to Erionite. The thorium-treated Eastgate shows no decrease in intensity and therefore no loss in crystallinity of the sample. The only significant change between the Eastgate sample and its thorium-treated sample was the enlargement of a peak at a  $2\theta$  value of  $43.148^\circ$  and this peak, labelled A on FIG. 72, had a relative intensity of 17.3%.

The X-ray powder diffractograms are described in terms of Relative Intensities. The peak with a maximum intensity was designated as having 100% intensity. All other peaks described in terms of percentage intensities were relative to this peak of greatest intensity. The only peak which experienced any loss in intensity was a peak at a  $2\theta$  value of  $29.391^\circ$  which lost upto 17% intensity after the sample was treated with thorium.

FIGS. 73 AND 74 show the X-ray powder diffractograms of clinoptilolite and an acid-treated thorium clinoptilolite. A loss of crystallinity of the clinoptilolite was evident. Three new peaks had appeared [FIGURE 74] labelled A, B and C. These peaks were sharp and corresponded to  $2\theta$  values of  $22.400^\circ$  (peak A),  $30.236^\circ$  (peak B) and  $48.321^\circ$  (peak C). Peaks A, B and C have



d-spacings of 3.9658, 2.9535 and 1.8820 Å respectively. Comparing these d-spacings with those of  $\text{ThO}_2$ ,  $\text{ThO}$  and  $\text{K}_2\text{ThO}_3$  [TABLE 63] it can be seen that peaks A, B and C most closely resemble  $\text{ThO}_2$  and also  $\text{ThO}$  and  $\text{K}_2\text{ThO}_3$ . FIG. 75 shows a colour overlay comparison of clinoptilolite in purple, thorium-treated clinoptilolite in orange and  $\text{ThO}_2$  in green. Many of the thorium-treated clinoptilolite peaks corresponded to  $\text{ThO}_2$ .

TABLE 63

The d-spacings (Å) of  $\text{ThO}_2$ ,  $\text{K}_2\text{ThO}_3$ , and Peaks A, B and C [FIG. 74]

FIG 74 A, B AND C	$\text{ThO}_2$	$\text{K}_2\text{ThO}_3$	$\text{ThO}$
3.9658	3.95	—	—
2.9535	2.94	3.06	3.06
1.882	1.88	1.88	1.87

FIGS. 76 AND 77 represent the X-ray powder diffractograms obtained for NaZ900 and the thorium treated zeolite. There was little difference between the two spectra and there were no peaks corresponding to  $\text{ThO}_2$  which were evident.

FIGS. 78 TO 81 represent the X-ray powder diffractograms obtained for other zeolites used in this work.

#### 8.16 ENERGY DISPERSIVE X-RAY SPECTRA (EDX)

FIGS. 82 AND 83 show the EDX spectra obtained for thorium treated clinoptilolite. FIGURE 82 shows the spectrum of a typical particle. There was a thorium peak which corresponded to thorium on the surface of the zeolite, as these spectra show the peaks of elements on the surface, and within the bulk zeolite, to a depth of a few microns.

FIGURE 83 shows the spectrum of a particle that had bright areas on its surface, shown by SEMs (see section 8.20). The bright areas were scanned by EPMA and were found to contain large amounts of thorium. There was a large thorium peak corresponding to thorium on the surface of the clinoptilolite (shown by FIG. 83). The elemental peak was greater than that of silicon.

FIG. 84 is the EDX spectrum of thorium treated Eastgate where the thorium had been washed off the sample by treatment with firstly 0.01M  $K^+$  and then with hydrochloric acid (1.0% v:v). According to the wet chemical analysis, there should be more magnesium present than potassium but the elemental analysis of the Eastgate surface in FIGURE 84 showed the reverse. Treatment with  $K^+$  solution and hydrochloric acid clearly removed magnesium from the sample and increased the  $K^+$  content of the sample. A slight hump in the EDX spectrum indicated a very small amount of thorium left on the surface.

FIGURE 85 shows no indication of surface thorium and the acid washing of the sample ensured this.

FIGURE 86 is the Energy Dispersive X-ray spectrum obtained for the CaY column sample treated with Th-232. Small amounts of thorium had accumulated on the surface of the CaY, even in the presence of 0.1M nitric acid.

FIGURE 87 is the typical X-ray spectrum obtained for a sample of clinoptilolite treated with 0.1N thorium-232 in a batch experiment and FIGURE 88 is the same sample with both sets of axes of the spectrum expanded. As seen in section 8.6 clinoptilolite removed more thorium from less concentrated solutions. Much of the thorium was on the surface of the zeolite particle [FIG. 83]. At higher concentrations there were small amounts of thorium on the surface with a possibility of thorium being within the bulk of the sample.

## 8.17 DIFFERENTIAL THERMAL GRAVIMETRY

FIGS 89 AND 90 show the thermograms of clinoptilolite and a thorium-treated clinoptilolite giving water contents of 14.11% and 26.55% respectively. The natural clinoptilolite showed a broad peak at about 76°C. The thorium-treated clinoptilolite showed a very regular water-loss peak uncharacteristic of a zeolite and a higher water content. This was attributed to thorium present as hydrated oxide. The water loss peak has its peak maximum at 115°C. (The curve has been smoothed).

FIGS. 91 AND 92 represent the two phases of the thorium-treated clinoptilolite [SEE SECTION 6.7] i.e. the caked phase and the powdery phase respectively. Both phases contain more water than the untreated natural zeolite but the caked phase [FIG. 91] contains more water than the powdery phase, as expected. It is reasonable to assume that the caked phase contains more thorium than the powdery phase.

FIGS. 93 AND 94 represent the differential thermograms for Na clinoptilolite and K clinoptilolite respectively. The Na clinoptilolite had the greater water content.

FIGURE 95 is the differential thermogram of Eastgate and the water content of this sample was found to be 13.37%. Between the temperatures 600°C and 750°C there was a series of water peaks. This was not due to noise on the instrument and the thermogram was entirely reproducible. There was a likelihood that the series of water peaks was due to the co-ordinated water molecules

associated with the  $\text{Mg}^{2+}$  cations being released at these temperatures. From the wet chemical analysis of the Eastgate sample, it has been shown that Eastgate contains small amounts of magnesium.

FIGURE 96 demonstrated the decomposition of  $\text{Th}(\text{OH})_4$  when heated.

FIGS. 97 AND 98 represent the thermograms of NaY and a thorium-treated sample of NaY respectively. Although the water losses for each sample were similar, the thorium-treated zeolite gave a slightly larger water content, there were other differences between the samples. The water loss peak for NaY occurred at a peak maximum temperature value of  $100^\circ\text{C}$ , whereas that for the thorium-treated sample occurred at  $70^\circ\text{C}$ . Both results for thorium-treated clinoptilolite and thorium-treated NaY indicate a hydrated thorium oxide species with loosely bound water present.

#### 8.18 $\gamma$ -SPECTRA

FIGS. 99 AND 100 display the  $\gamma$ -spectra obtained for a solvent-extracted Th-232 solution and a solvent-extracted Th-232 daughters solution. The Th-232 solution [FIG. 99] showed that a few of Th-232 daughter isotopes either had been extracted into the Th-232 solution or had grown into the Th-232 by the spontaneous radioactive decay of the Th-232. The isotopes present were  $^{212}\text{Pb}$ ,  $^{228}\text{Ac}$  and  $^{208}\text{Tl}$ . As can be seen from Appendix III these were the daughter products with the shortest half-lives, and therefore the highest activity and it was most likely that these isotopes had grown into the solution between the time of extraction and the time of obtaining the spectrum. FIGURE 100 shows that the

daughter isotopes Ac-228, Pb-212, Tl-208 were present in greater concentration.

FIGS. 101 TO 103 show the  $\gamma$ -spectra of zeolites that had been treated with thorium solutions on columns. FIGURE 101 represents the  $\gamma$ -spectrum of Eastgate treated with thorium-232 solutions. There was a large presence of Th-232 daughter isotopes which had been sorbed onto the zeolite, even after acid-washing of the zeolite. FIGURE 102 represents the  $\gamma$ -spectrum of clinoptilolite treated with Th-232 equilibrium solution. The spectrum was obtained under the same conditions as those for the Eastgate sample. However, the total counts obtained for the adsorbed Th-232 daughters were 3 times as great as those for Eastgate. FIGURE 103 shows the  $\gamma$ -spectrum for acid-washed clinoptilolite treated with Th-232 solution. There was a large presence of Th-234 within the sample with only small amounts of U-238 daughter products mainly Pa-234 which were growing into equilibrium. (Note: The ordinate axis of this spectrum has been reduced in scale to show the daughter isotopes).

FIGS. 104 TO 106 show  $\gamma$ -spectra obtained for a sample which had undergone an isotherm experiment. That of the isotherm equilibrium solution is shown in FIGURE 104 and a wide range of Th-232 daughters can be seen. FIG. 105 shows the spectrum obtained for the zeolite solid after equilibration in the isotherm experiment. Only Ac-228 was present. FIGURE 106 shows an isotherm control solution where the initial Th-232 daughter content can be seen. A comparison between FIGS. 104

and 106 showed that daughter  $\gamma$ -emitters had decreased in amount after contact with the zeolite, (clinoptilolite).

FIGURE 107 shows the  $\gamma$ -spectrum of Th-234 that had been solvent extracted from U-238. Again the Th-234 peaks represented high counts and in order to see the Th-234 daughter isotopes the ordinate was reduced as before.

FIGS. 108 AND 109 show the  $\gamma$ -spectra obtained for the stripped raffinate solution (with  $1\text{ g l}^{-1}$  thorium-232 added) and a clinoptilolite sample that had been treated with the raffinate solution respectively. FIGURE 108 shows that Th-234 and Th-232 daughters were present and FIGURE 109 showed that the clinoptilolite has removed some of the isotopes from solution even in the rather low pH conditions of the raffinate.

#### 8.19 $\beta$ -SPECTRA

FIGS. 110 AND 111 represent the  $\beta$ -spectra obtained for H-3 and C-14 respectively. These isotopes were used to produce calibration data for the  $\beta$ -spectrometer.  $E_{\text{max}}$  values of 18.6 keV for H-3 and 146.0 keV for C-14 were used. [REF. 96].

FIGURE 112 is the  $\beta$ -spectrum obtained for Tl-204 giving an  $E_{\text{max}}$  value of 763.0 keV showing the calibration to be correct and FIGURE 113 is the  $\beta$ -spectrum of Th-234 with an  $E_{\text{max}}$  value of 191.07 keV. TABLE 62 shows the channel numbers used to calculate the  $E_{\text{max}}$  energy [SEE APPENDIX II].

## 8.20 SCANNING ELECTRON MICROGRAPHS

PLATE 1 shows the Scanning electron micrographs obtained for thorium-treated clinoptilolite, (1) denotes a typical particle and (2) shows a particle with high surface thorium content. The bright areas on PLATE 1 (2) are the parts which contained high thorium quantities given by qualitative electron probe microanalysis. Clinoptilolite of the Mudhills origin produced scanning electron micrographs which showed some of the characteristic platy structure of clinoptilolites.

PLATE 2 (1) shows the scanning electron micrograph of the thorium-treated clinoptilolite particles from a column. The particles were between 150 and 200  $\mu\text{m}$  in diameter.

PLATE 2 (2) shows the scanning electron micrograph of acid-washed, thorium-treated Eastgate. Although some of the crystals have been eroded by the acid-treatment, the crystals may be seen to be fibrous in nature, thus illustrating the likely possibility of the presence of mordenite of a sedimentary character [REF. 12].

PLATE 3(1) shows an acid-washed thorium-treated NaZ900 sample.

PLATE 3 (2) shows an acid-washed CaY sample that had been treated with thorium. Acid-washing severely affected the crystal structure, which was not clearly visible from this scanning electron micrograph.



CHAPTER 9

GENERAL DISCUSSION

CONCLUSIONS AND

SUGGESTIONS FOR FURTHER

WORK

## 9. GENERAL DISCUSSION AND CONCLUSIONS

### 9.1 THORIUM

From the results obtained by the thorium uptake experiments, it was clearly shown that zeolites removed thorium most efficiently from lower thorium concentration solutions. Eastgate, clinoptilolite, NaY, NaZ900 and chabazites 1 and 3 removed thorium from dilute solutions. The uptakes of thorium for Eastgate and the chabazites were comparable. In acid solutions, uptakes of thorium were reduced for all zeolites due to a) preferential exchange of  $H^+$  or  $H_3O^+$  over thorium and b) the increasing quantities of bulky thorium nitrate complexes (cationic, neutral and anionic), that were present [REF. 62] in acidic solutions of thorium which were excluded sterically from the zeolite channels and pores.

Competing cations in the presence of thorium reduced the uptakes of thorium in most of the zeolites studied, with the exception of Eastgate.

### 9.2 ISOTHERMS AND CATION POSITIONS

#### 9.2.1 CLINOPTILOLITE

The isotherm data revealed that, at low concentrations of thorium in equilibrium solutions, thorium was the preferred ion and the zeolites clinoptilolite, Z900 and NaY removed thorium selectively at these concentrations. At 0.01N initial concentrations of thorium, the isotherm for clinoptilolite

indicated that approximately 20% of the cation sitings in the zeolite were occupied by thorium [FIG. 50]. Approximately 30% of sites within clinoptilolite remained unexchanged in agreement with the observed difficulty in the replacement of ions like calcium and magnesium from the sites such as M(4) [REF. 124]. At 0.001N initial thorium concentrations, in the presence of potassium, approximately 40-50% of the cation sites for clinoptilolite were filled [FIG. 51]. Detailed structural information for an Agoura clinoptilolite has been proposed by KOYAMA et al [REF. 113] and some cation sites have been reported by DYER et al [REFS. 40, 14] in a Hector clinoptilolite. The presence of a potassium ion at the M(3) cation position, in the vicinity of the centre of the 8-membered oxygen ring in channel C of clinoptilolite is unlikely to partake in ion-exchange with thorium [REF. 113]. This has been found to be in agreement with the analysis of solutions in TABLE 36 and no potassium was found in the solutions. It is far more likely to be the sodium ions (in cation positions M(1) and M(2)) that are exchanging for thorium in channels A and B of clinoptilolite. The Mudhills clinoptilolite used in this work had a pore size of  $4\text{\AA}$  [REF. 104], and this has been assumed to be the aperture diameter of the ten-membered oxygen ring of channel A, (the main channel). Provided that the thorium species removed from solution has a diameter of less than  $4\text{\AA}$ , ion-exchange would be expected to occur.

It was shown that two sodium ions were removed from the clinoptilolite for every  $\text{Th}^{4+}$  ion taken up by the zeolite [TABLE 38]. It was very likely, however, that a species such as a hydrated thorium oxide species was being sorbed by the zeolite. This involvement of a species such as  $\text{ThO}^{2+}$  or  $\text{Th}(\text{OH})_2^{2+}$  [REF. 58] and their hydrolysis products were far more likely to occur in non-acidic solutions of thorium, i.e. above an approximate pH of 3. The Th—O ionic bond length is  $2.53\text{\AA}$  [REF. 50]. The arisal of these polymeric thorium species could also have been accelerated by the fact that zeolites have an alkaline surface ( $\text{pH}\sim 12$ ) due to the presence of crystal-terminating hydroxyl groups. FREUDE et al [REF. 92] have discussed surface and framework hydroxyl groups in zeolites.

#### 9.2.2 NaY

TABLE 38 shows that a 1:1 milliequivalent exchange occurred between thorium in aqueous solution and sodium from NaY. From FIGURE 63, it can be seen that the isotherm for NaY equilibrated with thorium and sodium binary solutions, terminated at an  $A_c$  value of 0.26 for thorium. (At this point it should be noted that the  $A_s$  and  $A_c$  values were not normalized, as it was contemplated that simple ion-exchange of a binary system was not occurring with thorium). Ion-exchange in NaY with tervalent rare earth cations has been studied by REES et al [REF. 32] and  $\text{La}^{3+}$  ion-exchange behaviour in zeolites X and Y has also been studied [REF. 116]. REES has proposed that  $\text{La}^{3+}$  and other rare

earth ions were located in the supercages of zeolite Y [REF.32].

In this thesis, the isotherm shown by NaY illustrated a speciation effect with respect to thorium in the presence of sodium [FIG. 53]. At low-concentrations, the zeolite showed a great affinity for thorium upto a value of  $A_c = 0.06$ . From this value onwards, the behaviour of the isotherm was different to that of clinoptilolite for instance and possibly showed that a different thorium-zeolite phase existed. Exchange was complete and even though NaY has been shown to prefer ions of high charge density, such as  $\text{Lu}^{3+}$  [REF. 32], it was considered unlikely that ion exchange was the dominant mechanism at the higher thorium concentrations in contact with zeolite NaY. The first 23% of site occupancy of thorium within NaY (low concentrations of thorium) was attributed to  $\text{Th}^{4+}$  exchanging for ions within the supercages at sites M(II), M(III) and M(IV) [SEE Fig. 7]. It was unlikely that the cation sites within the  $\beta$ -cages would have been accessible to thorium. The  $\text{Th}^{4+}$  ion has an ionic diameter of  $1.98\text{\AA}$  [REF. 50] and is prone to high numbers of co-ordinated water molecules in aqueous solution [REF. 51]. Complete exchange was most likely to be due to a precipitation of thorium at the higher concentrations of thorium.

Over exchange and irreversibility of heavy metals in zeolites has been studied by TOWNSEND et al [REF. 112] and was attributed to hydronium ion-exchange although other explanations were proposed such as hydroxide precipitation, and the presence of occluded aluminium.

BOLTON has described in his review, that NaY removed thorium from acidic solutions [REF. 46]. In his work, a 1:1 mole ratio of thorium for sodium ion-exchange occurred in NaY and correlated with the exchange carried out in this work [TABLE 38]. BOLTON has suggested that the sum of the number of moles of cations, expressed as a ratio with the zeolite aluminium content is as follows:  $(4\text{Th}^{4+} + \text{Na}^+)/\text{Al} = 1$ , and that subsequent exchanges were possible. It was therefore proposed that the thorium exchanged as  $\text{Th}^{4+}$ , however, reservations were expressed because of the possibility of  $\text{H}_3\text{O}^+$  ion-exchange and thorium precipitation can also bring about a value of unity in the expression above.

Work has also been conducted on a zeolite 225 column. HUBICKI et al [REF. 121 abstract only] used this zeolite to separate a mixture of uranium, thorium and lanthanides, and it was found that this particular zeolite selectively removed thorium and the lanthanum content of the lanthanides by ion-exchange but eluted  $\text{UO}_2^{2+}$ . They gave no details of the nature of zeolite 225.

### 9.2.3 ZEOLITE Z900

The isotherm shown in FIGURE 52 for KZ900 depicts only about 50% completion of exchange of thorium for potassium, at total concentrations of 0.02N and of this exchange, approximately 40% of the available cation sites were shown to be occupied. The isotherm for potassium shows that this ion was not preferred.

Reversibility points calculated for thorium showed that the thorium exchange was irreversible and hence, an ion-exchange mechanism was unlikely.

### 9.3 ISOTHERMS : URANIUM

#### 9.3.1 CLINOPTILOLITE

Two very different isotherms were exhibited by clinoptilolite with potassium and sodium equilibrium solutions with the  $\text{UO}_2^{2+}$  ion. Very little preference for uranium was exhibited by clinoptilolite with sodium solutions, and any  $\text{UO}_2^{2+}$  removed by the zeolite was not reversible. The exchange was not complete and only 48% replacement occurred. It was therefore unlikely that ion-exchange occurred. In the presence of potassium a great affinity for uranyl ions was displayed initially with about 20% of the clinoptilolite cation sites being occupied by  $\text{UO}_2^{2+}$ . Exchange was incomplete and there was a large degree of exclusion of  $\text{UO}_2^{2+}$  from the framework cation sites of clinoptilolite. The  $\text{U}=\text{O}$  bond length has been shown to be  $1.94\text{\AA}$  [REF. 115], and since the  $\text{UO}_2^{2+}$  ion is linear, it can be expected to have a diameter of  $3.8\text{\AA}$ , i.e. well within the limiting  $4\text{\AA}$  pore size of the main channel in clinoptilolite. It was quite possible that the  $\text{UO}_2^{2+}$  was hydrated [REF. 117], thus preventing substantial exchange.

Uranyl ions have been used by many workers to study radioactive ion removal by zeolites. HAFEZ et al [REF. 117] described ion-exchange of  $\text{Cs}^+$  and  $\text{Sr}^{2+}$ , and adsorption of uranyl ions as positively charged hydrolysis species attracted to the

negatively-charged harmotome zeolite surface. ANDREEVA et al [REF. 49] also described a sorption of uranyl onto clinoptilolite.

### 9.3.2 Z900

Little preference was shown for  $\text{UO}_2^{2+}$  over sodium in Z900 as indicated by the isotherm in FIGURE 63.(1). Exchange was only 25% complete at the total concentration of 0.02N. FIGURE 63.(2) indicated that  $\text{UO}_2^{2+}$  was selectively removed from potassium solutions only at the lower concentration end of the isotherm, with about 20% of the cation sites of the Z900 being filled by  $\text{UO}_2^{2+}$ . Steric limitations of the  $\text{UO}_2^{2+}$  ion was not thought to be of significance with this zeolite, as the effective pore diameter of NaZ900 is  $7\text{\AA}$  [REF. 105].

### 9.3.3 ZEOLITE NaY

NaY was highly selective for  $\text{UO}_2^{2+}$  ions over sodium ions at 0.02N total concentrations and the isotherm maybe seen in FIGURE 64. Approximately 80% of the exchange sites in the zeolite were filled and exchange was complete. KY showed an incomplete exchange (only 34% exchange), and a step-like curve, although high selectivity for  $\text{UO}_2^{2+}$  was shown initially indicating that approximately 10% of the ion sites available in KY were filled. Work has been carried out on  $\text{UO}_2^{2+}$  ion-exchange onto synthetic faujasite-type zeolites by HOČEVAR [REF. 103]. The total concentration of sodium and uranyl was fixed at 0.2N. Comparing the isotherm obtained by HOČEVAR et al, in sodium solutions with that obtained by this work, it may be seen that



at the lower normality end of both isotherms, the  $\text{UO}_2^{2+}$  ion is the preferred ion by NaY. HOČEVAR et al suggested some zeolite phase changes at the total concentration of binary mixtures that he used. HOČEVAR found that exchange was complete.

REES et al have published isotherm data for  $\text{UO}_2^{2+}$  ion-exchange into zeolite X in sodium solutions, and have found that only 50% ion-exchange occurs at 0.1N total concentration with selectivity for sodium ions and this has been said to be due to the size of the  $\text{UO}_2^{2+}$  ion [REF. 102]. The work done by REES and HOČEVAR demonstrate the differences in zeolites X and Y, where a type of ion sieve effect was occurring. Migration of cations, from within the supercages of zeolite Y, to the  $\beta$ -cages appeared to be occurring.

Further studies of zeolite Y and the  $\text{UO}_2^{2+}$  ion have been published in the literature claiming that most of the  $\text{UO}_2^{2+}$  was within the bulk of the zeolite [REFS. 110, 111]. The same reference also compared the high concentration of bulk uranyl in zeolite Y with the high surface concentration (about 90%)  $\text{UO}_2^{2+}$  found on the surface of zeolite A.

#### 9.4 LANGMUIR ADSORPTION

Langmuir-type adsorption was not displayed for thorium-232 ions by clinoptilolite, Z900 or NaY. However, the total activity plot of the Th-232 parent-daughter equilibrium solution contacted with clinoptilolite, displayed Langmuir-type adsorption. Langmuir-type adsorption was also shown by the  $\beta$ -emitter daughters of

Th-232 (Ac-228/Ra-228) with zeolites clinoptilolite and Z900. The Langmuir constant,  $K$  and  $q_{\max}$  could not be calculated as the exact concentrations of  $\beta$ -emitter daughters could not be assessed.

The total activity Langmuir plots for the U-238 parent-daughter equilibrium solution were thought to be unreliable as half-life effects were evident which could not be corrected for.

Useful information, however can be made from U-238 determinations and the Langmuir plots obtained from them: [FIGS. 68 AND 69]. Zeolite NaZ900 showed Langmuirian adsorption and  $K$  and  $q_{\max}$  were calculated as  $1.9 \times 10^{-3} \text{ mg g}^{-1}$ . K-clinoptilolite showed a Langmuir-type of adsorption and  $q_{\max}$  was obtained at  $7.43 \text{ mg g}^{-1}$ . However, the line passed through the origin showing  $K$  to be zero.

Work on the  $\text{UO}_2^{2+}$  adsorption onto zeolite A has been published by workers in Japan [REF. 93]. In those investigations it was found that Langmuirian adsorption occurred with  $\text{UO}_2^{2+}$  and zeolite A.

Work illustrated in this thesis shows that the type of adsorption which occurred on clinoptilolite and Z900 in binary mixtures of  $\text{UO}_2^{2+}$  and counter ions, depended upon the counter ion present. For example, clinoptilolite showed Langmuirian adsorption if the counter-ion was  $\text{K}^+$  but if the counter-ion was  $\text{Na}^+$ , a different type of sorption occurred and this was also demonstrated by Z900 as  $\text{Na}^+$  allowed Langmuirian adsorption, but  $\text{K}^+$  did not. It was difficult to assess why this occurred as surface precipitation

analysis was not conducted for uranium.

WIERS et al [REF. 118] have studied the ion-exchange of a range of di- and trivalent cations onto zeolite A and have proposed an initial Langmuirian type of adsorption for  $\text{Ca}^{2+}$  ions and zeolite A.

HIGGO et al have studied the loadings of the actinides neptunium, americium, and plutonium onto deep-sea sediments and have proposed a sorption mechanism [REF. 119] and sorption of the actinides onto clays has been evaluated by other workers [REF. 120].

#### 9.5 SURFACE PRECIPITATION OF THORIUM

Patents published in the literature suggest that  $\text{ThO}_2$  has been exchanged into zeolites [REFS. 47,48,108,109]. From the ion-exchange isotherm data in this work, it was certainly evident that zeolites exhibited selectivity for the thorium ion at low concentrations. From the analysis of exchange solutions it was likely that for clinoptilolite, exchange occurred as  $\text{Th}(\text{OH})_2^{2+}$  or  $\text{ThO}^{2+}$  and NaY exchange was occurring with thorium as  $\text{Th}^{4+}$  or  $\text{Th}(\text{OH})_2^{2+}$  depending on the pH of the solution. Ion-exchange was not entirely responsible for the removal of thorium from solutions. X-ray diffraction data showed some  $\text{ThO}_2$  or ThO presence in clinoptilolite but was unlikely to indicate  $\text{Th}(\text{OH})_4$  species as they are amorphous to X-rays. A far more indicative method of showing surface thorium is the energy-dispersive X-ray microanalysis technique. The energy-dispersive X-ray spectra of unwashed clinoptilolite samples clearly showed surface thorium. Differential thermograms of zeolites treated with thorium in general, showed higher water

losses than untreated zeolites and indicated that the thorium was present as a possible hydrolysis product.

#### 9.6 REPRODUCIBILITY OF RESULTS

Uptake experiments and isotherm data may not have been entirely reproducible due to possible inconsistencies in the natural zeolites used. Slight variations in the composition of each sample of the same zeolite may have accounted for fluctuations in uptake results obtained for thorium and uranium. However, any subsequent experimentation on the natural zeolites used, should show the same trends as the results shown in this work.

#### 9.7 THERMODYNAMIC PARAMETERS FOR ISOTHERMS

All of the natural zeolites used in this work were unpurified and as such would have led to inaccurate calculation of parameters for ion-exchange. The main reason for not assessing thermodynamic data in this work was because of the possibility of surface precipitation of thorium and uranium onto zeolites, as demonstrated for thorium. It has also been shown in this thesis, that simple binary ion-exchange does not occur with thorium solutions which exist in their parent Th-232-daughter equilibrium form. Sorption of the thorium daughter-isotopes has been shown to occur simultaneously as ion-exchange with Th-232 in zeolites. Therefore it would have been impossible to consider any calculation of an accurate diffusion constant for ion-exchange. Ion-exchange with  $H^+$  or  $H_3O^+$  may also have been occurring in the zeolites tested.

AMES et al [REF. 123] has shown that radium has been sorbed onto zeolites and clays. The hydrated radium ionic radius is  $3.98\text{\AA}$  [REF. 100]. Thorium, as  $\text{Th}^{4+}$ , would be expected to be similar to radium.

No isotherms were plotted for Eastgate because total thorium—removal occurred in both sodium and potassium solutions, and the zeolite was known to be a mixture of at least two zeolites, mordenite and clinoptilolite, the major constituent being mordenite.

#### 9.8 EASTGATE - A SPECIAL CASE

From this work, it was clear that Eastgate was superior, in its thorium-removal ability, to all other natural and synthetic zeolites tested. The ability of Eastgate to remove thorium from solution appeared not to be hindered by competing ions such as sodium or potassium, and its capability to remove thorium from acidic solutions, was found to be far greater than other zeolites.

The zeolite was not fully characterized and this work attempted to elucidate the constituents of Eastgate to some extent, in order to explain its thorium-uptake capability. The only fact known about the Eastgate (as received), was that it was from the Eastgate deposit in the Shoshone Range, Nevada, U.S.A. It is known that erionite also originates from the Shoshone Range and is found with mordenite and clinoptilolite [REF. 95].

The differential thermogram of Eastgate, Churchill County, Nevada shown by GOTTARDI [REF. 95] was not similar to that obtained in this work [FIG. 95]. However, the sample of Eastgate resembles that of a Churchill County Eastgate which has its main

constituent as mordenite [REF. 122]. The water peak obtained for the Eastgate used in this work, was less broad and had its peak maximum at a lower temperature and several water peaks were obtained between 600 and 700°C. The peak maximum at 70°C was similar to that obtained by Mudhills clinoptilolite [FIG. 89]. Wet chemical analysis of the Shoshone Eastgate showed a similar composition to erionite but with approximately 2.5% MgO content. The Si/Al ratio was 4.24. The water contents of erionite, mordenite and clinoptilolite are respectively as follows: 26-28%, 12.96-15% and 16.8-25.8%[REF. 95]. The water content of the Eastgate (13.37%) most closely resembles that of mordenite.

The X-ray diffractogram of the Eastgate sample was not similar to erionite but showed that most of the major peaks corresponded to those of mordenite and clinoptilolite. It can be therefore concluded that the sample of Eastgate zeolite used in this work, was a mixture of mordenite and clinoptilolite and this was supported by the fact that it was originally supplied by Anaconda Copper Company in 1983. The company, at that time, owned the Eastgate claim now worked by East-West Minerals and are said to produce a mixture of mordenite and clinoptilolite.

An interesting paper published by CARLAND et al [REF. 43] shows that an Eastgate sample from Nevada contained 96% erionite and 1% chabazite, the rest of the mixed zeolite being made up of calcite and quartz. The sample removed  $\text{Cu}^{2+}$  from acidic solutions and the paper shows, that although the stability series of four zeolites in acidic solution (pH 3) was as follows:

mordenite > clinoptilolite > Eastgate > chabazite,

their  $\text{Cu}^{2+}$  removal ability from acid solution was:

Eastgate > chabazite > clinoptilolite >> mordenite.

This series was found to be similar to that for thorium in acid solutions in this thesis, with the exception of chabazite, which was not tested.

## 9.9 RADIOCHEMISTRY

### 9.9.1 EQUILIBRIUM SOLUTIONS

Analar thorium nitrate was used in all of the thorium experiments and had been industrially purified by the manufacturer, Koch-Light. Between the time of purification and use it was assumed that the Th-232 parent-daughter equilibrium had been achieved. The equilibrium quantities presented as a weight-fraction of unit Th-232 would have the values shown in APPENDIX V. It can be seen that the daughters were present in very small quantities but probably exhibit high count rates, especially when LSC was the method of measurement.

A parent-daughter equilibrium will re-establish itself by spontaneous radioactive decay when a particular isotope has been removed from the equilibrium solution, e.g. by the sorption effect of a zeolite.

### 9.9.2 ČERENKOV COUNTING

In this work, Čerenkov counting was adequate to count Th-234 solutions quantitatively and was most useful in counting Th-234 in highly acidic solutions as the Čerenkov radiation was not quenched by nitric acid.

It was also shown that the  $\beta$ -emitter daughters Ac-228 and Ra-228 could be counted in water, using the Čerenkov technique to assess their behaviour on contact with zeolites.

It was revealed that, although Th-232 was being removed selectively by zeolites from aqueous solution, so were the  $\beta$ -emitter daughters.

### 9.9.3 LIQUID SCINTILLATION COUNTING

When considering equilibrium solutions of parent Th-232 and its daughters, liquid scintillating may only be used to assess the removal of total activity of all of the equilibrium decay-chain components by zeolites. Potassium, sodium and aluminium solutions of low concentration showed little quenching in the counting systems used for thorium and uranium, however acid, especially nitric acid, was known to show quenching in these systems [REF. 87]. When counting a pure isotope of Th-232 liquid scintillation counting was probably the best method to use for its quantitative determination as the high count rates produced were less prone to error than other methods of determination. However, it must not be forgotten that immediately after separation of Th-232 from its daughters, the daughters will grow back into solution and a suitable extracted Th-232 standard must be counted with every sample.



#### 9.9.4 COUNTING METHODS AND DAUGHTER REMOVAL BY ZEOLITES

The methods used in sections 9.9.2 and 9.9.3 have demonstrated that thorium daughters exhibited the Langmuir-type of adsorption onto zeolites at the same time as the zeolites removed the parent Th-232 from solution.

#### 9.9.5 THORIUM-232 AND URANIUM-238

The best methods to determine thorium-232 and uranium-238 in the solutions of various compositions used in this work were the colourimetric analyses. These methods of analysis gave accurate determinations of the aforementioned isotopes in isotherm experiments and uptake experiments. Since the isotopes Th-232 and U-238 had very long half-lives, colourimetric determinations were not prone to half-life phenomena and no such corrections needed to be made. Colourimetric analysis was possible in solutions containing the daughters of Th-232 and U-238 [REF. 73].

#### 9.10 $\gamma$ - and $\beta$ -SPECTROSCOPY

##### 9.10.1 $\gamma$ -SPECTROSCOPY

$\gamma$ -Spectroscopy was used as a purely qualitative tool and was most useful in observing the sorption of thorium-daughters onto zeolites.

##### 9.10.2 $\beta$ -SPECTROSCOPY

The  $\beta$ -spectrum of Th-234 was used to characterize a solvent-extracted solution of Th-234 from U-238 and was found to be adequate for this purpose.

### 9.11 ZEOLITES AND ACID SOLUTIONS

Results pertaining to stripped raffinate solutions were disappointing with respect to Z900 and clinoptilolite, but not unexpected. The presence of thorium nitrate hydrated species within this solution warranted their exclusion from the zeolite apertures. Sodium Y could not withstand the highly acidic pH's involved.  $H^+$  and  $H_3O^+$  exchange was preferred by the zeolites in these acidic solutions.

A more promising result was shown by Eastgate in simulated raffinate solutions of the lowest total ionic concentrations. This zeolite remained reasonably stable in the low pH solutions and removed upto 42% thorium. Unfortunately, time did not allow for the screening procedure of Eastgate with stripped raffinate solutions but it was expected that Eastgate would give a better removal of thorium than clinoptilolite or Z900.

NaZ900 removed no thorium from any acidic solutions and  $H^+$ -exchange from acid solutions was expected. NaZ900 also had the highest  $SiO_2/Al_2O_3$  ratio of all the zeolites used, the ratio being 10 and was known to be stable in acidic solutions [REF. 21]. However GREBENSHCHIKOVA has published data for the adsorption of Th(IV) from nitric acid solutions of pH 1.9 on Na-mordenite. The adsorption was said to be 90% and the mechanism was of the ion-exchange type. Adsorption of Th(IV) was increased with decreasing acid concentration however, sodium ions reduced the

adsorption and the presence of caesium ions inhibited adsorption of Th(IV) completely [REF. 120 (abstract only)].

Clinoptilolite removed approximately 5% thorium from the simulated raffinate solutions and this was due to preferred exchange of  $\text{Na}^+$ ,  $\text{K}^+$  and  $\text{H}^+$ .

#### 9.12 CONCLUSIONS OF THIS WORK : THORIUM

Zeolites, both natural and synthetic can remove thorium efficiently from dilute solutions of pure thorium. They also removed the thorium daughters from a Th-232 parent-daughter equilibrium solution. Eastgate was superior to all other zeolites in its capability to remove thorium from solutions containing competing cations such as sodium and potassium. Clinoptilolite, NaY and NaZ900 showed reduced uptakes of thorium in the presence of sodium and potassium. These particular zeolites showed greatly reduced uptakes of thorium in acidic solutions however Eastgate was the least affected with respect to acid  $\text{H}^+$  interference.

In simulated raffinate solutions, the abilities for the uptakes of thorium were as follows for the zeolites tested: Eastgate >> clinoptilolite > NaY and NaZ900. This sequence corresponded to a 42% removal of thorium from solution by Eastgate to no removal at all by NaY and NaZ900.

Isotherms for clinoptilolite, NaY and Z900 and thorium all showed high selectivities for thorium at low solution concentrations of thorium solution. Langmuirian adsorption was

shown by the Th-232 daughters in conjunction with the partial exchange of Th-232 with the zeolites.

Eastgate was found to be a predominantly mordenite-clinoptilolite mixed zeolite and no isotherm could be plotted.

The uranium isotherms demonstrated that clinoptilolite, NaY and Z900 had high selectivities for uranyl ions at low concentrations of uranyl, especially NaY in sodium/uranyl binary mixtures. The uranyl ion underwent a Langmuirian-type of adsorption in the case of NaZ900.

Column work has shown that Eastgate had the highest loading capacity for thorium and that most of the thorium could be rapidly eluted with dilute hydrochloric acid. From ion-exchange data, thorium was most probably being sorbed onto the zeolites as  $\text{Th}(\text{OH})_2^{2+}$  or  $\text{ThO}_2^+$  or some other hydrated thorium oxide species. In more acidic solutions sorption was possibly occurring as  $\text{Th}^{4+}$ . Total ion-exchange was unlikely as a correlation of X-ray diffraction data, differential thermal gravimetry and energy-dispersive X-ray microanalysis data showed that there was precipitation of thorium onto zeolites.

#### 9.13 SUGGESTIONS FOR FURTHER WORK

Further experimentation is necessary on the Eastgate zeolite, especially in stripped raffinate solutions. This authoress feels that, due to the success of Eastgate in simulated raffinate solutions, it may be possible to find an optimum simulated raffinate solution composition at which Eastgate could be more efficient at selectively removing

thorium from solutions of interfering cations in nitric acid. Uptakes of thorium in pure thorium and nitric acid solutions could be improved if the thorium was in lower concentrations of  $H^+$ . More investigation of a systematic nature is required to find out which cation sites, if any, are involved or whether the thorium uptake on Eastgate is totally due to precipitation. The further use of energy dispersive X-ray microanalysis would be most beneficial.

## APPENDIX I

## APPENDIX I

### CALIBRATION OF THE MULTICHANNEL ANALYSER FOR $\gamma$ -SPECTROMETRY

The Multichannel Analyser (MCA) displayed counts or intensity on the ordinate axis. The base line (abscissa) was calibrated using a sealed  $\gamma$ -source, usually Na-22, to read energy in any programmed units. The uncalibrated abscissa consisted of 0-4095 channel numbers, where 4096 is the binary factor,  $2^{12}$ .

Since the GeLi detector was linked to the MCA via a linear input, it was a relatively simple matter to convert the linear channel numbers to linear energies and the machine used the simple linear relationship:

$$E = k.CH\# + c \qquad \text{Equation (I)}$$

Where: E represents energy

k and c are constants

CH# represents a particular channel number.

The Na-22 source gave two distinct peaks with maximum heights in two of the 4096 channel numbers and the machine performed an automatic calibration after the user had input these two channel numbers and the peak energy values (from referenced tables) for Na-22.

## APPENDIX II



## APPENDIX II

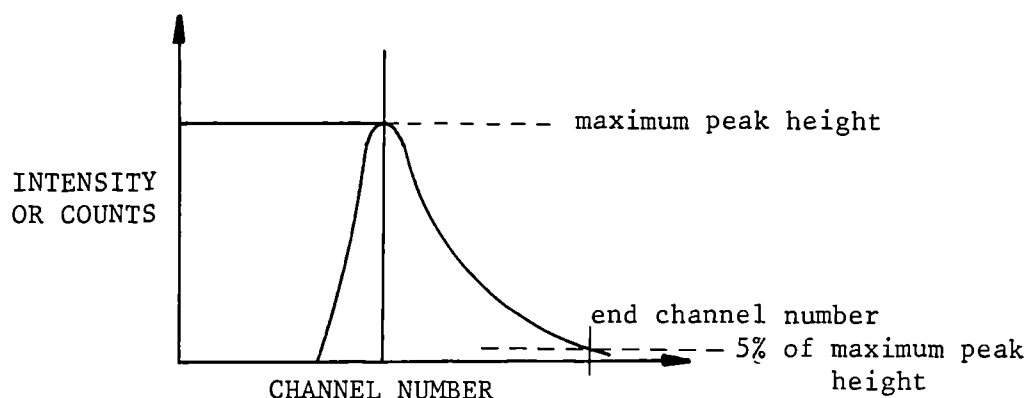
### CALIBRATION OF THE MULTICHANNEL ANALYSER FOR $\beta$ -SPECTROMETRY

Calibration of the MCA for use in  $\beta$ -spectrometry was not automatic unlike that for  $\gamma$ -spectrometry in APPENDIX I and consisted of two steps:

- a) Finding and labelling the correct end channel number corresponding to the maximum end energy ( $E_{\text{max}}$ ) of the  $\beta$ -spectrum.
- b) Deriving an equation from data obtained by using standard  $\beta$ -emitters with known  $E_{\text{max}}$  values (from referenced tables) and end channel numbers found by experiment and applying the equation so that  $\beta$ -spectra obtained from unknowns can be interpreted.

#### a) FINDING THE END CHANNEL

##### DIAGRAM OF A GENERAL $\beta$ -SPECTRUM



The end channel number was taken to be the channel number in which 5% of the maximum peak height had been obtained after background subtraction.

b) PROCEDURE TO CALIBRATE THE ENERGY SCALE TO OBTAIN  $E_{\max}$  VALUES

The detector used was an SL30 Intertechnique Liquid Scintillation counter linked to a Canberra Series 35 MCA via a logarithmic amplifier output. The MCA was unable to convert linear channel number (x-axis) on the screen to logarithmic energy automatically, as it used a linear-linear relationship, as shown in APPENDIX I. A linear-log relationship was used as follows after placing 1) a tritium  $\beta$ -emitter standard in the detector and collecting its  $\beta$ -spectrum on the MCA screen as counts 'vs' channel number. 2) Placing a C-14  $\beta$ -emitter standard in the detector and collecting its  $\beta$ -spectrum on the MCA screen in the same way as for 1) noting the end channel number in each case.

$$E_{(H-3)} = k \ln[CH(H-3)] + c \quad \text{Equation (II)}$$

$$E_{(C-14)} = k \ln[CH(C-14)] + c \quad \text{Equation (III)}$$

Where:  $E_{(H-3)}$  represents  $E_{\max}$  of tritium (keV).

$E_{(C-14)}$  represents  $E_{\max}$  of carbon-14 (keV).

k and c are constants.

CH(H-3) represents the end channel number for tritium.

CH(C-14) represents the end channel number for C-14.

Subtracting the equations (II) - (III)

$$E_{(H-3)} - E_{(C-14)} = k \left( \ln[CH(H-3)] - \ln[CH(C-14)] \right)$$

$$E_{(H-3)} - E_{(C-14)} = k \ln \left[ \frac{CH(H-3)}{CH(C-14)} \right] \quad \text{Equation (IV)}$$

$$k = \frac{E_{(H-3)} - E_{(C-14)}}{\ln \left[ \frac{CH(H-3)}{CH(C-14)} \right]} \quad \text{Equation (V)}$$

From experiment : CH(H-3) was found to be 2262

CH(C-14) was found to be 2933.

From reference  $\beta$ -energy tables :  $E_{(H-3)} = E_{\max}$  for H-3 = 18.6 keV

$E_{(C-14)} = E_{\max}$  for C-14 = 146.0 keV.

$$k = \frac{18.6 - 146.0}{\ln \left( \frac{2262}{2933} \right)}$$

$$k = \frac{-127.4}{-0.2598}$$

$$k = 490.42$$

Therefore, by having placed a sample in the detector, collecting its  $\beta$ -spectrum and noting the end channel number, having ascertained k from standards of known  $E_{\max}$ , its  $E_{\max}$  can be obtained using

$$E_{\max} = e^{\left( \frac{CH(\text{sample})}{k} \right)} \quad \text{Equation (VI)}$$

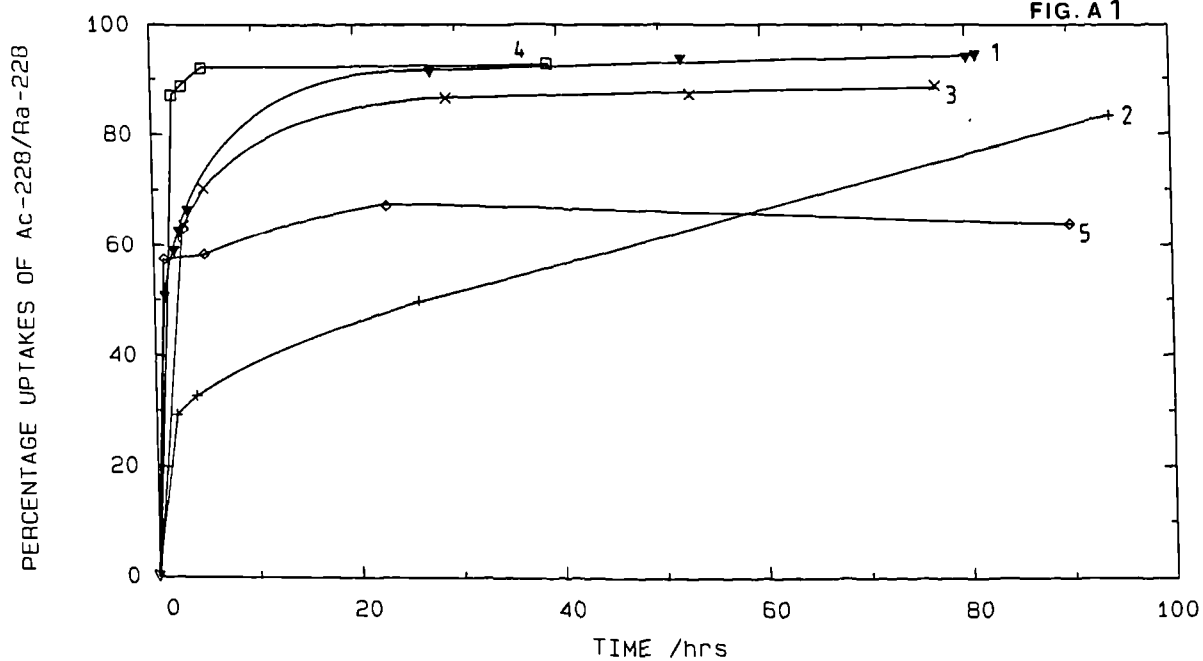
APPENDIX IIIHALF-LIVES OF SOME RELEVANT ISOTOPES

ISOTOPE	HALF-LIFE
Ac-228	6.13h
Th-228	1.91a
Pb-212	10.64h
Bi-212	60.50min
Tl-208	3.10min
Pa-234	6.66h
Th-230	$8.0 \times 10^4 \text{ a}$
Ra-226	1622a
Pb-214	26.8min
Bi-214	19.70min
Tl-210	1.32min

#### APPENDIX IV

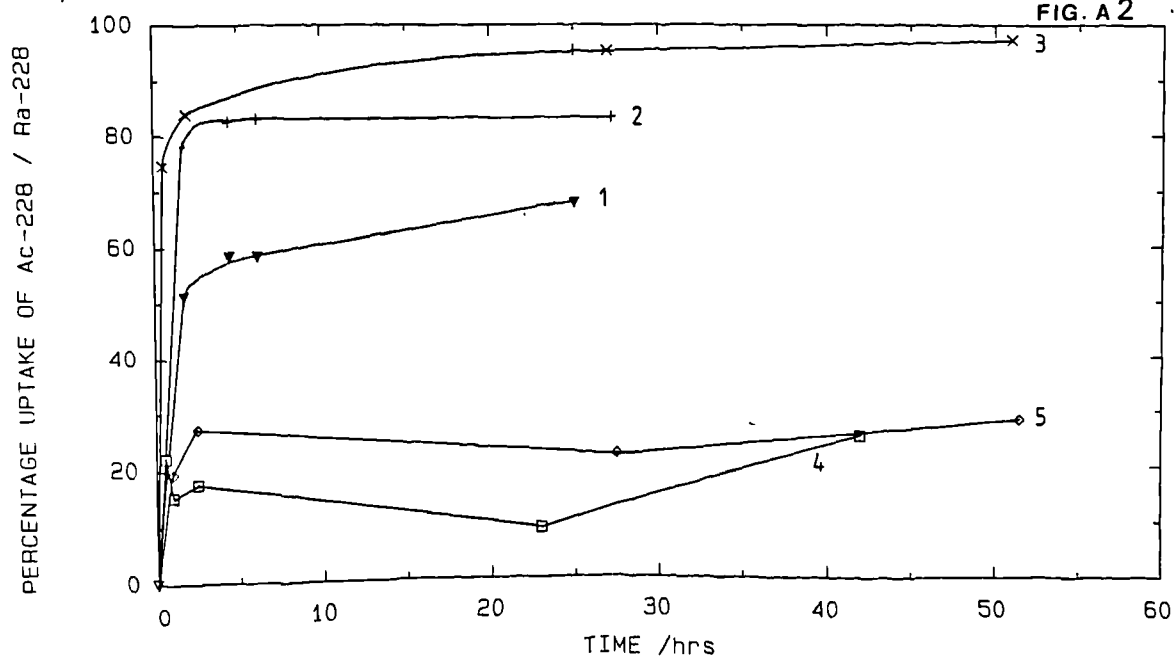
Ac-228/Ra-228 UPTAKE CURVES 1) CLINOPTILOLITE 2) EASTGATE  
3) CHABAZITE-1 4) CHABAZITE-2 5) CHABAZITE-3

FIG. A 1

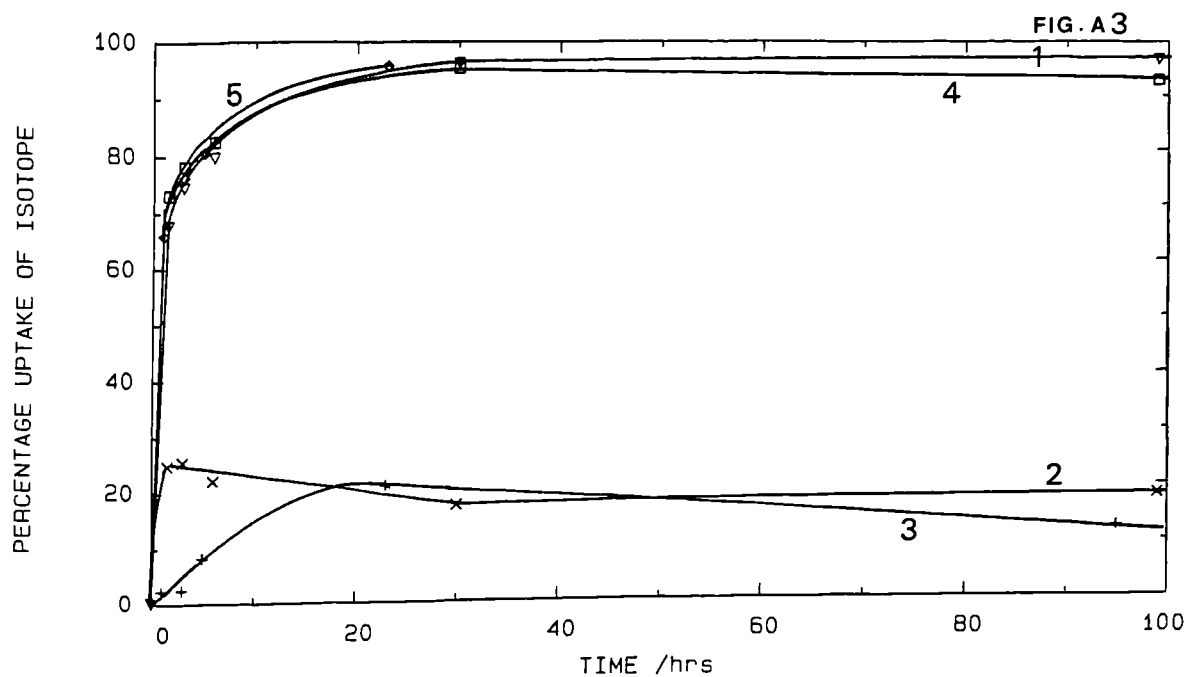


Ac-228/Ra-228 UPTAKE CURVES 1) MORDENITE 2) PHILLIPSITE  
3) ERIONITE 4) BREWSTERITE 5) COWLESITE

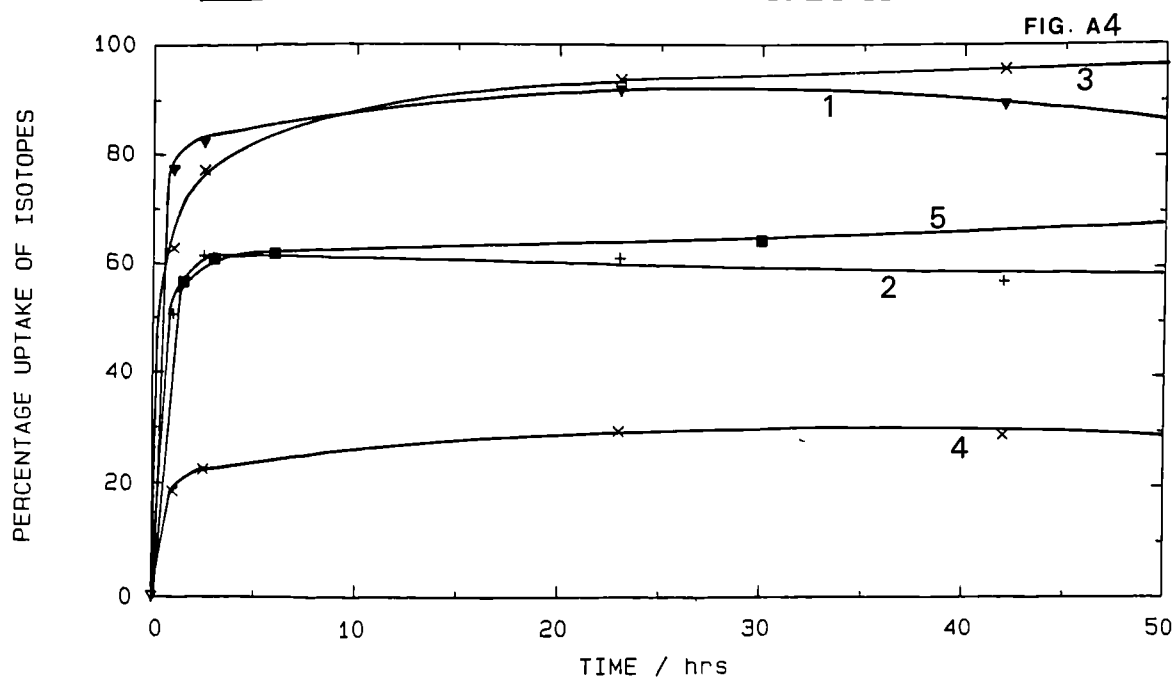
FIG. A 2



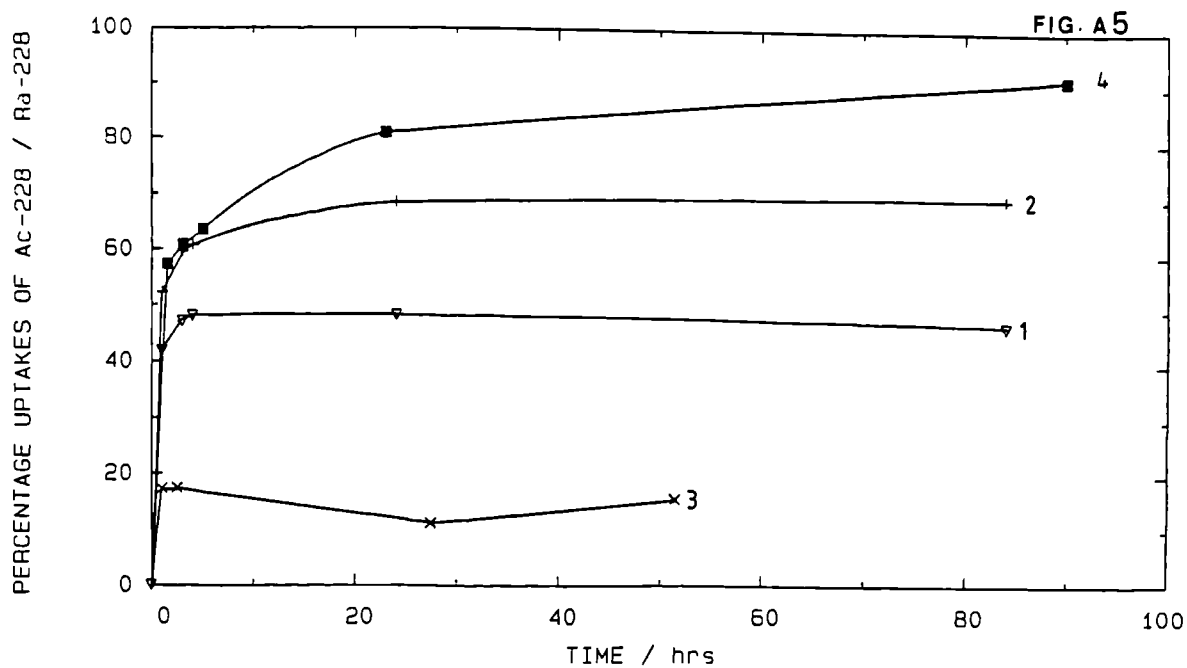
Ac-228/Ra-228 UPTAKES 1) 1010A 2) 5A (BINDER) 3) 5A (POWDER)  
4) 5050L 5) 5050F.



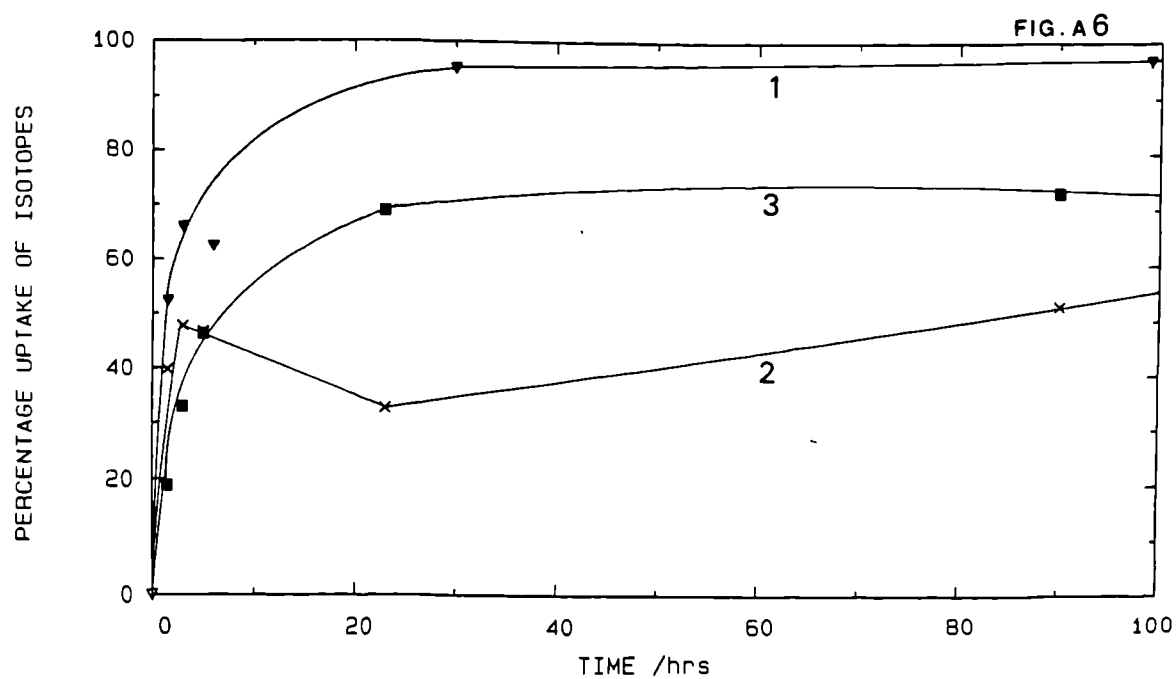
Ac-228/Ra-228 UPTAKE CURVES 1) NaY 2) 13X 3) NaZ900 4) 4A 5) K-L



Ac-228 / Ra-228 UPTAKE CURVE 1) PALAGONITE 2) PALAGONITE  
CONTAINING ZEOLITE 3) NATROLITE 4) ASHY LAYER IN LAVA FLOW

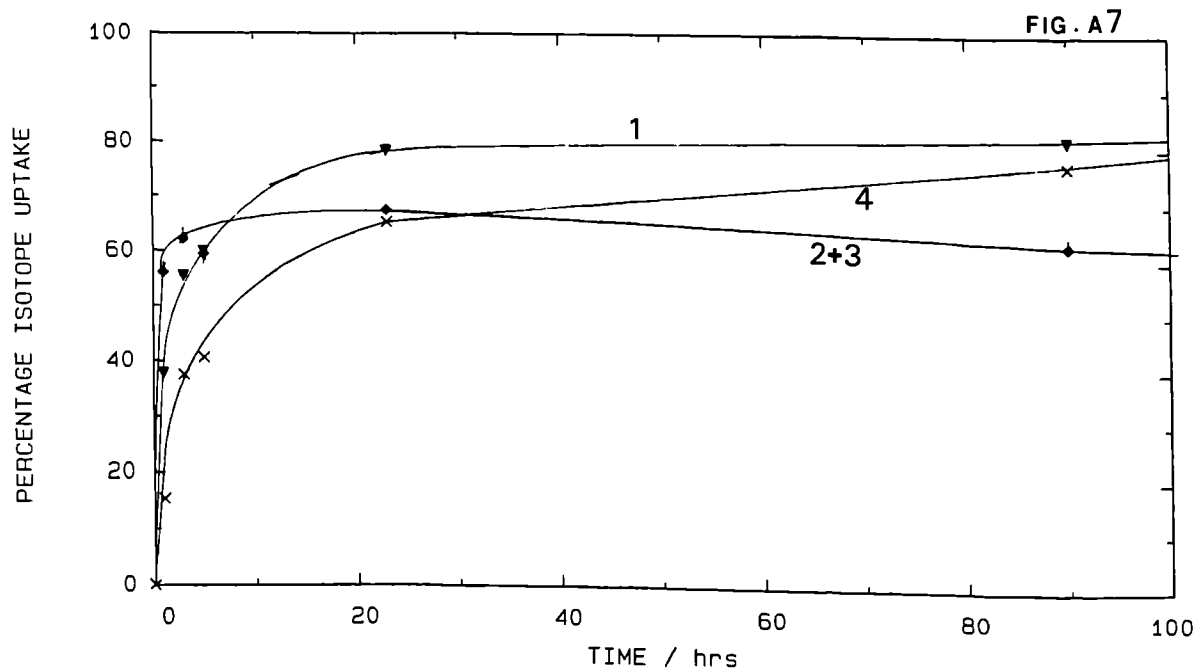


Ac-228\Ra-228 UPTAKES 1) FERRIERITE 2) BROWN TUFF  
3) HEULANDITE

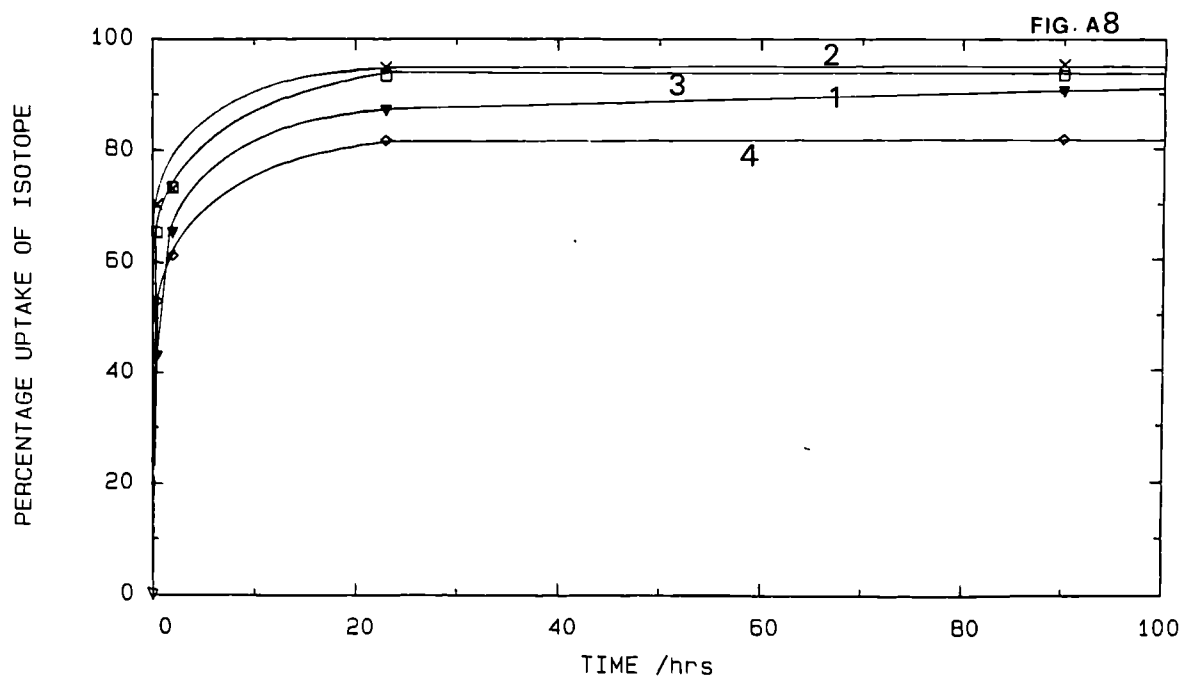




Ac-228\Ra-228 UPTAKE CURVE 1) CLINOPTILOLITE 2) CHABAZITE-3  
3) CHABAZITE-2 4) FERRIERITE in 10ppm Na

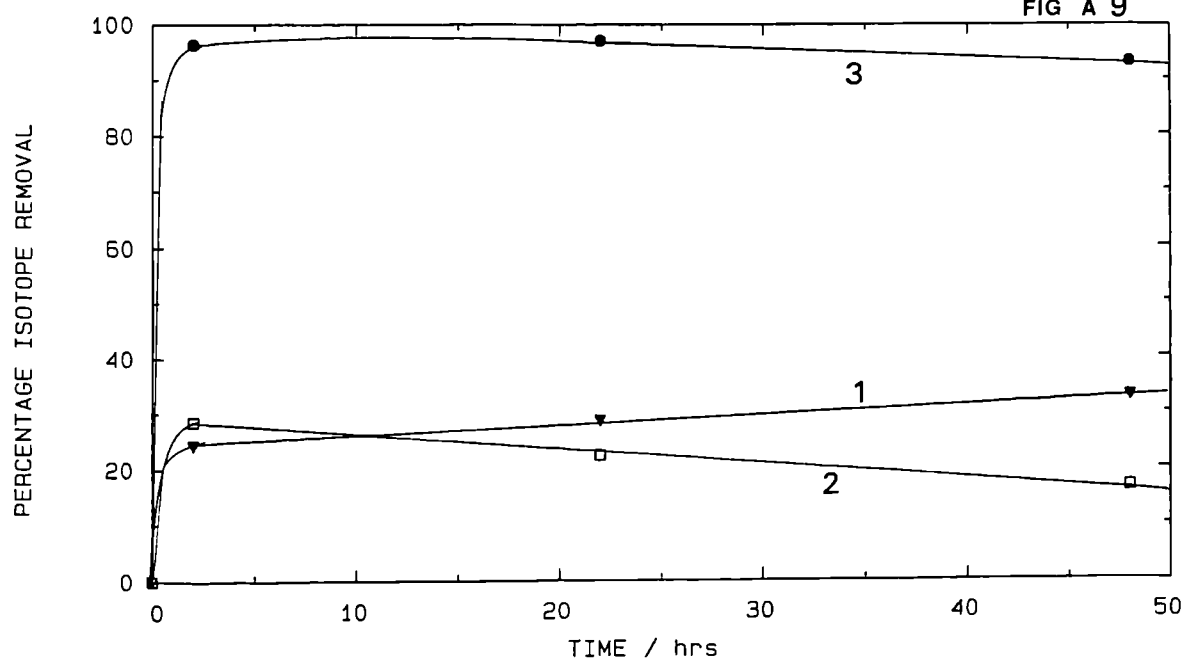


Ac-228\Ra-228 UPTAKES 1) CLINOPTILOLITE 2) CHABAZITE-3  
3) CHABAZITE-2 4) EASTGATE IN 400ppm K.



URANIUM  $\beta$ -DAUGHTER UPTAKES ONTO 1) CLINOPTILOLITE 2) Z900 3)  
NaY in 0.1N NITRIC ACID

FIG A 9



APPENDIX VEQUILIBRIUM COMPOSITION OF THORIUM AND ITSDISINTEGRATION PRODUCTS [REF. 51].

ISOTOPE	WEIGHT FRACTION
Th-232	1.0
Ra-228	$4.81 \times 10^{-10}$
Ac-228	$5.05 \times 10^{-14}$
Th-228	$1.37 \times 10^{-10}$
Ra-224	$7.17 \times 10^{-13}$
Rn-220	$1.24 \times 10^{-16}$
Po-216	$3.61 \times 10^{-19}$
Pb-212	$8.72 \times 10^{-14}$
Bi-212	$8.29 \times 10^{-15}$
Po-212	$4.51 \times 10^{-25}$
Tl-208	$1.43 \times 10^{-16}$

REFERENCES

INCLUDING BIBLIOGRAPHY

REFERENCES INCLUDING BIBLIOGRAPHY

1. "Radiation Research : Biomedical, Chemical and Physical Perspectives." Proceeding of the Fifth International Conference of Radiation Research. Ed : NYGAARD, O.F; ADLER, H.I; SINCLAIR, W.K.
2. CAMPBELL, M.H. "High-Level Radioactive Waste Management." Am. Chem. Soc., Washington (1976).
3. AERE REPORT R. 12338. Seminar on Long Term Research into Liquid Effluent Treatment. HARWELL (Jan. 1986). Ed : HOOPER, E.W. (Feb. 1987).
4. MUMPTON, F.A. and SAND, L.B. "Natural Zeolites." Chapter 1. Pergamon Press [First Edition 1978].
5. ECCLES, H. in "Ion Exchange Technology." Eds : NADEN, D. and STREAT, M. pp. 668-708. Ellis-Horwood (1984).
6. HOOPER, E.W. (HARWELL, U.K.). AERE G. 3857 D.O.E. Report RW.86. 088(1986).
7. JAMIL, M; Ph.D. Thesis, University of Salford (1987).
8. STREAT, M; SHAHBANDAH, M.R; J. Chem. Tech. Biotechnol. 32,580(1982).
9. DYER, A; HELPS, K.D; HUDSON, M.J; SHARP, C. Rec. Dev. Ion-Exch., [Pap. Int. Cont. Ion Exch. Processes] pp 155-64. Eds : WILLIAMS, P.A; HUDSON, M.J. (Elsevier, 1987).

10. RHODES, D.W; WILDING, M.W; "Decontamination of Radioactive Effluent with Clinoptilolite." REPORT IDO-14657, (July 1965).
11. RODDEN, C.J. and WARF, J.C., "Analytical Chemistry of the Manhattan Project", Chapter 2.
12. BANKS, C.V. and BYRD, C.H; *Analyt. Chem.* 25(3) pp. 416-419 (1953).
13. SARASWAT, I.P; SRIVASTAVA, S.K; BHATTACHARJEE, G; *Anal. Sci.*, 2(4), pp. 343-6(1986).
14. MERCER, B.W. and AMES, L.L., in "Natural Zeolites" Ed: MUMPTON, F. and SAND, L.B., 451-459 (1978).
15. ADAMS, B.A. and HOLMES, E.L.J., *Soc. Chem. Ind.* 54, 17, (1935).
16. HOWDEN, M and PILOT, J., in "Ion-Exchange Technology" Eds: NADEN, D and STREAT, M. Ellis Horwood 1984.
17. GUTMAN, R.G; TURNER, A.D; HOOPER, E.W. (AERE HARWELL, U.K.) ENC 1986 Transactions, Geneva. pp. 655-659 (June 1986).
18. DYER, A and KEIR, D. *Zeolites.* 4, pp. 215-217 (July 1984).
19. DYER, A. *Chemistry and Industry.* 2 pp. 241-245 (April 1984).
20. DYER, A. and MIKHAIL, K.Y. *Mineralogical Magazine* 49, pp. 203-210, (April 1985).
21. KEIR, D. Ph.D. Thesis, University of Salford (1986).
22. BOCK, R and BOCK, E. : *Z. anorg. Chem.*, 263 pp. 146 and pp. 168, (1950).

23. SMOLKA, H.G. and SCHWUGER, M.J. "Natural Zeolites." Eds. MUMPTON, F.A. and SAND, L.B. pp. 487-493.
24. DYER, A. and ENAMY, H. Zeolites 5, pp. 66 (March 1985).
25. BARRER, R.M. J. Soc. Chem. Ind. 64, pp. 130 (1945).
26. MUMPTON, F.A. in "Natural Zeolites - Occurrence, Properties and Use." pp. 3-30 Eds : SAND, L.B. and MUMPTON, F.A. (Pergamon (1978)).
27. WHITE, J.L. and OHLROGGI, A.J. : Canadian Patent. 939181, (2nd Jan. 1974).
28. DYER, A; WELLS, P.D. and WILLIAMS, C.D. G.B. Patent. Appl. 86/6,468. 15 Mar. 1986. pp. 20.
29. MORGAN, S. REPORT (1st year), University of Salford (1989).
30. AMIN, S. MSc. Thesis, University of Salford (1988).
31. BRECK, D.W.; EVERSOLE, W.G; MILTON, R.M. J. Am. Chem. Soc., 78, pp 5963, (1956).
32. REES, L.V.C. and ZUYI, T. Zeolites 6, pp. 201-205 (May 1986).
33. ABOUL-GHEIT, A.K; MENOIFY, M.F.; EL-MORSI, A.K. and ABDEL-HAMID, S. : Zeolites, 7, pp. 353-359, (July 1987).
34. BRECK, D.W. "Zeolite Molecular Sieves", Chapters 1 and 2, Wiley, U.K. (1974).
35. BARRER, R.M. : Chem. and Ind. pp. 1203 (1968).

36. DWYER, J. and DYER, A. Chem. Ind. 7, pp. 237-24 (1984).
37. BARRER, R.M. "Zeolites and Clay Minerals", (Academic Press (1978)).
38. KERR, G.T.; DEMPSEY, E; MIKOVSKY, R.J. J. Phys. Chem. 69, pp. 4050 (1965).
39. SMITH, J.V. and BENNETT, J.M. Nature 219, pp 1040 (1968).
40. DYER, A. and ARAYA, A. J. Inorg. Nucl. Chem. 43, (3), pp. 589-594, (1981).
41. ALBERTI, A. Tschermaks. Min. Petro. Mitt., 22, pp. 25 (1975).
42. MERKLE, A.B. and SLAUGHTER, M. Amer. Miner. 53, pp. 2210, (1968).
43. CARLAND, R.M. and ARPLAN, F.F; ACS Symposium Series 368. "Perspectives in Molecular Sieve Science." Chapter 18, Eds : FLANK, W.H. and WHYTE Jr. T.E. (1988).
44. STEVENS, F.S. and HILL, R.J.; Br. J. Cancer. 58, pp. 610-613 (1988).
45. VAUGHAN, P.A.; Acta. Crystallogr. 21, pp 983-990 (1966).
46. BOLTON, A.P. "Experimental Methods in Catalysis" Vol. 2. Eds : ANDERSON, R.B. and DAWSON, P.T. (Academic Press, 1976).
47. MILLER, J.T. and HENSLEY, A.L. U.S. Patent no. 4,551,572 (Nov. 5th, 1985).



48. BURRESS, G.T. U.S. Patent no. 4,629,818. (Dec. 16th, 1986).
49. ANDREEVA, N.R. and CHERNYAVSKAYA, N.B. Soviet Radiochemistry, 24(1), pp. 6-10, (1982).
50. SEABORG, G.T. and KATZ J.J. "The Actinide Elements". pp. 787 (First Edition : McGraw-Hill. 1954).
51. RYABCHIKOV, D.I. and GOL'BRAIKH, E.K. "The Analytical Chemistry of Thorium." Pergamon Press, U.K. (1963).
52. ANSELL, V.E. and CHAO, G.Y. Canadian Mineralogist 25, pp. 181-183, (1987).
53. THOMPSON, R. (ED.) "Modern Inorganic Chemicals Industry." Ch. 5 : "The Inorganic Chemistry of Nuclear Fuel Cycles." FINDLAY, J.R; GLOVER, K.M; JENKINS, I.L; LARGE, N.R; MARPLES, J.A.C; POTTER, P.E; SUTCLIFFE, P.W. Royal Society of Chemistry (1977).
54. LANE, J.A; ALEXANDER, L.G; BENNET, L.L; CARTER, W.L; PERRY, A.M; "Peaceful Uses of Atomic Energy," Procs. of the 3rd. Int. Conf., Geneva, (U.N. New York 1965).
55. CORDFUNKE, E.H.P. "The Chemistry of Thorium", [Elsevier, 1969].
56. PICKERING, M. and DAVIS, R. J. Chem. Ed. 49(6), pp. 432-433, (June, 1972).
57. SHARPE, A.G. "Inorganic Chemistry." (U.K. Longman. 1981).
58. COTTON, F.A. and WILKINSON, G. "Advanced Inorganic Chemistry." pp. 1095 (3rd Edition. Wiley Interscience, 1972).

59. KUMAR, N and TUCK, D.G. Can. J. Chem. 62 pp. 1072 (1984).
60. BOSWELL, G.G.J. and SOENTONO, S. J. Inorg. Nucl. Chem. 43, pp. 1625, (1981).
61. McDEVITT, N.T. and BAUN, W.L. : Spectrochimica Acta, 20, pp. 799-808, (1964).
62. ENTWISTLE, J.R. Private Communication with BNF plc.
63. McGLYNN, S.P. and SMITH, J.K. J. Molec. Spectroscopy 6, pp. 164 (1961).
64. DYER, A; ENAMY, H. and TOWNSEND, R.P. Separation Science and Technology. 16(2), pp. 173-183 (1981).
65. BRECK, D.W. in "Zeolite Molecular Sieves." Chapter 7, Wiley-Interscience (1974).
66. BARRER, R.M; DAVIES, J.A. and REES, L.V.C. : J. Inorg. Nucl. Chem. 30, pp. 3333 (1968).
67. ENAMY, H. and CHOW, J.K.K. (Private Communication).
68. EBERLY Jr. P.E; J. Phys. Chem. 72, pp. 1042 (1968).
69. BAES, C.F. and MEYER, N.J. Inorganic Chemistry. I pp. 780, (1962).
70. RUSH, R.M; JOHNSON, J.S. and KRAUS, K.A. Inorganic Chemistry, 1, pp. 378, (1962).
71. TOTH, L.M; FRIEDMAN, H.A; BEGUN, G.M; DORRIS, S.E; J. Phys. Chem. 88, (23), pp. 5574-5577 (1984).

72. FLETCHER, M.H. and MILKEY, R.G. *Analytical Chemistry* 28(9) pp. 1402-1407 (1956).
73. SANDELL, E.B. "Colourimetric Determination of Traces of Metals." (Wiley Interscience. U.S., 1978).
74. SNELL, F.D. and SNELL, E.B. "Colourimetric Methods of Analysis." (3rd Edition, Vol. II, Van Nostrand, 1959).
75. RABINOWITCH, E and BELFORD, R.L. "Spectroscopy and Photochemistry of Uranyl Compounds". (Pergamon Press, 1964).
76. SILVERMAN, L. and MOUDY, L. *Nucleonics*. 12(9) pp. 60-62, (1954).
77. FOREMAN, J.K; RILEY, C.J; SMITH, T.D. *Analyst*. 82, pp. 89, (1957).
78. OBRENOVIĆ-PALIGORIĆ, I; GAL, I.J; VAJGAND, V. *Anal. Chim. Acta*. 40, pp. 534-537, (1968).
79. VOGEL, A.I. "Quantitative Inorganic Analysis." (4th Edition, Longman, London, 1978).
80. FOX, B.W. : Radiochemistry, 3, Specialist Periodical Reports. (The Chemical Society, London. 1976).
81. FRIEDLANDER, G; KENNEDY, J.W; MILLER, J.M. "Nuclear and Radiochemistry". (3rd Edition, Wiley, 1981).
82. PERKINS, R.W. and KALKWARF, D.R. *Analytical Chemistry*. 28 (12), pp. 1989-1993, (Dec. 1956).
83. BANKS, C.V. and BYRD, C.H. *Analytical Chemistry*. 25(3). pp. 416-419 (March 1953).

84. SARMA, D.V.N. and RAG HAVA RAE, B.H.S.V. J. Ind. Chem. 13  
pp. 142-149 (March 1955).
85. "Liquid Scintillation Counting Practice." DYER, A. (London,  
Heyden. 1980).
86. CARMON, B. and DYER, A. J. Radioanal. and Nucl. Chem.,  
Articles, 98(2), pp. 265-273, (1986).
87. DYER, A; FAWCETT, J.M; POTTS, D.U. Int. J. Applied Radiation  
and Isotopes. 15, pp. 377-380, (1964).
88. TALIBUDEEN, O. and YAMADA, Y. J. of Soil Sci. 17(1) pp. 107-119,  
(1966).
89. "Scanning Electron Microscopy and X-Ray Microanalysis."  
GOLDSTEIN, J; NEWBURY, D.E; ECHLIN, P; JOY, D.C; FIORI, C;  
LIFSHIN, E. [Plenum Press, 1975].
90. "γ-Rays of Radionuclides in order of Increasing Energy."  
SLATER, D.N. [Butterworths, London 1962].
91. EL-YAMANI, I.S. and SHABANA, E.I. Talanta. 31(8), pp. 627-629  
(1984).
92. FREUDE, D; HUNGER, M; PFEIFER, H. and SCHWIEGER, W.  
Chem. Phys. Letts. 128(1), pp. 62-66 (1986).
93. YOSHINO, I. Kakuriken Kenkyu Hokoku (Tohoku Diagaku). 21(1),  
pp. 71-77, (1988).
94. BARRER, R.M. and ROBBINS, A.B. : Trans. Farad. Soc. 49,  
pp. 807 and pp. 929, (1953).

95. "Natural Zeolites." GOTTARDI, G. and GALLI, E. pp. 208  
Springer-Verlag 1985.
96. HARRISON, R.D. (Ed.) "Book of Data : Chemistry, Physics"  
(Nuffield, (1972)).
97. SEYFARTH, M. in "Natural Zeolites - Occurrence, Properties."  
pp. 517 (Eds. as in REF. 4).
98. BARRER, R.M. "Molecular Sieves." : Endeavour, 23, pp. 122-130  
(1964).
99. Inorganic Phases (JPCDS) Joint Committee on Powder Diffraction  
Standards (1984). no. 35-103.
100. GOLDSCHMIDT, V.M. Trans. Farad. Soc. 25, pp. 253-283, (1929).
101. "The Geology of Northern Skye." ANDERSON, F.W. and DUNHAM, K.C.  
(Members of the Geological Survey, Scotland), Her Majesty's  
Stationary Office , Edinburgh, 1966.
102. REES, L.V.C. and WILLIAMS, C.J.J. Farad. Soc. Trans. 66,  
pp. 1486-1487 (1965).
103. HOČEVAR, S. and DRZAJ. B. J. Inorg. Nucl. Chem. 41 pp. 91-94  
(1979).
104. PHELPS-DODGE Zeolite Company : Mudhills Clinoptilolite  
Data Sheet.
105. NORTON Chemical Process Company : ZEOLON 900 Technical  
Data Sheet.

106. WILLIAMS, C.D. Ph.D. Thesis. University of Salford (1988).
107. BUCK, M.J., LAPORTE Industries, Widnes, Cheshire. (Supplier of batch CaY.)
108. POP, G; MUSCA, G; SERBANS, S; POP, E. and TOMI, P. :  
Int. Cong. Catal. (Procs)., 8th Meeting, 3, pp. 1559-1568, (1984).
109. GOUDEAU, J.C; BENGUEDACH, A; JULIEN, L. Entropie 22 (130/131)  
pp. 39-42 (1986).
110. BAUMAN, S; STRATHMAN, M.D; SUIB, S.L. : J. Chem. Soc.,  
Chem. Commun. pp. 308-309 (1986).
111. SUIB, S.L. and CARRADO, K.A. Inorg. Chem. 24, pps. 200-202  
(1985).
112. TOWNSEND, R.P. and O'CONNOR, J.F. Zeolites. 5, pp. 158-164  
(May, 1985).
113. KOYAMA, K. and TAKEUCHI, Y. : Z. Kristall. 145, pp. 216 (1977).
114. DYER, A. and ARAYA, A. J. Inorg. Nucl. Chem. 43(3)  
pp. 595-600 (1981).
115. KENT ~~---~~ DALLEY, N; MUELLER, M.H. and SIMONSEN, S.H. : Inorg.  
Chem. 10(2) pp. 323 (1971).
116. PICKERT, P.E; RABO, J.A; DEMPSEY, E. and SCHOMAKER, V :  
Proc. Third Int. Congr. Catal. pp. 714 (1965).

117. HAFEZ, M.B; NAZMY, A.F; SALEM, F; ELDESOKI, M : J. Radio analytical Chem. 47, pp. 115-119, (1978).
118. WIERS, B.H; GROSSE, R.J. and CILLEY, W.A. : Environ. Sci. Technol. 16, pp. 617-24 (1982).
119. HIGGO, J.J.W. and REES, L.V.C. : Environ. Sci. Technol. 20, pp. 483-490, (1986).
120. GREBENSHCHIKOVA, V.I; CHERNYAVSKAYA, N.B; ANDREEVA, N.R. : Radiokhimiya. 15(3), 308-11 (1973). Chemical Abstract CA 79(16) : 97312v.
121. HUBICKI, W; HUBICKI, Z; JUSIAK, S; KRUPINSKI, A : Ann. Univ. Mariae Curie-Sklodowska, Sect. AA, Volume date 1973, 28, pp. 383-92 (1977). Chemical Abstract. CA88(20):145501r.
122. "The Economics of Zeolites" 1988 (First Edition), Roskill Information Services Ltd. London.
123. AMES, L.L; McGARRAH, J.E; WALKER, B.A : Clays. Clay. Miner. 31(5) 335-42 (1983).
124. WHITE, K.T. Ph.D. Thesis. The University of Salford (1988).